2

NASA CR-114641
Contract NAS2-7204

AVAILABLE TO THE PUBLIC

Final Report

A Study of an Orbital Radar Mapping Mission to Venus

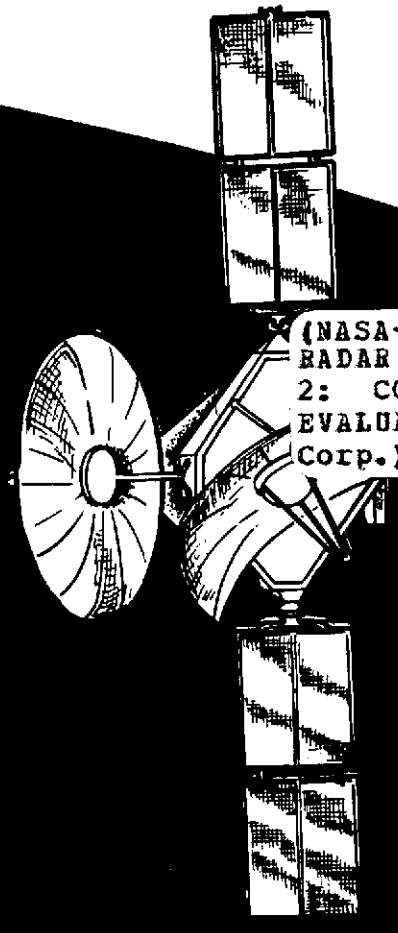

Volume II

Configuration Comparisons and Systems Evaluation

September 1973

NASA CR 114641

A STUDY OF AN ORBITAL RADAR MAPPING MISSION TO VENUS

FINAL REPORT

VOLUME II CONFIGURATION COMPARISONS AND SYSTEMS EVALUATION

September 1973

Approved

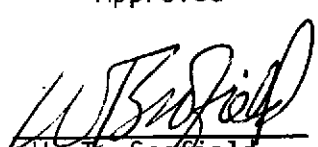

W. T. Scofield
Program Manager

D. B. Cross
Technical Director

Prepared Under Contract No. NAS2-7204 By

MARTIN MARIETTA AEROSPACE
DENVER DIVISION
Denver, Colorado 80201

for

NATIONAL AERONAUTICS AND SPACE ADMINISTRATION
AMES RESEARCH CENTER

FOREWORD

This report has been prepared in accordance with the requirements of Contract NAS2-7204 and under the direction of the NASA Contract Monitor John S. MacKay. The data and conclusions are the result of a nine month technical effort conducted for the Ames Research Center by the Martin Marietta Aerospace, Denver Division and the Environmental Research Institute of Michigan (ERIM) as a subcontractor. The report is divided into the following volumes:

Volume I	Summary
Volume II	Configuration Comparisons and System Evaluations
Volume III	Parametric Studies and Subsystem Comparisons

The report is arranged so that Volume I provides a concise overview of the study, Volume II provides an appreciation of the major mission and system integration considerations as well as cost and schedule implications and Volume III provides the detailed supporting tradeoff studies down to the subsystem level.

ACKNOWLEDGEMENTS

We acknowledge the following individuals and companies for their contributions through making data available, reviewing the work accomplished, suggesting problem solutions and contributing to the establishment of science goals.

Byron L. Swenson, NASA ARC

John S. MacKay, NASA ARC

Louis O. Friedman, JPL

Walt Brown, JPL

Alan Laderman, JPL

J. R. Hall, JPL

Kurt Heftman, JPL

Dr. Gordon Pettengill, MIT

Tony England, U.S.G.S.

Gerry Schaber, U.S.G.S.

Technology Service Corporation

STUDY TEAM

The following individuals participated in this study and their efforts are greatly appreciated. The Environmental Research Institute of Michigan (ERIM) personnel are acknowledged for their able participation as a subcontractor.

Program Manager	W. T. Scofield
Technical Director	D. B. Cross
Technical Team	
Science Analysis	D. C. Wychgram Dr. B. C. Clark
Mission Analysis	S. K. Asnin T. W. Locke
Radar & Antenna System	F. A. Vandenberg Dr. R. Bayma, ERIM
Data Handling & Communication System	R. W. Stafford; Dr. R. Bayma, ERIM Dr. J. Zelenka, ERIM R. Larson, ERIM Dr. R. Lewis, ERIM Dr. P. McInnes, ERIM
Attitude Control System	F. D. Hauser R. S. Jackson
Spacecraft Systems Lead	O. O. Ohlsson
Power	A. A. Sorensen
Thermal	T. Buna
Design	N. M. Phillips
Mass Properties	W. D. VanArnam
Antenna Technology	W. Koppl Dr. K. F. Broderick

CONTENTS

LIST OF FIGURES

LIST OF TABLES

I. INTRODUCTION

The primary intent of this volume is that of consolidating, summarizing, and highlighting all systems and mission design conclusions which rest on the parametric analyses presented in depth in Volume III. A number of specific concerns which relate to the feasibility of the Venus Orbital Radar mission are addressed. Designs are recommended which best satisfy the science objectives of the Venus radar mapping concept. Attention is given to the interaction and integration of those specific mission-systems recommendations with one another, and the final proposed designs are presented as complete, cohesive, and complementary configurations. The feasibility, cost, and scheduling of these configurations are evaluated against assumptions of reasonable state-of-the-art growth and space funding expectations. This volume also indicates areas of concern disclosed by the mission parametrics and system design considerations, and suggests the most productive directions for additional study. In addition, those technology items which offer the greatest potential for mission enhancement or science return are pointed out.

While the parametrics of Volume III have carried mapping orbit eccentricity as a variable through all design studies, this volume concentrates on an orbit design of 0.5 eccentricity with polar inclination as a recommended reference. All configurations are related to this reference. The problems associated with radar systems when mapping from an eccentric orbit have been brought under control by the technique of employing a variable side-look angle over each mapping pass. As a result, surface resolution ranging from 50 meters at the Venus equator to 200 meters near the poles can be achieved, with the potential for 100% coverage of the planet surface.

Our study has drawn in part from other sources which have recently examined areas related to the concept of orbital radar mapping of Venus topography. The Jet Propulsion Laboratory's report, "Planetary Imaging Radar Study," (JPL Report 701-145, June 1972) has concentrated on the definition of a radar system suitable for orbital mapping, and has contributed to our understanding of radar system design. A subsequent JPL study to be published soon, entitled "Venus Orbiting Imaging Radar," is essentially an expansion of their early report into the related mission and system aspects of a Venus orbital radar. This report has also detailed important science considerations for the radar exploration of Venus. Much of their analysis involves the design of radar imaging from a circular mapping orbit. The Ames Research Center study, "A Preliminary Analysis of a Radar Mapping Mission to Venus," has formed a broad foundation for much of the mission design and systems evaluations undertaken by Martin Marietta. Their work has been instrumental in stimulating productive directions of investigation which have been followed in our assessment of Venus Radar Mapping missions for the 1980s.

II. SCIENCE RATIONALE

Although Venus is Earth's nearest planetary neighbor, very little is known about the planet in terms of its geology and surface characteristics. The planetological similiarities of density and size which exist between Earth and Venus suggests that the two planets may have comparable origins and geologic histories. The study of Venusian geologic history and surface processes will undoubtedly provide insight in understanding the origin and evolution of the solar system and Earth.

The exploratory mission under consideration is for the mid to late 1980 time period. It is assumed that basic atmospheric, planetary dimensions and shape, mass distribution, magnetic field and similar characteristics will have been defined from precise orbit tracking, fly-bys, probes, and analysis of Earth-based observations prior to the mission.

The overall science goal of the exploratory mission is to determine the geologic history of Venus and its mode of origin. This objective can best be accomplished by obtaining high resolution topographic data of the planet's surface. Secondary objectives are to map the major topographic features of Venus and provide detailed geologic and terrain analysis of potential landing sites.

First order geologic information can be obtained from study of a planet's surface morphology. Surface morphology, which is described by topographic data, can be interpreted by the geologist for information on the uniformity of the crust, general rock type, geologic structure, stratigraphy and constructional/destructional surface processes. This information is used to construct the historical evolution of the planet.

In view of the primary importance of topographic data, it is mandatory that the surface imaging system be designed to maximize

the amount of quality of topographic data obtained. Remote sensor systems which employ the visible and near infrared regions of the electromagnetic spectrum have been highly developed and are proved to be well suited to obtaining topographic data. The thick Venusian atmosphere is opaque to these shorter wavelengths forcing the use of an alternative system. Side-looking radar can provide imagery with high topographic data content and selection of the proper operating frequency will permit atmospheric penetration (see Volume III, Section II). Synthetic aperture radar techniques have been developed over the past few years which minimize power and antenna requirements and yet provide a high degree of resolution. Proper specification of radar variables will make a synthetic aperture radar system ideally suited for the Venus orbital mapper mission.

The science requirements can be satisfied with a baseline mission which employs a single frequency (3.0 GHz, 10 cm wavelength) single polarization imaging system. A radar altimeter is virtually required auxiliary instrumentation. At least one entire hemisphere of coverage, including the pole, is required with total coverage desirable. A basic resolution of 100 meters, with limited higher and lower resolution coverage, will accomplish the science objectives. These ground rule science requirements evolved from the parametric data of this study and the data presented early in the JPL study "Venus Orbiting Imaging Radar." The rationale is completely expressed in Volume III Section II of this report.

III. MISSION ANALYSIS

INTRODUCTION

Launch Opportunity Analysis

Definition of launch opportunities during the 1980s for the Venus orbital radar concept is a strong function of Venus arrival conditions. With a planetary orbiter mission, arrival Vhp (hyperbolic excess velocity) is always a principal element in launch window selection, since this parameter is a direct measure of the amount of energy which must be removed from the heliocentric trajectory to achieve an orbit. The nature of our parametric study involved the consideration of a wide range of orbit sizes; from 0. to 0.8 eccentricity with periapsis at 400 km altitude. Evaluation of mission years and launch window optimization has therefore been based upon insertion into a mean orbit size of 0.3 eccentricity, a value between the tight circular orbit case and the relatively loose orbits of up to 0.8 eccentricity.

Launch energy considerations are of course important to the analysis of mission opportunity, and are also influenced by the mission concept. Where Vhp measures inserted weight in orbit capability, launch energy (C_3) measures the capability of the assumed launch window to deliver weight to a target planet. Titan IIIE/Centaur has been considered the prime launch vehicle for the Venus Radar Mapper mission. A launch window duration of 20 days has been selected as most representative of current mission design philosophy. If a shorter window were considered, overall performance would be enhanced since the optimal performance region would be more closely bracketed. The reverse would hold for a longer launch window. Charts of launch energy and arrival Vhp for all mission years are presented in the Mission Description subsection of this volume.

Where the alternative launch system of a Shuttle/Centaur can be considered as viable, the influence of mission concept on launch opportunity analysis modifies somewhat. With this increased launch capacity, nearly double that of Titan/Centaur, C_3 becomes even less of a launch window determinant for a single spacecraft mission. But of greater importance, the doubled delivered weight capability opens up the attractive option of a dual spacecraft mission. A promising dual mission concept at this point appears to be that of placing the two spacecraft into identical, but lagging, orbits. The leading orbiter would serve as a wide area, contiguous coverage, mapper, while the role of the trailing orbiter would be to map in a high resolution mode specific sites selected in near real time for detailed study. The definition of the optimum dual spacecraft mode of operation is beyond the scope of this study. Consideration of the Shuttle/Centaur, then, provides a flexibility in mission design beyond the simple enhancement of existing launch opportunities or opening of marginal opportunities.

Orbit Design

A primary influence on the design of the mapping orbit derives from the constraints associated with the side-looking radar system. Radar design work has concentrated on the integration of antenna configuration, beamwidth, PRF (pulse repetition frequency) constraints, power, and mapping frequency to gain the greatest return from orbits of various sizes (e = 0. to 0.5). The resulting radar system in turn influences orbit orientation for each eccentricity, specifically the location of periapsis. As true anomaly increases in an eccentric orbit, so does the altitude, radar range, radar power requirements, and swath width for a fixed beamwidth - fixed side-look angle system. The result of this situation is 1) a limit to the true anomaly imposed by power limits, and 2) a second limit on true anomaly arising from ambiguities in the processing of the radar signal for large swath widths.

Although the radar systems presented in this volume are designed to minimize the problem of limited true anomaly, their configurations do influence the amount of planet coverage and the position of periapsis. For Configurations A and B (see Section VI), true anomaly limits are set at $\pm 55^{\circ}$ for 0.5 eccentricity, and since polar coverage is desired, periapsis has been located at a latitude of 35°. With Configuration C (see Section VI), which employs the technique of variable side-look, $\pm 90^{\circ}$ is the usable true anomaly range for mapping, and periapsis is located at the equator to balance the radar range profile over each hemisphere.

A second important influence on the orbit design comes from the capability of the insertion propulsion system considered. Here the propulsion limits constrain the set of orbit sizes and eccentricities, which can be achieved for the various mission years and set a lower bound on eccentricity. As eccentricity decreases, more energy must be removed from the hyperbolic approach trajectory to insert into the orbit. The extensive analysis presented in Volume III which treats the problem of orbit insertion, indicates that the lower limit on orbit size ranges from $e = 0.3$ to $e = 0.5$ for Viking class propulsion, varying with mission opportunity as the associated Vhp characteristics vary. Below an eccentricity of 0.3, the use of a space storable insertion system is necessary to provide sufficient insertion capability for the set of 1980 missions.

A variety of other systems such as power acquisition, telecommunications, and thermal do interrelate with the orbit design, but their role at this point of the feasibility assessment is not one of shaping the reference orbit. Instead, they serve to define such things as frequency of mapping, communication schedules, and spacecraft orientation at various mission phases. Their influence is directed toward the sequencing of mission events and spacecraft

orientation, and they tend to be tailored to the particular trajectory characteristics of the considered missions and orbit designs.

LIMITING CRITERIA

Orbit Orientation

From the parametrics of Volume III a set of limiting criteria has been developed which relates to the orientation of the mapping orbit. Given the double-valued nature of periapsis latitude solutions possible with polar orbit insertion, the variability of Vhp declination with mission year, and limits to the amount of apsidal shift capability which can be reasonably assumed, there exists a mission year dependent restriction on periapsis latitude possibilities. And as a consequence, where a specific periapsis latitude is designated, this situation indicates the degree of apsidal shift which will be needed over the launch window of each opportunity, and in this way becomes a potential limiting factor on the viability of certain mission years.

The same dual periapsis latitude solutions associated with nominal, coplanar insertion are interrelated with orbit motion in that they correspond to the possibilities of descending or ascending mode motion about periapsis. Specifically, descending motion is associated with Northern periapsis latitudes, and ascending motion with a Southern periapsis. The effect of this is a limitation of the orbital motion during the mapping phase, with all the associated implications for event scheduling, when a particular hemisphere is designated for periapsis placement.

In addition to these limiting aspects of orbit orientation, Volume III discloses the significant influence of periapsis latitude on orbit stability. For eccentric polar orbits the degree of periapsis altitude instability was found to be a strong function

of the periapsis offset in latitude from the Venus orbit plane equator. The limit here is on orbit size, suggesting that the more highly eccentric orbits may be insufficiently stable for all considered periapsis locations.

Orbit Size

The important limiting criteria to orbit size, periapsis altitude and eccentricity, derive from a variety of otherwise unrelated analyses. Periapsis altitude for this mission concept must balance the desire to keep altitude low for adequate mapping resolution (a science objective) with the mission necessity of remaining high enough to avoid contact with the dense Venus atmosphere. For our study, an initial periapsis altitude of 400 km has been selected for its capacity to absorb an insertion dispersion of about 75 km and still remain 300 km above the surface - deemed sufficient for the orbit designs considered appropriate to keep any altitude decay from reaching the atmosphere.

Characteristics of the various propulsion systems serve to establish lower limits on orbit eccentricity. The performance of Titan IIIE/Centaur translates into a maximum weight which can be delivered to Venus for any given launch opportunity, and limits the size of the insertion propulsion system that can be used to transfer to the mapping orbit. This pre-insertion weight limit for most cases is about 4000 kg. With a 3-engine Viking insertion propulsion system as our reference, tailored to the launch vehicle capability, eccentricity is bounded on the low side at $e = 0.3$ in 1983 and 1984, and $e = 0.5$ in 1988. Orbit eccentricities below these limits would require a much higher performance insertion system, such as a space storable configuration.

Upper limits to eccentricity derive from the periapsis altitude instabilities associated with polar orbits for certain periapsis

latitude locations. As indicated in Volume III, these instabilities can reach unacceptable levels when periapsis latitude is as much as 20^{o} for orbit eccentricity of 0.6 or greater. Since an off-equatorial periapsis is desirable for our Configurations A and B, the 0.6 eccentricity has been established as the upper bound on orbit size.

In addition to these bounds on eccentric orbit size, there exist limits to size which arise from the problems inflicted upon the radar system when the altitude increase is large with increased true anomaly. The specifics of these problems are addressed in the major section on Radar and Antenna Systems of this volume. When ambiguity, processing, and power limits are considered, the practical upper limit on eccentricity becomes closer to 0.5; and even at this size surface coverage is sacrificed for the dual-beamwidth strategy of the A and B spacecraft.

MISSION DESCRIPTIONS

This section presents characteristics of the entire Venus orbital mapper mission, from launch conditions through orbit insertion to specific aspects of the surface coverage achieved by the radar. Emphasis is on the illustration of all mission phases and involves representation of the reference missions that have become associated with both the dual beamwidth radar system (Configurations A and B) and the technique of variable side-look angle (Configuration C). All of the relevant conclusions which have been derived from the parametric analyses of Volume III are summarized. The detailed rationale underlying those conclusions, however, is best obtained by direct reference to that volume.

Interplanetary Trajectory Characteristics

The heliocentric transfer trajectories for the missions to Venus orbit are all direct, of both Type I and II classification. Use of multiple-revolution transfer is not indicated at this point of the study due to the existing variety of direct Earth-Venus opportunities available during the decade of the 1980s. For all mission years considered, 1983, 1984, 1986, 1988, and 1989, a Type I trajectory (transfer angle $< 180°$) exists with attractive performance potential. For missions in 1983 and 1984, Type II trajectories with performance comparable to Type I transfers have been found. Figures III-1 and III-2 illustrate both trajectory types in a heliocentric system - Type I in 1983 and Type II in 1984. Positions of Earth and Venus are indicated at launch and Venus arrival, and 20-day flight time intervals are denoted by the smaller dots along the path of the transfer trajectory.

Specific aspects of the geometries associated with both trajectories are presented in Figures III-3, III-4, and III-5. The curves of Figure III-3 present the history of Sun-Earth-vehicle angle (SEV) during interplanetary cruise for both cases. SEV angle becomes critical as it approaches zero, indicating possible solar interference with tracking signals between Earth and spacecraft. For neither trajectory does the timing of zero SEV occur during prime tracking periods. In Figure III-4 are shown histories of spacecraft equatorial declination. Again the effect of this parameter is felt primarily as it approaches a zero value, and the effect is a general degradation to the navigation process. Here too, neither trajectory shows a zero-declination problem during prime tracking time. Figure III-5 illustrates the range histories from Earth and sun. The important characteristic of note here is that Earth range at Venus encounter is only around 0.6 to 0.7 AU, a proximity favorable to navigation and orbit determination. On

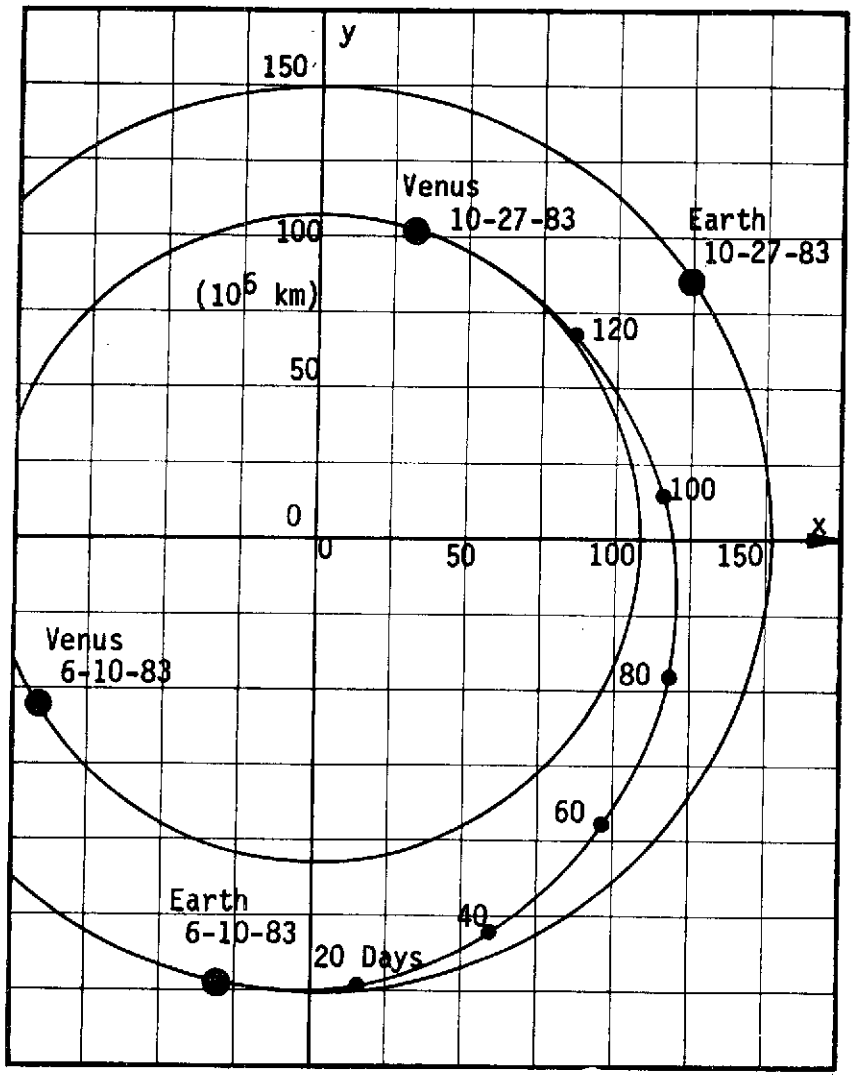

Figure III-1 Heliocentric Trajectory, 1983 Type I Mission

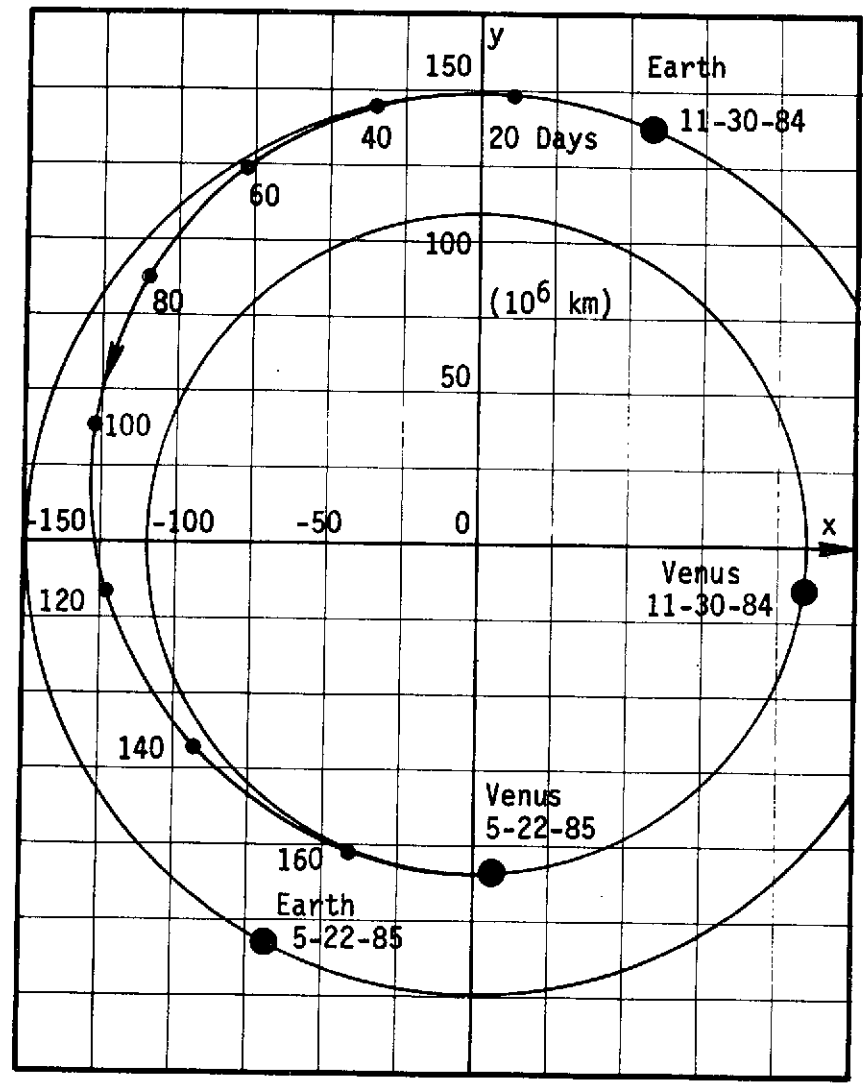

Figure III-2 Heliocentric Trajectory, 1984 Type II Mission

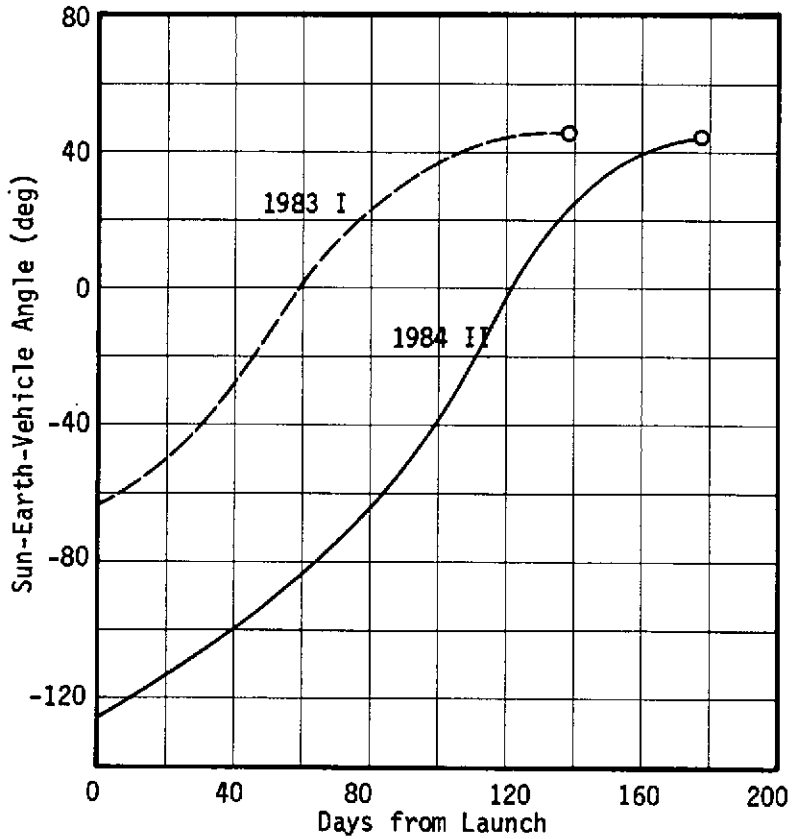

Figure III-3 Sun-Earth-Vehicle Angle Histories

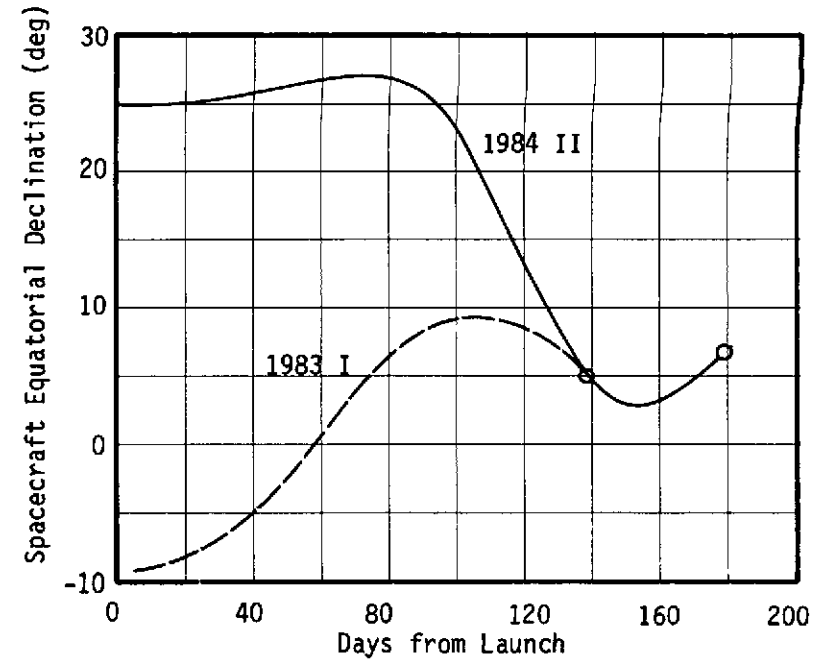

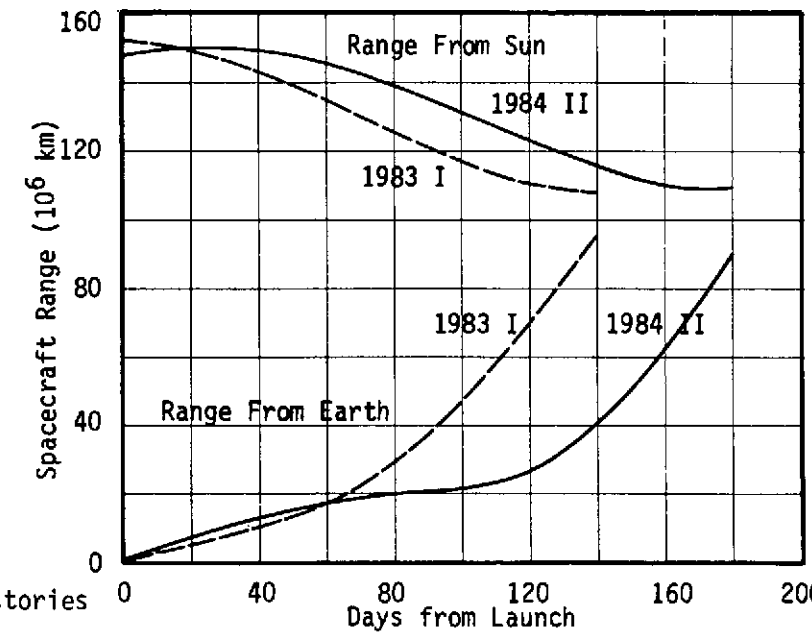

Figure III-5 Spacecraft Range Histories

Figure III-4 Spacecraft Equatorial Declination Histories

balance, the nature of this overall geometrical picture exhibits a lack of any unfavorable navigation features, a situation which should be, and is, reflected by the results of the navigation analysis.

In assessing the actual performance characteristics for each mission year opportunity, the critical parameters are launch energy, C_3, and hyperbolic excess velocity at arrival, Vhp. The first parameter measures the potential for delivering weight to Venus; the second parameter measures the cost of inserting that weight into some specified orbit. Both measure the potential value of each mission year in terms of a useful orbiting science payload. Launch energy for all considered opportunities is shown by the bar chart of Figure III-6, and Vhp is similarly presented in Figure III-7. In all cases, the maximum value of each parameter over an optimized 20-day launch window is presented. Translation of these parameters into useful weight in orbit will be done in the subsection, Orbit Insertion.

Navigation

A complete navigation analysis has been performed for two reference trajectories selected as representative of the entire mission set considered - a 1984 Type II and a 1988 Type I. Details of this analysis are discussed at length in Volume III and only the results and conclusions of the study are presented here.

For both trajectory types, two midcourse corrections are adequate. An initial midcourse is executed 5 days after launch to remove injection errors, and a second correction is performed 10 days prior to Venus arrival to reduce trajectory errors which have grown from the execution uncertainties of the first midcourse correction. The total ΔV load (mean + 3 sigma) associated with this midcourse scheme is 36.5 m/sec for 1984 Type II and 30.0 m/sec for the 1988 Type I. This relatively low magnitude of midcourse requirement was anticipated and reflects the generally favorable navigation geometries.

Encounter error levels associated with the resulting trajectory dispersions were, however, larger than expected for encounter radius. One-sigma errors in radius were found to be 38 km for the 1984 trajectory and 112 km for the 1988 mission. At these levels a design calling for insertion into an orbit of 400 km periapsis would require some degree of aimpoint bias to ensure avoidance of the Venus atmosphere. The initial insertion would be into an orbit with a higher periapsis of perhaps 1000 km, which would be followed by an orbit trim to lower periapsis to its nominal value. Yet the size of the radius error is actually a function of the pessimistic station location error assumptions made for the analysis, rather than a function of poor navigation geometry. The error level for encounter dispersions could, for example, be halved with the inclusion of changed particle calibration (a navigation technique) in the navigation process. This simply requires the incorporation of X-band and S-band capability onboard the spacecraft, and would be the preferred solution from the mission analysis view. Other encounter errors were found to be more reasonable, even with the pessimistic navigation assumptions. One-sigma errors in periapsis latitude are about 0.5^{o}, and in-orbit inclination, from 0.2^{o} to 0.6^{o}.

Orbit Insertion

The parametric study of orbit orientation possibilities for nominal transfer into polar orbit has produced a picture of periapsis latitude accessibility varying considerably with mission year. In conjunction with this variability and the desire from science considerations to provide some freedom to position periapsis over specific latitude regions for different mapping strategies, an apsidal shift provision of $\pm 20°$ has been included in all of the orbit insertion analysis. Given this flexibility, each mission opportunity can be examined to determine its suitability for our reference orbit designs corresponding to Configurations A, B, and C. Accessible

periapsis latitude ranges for all opportunities are presented in bar chart format by Figure III-8. The indicated ranges correspond to a $\pm 20°$ spread about the nominal latitudes for mid-window launch. Variation in nominal latitude over the 20-day window duration is sometimes significant, and the degree of this variation is assessed in Volume III.

If the 0.5 eccentricity orbit is considered our reference orbit size, and with the assumption that polar coverage is highly desirable, Configurations A and B (dual beamwidth) must seek a periapsis location at 35° latitude, North or South, since mapping is limited to $\pm 55^{\circ}$ true anomaly. Configuration C, with variable side-look, is able to map $\pm 90^{\circ}$ in true anomaly, so therefore seeks an equatorial periapsis. With these conditions as a guide to mission year suitability, reference to Figure III-8 indicates that missions in 1983, 1984, and 1989 are adequate for all configurations, while in 1986 and 1988 periapsis location is limited to regions around the pole and regions around the equator. Mid-latitudes would not be accessible in those two years for Configurations A and B, implying the sacrifice of either polar or equatorial coverage.

Given this 20° apsidal shift allocation for orbit insertion, the actual orbit insertion maneuver has been evaluated in depth. A complete analysis is presented in Volume III, including all related parametrics. A primary consequence of that analysis was disclosure of the significance of finite burn loss effects with a fixed attitude burn, arising from excessively long burn times at low thrust to initial weight ratios (T/W). The study led to the treatment of a 3-engine Viking Class insertion system as our reference design to minimize those losses. With this design, all mission opportunities can be assessed for 1) their performance <u>capability</u> assuming rubber payload in orbit and rubber propellant tanks, and 2) their <u>realizable</u> performance value assuming a realistic fixed payload weight and reasonable tank growth.

Figure III-6 Launch Energy Range for All Missions (20 Day Window)

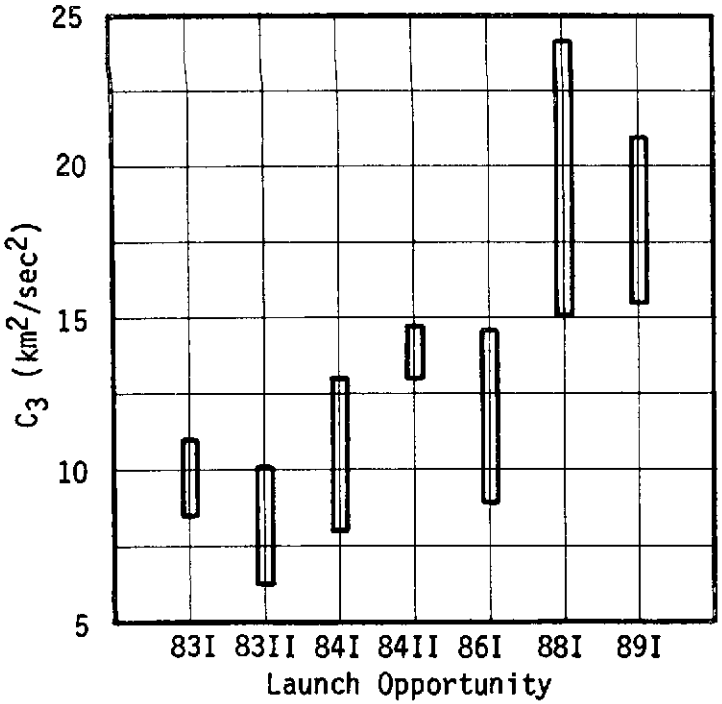

Figure III-7 V_{hp} Range for All Missions (20 Day Window)

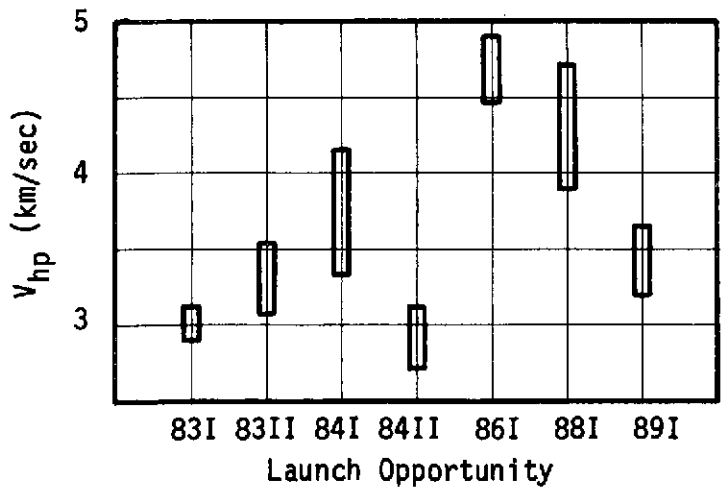

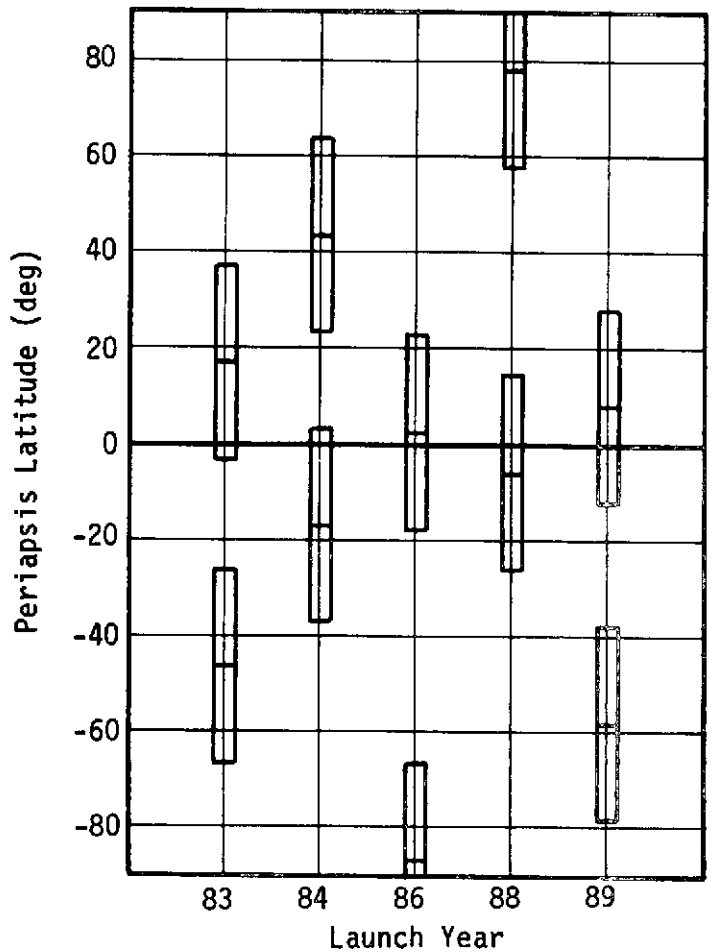

Figure III-8 Accessible Periapsis Latitudes With ±20° Apsidal Shift for All Mission Years, in Polar Orbit

A performance capability picture is presented in Figure III-9 for all mission years. The chart illustrates payload weight in orbit potential for each year based on worst day conditions of the associated launch windows, and reflects the assumptions discussed, including apsidal rotation provision, finite burn effects, and 3-engine propellant inerts. The impact of varying eccentricity can be seen by comparisons of the three considered eccentricities of 0.,0.3, and 0.5. This picture of performance capability is essentially a representation of the combined effects of launch energy and Vhp which were shown in similar format in Figures III-6 and III-7.

Realizable performance, on the other hand, is an illustration of the actual characteristics required of our insertion propulsion system once a specific payload weight in orbit has been defined. In our study, that weight has been assumed to be 750 kg and is based on extensive analysis of all spacecraft systems. For this picture the underlying assumptions are somewhat different. A limit to finite burn loss of 400 m/sec has been imposed as an arbitrary upper bound for manageability. This limit in turn sets a minimum T/W for various levels of impulsive ΔV, which translates into upper limits on initial (pre-insertion) weight as thrust is equated to the 1, 2, 3, and 4 engine Viking class systems. The result is then a criterion for determining points, based on the initial weight requirements, which indicate the necessary engine combination to hold down finite burn losses to acceptable levels. Initial weight requirements are a direct function of ΔV with fixed payload in orbit; hence, are functions of arrival Vhp and the eccentricity of the desired orbit.

Figure III-10 presents the realizable performance characteristics for all mission years, as illustrated by their initial weight requirements, with the assumptions of 1) 750 kg payload, 2) 20

Figure III-9 Useful Weight In Orbit Capability for
All Mission Years, 3-Engine Viking Propulsion Assumptions

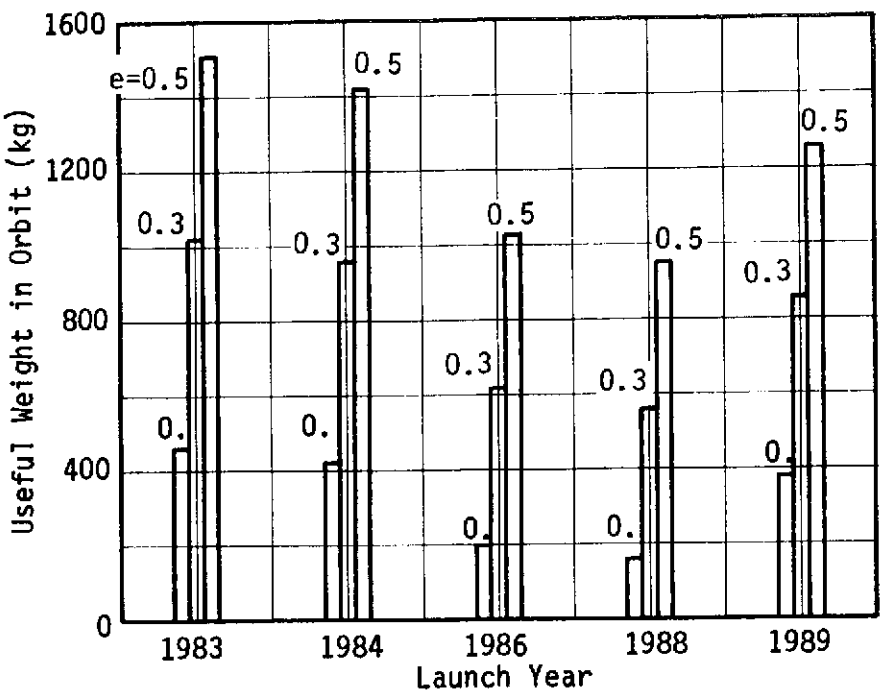

Figure III-10 Mission Year Performance for Fixed Useful Weight In Orbit (750 kg)

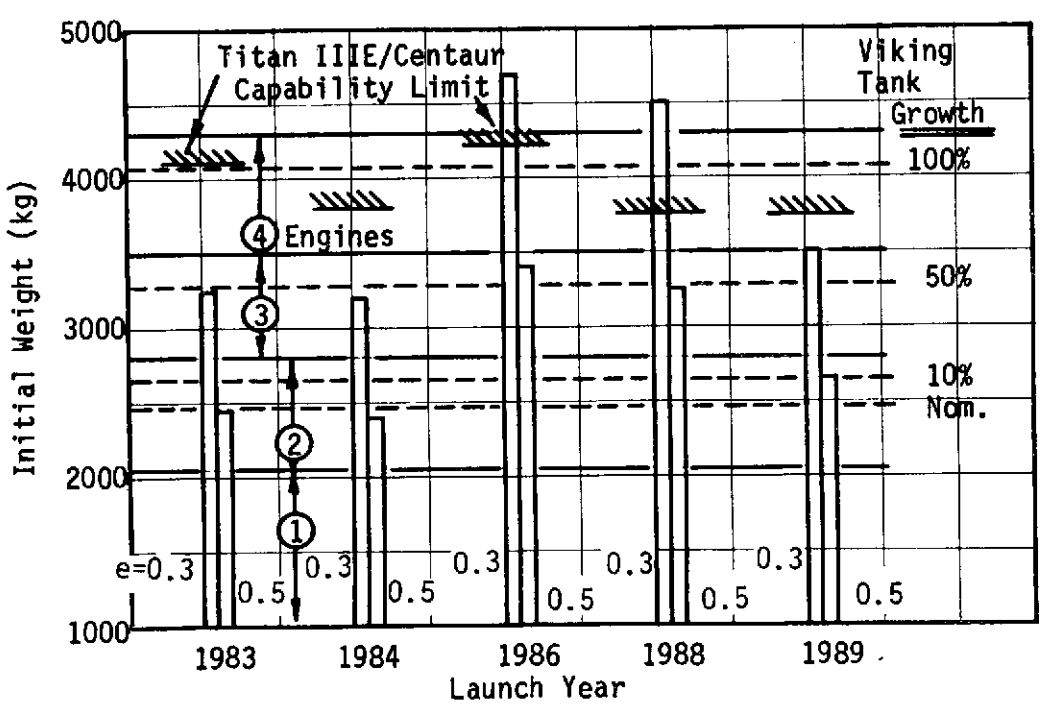

apsidal shift, 3) 400 m/sec burn loss, and 4) worst case Vhp for each window. Superimposed on the chart are the necessary engine combinations and the corresponding propellant load expressed as a percentage of current Viking tank capacity. Also indicated are the limits to delivered weight which derive from the performance limits of Titan IIIE/Centaur and the associated C_3 for each mission. With an orbit eccentricity of 0.5, all mission years can achieve the desirable payload with a propulsion system comprised of 3-engines; the most attractive propulsion growth alternative from the systems' view. For an eccentricity of 0.3, however, missions in 1986 and 1988 exceed the capability of Titan/Centaur for any combination of insertion engines, while missions in 1983, 1984, and 1989 are still viable with three engines but require increased propellant and tankage growth. Insertion into the circular orbit, e = 0, would require, for all years, performance capability greater than a Titan/Centaur launch system, or a space storable insertion system, along with much greater propellant load requirements.

The principal conclusion to be drawn at this point is the attractiveness of the 0.5 eccentricity orbit in terms of what can be achieved for a minimal growth in existing Viking class hardware. All launch year opportunities are viable and the nominal science payload can be achieved in each case with the flexibility preserved for providing the 20° apsidal shift capability within the insertion maneuver.

Orbiter Mission

Mapping orbits considered for all vehicle configurations are at polar orbit inclination. Some inclination offset would be desired to map the true Venus pole, but analyses discussed in Volume III have indicated that, for orbits within $\pm 15^{\circ}$ of polar, orbit lifetime and occultation characteristics are essentially the same. The simplifying polar inclination assumption is therefore made for all missions discussed here.

Orbit sizes which have been investigated in detail by both mission analysis and systems design correspond to eccentricities of 0. (circular), 0.3, and 0.5 with periapsis altitude at 400 km. The 0.5 eccentricity has become, however, our preferred design for all configurations. Orbit stability analysis for the Venus polar orbits, with solar perturbation effects assumed dominant, indicates that an eccentricity of about 0.6 is an effective upper limit for maintaining periapsis altitude within a reasonable band around 400 km. For an eccentricity of 0.5, with periapsis at latitudes of up to 35^{o}, periapsis altitude can be held to within $\pm$10 km of 400 km with two orbit trims of 5 m/sec each over the 243-day mission duration. From examination of orbit insertion requirements, assuming Viking class insertion propulsion in various combinations, the 0.5 eccentricity was also found to represent the smallest orbit size which preserved mission viability for all considered launch years of the 1980s.

The location of periapsis in latitude, and the orbital motion about periapsis associated with the latitude location, were discussed in the subsection, Orbit Insertion. To summarize, Configuration A and B require periapsis offset from the equator for polar coverage given their mapping true anomaly limits. Periapsis latitude must be 35^{o} (North or South) for the 0.5 orbit with mapping $\pm 55^{o}$ true anomaly, and 25^{o} (North or South) for the 0.3 orbit with mapping $\pm 65^{o}$ true anomaly. Where periapsis is located South, ascending orbit motion is specified about periapsis, and for Northern locations descending mode motion is specified. In the circular orbit case $\pm 90^{o}$ mapping is possible, and altitude is of course constant around the orbit at 400 km. For Configuration C with programmed variable side-look angle, $\pm 90^{o}$ mapping is achieved for all orbit sizes so that here an equatorial periapsis is desired in each case.

Given this description of the orbits considered by the study, their characteristics relating to mission and systems event timelines can be addressed. For systems design, maximum periods of Earth and Sun occultation have been treated for all orbit configurations. In Figures III-11, III-12, and III-13, pictorials of maximum occultation periods are shown with shadow entry and exit times denoted in hours from periapsis passage, for 0.5, 0.3, and 0. eccentricities with periapsis at the equator. The orbits are presented approximately to scale to better reflect occultation differences. These representations are appropriate to the C configuration. Figures III-14 and III-15 illustrate similar occultation characteristics but for the periapsis latitude offset configurations (A and B) where periapsis is located -35^{o} for e = 0.5 and -25^{o} for e = 0.3. These particular cases are shown for one launch/arrival date opportunity of the 1984 Type II mission but are, in general, representative of all mission years. The timing of the complete occultation history was found to vary up to 30 days from orbit insertion as mission year varied, but for all missions the same worst case occultation periods were encountered. Superimposed on these pictures is the standard mapping swath in true anomaly appropriate to each configuration.

A general mission event timeline is presented in Table III-1 for a 1984 Type II mission with a 0.5 eccentricity mapping orbit. For this case periapsis has been assumed to be at the -35^{o} latitude so that the timing for orbit trims can be included. The timeline extends from launch through the interplanetary cruise with midcourse corrections called out, and ends after 243 days in mapping orbit.

The ultimate result of the orbit design and radar/antenna systems studies is shown by the mapping coverage actually realized with the various configurations. Our current mapping cycle

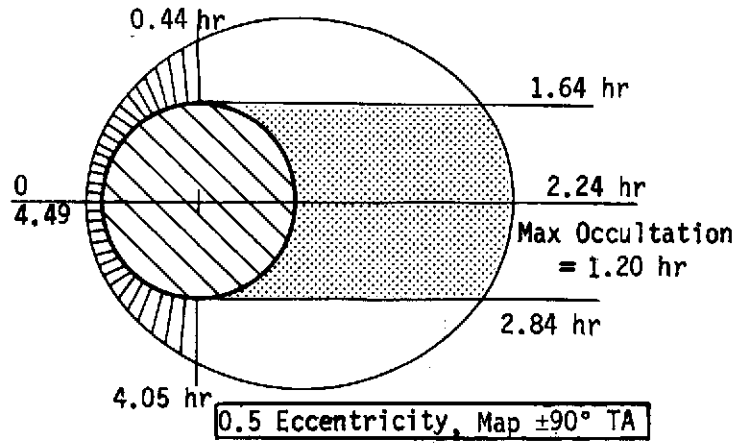

Figure III-11 Orbit Timeline

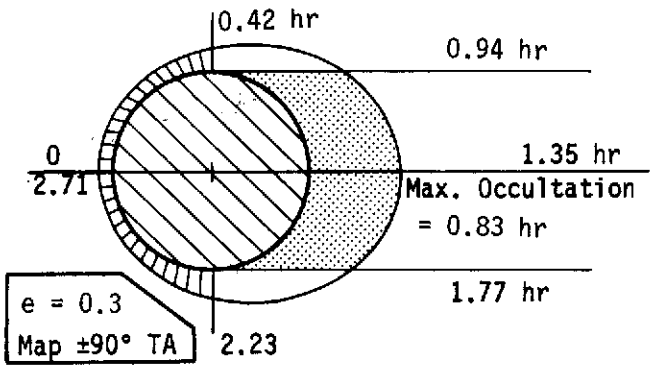

Figure III-12 Orbit Timeline

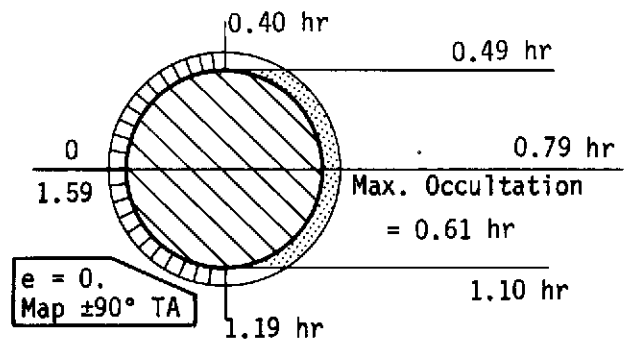

Figure III-13 Orbit Timeline

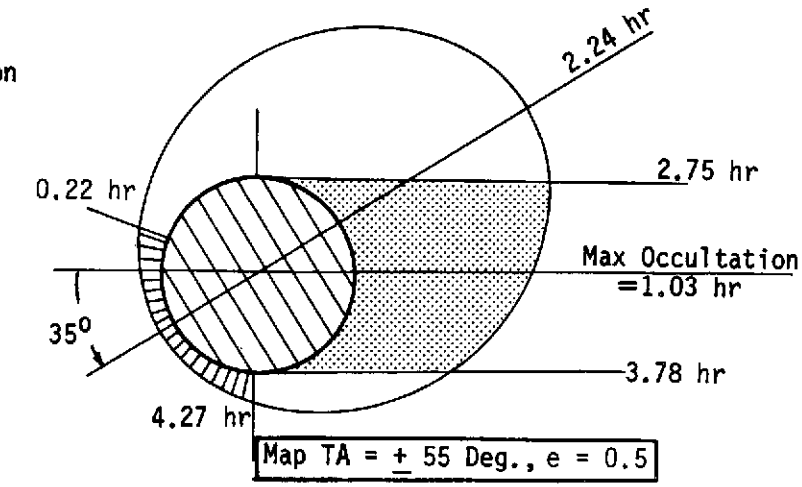

Figure III-14 Orbit Timeline

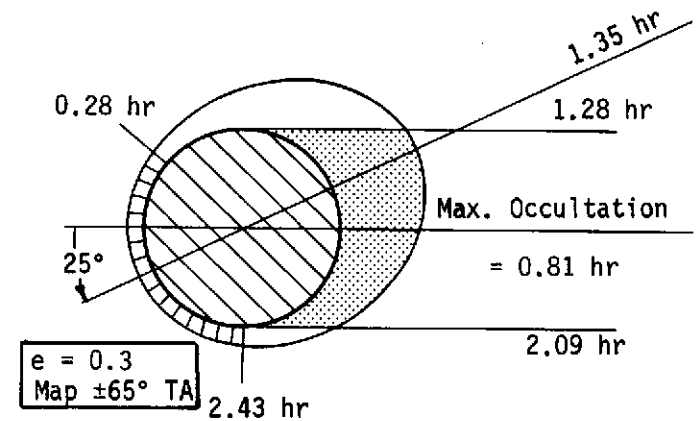

Figure III-15 Orbit Timeline

Table III-1 General Mission Timeline for 1984 Type II
(e = 0.5, Periapsis Latitude = -35°)

	Mission Day	Orbiter Day	Earth Range (AU)	Sun Range (AU)	Event
Cruise	0		0.00	0.99	Launch 11-30-1984
	5				M/C #1, ΔV = 28.5 m/sec
	40		0.08	1.00	
	80		0.13	0.94	
	120		0.17	0.83	
	160		0.41	0.74	
	165				M/C #2, ΔV = 8.0 m/sec
	175		0.55	0.73	Venus Encounter, Earth Occultation, 5-24-1985
Orbiter	175	0			Orbit Insertion, V = 2000 m/sec
	189	14			Sun Occultation at Periapsis
	215	40	0.87	0.73	
	225	50			Orbit Trim, ΔV = 5 m/sec
	229	54			End Earth Occultation at Periapsis
	255	80	1.16	0.72	
	273	98			End Sun Occultation at Periapsis
	295	120	1.40	0.72	
	305	130			Begin Earth Occultation near Apoapsis
	322	147	1.53	0.72	Maximum Earth Occultation = 1.02 Hours
	329	154			Begin Sun Occultation near Apoapsis
	335	160	1.58	0.72	
	341	166			End Earth Occultation near Apoapsis
					Orbit Trim, ΔV = 5 m/sec
	342	167	1.60	0.72	Maximum Sun Occultation = 1.03 Hours
	357	182			End Sun Occultation near Apoapsis
	375	200	1.68	0.72	
	413	238			Begin Earth and Sun Occultation at Periapsis
	418	243	1.71	0.73	End of Mission, 1-22-1986

philosophy has set mapping orbit frequency at once every 5 orbits for the circular, every other orbit for e = 0.3, and every orbit for e = 0.5. Since the 0.5 orbit has generally been accepted as the reference design, particular aspects of the coverage will be illustrated for that case. Figure III-16 presents on a global picture of Venus the nature of the dual beamwidth mapping swath, centered here at a latitude of 35°. Side-look angle is constant over all true anomalies at a value of 30°. The wide beam (3.18°) is used for true anomalies between -40° and +21° which corresponds in this case to latitudes between -5° and +56° (ascending motion). For other true anomalies farther removed from periapsis the narrow beam (1.59°) is turned on. Mapping occurs over ±55° true anomaly - theoretically from -20° to +90° in latitude. In the figure individual swaths are shown spaced at 10 orbit intervals for clarity, consistent with the above description. The orbit trace corresponding to the first swath on the left is also shown, with periapsis location indicated. As can be observed from the swath ends, the true planet pole is not imaged with an exact 90° inclination. For Configurations A and B, the required inclination offset to achieve true pole coverage would be 8.4°.

Figure III-17 illustrates the global coverage picture for the C configuration mapping strategy, with mapping ±90° true anomaly. Side-look angle is variable in this case, ranging from 50° at the equator to 12° near the poles, as shown by Figure III-18. Beamwidth is a fixed 2.13°. Again with the exact 90° inclination orbit, coverage of the true pole is not achieved, and the inclination offset required to gain this coverage is 7.4° for Configuration C. Individual swaths are shown for 10 orbit intervals, and the orbit trace associated with the first swath is indicated with periapsis located on the equator. The swath advances with time

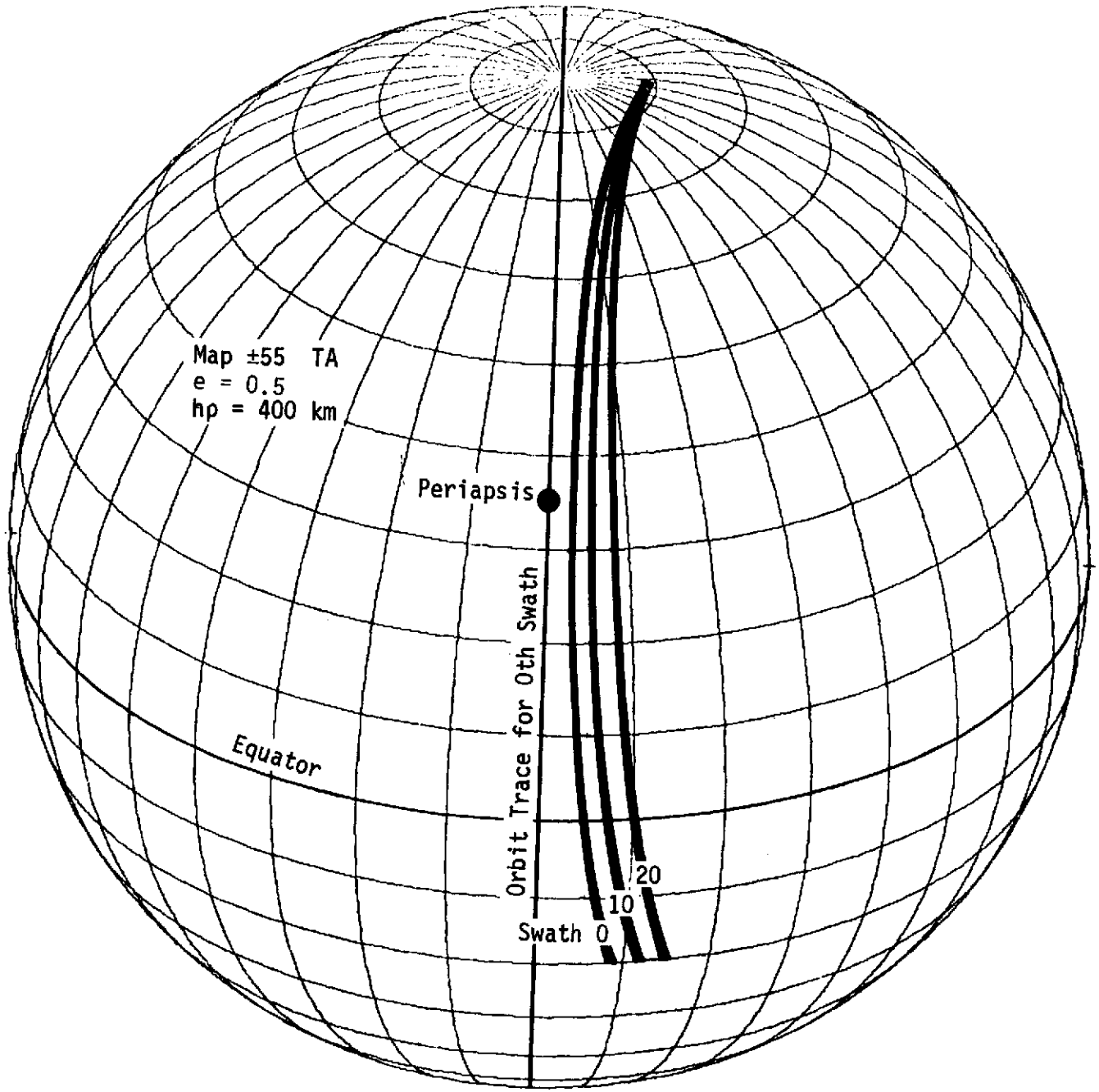

Figure III-16 Typical Dual-Beamwidth Coverage, 0.5 Eccentricity

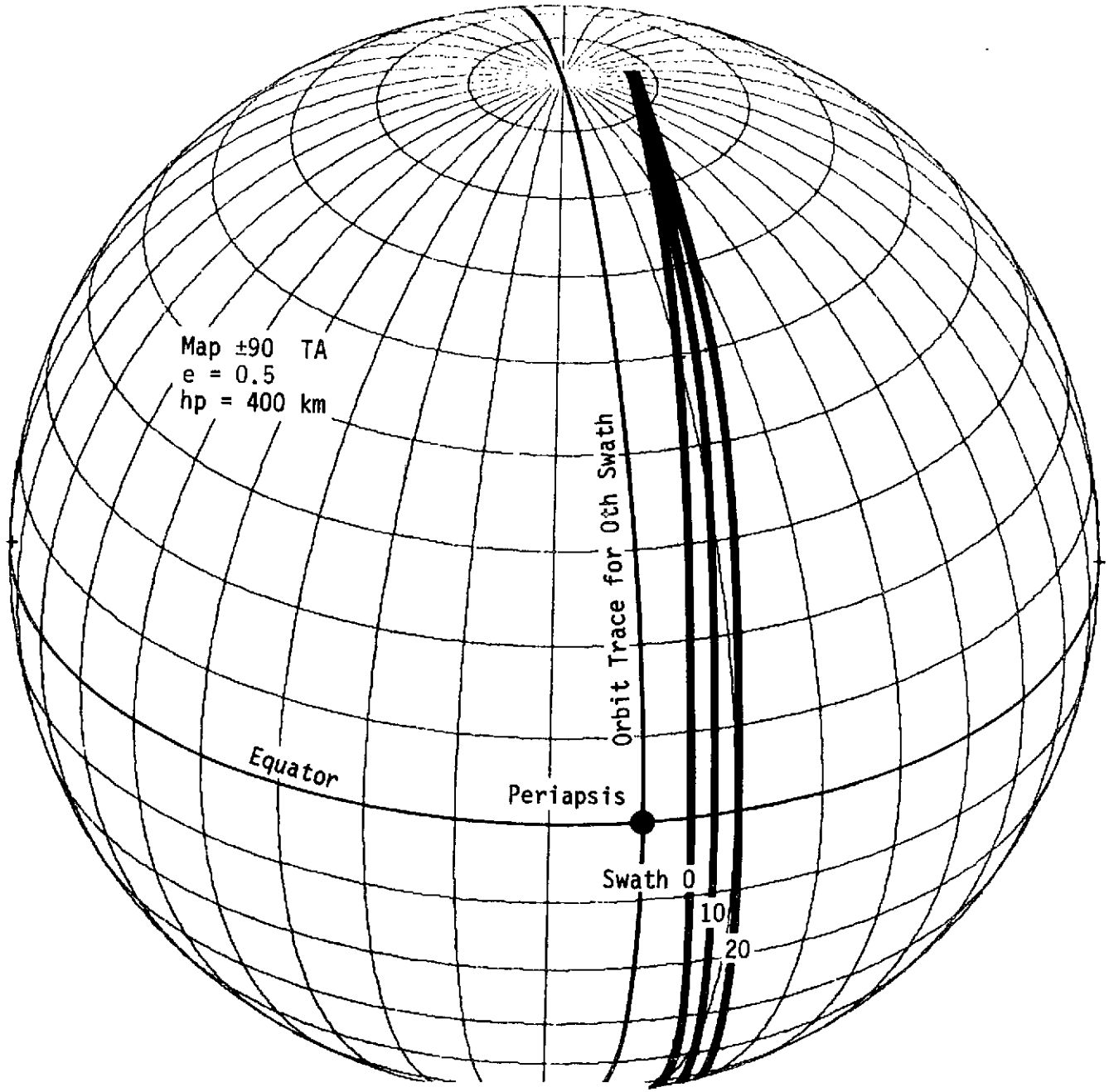

Figure III-17 Typical Variable Side-Look Coverage, 0.5 Eccentricity

from west to east as the planet's reverse spin causes the inertial orbit to progress in that direction with respect to surface points. (Directions noted are consistent with the Venus orbit plane system, where north is in the direction of north ecliptic - see Volume III.)

Swath overlap gained by these mapping techniques is illustrated by Figure III-19 and III-20. Minimum overlap for Configurations A and B is 20%, where overlap has been computed as:

$$\% \text{ OVERLAP} = 100 * \frac{\text{SWATH WIDTH - ORBIT SPACING}}{\text{SWATH WIDTH}}$$

Overlap approaches 100% at the polar region where, as can be seen in Figure III-16, there is much coverage redundancy.
For Configuration A the minimum overlap is about 30% at the equator, and again overlap approaches 100% over the polar regions where for this case, too, much redundancy exists in that area.

A comparison of the radar swaths for both techniques shows the obvious superiority of Configuration C in terms of more complete and balanced treatment of both hemispheres. Due to this greater coverage capability, the variable side-look mode has become our preferred design.

For much of the surface coverage/radar design analysis of this study, the radar beam orientation has been assumed to be a measured angular distance from the radius vector, perpendicular to the orbit plane. That distance is defined by the side-look angle. An alternative orientation for radar mapping is alignment of the radar beam in a plane perpendicular to the orbit plane as before, but containing the zero-doppler line. Side-look angle is then measured from the zero-doppler line to the center of the radar beam. The zero doppler line is simply the line in the orbit plane which is perpendicular to the velocity vector and intersects the planet surface. Both geometrical configurations are shown in Figure III-21.

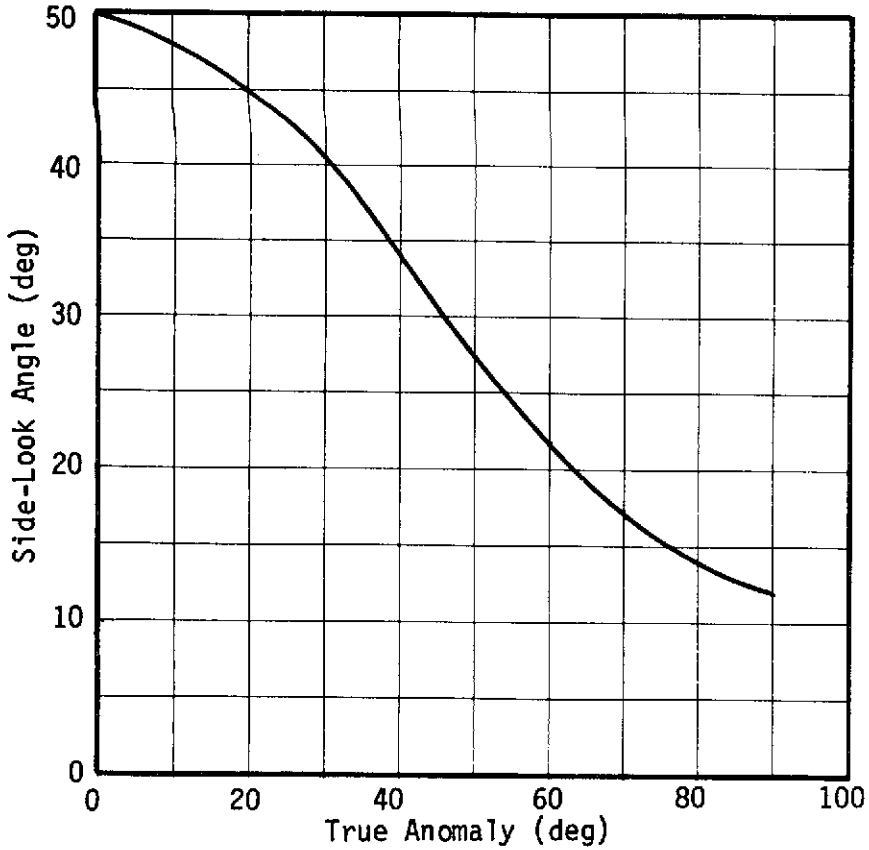

Figure III-18 Variable Side-Look Angle History, 0.5 Eccentricity

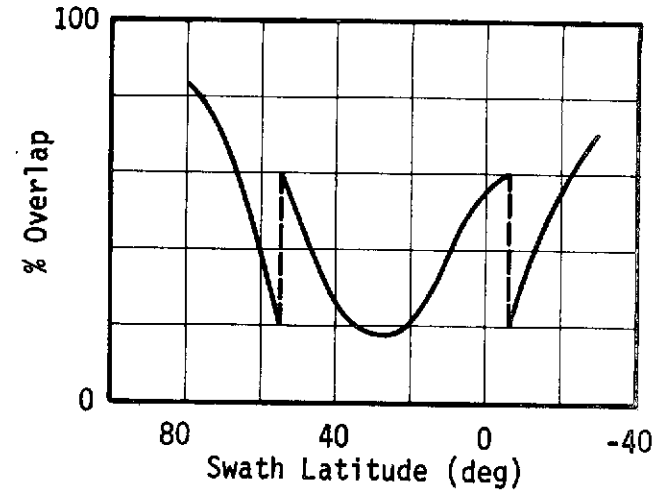

Figure III-19 Swath Overlap for Dual Beamwidth, 0.5 Eccentricity

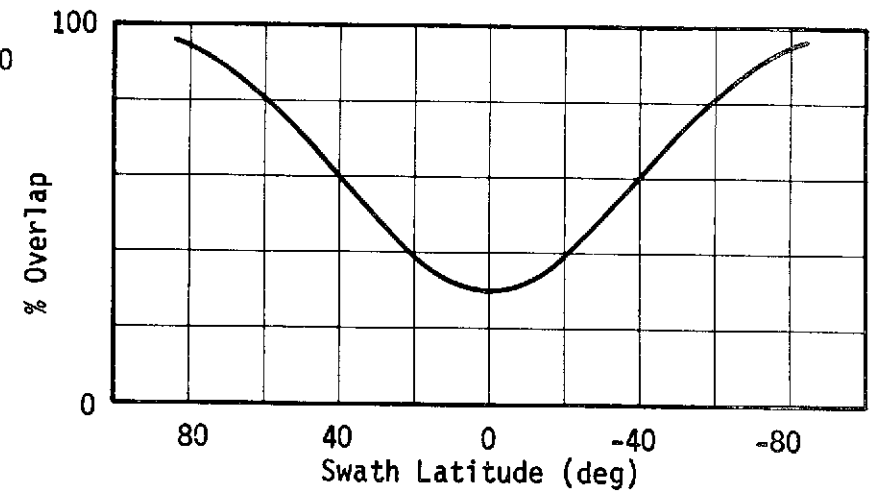

Figure III-20 Swath Overlap for Variable Side-Look, 0.5 Eccentricity

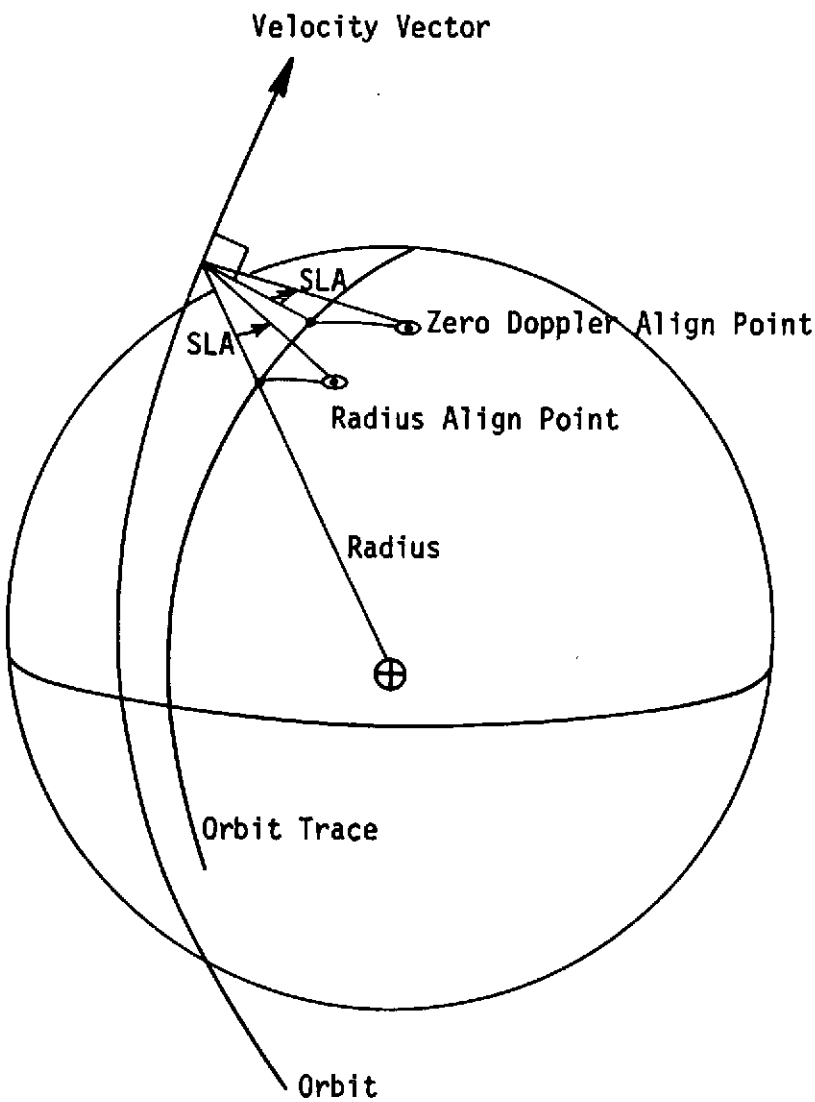

Figure III-21 Radius Align and Zero-Doppler Align Geometries

The effect of considering a zero-doppler alignment as opposed to a radius alignment is somewhat different for the dual beamwidth and variable side-look configurations. For both cases, the zero-doppler align trails radius align at true anomalies before periapsis, and leads after periapsis. The implication here is that a fixed latitude spread around periapsis can be mapped with a smaller spread of true anomaly, or conversely, assuming a fixed true anomaly spread, a wider latitude range can be achieved. This assumes that the increased range for the zero-doppler align does not constrain the problem. Quantitative differences between the two alignments are presented in Table III-2 as true anomaly is varied for Configurations A and C radar mapping. For Configuration A, mapping $\pm 55°$ true anomaly in the radius align mode, the same latitude range could be gained by mapping $\pm 50°$ in the zero-doppler align situation. With Configuration C nominally mapping $\pm 90°$ true anomaly with periapsis on the equator, zero-doppler align gains the same coverage of latitudes mapping only $\pm 80°$ true anomaly. In addition, the radar range at $\pm 80°$ true anomaly with zero-doppler align is roughly the same as with radius align at $\pm 90°$.

In summary, considering zero-doppler radar alignment will tend to either 1) provide greater latitude coverage capability, or 2) provide a longer portion of the orbit timeline for use by systems other than radar mapping. Of course radar system implications vary the significance of the results and are discussed in Section IV.

CONCLUSIONS AND CONCERNS

The principal conclusion which has evolved from the mission analysis/radar system interaction is that Venus surface mapping objectives can be achieved from an eccentric orbit with current state-of-the-art propulsion technology. An orbit eccentricity

Table III-2 Radius and Zero Doppler Alignments for Configurations A and C

True Anomaly (deg)	S/C Latitude (deg)	Swath Latitude (deg)	
		Radius Align	Zero-Doppler Align
Configuration A, Dual Beamwidth, For 0.5 Eccentricity			
-55	-90	-81.58	-79.81
-50	-85	-81.21	-82.25
-45	-80	-78.25	-80.36
-15	-50	-49.93	-50.32
0	-35	-39.97	-34.97
35	0	0.00	1.61
55	20	19.78	24.45
Configuration C, Variable Side-Look, For 0.5 Eccentricity			
-90	-90	-82.58	-68.21
-80	-80	-77.90	-81.30
-70	-70	-69.00	-76.81
-60	-60	-59.34	-64.87
-20	-20	-19.91	-20.53
0	0	0.00	0.00
20	20	19.91	20.53
60	60	59.34	64.87
70	70	69.00	76.81
80	80	77.90	81.30
90	90	82.58	68.21

of 0.5 is suggested for the mapping orbit, with a periapsis altitude of 400 km. This orbit size, in an orientation of polar to near-polar inclination, is sufficiently stable over the 250 day mission life for minimal altitude maintenance requirements (orbit trims require less than 10 m/sec V load) and allows orbit insertion with a 3-engine Viking class propulsion system for all mission years considered. For the variable side-look radar configuration, mapping can be gained over $\pm 90°$ true anomaly, and periapsis should therefore be positioned over the equator. This periapsis location can be achieved for all years with the allocated 20° apsidal shift capability at orbit insertion.

Concerns which have been identified by the study involve the problem of long orbit insertion burns at fixed attitude and the large errors in Venus encounter radius for the navigation assumptions considered. Finite burn loss has been brought to manageable levels by employment of a multiple-engine Viking insertion propulsion system with increased thrust level. Other techniques should be investigated in any subsequent study and these include 1) an optionally programmed attitude history for the insertion maneuver, and 2) a phased insertion sequence with multiple impulses to one or more intermediate transfer orbits. Errors in Venus encounter radius are the result of pessimistic navigation assumptions considered in the midcourse analysis. These errors could be treated by either 1) a biased aimpoint scheme with insertion into an intermediate orbit of higher periapsis altitude, followed by an orbit trim to gain the desired mapping orbit periapsis of 400 km, or 2) inclusion of charged particle calibration in the navigation process, which should halve encounter errors but requires X-band and S-band capability onboard the spacecraft. The effect of each technique on increased mission complexity and error reduction capacity must be given a quantitative assessment. No other areas of concern have been disclosed which have crucial, negative impact to the Venus radar mapper mission feasibility.

IV. RADAR AND ANTENNA SYSTEMS

INTRODUCTION

This section will discuss the radar and antenna subsystem design for the selected configurations: Configuration A which is considered an attractive alternate; Configuration B which is the least attractive and will not be discussed as thoroughly as the others; and Configuration C which is the preferred configuration.

Early in this study it was recognized that there are two distinct classes of radar and communications subsystems, corresponding to two schemes for mapping the surface and transmitting the mapping data to Earth. One of these schemes involves time-sharing the same antenna for mapping and communication, while the other scheme employs separate antennas. These schemes are referred to as the shared antenna configuration and the dedicated antenna configuration, respectively. The twenty-six original designs which are discussed in Volume III (Section VII: Preliminary Evaluation of Compatible Groupings) are variations of these basic configurations. Configuration A is a shared antenna design, while Configurations B and C are dedicated antenna designs.

SYSTEM DESCRIPTIONS

Configuration A

Configuration A is an attractive design as it uses the same antenna to do the mapping and communicating. This is a desirable characteristic in terms of needing only one antenna, but this design is not efficient in terms of getting the data to Earth. Time is needed between the phases to reacquire the new targets.

The Earth must be acquired at the end of the mapping phase, and the antenna must be pointed to the mapping orientation at the beginning of the mapping phase. Mapping and communications are mutually exclusive and the antenna must be designed for both frequencies. For this reason the antenna design cannot be optimum for both functions. The decreased utilization and mutually exclusive use of the same antenna makes this configuration less attractive than Configuration C because the Venus mapping mission is usually limited by the data that can be sent to the Earth. Even so, this configuration is considered an attractive design and can do the mission in special situations. In fact, a similar design was suggested by JPL (Ref. IV-1) as the preferred design to map Venus from circular orbits.

Configuration A looks similar to the Viking Orbiter and is discussed in Section VI. In fact, a modified Viking Orbiter will be used in this study to map Venus from elliptical orbits. The antenna gimbal is mounted on one side of the body and a thermo-radiator on the other side. The antenna has two gimbals (one for azimuth pointing and one for elevation pointing) and has a fixed side look angle of 30 degrees built into the arm. A dual beamwidth antenna is utilized with the constant side look angle, but a variable side look angle can be used if a third gimbal and an antenna control system are added. The spacecraft (solar array) is always pointed toward the Sun, which is sensed by the existing Sun sensor system that is relocated on the solar panels. The antenna azimuth arm is controlled to be perpendicular to the spacecraft orbital plane during the mapping phase. The elevation gimbal command is a fixed command as a function of the orbit the spacecraft is in. These commands can be calculated by Earth based computers and transmitted to the spacecraft to be stored in control computer as a function of the orbit. The elevation gimbal is controlled by a clutterlock system in an antenna pointing system. The clutterlock system

generally points the antenna boresight along the zero doppler line. The clutterlock system is described in a later section in detail.

If the dual-beamwidth antenna is used, the antenna subsystem must be switched to a different beamwidth antenna when needed. The antenna probably would be switched by an altitude discrete from the control computer as sensed by the radar altimeter.

At the end of the mapping phase, the antenna is pointed toward the Earth using fixed gimbal commands relative to the body oriented inertial reference system. At the end of the communication phase, the antenna is pointed to the attitude needed at the start of the mapping phase. The spacecraft inertial reference system will be able to point the antenna toward the zero doppler line or other orientation well within the main lobe of the antenna pattern, so no beam stepping system will be needed. The clutterlock system will acquire the zero doppler line within a minute. This short zero doppler acquisition time is achieved because the antenna control system has a very accurate pointing capability. A total acquisition time of 18 minutes is allotted for Earth and zero doppler acquisitions.

The suggested radar and antenna subsystem design specifications for the shared antenna configuration (Configuration A) is shown in Table IV-1. A spacecraft using a constant side look angle of 30 degrees and an S-band (λ = 10 cm) radar operating frequency is assumed for this subsystem design. The 30 degree side look angle is optimum in terms of the power required to get the required resolution. A reflector type antenna is used to minimize solar occultation of the solar panel and not be dependent on technology predictions. Swath widths to give at least 20 percent overlap at periapsis are suggested. A transmitted pulse width of 33 μsec is used to give 100 m

Table IV-1 Suggested Radar and Antenna Subsystem Design Specifications (Shared Antenna Configuration)

PARAMETER	VALUE		
Eccentricity	e = 0.0	e = 0.3	e = 0.5
Mapping Strategy	N = 5	N = 2	N = 1
Mapping Coverage	TA = $\pm 90^{o}$	TA = $\pm 65^{o}$	TA = $\pm 55^{o}$
Mapping & Communication Time	7.93 hrs	5.40 hrs	4.4 hrs
Resolution	$r_a = r_r$ = 100m	$r_a = r_r$ = 100m	$r_a = r_r$ = 100m
Antenna Type	Reflector	Reflector	Reflector
Azimuth Dimension	4.0 m	4.57 m	3.66 m
Range Dimension	1.0 m	2.90 m	3.5 m
Beamwidth	Single	Multiple	Multiple
Wavelength (λ)	10 cm (S-Band)	10 cm (S-Band)	10 cm (S-Band)
Side Look Angle (θ)	0.53 (30^{o})	0.53 rad	0.53 rad
PRF	4000 PPS	3750 PPS	5000 PPS
Swath Width (W)	65 km	44 km	36 km
Overlap (%)	20%	20%	20%
Transmitted Pulse Width	33 μsec	33 μsec	33 μsec
Radar Altimeter	Yes	Yes	Yes
Polarization	Single	Single	Single
Average Trans Power	28W	105W	166W
Peak Radiated Power	209W	850W	1050W
Input Power Requirement	183W	415W	600W
Subsystem Weight (1980 est)	26.5 kg	54.9 kg	58.3 kg
Volume (Electronics)	0.016 m^3	0.024 m^3	0.026 m^3
Pulse Compression Ratio	100	100	100

resolution at periapsis with a range compression ratio of 100. A radar altimeter is considered an essential instrument to have on-board to give altitude discretes, altitude profiling and to augment the science these design specifications are for a minimum cost design; additional capabilities will be considered accessory items that will add additional cost.

The subsystem weight was calculated for a TWT transmitter system from the weight equations described in the PIRS report (Ref. IV-2) based on the functional block diagram shown in Figure IV-1.

The following weight equations were used for each component in the TWT system:

$$W_T = \text{TWT weight} = 0.544\ (\lambda/0.3)^{0.4} P^{0.6}\ \text{kg} \qquad \text{(IV-1)}$$

$$W_{HV} = \text{High Voltage Supply Weight} = 4.54 + 0.454\ (P/0.4)^{0.5}\ (\lambda/0.3)^{-0.57}\ \text{kg} \qquad \text{(IV-2)}$$

$$W_M = \text{Modulator Weight} = 3.18\ \text{kg} \qquad \text{(IV-3)}$$

$$W_E = \text{Energy Storage Capacitor Weight} = (34.47/PRF)(P/0.4)(\lambda/0.3)^{-0.57}\ \text{kg} \qquad \text{(IV-4)}$$

$$W_F = \text{Filament Current Supply Weight} = 1.36\ \text{kg} \qquad \text{(IV-5)}$$

The PIRS report states that a TWT or solid state transmitters can be used for frequencies greater than 1 GHz. If the power is greater than $(\lambda/9) \times 10^4$ watts, a TWT is required on the basis of today's technology. At S-band, a TWT transmitter would be needed if the average RF power is greater than 10 watts. Since all of the cases con- estimate is based on 2.44 kg/m^2 (0.5 lbs/ft^2) for a deployable antenna, where typical densities are from 0.3 to 0.5 pounds per sq ft of aperture subsystems are discussed in detail in Volume III. The antenna weight is based on 2.44 kgm/m^2 (0.5 lbs/ft^2) for a deployable antenna, where typical densities are from 0.3 to 0.5 pounds per sq ft of aperture area of the antenna. A packaging density of 880 kg/m^3 (55 lb/ft3) is used for the radar subsystem electronics.

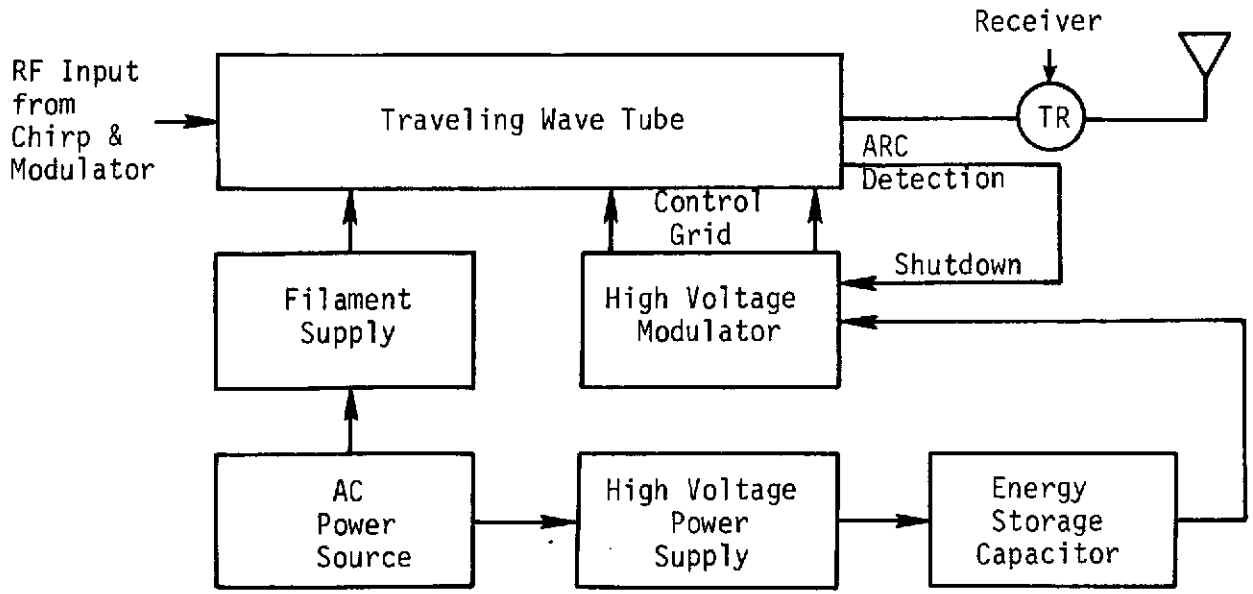

Figure IV-1 Functional Block Diagram of a Typical TWT Transmitter

Based on simple geometry and coverage analyses (Vol III Section IV) a spacecraft in a circular orbit can map every fifth orbit to get full planet coverage. A single beamwidth antenna with the dimensions of 1 x 4 meters and a constant side look angle of 30 degrees can be used for this orbit. The radar subsystem design is simplified for the circular orbit because the upper and lower PRF constraints are constant throughout the phase.

Mapping to $\pm 65^{o}$ true anomaly is achieved when the spacecraft is assumed to be in a 0.3 orbit and mapping every other orbit. A dual beamwidth antenna is used with the dimensions of 2.9 x 4.6 m. This orbit and mapping strategy yields greater surface mapping and less power than an 0.5 orbit. Range ambiguities limit the planet coverage that can be obtained (see Vol III Section IV).

The mapping strategy of using an 0.5 orbit and mapping every orbit is favored because a Viking Orbiter spacecraft can be used with the present propulsion capabilities. A dual beamwidth antenna (3.5 x 3.66 m) is needed to achieve a mapping capability to $\pm 55^{o}$ true anomaly. Input power of 600 watts to the radar subsystem is required for this mission. The input power is calculated by assuming that the transmitter is 33 percent efficient and that the other components in the radar subsystem require 100 watts.

Configuration B

Configuration B is the least attractive of three selected configurations and utilizes separate (dedicated) antennas. This design controls the vehicle to point the body mounted radar antenna in the zero doppler direction by maneuvering the vehicle during the mapping phase. The spacecraft power is obtained principally from

batteries during the mapping phase. During the transition from the mapping phase to the communication phase, the vehicle must acquire the Sun and Canopus by maneuvering the vehicle to the Sun pointing orientation. The two degrees of freedom communication antenna must then acquire the Earth and start transmitting data. The communications antenna is pointed by fixed command, which is a function of the orbit it is in. These commands are calculated on the ground and transmitted to the spacecraft as a batch of data and used later. About 0.45 hour would be needed for this phase to acquire the Sun and Canopus. An equal amount of time would be needed to go back to the zero doppler orientation during the transition from the communication phase to the mapping phase. During the communication phase the vehicle is controlled to point at the Sun while its articulated communication antenna points at Earth and transmits the radar data to Earth.

Since this configuration is the least attractive this design will not be discussed in detail. The radar and antenna subsystem design specifications are essentially the same as the shared antenna configuration shown in Table IV-1 except for a few differences that will be discussed below. A planar array (PA) is used because it is easier to package during the launch phase. A vertebra-beam-ground-plane type of planar array is used, which is shown in the technology prediction section of this report. A two gimbal, 3-meter diameter parabolic antenna is used to transmit the data to Earth. The weight of the antenna subsystem would be slightly heavier than Configuration A, but the total weight of the radar and antenna subsystem for both configurations would be about the same. Planar array designs that utilize continuous-vertebra-beam-slab, vertebra-beam-ground-plane, or self-forming sandwich designs can be used. These planar arrays are described in the antenna technology prediction section of Volume III. As will be shown later, this configuration

is the least attractive because the existing VO attitude control system (ACS) cannot be modified to do the mission using this configuration.

Configuration C

Configuration C integrates as many of the desired subsystem characteristics as possible and as expected turns out to be the preferred configuration. The flexibility and additional capability of this design at comparable cost and complexity is the reason Configuration C is the preferred configuration. The variable side look angle is also integrated into this design as a desired characteristic to give full planet coverage at some additional cost.

Configuration C has separate antennas, so the vehicle can communicate at all times except when the Earth is occulted. The azimuth gimbal of the communication antenna needs 90° of travel. The elevation gimbal on this antenna must point only a few degrees out of the ecliptic ($\pm 5°$), but must flip over 180° once per Venus year when the spacecraft is maneuvered to map on the other side of the spacecraft. Articulated solar panels are needed so that the spacecraft can be inertially pointed perpendicular to the orbital plane. The operational aspects of this configuration when mapping Venus will be discussed in the spacecraft system section.

A 4.1 by 3.24 meter radar antenna is used with an azimuth capability of 360° for both the variable and constant side look angle schemes. An additional gimbal is needed when a variable side look angle is used and is shown as the outer gimbal in the configuration drawing of Section VI. The antenna subsystem shown is for a variable side look angle.

The suggested radar and antenna subsystem design specifications for a variable side look angle is shown in Table IV-2. The specifications for the circular orbit are the same as those used for the other two configurations, since a constant side look angle is needed.

Table IV-2 Suggested Radar and Antenna Subsystem Design Specifications (Specialized Spacecraft Design)

PARAMETER	VALUE		
Eccentricity	e = 0.0	e = 0.3	e = 0.5
Mapping Strategy	N = 5	N = 2	N = 1
Mapping Coverage	TA = $\pm$ 90°	TA = $\pm$ 90°	TA = $\pm$ 90°
Mapping & Communication Time	7.93	5.40	4.4
Resolution	$r_a = r_r$ = 100 m	$r_a = r_r$ = 100 m (60°)	$r_a = r_r$ = 100 m (60°)
Antenna Type	Reflector	Reflector	Reflector
Azimuth Dimension	4.0	3.66	4.1 m
Range Dimension	1.0	2.65 m	3.24 m
Beamwidth	Single	Single	Single
Wavelength (λ)	10 cm (S-band)	10 cm (S-band)	10 cm (S-band)
Side Look Angle (θ)	0.53 (30°)	$12 \leq \theta \leq 50°$ (Var.)	$12 \leq \theta \leq 50°$ (Var.)
PRF	4000 PPS	4500 PPS	4500 PPS
Swath Width (W)	65 km	44 km	36 km
Overlap (%)	20%	20%	20%
Transmitted Pulsewidth	33μ sec	24μ sec	24μ sec
Radar Altimeter	Yes	Yes	Yes
Polarization	Single	Single	Single
Average Transmitter Power	28 W	35 W	78W
Peak Radiated Power	209 W	392 W	750 W
Input Power Requirement	183 W	206 W	333 W
Subsystem Weight (1980 est.)	26.5 kg	36.6 kg	41.0 kg
Volume (Electronics)	0.016 m^3	0.021 m^3	0.026 m^3
Pulse Compression Ratio	100	72	72

The only advantages of the 0.3 orbit over the 0.5 orbit are that it requires a smaller antenna and less power. However, the 0.3 eccentricity also requires a larger propulsion capability than available on the VO spacecraft. Because of the propulsion problem, the 0.5 orbit is favored since the spacecraft has the power available.

The spacecraft uses an orbit with an eccentricity of 0.5 and maps every orbit to get full planet coverage. A transmitted pulse length of 24μsec is used to get a 100 meter resolution at 60° true anomaly (periapsis at the equator). The resolution will be degraded to about 200 m at the poles and a resolution of 48 m will be realized at periapsis. A single beamwidth reflector type antenna with a mesh type of reflector surface is suggested, so the solar panels will have minimum shadowing. A variable side look angle is used to give complete surface mapping and to reduce the power required. The spacecraft must supply 333 watts to power the radar subsystem.

Table IV-3 shows the microwave gains and losses that were used in the radar range equation to calculate the maximum power required. The atmospheric losses were calculated from an equation used in the PIRS (Ref. IV-2) report and is shown below:

$$L_A = \frac{630}{\lambda^2} = 0.7\ f^2 \text{ db} \qquad \text{(IV-6)}$$

where λ = wavelength (cm)

f = frequency (ghz)

System losses of 3.0 db and an antenna illumination efficiency of 0.85 were used, which were the same values as used in the SSD (Ref. IV-3) report. The normalized radar cross section, σ_o, is for a polarized radar as determined by Muhleman (Ref. IV-4). The total losses and signal-to-noise ratio of Table IV-3 compare within one db to the S/N requirement used in the PIRS report. This S/N requirement actually includes all of the losses shown separately in Table IV-3.

Table IV-3 Power Requirements (λ = 10 cm, e = 0.5, N=1, and Mapping $\pm 90^{o}$)

Parameter	Contribution	Remarks $P = \left(16\pi/C\right)\left(\sin\psi/\cos^3\theta\right)\left(H^3\lambda VKTLB(S/N)/A^2\sigma_0\right)$
$16\pi/C$	- 67.7	C = Speed of Light
$\sin\psi/\cos^3\theta$	- 6.5	$12 \leq \psi \leq 50^{o}$ (Variable)
H^3	+196.8	H = 3625 km (Spacecraft Altitude)
λ	- 10.0	S-Band (λ = 10 cm)
V	+ 37.6	5795 m/sec (Spacecraft Velocity)
KT	-200.2	$T = 700^{o}K$
L	+ 11.7	Atmos = 7.3. Sys = 3.0. Ant Eff = 0.85
B	+ 66.4	= 24 μsec (100 m at 60^{o}) (Bandwidth)
(S/N)	+ 10.0	
A^2	- 22.4	D_r = 3.24 m, D_a = 4.1 m, A = 13.3 m^2
σ_0	+ 3.2	$\sigma_0 = 0.0133\ \cos\theta/(\sin\theta+0.1\ \cos\theta)^3$-Polarized
Total	+ 18.9 db	P_{AV} = 77.7 Watts P_{IN} = 333 Watts

As can be seen by Table IV-2 and IV-3, a spacecraft using a variable side look angle can map with reasonable power to an altitude of 3600 km. A dual beamwidth antenna using a constant side look angle mapping to 1500 km required about twice as much power (Table IV-1). There are some questions as to whether some additional power would be needed for the variable side look case since the spacecraft is operating with a small incidence angle at the mapping extremities where the radar return has a large specular component. A higher power capability may be needed to compensate for the smaller side look angles.

Antenna Subsystem Design

Many things must be considered to determine the actual antenna designs that will be needed. Generally the cheapest and the most reliable design would be the best selection if one could get both the desired characteristics and provided adequate side lobe level. In the next decade the planar array probably would be the best selection in terms of flexibility and reliability, but with today's antenna technology, a reflector type antenna would be an adequate selection to do the Venus mapping mission and would avoid the technological risk of new antenna development.

Dual Beamwidth Antenna Designs - The dual beamwidth antenna can be implemented with a reflector type or a planar array antenna. The planar array would be sized for the narrow beamwidth, where extra elements would be switched out to narrow the antenna dimensions and increase beamwidth. Today, because of the weight and cost penalties of the antenna subsystem, a planar array would not be used unless beam steering or side lobe control is required. If a reflector type antenna were used to implement the dual beamwidth aperture, the narrow beamwidth would size the dimensions of the reflector that would be needed. A single feed would probably be

needed to implement the narrow beamwidth since the antenna is almost a full parabolic surface. When the wide beamwidth is implemented, a set of feeds (probably two) would be needed to form a line feed that would illuminate the truncated parabolic antenna. There is also the possibility that a shaped single feed could illuminate the surface. A parabolic-cylindrical reflector type antenna could also be used, but multiple line feeds would be needed and it would be a more costly design. The feeds must be designed to illuminate the surface needed. Other types of reflector-type antennas could be used provided they could be designed to meet the mapping specifications. In a more advanced study, an optimum antenna design would be determined to meet the ambiguity requirements.

Deployable vs Fixed Antenna Designs - There probably would not be any reason to use deployable antennas unless the antenna cannot be packaged within the shroud of the launch vehicle. Deployable antennas are not only less reliable but also illumination degradations must be assumed because these antennas are only an approximation of a parabolic surface.

At present, deployable reflector-type antenna technology is sufficiently developed to do the Venus mapping mission. Deployable planar array technology is in its infancy and probably not adequate to do the mission today. The deployable planar array technology should advance considerably in the next decade, and antennas of this type probably could be used for a 1981 mission.

Fixed planar array and reflector-type antenna technology is adequate today to do the Venus mapping mission, although the planar array would be a very heavy and costly subsystem. The advancement in the state-of-the-art of planar arrays would be to reduce weight, increase efficiency, and increase power transmission capability. The assessment of the state-of-the-art advancement in the next decade is discussed in Volume III of this report.

Phased Arrays vs Reflector Type Antennas - The phased arrays would not be used today unless side lobe control or beam steering is needed as they are too heavy and are too expensive to develop. It is felt that the well designed reflector type antenna is adequate to do the Venus mapping mission because only a portion of the receiver bandwidth is used where a maximum presumming to 30 m is used. An ambiguity level of -20 db is considered adequate and unambiguous for the Venus mapping mission. In the future, planar or phased arrays may be competitive with reflector type antennas in terms of weight and cost. Our assessment of future technology discussed in Volume III predicts that the planar array will be a favorable antenna design to be used in the next decade.

Other Antenna Types - Another type of antenna that can be used is an inflatable antenna. Deployable parabolic or planar arrays can be implemented by using inflatable structures. The state-of-the-art of inflatable antennas is in its infancy and would have to be developed for the particular mission. Inflatable antennas at S-band would be feasible, but would not be rigid enough to be used at X-band. These designs would be costly to develop as they would have to be developed for the Venus mapping mission. Inflatable antennas are generally used where very large antennas are needed. Since we try to use small articulated antennas inflatable type antennas were not considered in our final design.

Antenna Gimbal Designs - The antenna gimbals would probably need digital encoders to sense gimbal position that would have resolution capability good enough to point the radar antenna. Encoders with at least 10-bit accuracy and probably 12-bit accuracy (per 360 degrees) would be needed to point the radar antenna. A simple antenna control system would be needed to control the antenna and is discussed in the attitude control section.

One problem with Configuration A where the mapping and communications functions are shared is that the antenna must be designed for two frequencies. Two frequencies (multi-channels) have to be "piped" through the rotary joints. Multi-frequency joints create tough design problems particularly when multirevolutional rotary joints are used. These types of rotary joints would be expensive and some future study should address the design of these joints. Configuration C has simple one frequency rotary joints.

The radar altimeter output would not have to be channeled through the rotary joints as the electronics can be placed on the last gimbal so that only the supply voltages have to be supplied to the electronics by means of slip rings or other means. Since the radar altimeter (RA) electronics weighs only about 10 pounds and can be mounted at the center of the antenna, the RA will not change the moment of inertia of the antenna appreciably.

Radar Electronics Subsystem Design

Figure IV-2 shows the block diagram for the suggested radar subsystem. The waveform generator generates the pulse to be transmitted whether pulse compression is used or not. The frequency deviable oscillator is not needed, if pulse compression is not used. The local oscillator generates the carrier frequency, W_1, which is mixed with the intermediate frequency, IF, to generate the sum and difference of these frequencies. The output signal, W_o, is amplified and the output pulse is transmitted via the transmit-receive, TR, switch and radar antenna. If range pulse compression is used then a frequency deviable oscillator, FDO, will be used to shape the pulse. The carrier frequency is used to lock in the FDO which is linearly frequency-modulated by a ramp signal. This ramp signal is mixed with

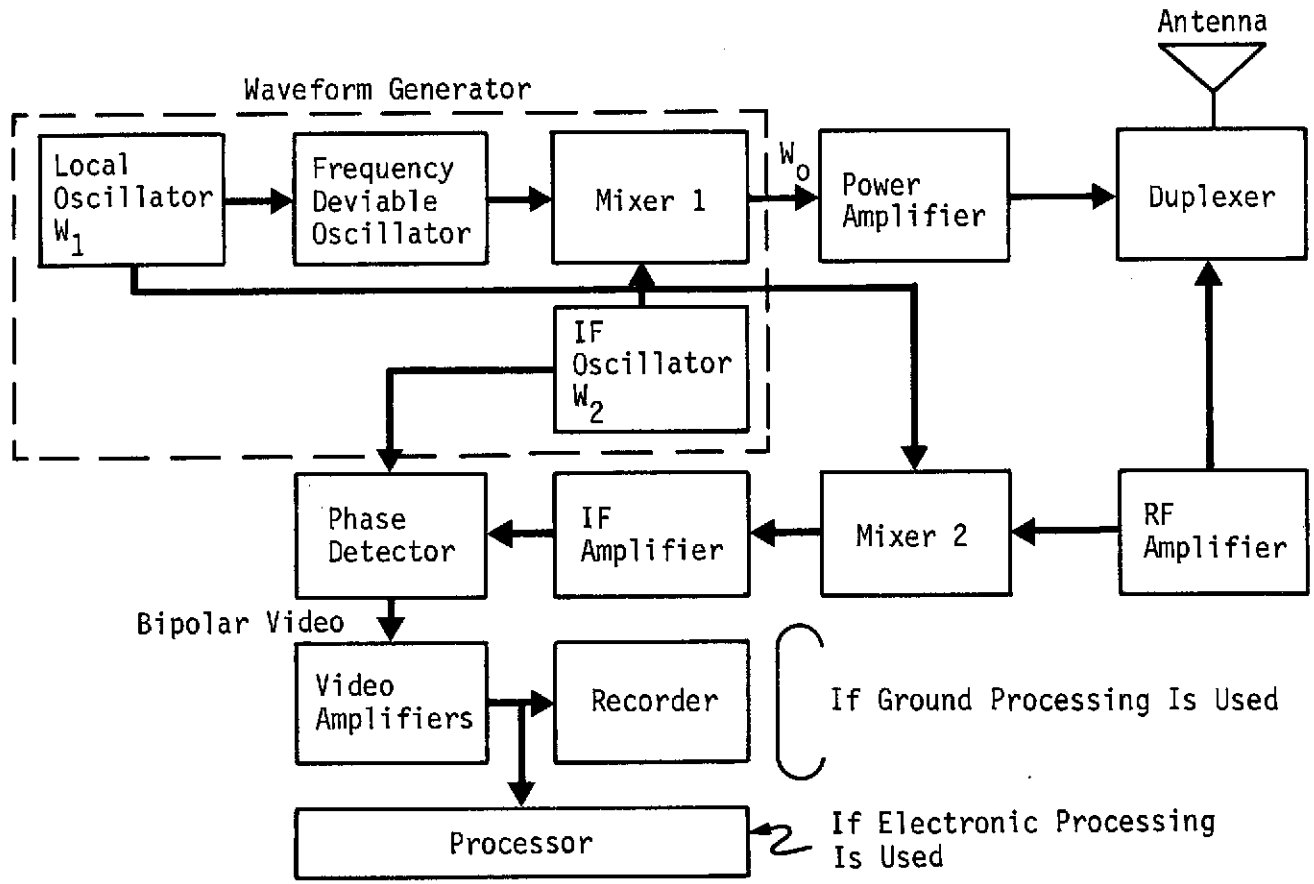

Figure IV-2 Coherent Radar Subsystem

the IF to generate the chirp signal which is power amplified before it is transmitted. The output from the mixer is amplified to the power required and radiated from the antenna on the transmit phase as determined by the duplexer. The return pulse is received when the TR switch connects the receiver to the antenna. The RF signal is amplified and mixed with the local oscillator frequency to give IF. The IF is amplified and fet into a phase sensitive detector to give a bi-polar video output signal. The bi-polar video signal is amplified before it is recorded for buffering if real time processing is not used. The signal is buffered so the raw data can be sent to Earth at a rate the communication system can handle. The video signal can be partially or fully processed on-board and then buffered and transmitted to Earth. A real time or non-real time processor can be used. Buffers may be needed before and after the processing. The processing options will be described in the data handling and communication system section.

The radar subsystem can be designed from today's state-of-the-art components and should be almost an off-the-shelf hardware item. One radar subsystem manufacturer, which has manufactured and flown mapping radars, claimed there was no advantage in modifying existing hardware to do the Venus mapping mission because it is practically an off-the-shelf design.

Radar Altimeter

The radar altimeter is used during the mapping phase to control the vehicle and to augment the science. The mapping radar can be used as an altimeter if the altimetry is time shared with the mapping function. If multi-orbit mapping phases are used mapping can be conducted during one orbit and altimetry can be conducted on another. If single orbit mapping phases are used, as for eccentricities of 0.5, then a separate altimeter must be used.

Since the 0.5 orbit is favored where we map every orbit, a separate, simple and lightweight altimeter is favored. A radar altim-

eter operating on a different frequency would maximize the science return and minimize the engineering risk. A 20-cm L-band frequency would be a good choice for a radar altimeter as it has minimum atmospheric losses and would probably not have much subsurface penetration to degrade the altimeter's accuracy.

The mapping radar also can be used to provide altitude data by timing each range pulse to generate the range for each range cell. This time is proportional to range which can be rectified to determine altitude and compared with the separate altimeter data. The altimetry will have the same range resolution as obtained in mapping but has azimuth resolution determined by the aperture of the antenna. Azimuth processing can be done to obtain the same resolution in this direction. A synthetic aperture has to be generated to get the same resolution as was obtained in range.

The planetary surface characteristics can be determined by comparing altimetry measurements by the altimeter and the mapping radar. The mapping radar can determine the range to a prominent feature by timing the return. The altitude can be determined from the range when the side look angle is known. This altitude can be compared to the one sensed by the altimeter to determine the subsurface penetration. Surface characteristics can be deduced from this information.

A wide beamwidth altimeter using a cavity backed cross slot antenna and a leading edge tracker like the Viking Lander uses would be a good selection to reduce costs of developing a new one. Table IV-4 shows the microwave gains and losses used in the radar range equation to determine peak transmitted power needed for a radar altimeter to operate to a maximum altitude of 4000 km. A transmitter with a peak power of about 25 watts will be required which requires 10 watts of input power assuming a 20 percent efficiency. The estimated weight of the altimeter electronics is about 4.55 kg (10 pounds) with an antenna weight of about 0.91 kg (2 pounds) and size of 0.35 m diameter.

Table IV-4 Radar Altimeter Specifications

Frequency = 1.5 GHz (L-band)

Pulse Width = 1 (10^{-3}) sec

PRF = 85 PPS

Duty Cycle = 8.5%

$$P_t = \frac{(4\pi)^3 R^4 KTB(NF)L(S/N)_{REQ}}{G^2 \lambda^2 \sigma}$$

Parameter	Contribution	Remarks
Maximum Range (R)	+264.0 db	H_{MAX} = 4000 km
$(4\pi)^3$	+ 33.0 db	
KT	-200.2 db	T = 700°K
B (bandwidth)	+ 30.0 db	1 millisec pulse
NF (noise figure)	+ 9.0 db	
L (losses)	+ 6.5 db	$L = 0.7 f^2$
$(S/N)_{REQ}$	+ 10.0	
G^2 (antenna gain)	- 29.6 db	0.35 m diameter antenna
λ^2 (wavelength)	+ 3.9 db	λ = 0.2 (L-band)
σ (normalized radar cross section)	-112.7 db	±20
	+ 13.9 db	
	P_T = +24.6 watts	
	P_{AVE} = 24.6/11.8 = 2.08 watts	
	P_{IN} = 10.0 watts (20% efficiency)	
	W = 4.6 kg (10 lbs)	
	Antenna = 0.91 kg (2.0 lbs)	

The Viking Lander (VL) radar altimeter has the following specifications:

20^{o} x 80^{o} fan shaped beam
transmitted pulse width = 1 millisec
power input = 33 watts
average power output = 5 to 19 watts
peak power output = 70 to 250 watts
PRF = 85 PPS
weight = 6.8 kg (15 lbs)
antenna = cavity-backed cross-slot
operating frequency = 1.0 GHz
volume = 0.00644 m^3

The VL radar altimeter is heavier and has a higher power capability than is needed. To save developmental cost, a modified VL radar altimeter could be used where it would be modified to reduce weight and power.

A block diagram of the suggested radar altimeter is shown in Figure IV-3. The carrier is modulated to form a one millisecond pulse which is amplified and transmitted via the transmit-receive, TR, switch and the altimeter antenna. The control logic controls the TR switch and controls the range gate tracker when the received signal is above the tracker threshold. The radar altimeter indicates when the leading edge is sensed. This means the radar altimeter senses the first return above the threshold which is within the antenna beamwidth as shown in the sketch:

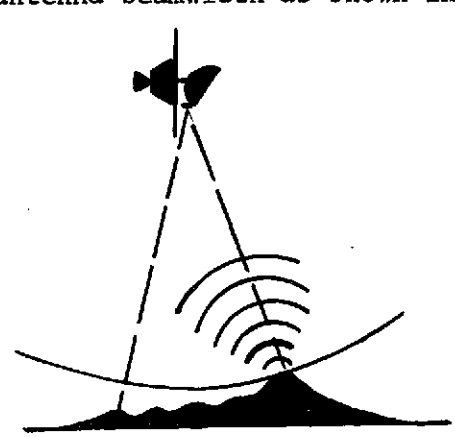

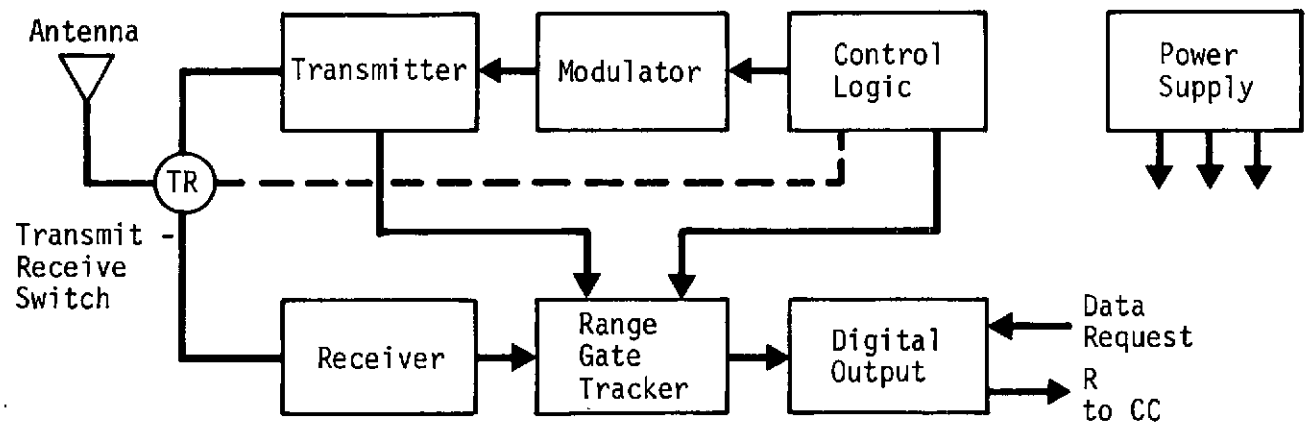

Figure IV-3 Block Diagram of the Radar Altimeter

As can be seen, the radar altimeter does not always sense altitude but the range to the closest surface to the antenna. However, it appears that the altitude data can be improved by comparison with imaging data.

Using a 1.5 GHz frequency and the output power required, the radar altimeter could be mechanized completely with solid state components. Using today's solid state technology, the radar altimeter estimated weight should be about 10 kg where the cavity-backed cross-slot antenna (0.35 m diameter) would have an estimated weight of about 0.91 kg. The volume required to package the radar altimeter would be 0.0041 m^3 (0.17 ft^3) based on 88.5 kg/m^3 (55 pounds/ft^3) as an average electronic packaging density.

The radar altimeter is designed to transmit a pulse every 100 m at a specified latitude. The radar altimeter will sense range under the spacecraft and has essentially 100 m resolution at the specified latitude.

Clutterlock System

These paragraphs describe a system for acquiring and tracking the zero doppler line for the Venus Mapping Radar. The following parameters are assumed for illustration purposes:

orbit eccentricity: $\epsilon = 0.5$

wavelength: $\lambda = 10$ cm

side look angle: $\theta = 10$ degrees

The azimuth look angle to the zero doppler line is

$$\theta_a = \tan^{-1} (\underline{v}_r / \underline{v}_t) \qquad \text{(IV-7)}$$

where $\underline{v}_r$ and $\underline{v}_t$ are the radial and tangential components of the spacecraft velocity vector. Here we note that the orbital velocity is

$$\underline{v} = \left(\underline{v}_r^2 + \underline{v}_t^2 \right)^{1/2} \qquad \text{(IV-8)}$$

In particular, we note that $\theta_a = 0$ at periapsis, θ_a is positive (forward) after periapsis passage, and negative prior to periapsis. We also note that the zero doppler line does not always intersect the planet

In the Mission Analysis Section of Volume III, it is shown that the zero doppler plane is tangent to the planet surface at $\pm 111.2^{\circ}$ true anomaly, and that the zero doppler plane intersects the planet at maximum or minimum latitude ($\pm 85.2^{\circ}$) at $\pm 78^{\circ}$ TA.

At the initial intersections of the zero doppler plane with the planet (111.2° TA), the range is approximately 9900 km and the grazing angle is 90°. At this point, the radar return would be too weak for clutterlock acquisition. Hence, we will arbitrarily assume clutterlock acquisition begins at -100° TA and tracking with radar mapping at -80° TA. Pertinent parameters are listed in Table IV-5 where

TA = orbital true anomaly
T = time from periapsis
Θ_a = angle between nadir and zero doppler plane
ψ = grazing angle
R = range
$\underline{v}$ = orbital velocity

From Table IV-5 we note that the time available for acquisition is 0.163 hour or approximately 580 seconds; considerably more than the estimated 30 seconds that are required.

Table IV-5 Initial Clutterlock Acquisition

TA (degrees)	T (hr)	Θa (deg)	ψ (deg)	R (km)	v (km/sec)
-100	-0.527	28.33	59.78	6170	6.012
- 80	-0.364	24.37	40.04	3374	6.914

Doppler Signal - The azimuth Doppler frequency is

$$f_d = \frac{2\underline{v}}{\lambda} \sin \Theta_a \qquad \text{(IV-9)}$$

where Θ_a is the angular displacement from the zero doppler plane to nadir. The two-sided doppler bandwidth is approximately

$$B_d = \frac{2\underline{v}}{D_a} \text{ Hz} \qquad \text{(IV-10)}$$

where D_a is the azimuth aperture dimension of the antenna. To prevent aliasing during mapping we require that

$$\text{PRF} > B_d \qquad \text{(IV-11)}$$

Let us now consider some values. We will assume that $D_a = 4$ m and that the maximum inertial uncertainty in the position of the zero doppler line is $\Theta_\epsilon = 20$ mrad ($\pm$ 10 mrad or $\pm 0.6°$). The azimuth beamwidth is

$$\beta_a = \frac{\lambda}{D_a} = 25 \text{ mrad} \qquad \text{(IV-12)}$$

At the beginning of mapping, the orbital velocity is $\underline{v} \approx 6.9$ km/sec. Then from Equation (IV-10), the doppler bandwidth is approximately 3.5 kHz.

The maximum Doppler spread is

$$\Delta f_d = \frac{2\underline{v}}{\lambda} \sin (\Theta_\epsilon + \beta_a) \approx 6.2 \text{ kHz} \qquad \text{(IV-13)}$$

To unambiguously resolve this received doppler with a pulse doppler radar requires a PRF in excess of 6 kHz which would introduce range ambiguities.

Acquisition - Now, let us assume a doppler spread of 10 kHz and a required resolution of 1 kHz. This resolution could be attained with a single 1 msec uncoded pulse. Note that doppler frequency is a function of angle only. Hence, range resolution is irrelevant and clutterlock can be attained with a

continuous wave, CW, radar. However, when a single antenna is used for transmission and reception, it is necessary to operate in a pulsed mode to prevent the transmitter from jamming the receiver. The maximum length pulse that can be received with the transmitter off is equal to the two-way propagation delay, or

$$T_{MAX} = \frac{2R}{C} \tag{IV-14}$$

Just prior to mapping, the range is 3374 km; then T_{MAX} = 22.5 msec. At initial acquisition, the range is 6170 km for which T_{MAX} = 41 msec. Hence, for clutterlock acquisition, one can easily obtain 1 kHz resolution with sufficient statistical averaging to unambiguously determine antenna pointing angle with a single pulse.

The use of a CW clutter acquisition signal also offers a significant advantage in SNR since the receiver bandwidth can be reduced to the clutter bandwidth. If we assume a 3 MHz receiver bandwidth for mapping and a 10 kHz bandwidth for clutterlock acquisition, a 300-to-1 or 25 db SNR improvement between the two is obtained. This full improvement is obtained just prior to mapping. At initial acquisition, some of the SNR improvement is lost due to the increased range.

Tracking - During mapping, clutter tracking can be accomplished using the received azimuth video. Let

$$z_n = x_n + iy_n, \quad n = \ldots -1, 0, 1, \ldots \tag{IV-15}$$

be the range-gated complex azimuth signal received at the nth transmission. Let

$$e_n = y_n x_{n-1} - x_n y_{n-1} \tag{IV-16}$$

be the unfiltered clutterlock error signal. Let $\hat{e}_n$ be the low-pass filtered error signal. Then it can be shown that $\hat{e}_n$ is an estimate of the imaginary part of the complex autocorrelation function of

z_n evaluated at a delay equal to the PRF interval, i.e.,

$$e_n = I_m \left\{ \overbrace{R_z (T)} \right\} \tag{IV-17}$$

where

$$T = \frac{1}{PRF} \tag{IV-18}$$

Now

$$R_z (T) = R_o (T) \exp \left\{ 2\pi i f_o T \right\} \tag{IV-19}$$

where $R_o(T)$ is the real-valued autocorrelation function of the zero offset doppler signal and f_o is the doppler offset. The imaginary part of $R_z (T)$ is

$$e(T) = R_o (T) \sin 2\pi f_o T \tag{IV-20}$$

From Equation (IV-20), we note that

$$e(T) = 0, \quad f_o = \frac{n}{2T}, \quad n = 0, \pm 1, \pm 2, \ \ldots \tag{IV-21}$$

The point $f_o = 0$ is the desired equilibrium point of the clutterlock. Odd values of n correspond to unstable equilibrium points. Even values of n, $n \neq 0$, correspond to stable ambiguous equilibrium points.

Let us now relate Equation (IV-21) to pointing error for ambiguous clutterlock operation. Equating Equations (IV-9) and (IV-21) gives the ambiguous equilibrium points

$$\frac{2v_o}{\lambda} \sin \theta_{a_n} = \frac{n}{2T}, \quad n = \pm 1, \pm 2, \quad \ldots \tag{IV-22}$$

Solving for θ_{a_n},

$$\theta_{a_n} = \sin^{-1} \frac{n\lambda}{4v_o T} \tag{VI-23}$$

Now

$$v_o T = \Delta x < D_a/2 \tag{IV-24}$$

is the azimuth spatial sampling interval.

Let us now assume that the azimuth doppler is sampled at the 26 db bandwidth. Then

$$\Delta x = \frac{D_a}{3.2} \tag{IV-25}$$

Then, Equation (IV-23) becomes

$$\theta_{a_n} = \sin^{-1} \frac{0.8n\lambda}{D_a} \approx 0.8n \beta_a \tag{IV-26}$$

Now we recall that odd values of n ($n = \pm 1, \pm 3, \ldots$) correspond to unstable equilibrium points (saddle points) and even values of n ($n = \pm 2, \pm 4, \ldots$) correspond to stable equilibrium points. If $\beta_a = 25$ mrad, the first pair of saddle points occur at ± 20 mrad and the first pair of stable ambiguous operating points occur at ± 40 mrad angular offset. In particular, if the initial error is less than ± 20 mrad, then the clutterlock will lock on the zero offset equilibrium point. If the initial error is between 20 and 60 mrad, then the clutterlock will acquire the 40 mrad offset point, etc. However, we have assumed an initial error of ± 10 mrad. Hence, if this tolerance cannot be held, initial acquisition will be ambiguous and the previous discussion on acquisition is largely academic.

We can generalize these results for arbitrary sampling intervals to account for different antenna sizes. From Equations (IV-23) and (IV-24),

$$\theta_{a_n} = \sin^{-1} \frac{n\lambda}{4\Delta x} \approx \frac{n\lambda}{4\Delta x} \tag{IV-27}$$

The first pair of saddle points and ambiguous operating points as a function of Δx, are shown in Table IV-6 for $\lambda = 10$ cm.

Table IV-6 Saddle and Ambiguous Operating Points

Δx (meters)	First Saddle Point (mrad)	First Ambiguous Operating Points (mrad)
10.0	$\pm$ 2.5	$\pm$ 5.0
5.0	$\pm$ 5.0	$\pm$10.0
2.0	$\pm$ 7.5	$\pm$15.0
1.6	$\pm$10.0	$\pm$20.0
1.0	$\pm$25.0	$\pm$50.0

Now, from Table IV-6, we observe that with an initial uncertainty of $\pm$10 mrad, the clutterlock will acquire zero angular offset for $\Delta x < 1.6$m, and will lock at a maximum ambiguous offset of $\pm$20 mrad for $\Delta x > 1.6$m.

Table IV-6 also indicates the operation of the Goodyear Aerospace Corporation Beam Stepping method of clutterlock acquisition described in the PIRS study (Ref. 12). Let us assume the clutterlock is initially locked to a 20 mrad ambiguity with a sampling of $\Delta x = 1.6$m. Now, by slowly increasing the sampling interval to slightly greater than 5 meters (decreasing the PRF), the ambiguous antenna angle would be reduced to less than 10 mrad. Instantaneously increasing the PRF interval to 1.6m would then place the offset error within the first saddle point forcing the clutterlock to lock on zero offset.

Effects of Clutterlock Error - We will consider two classes of error: 1) offset error about a stable equilibrium point, and 2) ambiguous lock about a nonzero equilibrium point.

For the first case, the azimuth doppler is presumed and processed at zero offset. The required angular beamwidth for an azimuth resolution of r_a meters is

$$\alpha_{min} = \frac{\lambda}{2r_a} \qquad \text{(IV-28)}$$

Then if λ = 10 cm and r_a = 100 m, α_{min} = 5.0 mrad. Let the two-way 6 db azimuth beamwidth be β_a. Then an offset error of $\pm(\beta_a - \alpha/2)$ will result in a maximum signal attenuation of 6 db at the presummer output. This is the only effect. If a 10 m antenna is used, β_a = 10 mrad and the range of permissible error is $\pm$4.5 mrad. However, if 10 m azimuth resolution is required, than α = 5 mrad and the permissible pointing error with a 10 m antenna is reduced to $\pm$5 mrad.

If the antenna is locked to an ambiguous angular offset, then effectively the radar is operating in a squinted mode. This does not affect the amplitude of the returned signal since the azimuth data is still received in the region of maximum antenna gain. If the squint angle is known, then it is easily corrected in processing. If the squint angle is unknown, then the resulting image will be displaced and skewed by the squint angle. For example, if the unknown squint angle is 20 mrad, then the image will be displaced by 20 km at 1000 km slant from the predicted position of zero doppler. This could be rectified after processing if the amount of skew can be determined from the image. In particular, overlapping portions of the image from successive passes could be used to estimate the displacement to permit post-processing correction.

Implementation - The zero doppler pointing angle and angular rates can be predicted from measured orbital parameters. Hence, it is assumed that the clutterlock will be used primarily as a closed-loop correction servo around a nominal open-loop antenna attitude control system. This minimizes the performance requirements of the clutterlock servo.

For the 0.5 eccentricity orbit, the maximum rate of change of the zero doppler line is approximately 1.5 mrad/sec and occurs at periapsis. Then a clutterlock loop gain of 1 rad/sec/rad would permit tracking with less than 2 mrad point error if no open-loop steering command is used. The open-loop steering signal would reduce the pointing error even further.

Because of the random nature of the clutterlock error signal, this signal is normally filtered with a time constant equal to the real aperture time of the azimuth beamwidth, i.e.,

$$\tau = \frac{R\beta_a}{v_o} \text{ sec} \qquad \text{(IV-29)}$$

For aircraft radars, longer time constants are often used to prevent the clutterlock from responding to dominant cultural targets. In a planetary mapping mission, a shorter time constant could be used since no strong isolated returns are expected. Using nominal values of R = 1000 km, v_o = 8 km/sec and β_a = 20 mrad, the time constant given by Equation (IV-29) is approximately 2.5 seconds. However, in practice, a time constant of the order of 0.25 seconds would probably be adequate.

One possible implementation of the clutterlock tracking system is shown in Figure IV-4. In this diagram, x_n and y_n represent the quantized (digital) range-gated inphase and quadrature video signals. Samples are taken at several ranges across the swath. These samples are delayed by one PRF interval (T) and then cross-multiplied and subtracted according to Equation (IV-16). The difference is then accumulated over several PRF intervals and the resulting sum is used as a rate command to the azimuth steering channel. We will assume that three range samples are used: near- mid- and far-range. Then six words of delay are required. Figure IV-4 shows two multipliers, an adder, and a subtractor. However, a single multiplier can be time-shared with the resulting product alternately added or subtracted with the contents of the accumulator. The accumulator is a digital integrate-and-dump circuit which would accumulate the error signal over several hundred PRF's and then transfer the resulting filtered error signal to the antenna azimuth attitude control servo. If we assume a nominal PRF of 4 kHz, then 250 μsec are available for the required six multiplications and additions. This time is more than

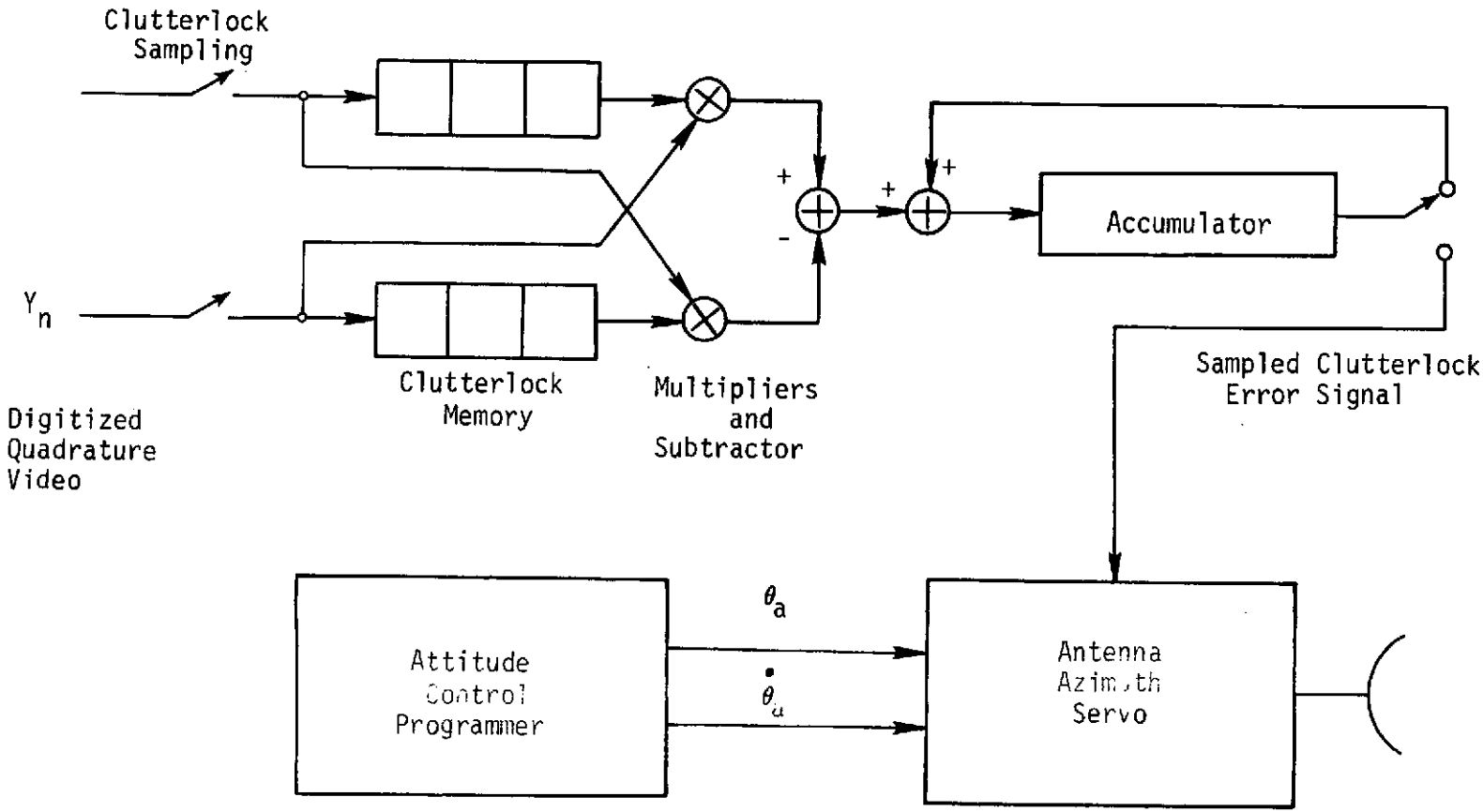

Figure IV-4 Clutterlock Tracking System

adequate to permit a multiplexed operation using a single arithmetic unit. It is then estimated that total hardware requirements for the digital clutterlock tracking circuit are approximately 100 bits of memory plus one six-bit adder. Hence, power and weight requirements are essentially negligible.

Implementation of the CW acquisition system described earlier would not be required if the inertial altitude reference error is less than $\pm 0.5°$ since, in this case, the clutterlock tracking circuit will lock within the first or second ambiguous angle about zero doppler. Subsequent variation of the PRF would quickly eliminate the ambiguity. If significantly larger initial pointing errors are expected, then implementation of the CW acquisition system is recommended. Since acquisition is done prior to mapping, the on-board processing hardware (presummer) could be programmed to do the filtering required for acquisition. Hence, a significant increase in size, weight, and power would not be required.

Alternative Systems - An alternate method of clutterlock implementation is to fix the antenna and change the receiver reference frequency to compensate for radial-velocity-induced doppler shift. For the 0.5 eccentricity orbit, the maximum radial velocity is 2.8973 km/sec at 90° T.A. The corresponding doppler shift is 58 kHz for $\lambda = 10$ cm. This is an order of magnitude greater than the PRF. However, because the radar data is sampled, the actual required offset frequency is equal to

$$f_o = \frac{2v_r}{\lambda} \text{ modulo (PRF)} \qquad \text{(IV-30)}$$

i.e., at a PRF of 4 kHz, a 58 kHz offset is equivalent to 2 kHz. Alternately offset errors equal to multiples of the PRF are transparent in the azimuth channel.

Implementation of the electronic offset clutterlock system is identical to the antenna steering system discussed earlier, with the exception that the clutterlock error signal is used to drive a voltage controlled oscillator, VCO, which shifts the reference frequency.

One important fact to note when electronic offset clutterlock is used is that antenna pointing errors are completely ambiguous with offset errors. That is, the reference VCO will automatically correct the doppler shift due to an antenna pointing error. However, if this pointing error is unknown, the resulting image will be shifted and skewed. Thus, implementation of electronic clutterlock assumes precise inertial pointing of the antenna.

Conclusions - The recommended clutterlock system is the closed-loop antenna tracking correction system. If the initial pointing error is small, then a sample sawtooth variation of PRF can be used to unambiguously acquire zero doppler. If the initial pointing error is large, then a pulse CW mode of radar operation can be used to rapidly acquire zero doppler. The size, power, and weight impact of a clutterlock system is negligible.

SYSTEM COMPARISON AND EVALUATION

Configuration C appears to be the preferred configuration for the radar subsystem because the vehicle pointing simplifies the radar antenna gimbal design and minimizes the antenna torques on the vehicle due to antenna articulation. The vehicle is inertially oriented; always pointing perpendicular to the orbital plane. The the center of gravity of the spacecraft, the antenna torques on the spacecraft are minimized. The mapping and communication subsystems have their own antennas so their utilization can be maximized and each antenna design can be optimized for its specific function. Very little communication antenna articulation is needed during the mission and, then primarily when the mapping side is changed once per mapping mission. Only one microwave frequency has to be "piped" through the rotary gimbals in the preferred configuration which is a cheap and standard design.

The solar panels and communication antenna point to an essentially inertial point throughout the mission so the torques on the vehicle are minimized.

A variable side look angle or a constant side look angle utilizing a dual beamwidth antenna can be used to eliminate ambiguities in elliptical orbits. The constant side look angle configuration uses a dual beamwidth antenna to narrow the beamwidth at the higher latitudes. A reflector type antenna is preferred and should be adequate to do the Venus mapping mission. The dual beamwidth antenna is a more expensive design but should not be a critical design. Mapping to $\pm 55^{\circ}$ TA can be achieved using a dual beamwidth antenna.

The variable side look, VSL, angle configuration is favored as it simplifies the antenna design and achieves greater mapping coverage. The variable side look angle configuration, where the antenna always points along the zero doppler line (ZDL), cannot be implemented in elliptical orbits, because the ZDL varies drastically from the radial direction. Mapping to $\pm 80^{\circ}$ latitude in a polar orbit can be achieved, but this configuration probably would require too much power to utilize the present VO solar panels (two panels) and would violate the PRF constraints at the higher latitudes.

The obvious solution is to "squint" the antenna forward or backward from the ZDL to point in the direction needed. An electronic offset clutterlock system, which is mentioned in Volume III, is one way to implement the VSL configuration. An additional gimbal is needed to vary the side look angle.

Another interesting solution is to squint the antenna a fixed angle forward the first half of the mapping phase and rearward the last half of the mapping phase. This scheme produces a variable grazing angle that approximates the grazing angles obtained in the previous case. One gimbal is eliminated by this scheme, since the spacecraft now can utilize a constant side look angle. The variable

grazing angle is obtained by the change in direction of the ZDL. A constant upper PRF constraint is not obtained, but the constraint does not limit mapping. Total planet coverage can again be achieved. In addition to the planet coverage, the power required is reduced considerably from the constant side look angle case with dual beamwidth.

A cursory study of the variable side look angle cases has been conducted and more in depth studies should be conducted to determine the best scheme. From this cursory study, the last implementation of the VSL angle configuration is favored, because complete mapping coverage of the planet is obtained and one gimbal is eliminated on the radar antenna.

As will be seen later, no modifications will be needed to the Canopus sensor except remounting, which has to be done for all three configurations. The Canopus sensor has to be remounted to point in the -X direction, which is along the South ecliptic. Inertial pointing has the disadvantage of having articulated solar panels, although very slow articulation capability is needed.

TECHNOLOGY ASSESSMENT

Advanced technology is not important for the radar subsystem designs as only present state-of-the-art components are needed to implement the designs needed for the Venus mapping mission. Improved technology should reduce system weight, and increase efficiency and reliability. The reliability can be increased by using many elements in a planar array where the failure of a few elements will not affect the output power appreciably. The efficiency of solid state components should increase considerably in the next decade. Advanced technology should augment the mission by reducing the side lobes, providing simple methods to do beam steering, and increasing the radar subsystem efficiencies and power per antenna

element. Planar array designs should be very competitive to reflector type antenna designs and have a much better specification in terms of side lobes, reliability and power efficiency in the next decade. For this reason, planar arrays will probably be used when their weight and cost compares favorably with reflector type antennas. The planar array by today's standards is too expensive and heavy a design to use in a minimum cost mission. A reflector type antenna is selected in most cases to reduce cost and weight. This type of antenna is also selected to minimize shadowing of the solar panels. A planar array is selected for the dedicated antenna configuration (Configuration B), so that the antenna can be packaged in the launch vehicle shroud.

The state-of-the-art of deployable planar arrays is in its infancy and should develop considerably in terms of workable and developed hardware in the next decade. The state-of-the-art of deployable reflector type antennas, specifically parabolic designs, is available and highly developed at the lower frequencies (S-band and lower), but is being developed for higher frequencies. Surface variations over a tenth of a wavelength cannot generally be tolerated in these designs.

CONCLUSIONS AND CONCERNS

Conclusions

Configuration C appears to be the most flexible design at comparable cost to the other alternate configurations and exhibits many desirable characteristics the subsystem designers want. Although Configuration C is the preferred design, Configuration A is a very attractive design. In fact, JPL selected a very similar configuration for their preferred design in their latest study (Ref. IV-1).

An orbit with an eccentricity of 0.5 and mapping every orbit appears to be the favored mapping strategy when a variable side look angle is used and total system design is considered. This mapping strategy is favored, because the VO'75 spacecraft can be used with essentially its present propulsion capability for a variety of mission opportunities. The radar subsystem itself requires less power in more circular orbits, but significantly modified Viking propulsion capability is required.

Present state-of-the-art technology for radar and antenna subsystem designs would be adequate to do the Venus mapping mission. Advanced technology might reduce the weight, increase the reliability and power capability, and add to the flexibility of the mapping radar subsystem. The design of the radar subsystem to do this mission is a straightforward design. The design of the antenna subsystem must be developed and optimized for the Venus mapping mission to guarantee the required side lobe levels. The expected side lobe specifications for the antenna subsystem are easy to meet and standard antenna designs should be adequate. Side lobe levels that are 20 db down (two way), should be adequate to do this mission, since very little of the doppler bandwidth is used.

The use of a reflector type antenna is favored and should be adequate to do this mission. The design of the reflector should be straightforward. The feed and the articulation subsystems will be a new design effort. If a deployable antenna is used, a new antenna design would probably be needed so that it can be packaged in the launch vehicle and articulated.

A wide beamwidth, L-band radar altimeter is suggested to augment the science and supply discretes to change the phases during the mapping mission. A different operating frequency is used for each system to minimize the coupling between the mapping radar and altimeter and to get additional information about the surface.

The Viking Lander radar altimeter can be used and has been baselined to save developmental costs. This instrument is 50% heavier and has a higher output power capability than is needed.

The clutterlock system should be a straightforward design, that uses the zero doppler reference to point the radar antenna. This system can be implemented as a component of the radar subsystem.

Concerns

The biggest concern during this study is to find ways to use reasonable-sized antennas which can be articulated when elliptical orbits are used. Elliptical orbits are needed if existing spacecraft are to be used with reasonable propulsive capability. The radar antenna has to be large in the azimuth direction because the PRF must be low. The antenna must be narrow in the range direction to illuminate the swath width at periapsis. This is discussed in the limiting criteria section of Volume III. In elliptical orbits a wider swath width is illuminated with a given antenna as altitude increases. The range ambiguity constraint becomes more restrictive for the wider swath widths. Very low PRF and very large antenna dimensions are needed to guarantee little range and doppler ambiguities, unless the illuminated swath width can be changed. Without some method to change the swath width, the antenna needed is generally too large to be articulated. If the antenna is not articulated, too much attitude control system (ACS) propellant is required to use a mass expulsion attitude control system. A new control moment gyro (CMG) control system would have to be developed which would increase the developmental risk and expense. Large antennas will also

be hard to package in the launch vehicle shroud and hard to point to the accuracy required. For this reason, we have tried to solve the range ambiguity problem that occurs in elliptical orbits by changing the illuminated swath width during the mapping phase.

Range gating has been suggested as one way to solve the problem, where a small portion of the illuminated swath width is processed to get the mapping area at the highest latitudes. The range ambiguity content would be too high to guarantee good mapping. This technique is rejected because good pictures cannot be guaranteed with side lobes that are not 20 db below the main lobe.

The second and straightforward approach is examined next, where a multi-beamwidth antenna is used. A reflector type antenna would probably be used for the earlier missions and may be competitive for the later missions. We assume the reflector type antenna will be used. Specifically, a dual beamwidth antenna is suggested to be used which would not allow full planet mapping. Mapping to $\pm 55^{\circ}$ latitude (periapsis at equator) and mapping from -90° to $+35^{\circ}$ latitude, if the one pole is mapped, can be achieved without violating the mapping ambiguity constraints. The more complex design of the reflector type antenna is some concern in terms of development risk even if this is considered a straightforward design. Side lobe levels and illumination patterns due to aperture blockage resulting from use of a dual set of feeds have to be investigated. Aperture blockage by a dual set of feeds will change the antenna illumination pattern so that the side lobe level and beamwidth cannot be guaranteed. This type antenna with its articulation system has to be a newly developed system and designed for this mission, but should not be a critical design with much developmental risk.

The concept of a variable side look angle looks attractive if small grazing angles can be achieved. The antenna is controlled by a clutterlock system which points the antenna along the zero doppler line (ZDL). At periapsis, the zero doppler plane includes the radial direction. At the mapping extremities the zero doppler plane deviates greatly from the radial direction, so that small grazing angles cannot be obtained unless the antenna is not pointed along the ZDL. An electronic offset clutterlock system can be used to control the antenna so that small grazing angles can be achieved. This system is described in the previous section that describes the clutterlock system. High grazing angles are produced by any zero doppler pointing system, whenever mapping is conducted at the higher latitudes in elliptical orbits. These high grazing angles require more power and exhibit wider illuminated swath widths at the higher altitudes to make the PRF constraints more difficult to meet. An electronic offset clutterlock system is only one way to solve the problem; later studies should investigate this problem in detail. The major concern in implementing a variable side-looking angle system is whether the small grazing angles can be achieved by using a scheme such as an electronic offset clutterlock system. A technique for using a radar squint mode and a constant side look angle is suggested as a solution in Volume III, which utilizes the VSL scheme. This scheme uses the variation of the VSL angle to implement a mapping system that gives 900 km overlap at the equator, which should give good stereo pictures. Complete planet coverage is also achieved, while eliminating one antenna gimbal.

REFERENCES

IV-1 Louis Friedman, et al: *Venus Orbiter Imaging Radar (VOIR)*. Final Oral Report to NASA Headquarters, April 27, 1973.

IV-2 Walter E. Brown, Jr., et al: *Planetary Imaging Radar Study*. JPL 701-145, June 1, 1972.

IV-3 John S. MacKay, et al: *A Preliminary Analysis of a Radar Mapping Mission to Venus*. NASA-OAST, October 11, 1972.

IV-4 D. O. Muhlman: "Interferometric Investigations of the Atmosphere of Venus." *Radio Science*, Vol. 5, February 1970.

V. DATA HANDLING AND COMMUNICATIONS

INTRODUCTION

The objective of this section is to formulate candidate subsystem implementations, assess feasibility, cross-correlate and evaluate interacting subsystem requirements, and define technology development activities.

This section is concerned with identification of representative subsystem performance specifications and metric characteristics such as volume, weight, power. The identification of such example specifications is accomplished with the purpose of testing or inferring technical feasibility and risk factors for the timeframe of the mission. The basic requirements are those derived and discussed in Section V, Volume III. The example designs and technology evaluation of this section are basically expanded point implementation taken around key areas of the parametrically derived requirements of Volume III, Section V.

Initially, the basic common denominators of the data management/communications subsystems studies are discussed and presented in a generic subsystem block diagram. The implementation guidelines are developed and candidate implementations discussed. Critical subsystem interrelationships and design susceptibilities are investigated next leading to technology status assessments and critical development concerns. Finally overall mission requirements, technology risk and additional advance research or development requirements are summarized.

SUBSYSTEM IMPLEMENTATION CONSIDERATIONS

Data Management/Communications Subsystem Common Denominators

Figure V-1 presents a subsystem block diagram which is simplified to display the basic elements which are common to all implementations. The requirements for individual elements are unique to each mission strategy. Referring to the diagram, the basic assumptions of the overall subsystem implementation are discussed below. Uplink command is at S-band with a nearly omnidirectional receive capability. A doppler transponder would provide for turn-around doppler ranging via either the "omni" or high gain antenna network. A continuous low data rate engineering telemetry link could be employed at X- or S-band via the medium gain/high gain antenna system. The medium gain gain parabolic reflector system. This applies to either Configuration C (dual antenna) spacecraft or Configuration A (shared antenna) spacecraft configurations. Uplink commands are received via the command receiver and are demodulated and stored in the command distri- the command receiver, demodulated and stored in the command distribution unit which is under control of a central control, computation and sequencing computer. Data is accessed from the radar subsystem and converted to a digital format by an analog to digital converter (ADC) unit. Auxiliary science data would share the ADC unit which itself would have the capability to convert both radar and auxiliary science and engineering data on a non-interference basis. A dedicated radar data processing unit would condition radar data for storage in a mass storage unit until the communications relay window occurs allowing high rate data relay. A data annotation/control unit catalogs and identifies radar and ancillary science and engineering data for storage in a digital mass storage unit.

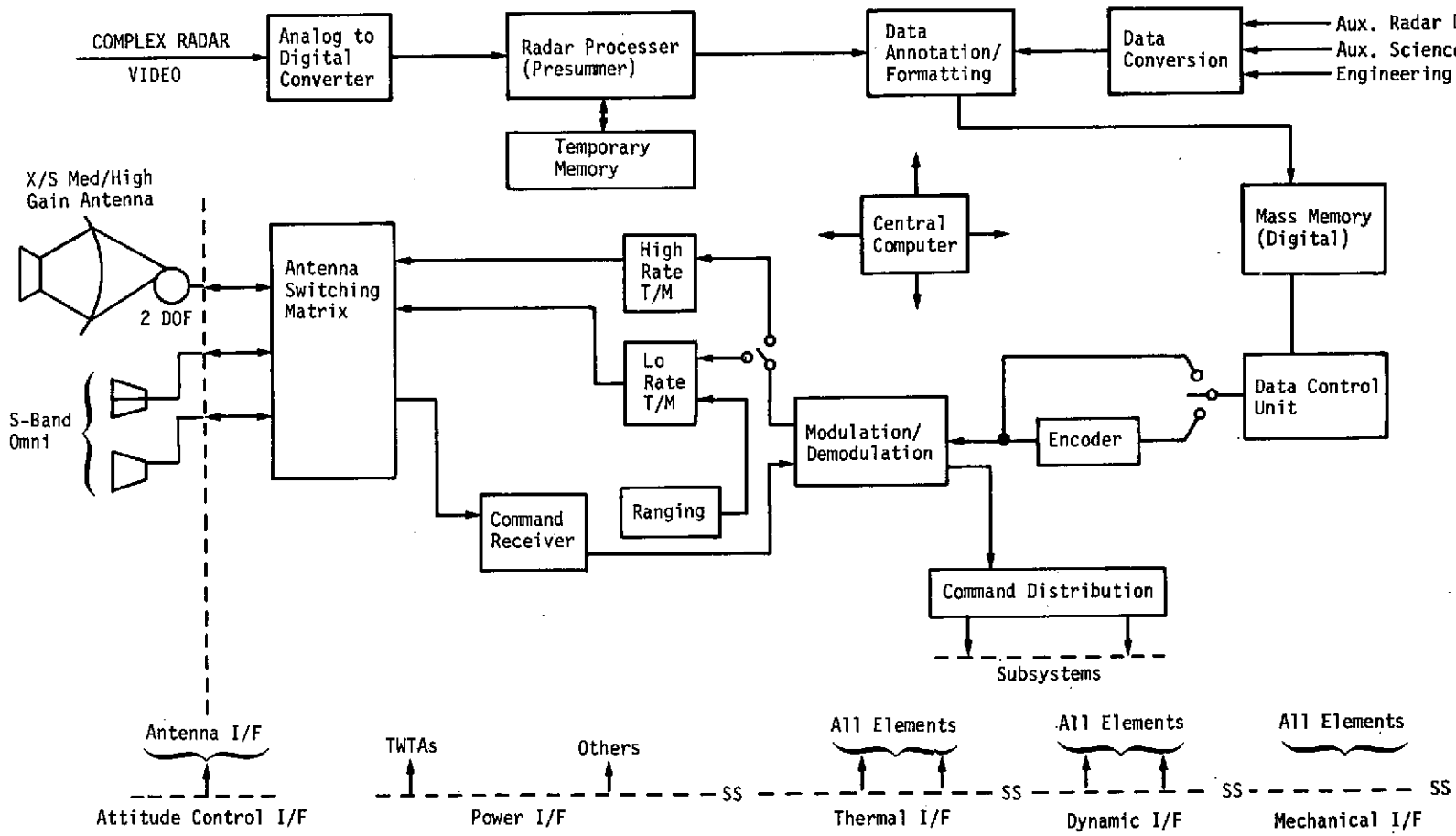

Figure V-1 Data Management/Communication Basic Block Diagram

During high rate data relay, data read out of the mass storage unit is converted to modulation on a carrier frequency by the modulation unit and traveling wave tube amplifier (TWTA) modulation exciter unit. High level radio frequency carrier power is formed by the TWT amplifiers (operating at X-band). This amplifier module could be composed of a single TWTA or a tandem assembly based on power requirements. An optional data channel encoder is shown to expose the fact that channel encoding can reduce TWTA power required due to data bit signal to noise requirement reduction for a given probability of error. The block diagram indicates the major subsystems interfaces of data management/communications; subsequent paragraphs will expand their limiting interactions, constraints, and requirements.

Implementation Guidelines and Ground Rules

Candidate implementations were derived at eccentricities of $e = 0$ (mapping every 5th orbit, 1:5), $e = 0.3$ (mapping every second orbit, 1:2) and $e = 0.5$ (mapping every orbit, 1:1) for a nominal 1984 mission lasting 250 days at Venus employing both Configurations C and A. All spacecraft configurations were attitude stabilized (3-axis).

The mission profile traverses minimum and maximum Earth-Venus slant ranges and experiences all possible occultation relationships including a short solar occultation near the end of the mission. The effect of solar occultation on communications is minimized by employing X-band with its narrower ground station antenna beamwidth. Designs presented are compatible with peak Earth occultation values to provide high quality data continuously and excess capability at the first of the mission. Radio frequency powers are computed to provide high quality data even at mission end. Power and thermal studies have shown that the corresponding required powers

are compatible with the reference attitude stabilized spacecraft concept employed (Viking orbiter class spacecraft) using approximately 14.9 m^2 (160 ft^2) of solar panel. Detailed timeline and power subsystem parametric studies are presented in Volume III, Section V and Volume III Section VI. Parametric studies have placed orbital periapse both at the equator and at latitude of -35 degrees for polar coverage reasons. The primary effect on data management/communications is to change the duration of peak Earth occultation and its time of occurrence in orbit. These changes were very small relative to the average communications window but are included in the reference design implementations of Configuration C spacecraft. The map time (according to radar subsystem studies) is affected by assumptions of antenna utilization strategies and is nominally the time to traverse ~180 degrees true anomaly around periapsis (Configuration C spacecraft) and ~110 degrees true anomaly (Configuration A spacecraft).

The operational scenario is based on reference time lines such as those outlined below. A detailed presentation of the overall system relative to these timelines is discussed in Volume III, Section VI, Power Subsystem Trades. These representative timelines typify the two characteristic Earth occultation situations such as presented in Figures V-2 and V-3 below.

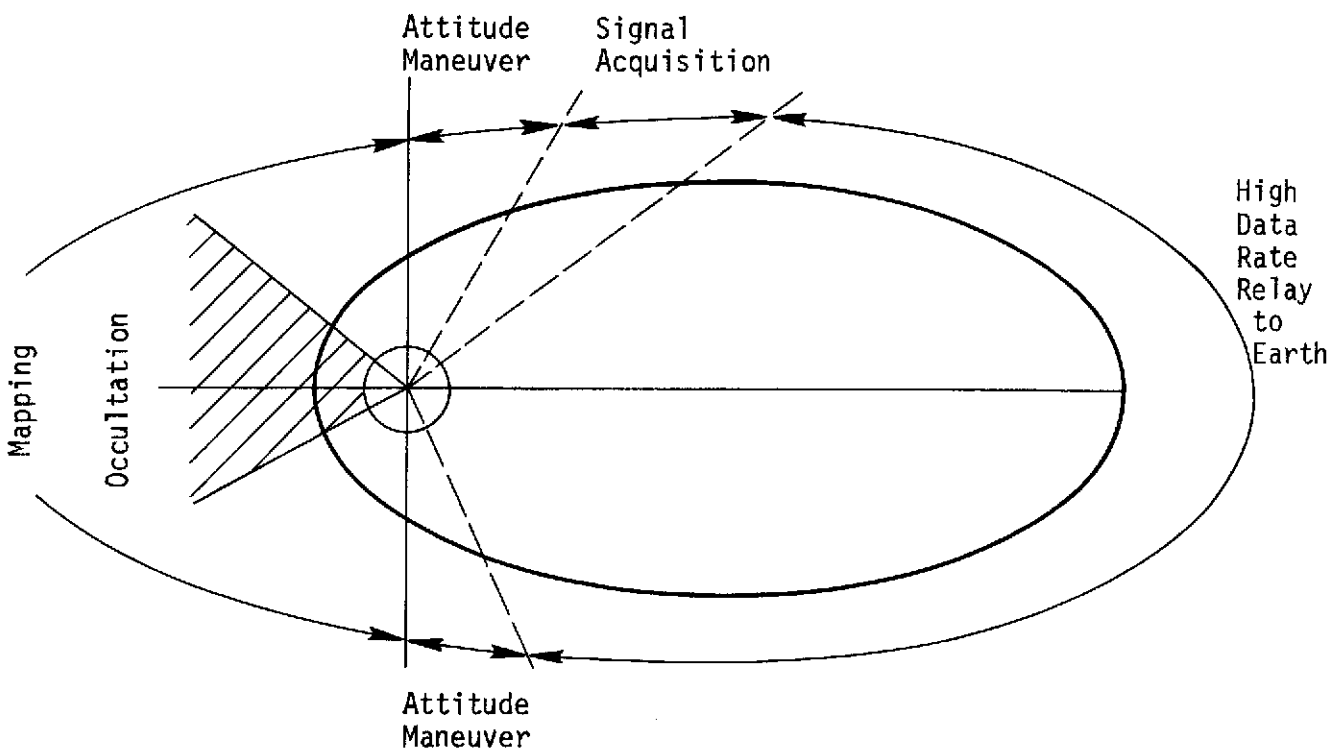

Figure V-2 Orbital Timeline - Periapsis Earth Occultation

Figure V-2 indicates the basic Earth occultation relationship existing upon arrival at Venus and again at mission end for Type II trajectories (the reference for this study). The salient characteristic of this geometry is that earth occultation occurs at periapsis at arrival and does not interfere with the nominal communications strategy (mutually exclusive mapping and high rate data relay) and Venus distance. Although not pursued in this study, the apoapsis Venus distance. Although not pursued under this study, the apoapsis occultation and periapsis occultation can be adjusted (nearly switched) by utilization of Type I trajectories with an additional spacecraft deflection velocity penalty at Venus.

The second characteristic timeline with earth occultation is sketched in Figure V-3 below.

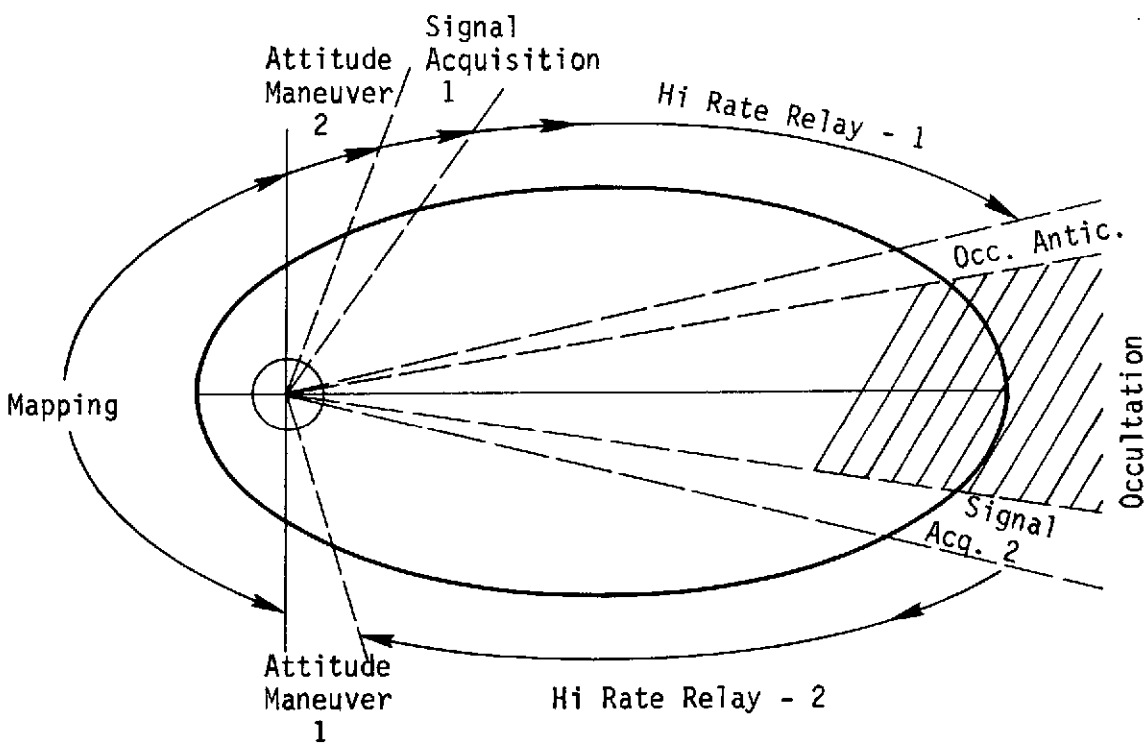

Figure V-3 Orbital Timeline - Apoapse Earth Occultation

The reference implementations, including power studies (Volume III, Section VI) and thermal studies (Volume III, Section VI) were based on the reference timeline of Figure V-3 using the Earth occultation characteristics at apoapse as the pacing communications geometry. The reference designs further assume the maximum Earth-Venus slant-range (data rates were presented parametrically over the entire mission in Volume III, Section V) for application of signal transit time to the

signal acquisition sequence. Signal acquisition is based on twice the transit time from Earth to Venus plus the DSN ground station typical signal acquisition and lock up time when a desired "close loop" acquisition philosophy is used. The closed loop signal acquisition sequence requires Earth to initiate the high data rate send command. An alternate scheme based on one way transit time plus signal acquisition time also appears feasible. With this philosophy repeated "send" commands would be issued from Earth while the spacecraft was in occultation. Thus, as soon as the spacecraft moves out of earth occultation, it would send a data header of length equal to the nominal signal lock-up time, then automatically initiate the high data rate sequence. All of these policies assume that the spacecraft attitude control system can maintain attitude pointing to Earth during the occultation time within the antenna half power beamwidth following the last inertial update.

Other reference criteria includes maintaining required radio frequency power less than 100 watts at X-band for the example designs. This is based on a technology survey and vendor contact to determine technology limitations. Iterative point analyses by the power subsystem analysis indicate that total prime power for the TWTA's should be 700 watts when approximately 160 sq ft of solar array is employed as a reference size in the 0.5 eccentricity orbit.

A major benefit of Configuration C is to remove the orbital timeline penalty due to attitude maneuvering, and to allow joint signal acquisition (at reduced TWTA power) and mapping at lower eccentricities since the communications antenna is continuously earth oriented at all times in orbit.

The mass storage subsystem is implemented on magnetic tape

nominally of the class specified for the Viking Orbiter which has a capacity of 1.3×10^9 bits. The subsystem itself is composed of two redundant recorders of approximately 0.65×10^9 bits.

Reference Processing Mode Definitions

The many alternative processing strategies possible have been collected into three reference modes plus a selectable telescope mode which can be applied to all cases. These reference modes are called: a) maximum presumming[1], b) minimum presumming, and c) mixed integration processing[2]. An additional mode, called telescope mode, is assumed to be available upon selection throughout any of the reference missions. The above modes primarily apply to the degree of processing in azimuth, or the along track direction.

The design reference for the range (cross track) direction is unprocessed data in all cases except for onboard mixed integration processing. That is, the range compression is accomplished on Earth.

---

[1] Presumming denotes the process of averaging corresponding range bins from subsequent sweeps in order to lower the azimuth bandwith prior to the actual image compression. Initial radar data is not a TV like image, but a hologram.

[2] Mixed integration processing forms images from several azimuth channels, then non-coherently integrates these to form a composite image with improved statistics. This could be done on the spacecraft or on Earth if the several azimuth channels were telemetered.

Range resolution is referred to as "nominal" because the ground range resolution is a function of the incidence angle of the radar beam at each point on the surface. The slant range resolution is fixed by the transmitted pulse and receiver bandwidth. Reference designs provide for a 50 meter fixed slant range resolution which converts to a varying ground range resolution depending on the range of incidence angles over the swath width (see Section IV, Volume III, Radar Parametric Studies for further details on this characteristic).

Maximum presumming refers to that processing mode (in azimuth) which accomplishes the maximum amount of data averaging (lowest data volume) without degrading the final azimuth resolution below a nominal 100 meters. Range resolution is a fixed 50 meters in slant range and a nominal 100 meters in ground range. Final resolution is $\rho_a = \rho_r = 100$ meters.

Minimum presumming refers to that level of azimuth data averaging which preserves the potential for 33 meter resolution in azimuth. Such data can be processed to this resolution or averaged non-coherently to the 100 meter resolution with a linear (i.e. 3 to 1) improvement in the final image (variance/mean^2) statistic. (See Volume III, Section V.)

Nominal range resolution relayed is 100 meter in ground range. This 33 meter azimuth resolution is a good fit with system capability, but further study should examine the "best" resolution goal desired from the timely evaluation of science and exploration objectives.

Fine Resolution Mode - A telescope mode is recommended for all missions which provides for an optional increased range bandwidth that allows $\rho_a = \rho_r = 33$ meters after compression. This mode should be selectable at will and would provide the higher resolution over a shorter swath (when mapping the same range of true anomaly), or full

swath with a shorter range of true anomaly.

The basis for telescope mode implementation for this study is that mass storage and communications would be nominally sized for one of the basic processing modes which would include telescope mode mapping at the expense of planetary coverage requirements. Should the mission be sized to account for some degree of telescope mode mapping without loss of coverage, then the mass storage and communications would be sized accordingly. Additional basic study is required to determine the requirements for telescope mapping beyond "The best you can get." Such studies would consider atmospheric turbulence, suspended particulate matter and densities, etc.

Mixed integration processing is the third reference onboard processing mode. This mode makes use of the excess doppler (azimuth) bandwidth to form an image based on many azimuth channels. The images from the many channels are then combined non-coherently to form a composite image of higher potential quality than those obtained by processing a single channel. This technique is carried because of the possible image quality advantage, but further study is needed to determine the engineering feasibility of incorporating a remote mixed integration processor on a spacecraft. However, in this case, all image corrections would not be accomplished on the spacecraft. Most standard television type enhancement and rectification would be accomplished on Earth.

Reference Antenna Size

The reference antenna size for the basic example design (e = 0.5, map every orbit) utilizing Configuration C spacecraft is a 3-meter diameter communications antenna operating at X-band. This antenna is very similar to the Pioneer F & G antenna

except that it would be articulated in two degrees of freedom. Attitude control studies (Volume III, Section VI) indicate that relative minor improvements over the current Viking Orbiter baseline are required to meet the positive requirements at X-band.

The antenna sizes shown for Configuration A are those determined by radar mapping requirements and shared by the communications subsystem.

Feasibility Testing Through Example Implementations

Subsystem feasibility is probed in this study by establishing candidate subsystem implementations based on the derived requirements of Volume III and comparing the component specifications required to technology status. Where technical risk is marginally high, performance enhancements options are available to reduce the demands on critical subsystem items.

Baseline Mission for Comparison - The reference baseline for the implementation comparisons of Tables V-1 through V-8 is mapping every orbit (1:1) from an orbit of 0.5 eccentricity. The values included in the tables for eccentricities of 0.3 (1:2) and 0. (1:5) are done so for comparative purposes so that the variation of requirements on data handling and communications can be understood. The emphasis is on the design at eccentricity of 0.5. The reference design can relay high quality data at 100 meter resolution at mission end. The tables are discussed in detail below.

The baseline data channel is uncoded and coherent due to the required high data rates and DSN ground station bandwidth constraints. It is noted that the required power can be lower if the data channel were encoded, and such an option is listed as a desirable performance enhancement item. Since decoders of high coding

Table V-1 Configuration C Spacecraft Specifications--Maximum Presumming - 1

	e = 0	e = 0.3	e = 0.5
Swath width (km) at equator	65	44	36
Map strategy	1:5	1:2	1:1
Map duration (degrees true anomaly)	180	180	180
Map time (hr)	0.80	0.85	0.88
Antenna (m) - Parabolic - Furled	3	3	3
Net comm. window (hr)/cycle	3.84	2.32	1.9
Maximum Presumming/4 Bit Quantization			
Data volume/cycle (MBit)	1080	880	883
Data rate to recorder (BPS)	368K	285K	251K
Required relay data rate (BPS)	76.8K	105K	129K
RF Power-TWTA (watt)	52.2	71.5	88
Prime power for TWTA (watt)	146.5	286	352
Support Subsystem Power (W)			
Recorder	45	45	45
Data control/annotation	44.3	44.3	44.3
Command reception	29.3	29.3	29.3
Engineering T/M	5	5	5
Articulation/control	35.3	35.3	35.3

NOTES:

1. Reference maximum data rate (BPS) uncoded, coherent, detection, 100 W RF
2. Signal acquisition at low power coincident with mapping at e = 0.35
3. Nominal resolution: $\rho_a=\rho_r=100$ m

Table V-2 Configuration C Spacecraft Specifications--Maximum Presumming - 2

	e = 0	e = 0.3	e = 0.5
Swath width (km) at equator	65	44	36
Map strategy	1:5	1:2	1:1
Map duration (degrees true anomaly)	180	120	110
Map time (hr)	0.80	0.56	0.44
Antenna (m) - Parabolic - Furled	3	3	3
Net comm. window (hr)/cycle	3.0	2.82	2.46
Maximum Presumming/4 Bit Quantization			
Data volume/cycle (MBit)	1080	590	446
Data rate to recorder (BPS)	368K	285K	251K
Required relay data rate (BPS)	100K	58K	50.5K
RF Power-TWTA (watt)	68.3	39.6	34.5
Prime power for TWTA (watt)	273.2	158.4	138.0
Support Subsystem Power (W)			
Recorder	45	45	45
Data control/annotation	44.3	44.3	44.3
Command reception	29.3	29.3	29.3
Engineering T/M	5	5	5
Articulation/control	35.3	35.3	35.3
NOTES:			
Reference maximum data rate (BPS) uncoded, 100 W RF maximum	146.5K	146.5K	146.5K
Nominal potential resolution $\rho_a=\rho_r=$ 100 meter			

Table V-3 Configuration C Spacecraft Specifications--Maximum Presumming - 3

	e = 0	e = 0.3	e = 0.5
Swath width (km) at equator	65	44	36
Map strategy	1:5	1:2	1:1
Map duration (degrees true anomaly)	180	120	110
Map time (hr)	0.80	0.56	0.44
Antenna (m) - Parabolic - Furled	4	4	4
Net comm. window (hr)/cycle	3	2.82	2.46
Maximum Presumming/4 Bit Quantization			
Data volume/cycle (MBit)	1080	590	446
Data rate to recorder (BPS)	368K	285K	251K
Required relay data rate (BPS)	100K	58K	50.5K
RF Power-TWTA (watt)	37.9	22	19.2
Prime power for TWTA (watt)	151.6	88	76.8
Support Subsystem Power (W)			
Recorder	45	45	45
Data control/annotation	44.3	44.3	44.3
Command reception	29.3	29.3	29.3
Engineering T/M	5	5	5
Articulation/control	35.3	35.3	35.3
NOTES:			
1. Reference maximum rate available (BPS) uncoded coherent detection 100 W RF maximum	264K	264K	264K
2. Nominal $\rho_a=\rho_r=$ 100 m			
3. Comm window @ peak occultation			

Table V-4 Configuration C Spacecraft Specifications--Minimum Presumming - 4

	e = 0	e = 0.3	e = 0.5
Swath width (km) at equator	65	44	36
Map strategy	1:5	1:2	1:1
Map duration (degrees true anomaly)	180	120	110
Map time (hr)	0.80	0.56	0.44
Antenna (m) - Parabolic - Furled	4	4	4
Net comm. window (hr)/cycle	3	2.82	2.46
Maximum Presumming/4 Bit Quantization			
Data volume/cycle (MBit)	3200	1650	1325
Data rate to recorder (BPS)	1104K	855K	753K
Required relay data rate (BPS)	296K	163K	150K
RF Power-TWTA (watt)	112	61.8	57
Prime power for TWTA (watt)	448	247.2	228
Support Subsystem Power (W)			
Recorder	45	45	45
Data control/annotation	44.3	44.3	44.3
Command reception	29.3	29.3	29.3
Engineering T/M	5	5	5
Articulation/control	35.3	35.3	35.3
NOTES:			
1. Ref. maximum rate available (BPS) uncoded, coherent detection 100 W @ RF max from TWTA assy.	264K	264K	264K
2. Nominal resolution potential: ρ_a=33m, ρ_r = 100 m			

Table V-5 Configuration A Spacecraft Specifications -- Maximum Presumming

	e = 0	e = 0.3	e = 0.5
Swath width (km) at equator	65	44	36
Map strategy	1:5	1:2	1:1
Map duration (degrees true anomaly)	180	120	110
Map time (hr)	0.80	0.56	0.44
Antenna (m) - Parabolic - Furled	1 x 4	2.9 x 4.57	3.5 x 3.66
Net comm. window (hr)/cycle	2.42	1.54	1.82
Maximum Presumming/4 Bit Quantization			
Data volume/cycle (MBit)	1080	590	446
Data rate to recorder (BPS)	368K	285K	251K
Required relay data rate (BPS)	124K	107K	68.5K
RF Power-TWTA (watt)	142	38.5	25.6
Prime power for TWTA (watt)	568	154	102.4
Support Subsystem Power (W)			
Recorder	45	45	45
Data control/annotation	44.3	44.3	44.3
Command reception	29.3	29.3	29.3
Engineering T/M	5	5	5
Articulation/control	35.3	35.3	35.3
NOTES:			
1. Ref. maximum data rate (BPS) uncoded, 100 W RF maximum	87.3K	278K	267K
2. Nominal resolution $\rho_a=\rho_r=100$ m			

Table V-6 Configuration A Spacecraft Specifications -- Minimum Presumming

	e = 0	e = 0.3	e = 0.5
Swath width (km) at equator	65	44	36
Map strategy	1:5	1:2	1:1
Map duration (degrees true anomaly)	180	120	110
Map time (hr)	0.80	0.56	0.44
Antenna (m) - Parabolic - Furled	1 x 4	2.9 x 4.57	3.5 x 3.66
Net comm. window (hr)/cycle	2.42	1.54	1.82
Maximum Presumming/4 Bit Quantization			
Data volume/cycle (MBit)	3200	1650	1325
Data rate to recorder (BPS)	1104K	855K	753K
Required relay data rate (BPS)	368K	298K	202K
RF Power-TWTA (watt)	422	107	75.8
Prime power for TWTA (watt)	1688	428	303
Support Subsystem Power (W)			
Recorder	45	45	45
Data control/annotation	44.3	44.3	44.3
Command reception	29.3	29.3	29.3
Engineering T/M	5	5	5
Articulation/control	35.3	35.3	35.3

NOTES:

1. Ref. maximum rate available (BPS), uncoded, coherent detection 100 W @ 8448 MHz from TWTA assy.
2. Nominal resolution potential (ground range): ρ_a=33m, ρ_r=100m
3. Comm window during peak occultation

Table V-7 Configuration B Spacecraft Specifications - Maximum Presumming

	e = 0	e = 0.3	e = 0.5
Swath width (km) at equator	65	44	36
Map Strategy	1:5	1:2	1:1
Map Duration (degrees true anomaly)	180	120	110
Map Time (hr)	0.80	0.56	0.44
Antenna (m) - parabolic furled	3	3	3
Net comm. window (hr)/cycle	2.42	1.54	1.22
Maximum Presumming/4 Bit Quantization			
Data volume/cycle (MBit)	1080	590	446
Data rate to recorder (BPS)	368	285	251
Required relay data rate (BPS)	124	107	102
RF power-TWTA (assy)-(watt)	84.5	38.5	69.5
Prime power for TWTA (watt)	338	154	278
Support Subsystem Power/(W)			
Recorder	45	45	45
Data control/annotation	44.3	44.3	44.3
Command reception	29.3	29.3	29.3
Engineering T/M	5	5	5
Articulation/control	35.3	35.3	35.3

Table V-8 Configuration B Spacecraft Specifications - Minimum Presumming

	e = 0	e = 0.3	e = 0.5
Swath width (km) at equator	65	44	36
Map strategy	1:5	1:2	1:1
Map duration (degrees true anomaly)	180	120	110
Map time (hr)	0.80	0.56	0.44
Antenna (m) - parabolic furled	3	3	3
Net comm. window (hr)/cycle	2.42	1.54	1.22
Minimum Presumming/4 Bit Quantization			
Data volume/cycle (MBit)	3200	1050	1325
Data rate to recorder (BPS)	1104	894	906
Required relay data rate (BPS)	368 K	298 K	302 K
RF power-TWTA (assy)-(watt)	251	203	206
Prime power for TWTA (watt)	1004	812	824
Support Subsystem Power/(W)			
Recorder	45	45	45
Data control/annotation	44.3	44.3	44.3
Command reception	25.3	25.3	25.3
Engineering T/M	5	5	5
Articulation/control	35.3	35.3	35.3
NOTES:			
1. Ref. maximum data rate @ 1.73 AU (KBPS); uncoded, coherent detection, $p(e) \sim 5 \times 10^{-3}$	146.5	146.5	146.5

efficiency ($\geq$50%) are not currently available within the DSN, the high data rates call for a basic implementation of an uncoded channel. Encoding is discussed in Volume III, Section V with a conservative definition of the power benefit when typical short constraint length, high efficiency codes are used.

The powers presented represent those required to meet maximum Earth-Venus range and peak occultation characteristics. This is reasonable since peak occultation and maximum range are nearly coincident. It is recognized that for the eccentricity = 0.5 orbit, the duration of occultation is the least.

A Recommended Mission Concept - Though there are many configurations presented in the previous tables which appear feasible at reasonable cost and technical risk, it is possible to recommend an approach to the mission which traverses the path of alternatives at an equitable cost or risk to all spacecraft subsystems. For the data handling and communications considerations, this recommended concept is shown below in Table V-9. This recommended concept requires data rates for the normal 100 meter resolution data which do not excessivly impact the DSN receiving and ground storage capability. Even with the included coding (high code rate) the resultant symbol rates appear reasonable. The onboard communications TWTA is specified at a power level compatible with current technology and not considered excessive. The pointing and maintenance of the 3-meter high gain antenna is compatible with the Viking '75 systems with minor improvements. The mass storage requirement is fully compatible with the proposed Viking orbiter/advanced Mariner technology at bandwidths $\leq$1 MHz and capacity of $\leq$ 1300 MBits.

The operating communications frequency is X-band which should be

Table V-9 Recommended Concept - Data Management/Communications

Spacecraft:	Configuration C (dual antenna, articulated solar panels)
Map Strategy:	1:1
Eccentricity:	0.5
Duration:	250 Days
Communications:	
Antennas:	3 meter, furlable, articulated 2 degrees of freedom Low gain and medium gain horns for telemetry and command.
Frequency:	X-band ($\sim$ 8448 MHz)
Data Channel:	Coded, convolutional (rate 1/2, short constraint length). Nominal rate 130 KBPS (260 KSPS) max.
Power Amplifier:	TWTA $\sim$ 50 watts @ X-band.
Radar Processor:	Multimode Presummer in Azimuth
	(a) 100 m x 100 m normal resolution (end of mission)
	(b) 33 m x 100 m selected resolution (near arrival)
	(c) 33 m x 33 m selectable fine resolution (any time)
	4 Bit quantization each; amplitude, phase
Mass Storage:	Digital Tape
	Bandwidth - 2 MHz Capacity - 1000 MBit
Command/Tracking:	Basic Viking/Mariner command reception.
	Doppler tracking.
Ground Stations:	3 Stations, 64 m @ X-band.
	High rate intra-station data relay.
	Central radar data reduction facility.

available in the DSN with current plans for early 1980s capability. Three ground stations with 64 meter dishes appear necessary for the full 250 days at Venus.

The data reduction is feasible with a digital Earth based facility. An optical processor is not necessarily required since the swath widths of the orbital mapping mission are relatively short compared to resolution dimensions.

The recommended radar processor is a presummer with multiple modes. The modes would include a) presum to 33-meter azimuth resolution (fine resolution mode), b) presum to 100-meter resolution for normal processing. Range data would be unprocessed on the spacecraft. Final image formation would be on Earth. Quantization is to 4 bits each of amplitude and phase, with annotation of radar receiver automatic gain control.

Tables V-1 through V-8 present example subsystem specifications for the baseline case of 0.5 eccentricity, mapping every orbit and compares them to requirements for e = 0.3 (1:2) and e = 0 (1:5). There are example specifications which can be relaxed in certain areas through the incorporation of one or more "performance enhancement items" identified in a later paragraph.

Table V-1 shows characteristics of a Configuration C spacecraft mapping cycle with a reference three meter parabolic, articulated communications antenna. The average RF power required with no data encoding is considered feasible in the time frame of the mission and marginal today for the e = 0.3 and 0.5 cases. The power in all cases, however, is considered feasible currently if data encoding were employed allowing the RF powers to be approximately

halved[1]. The recorder is within the capacity and bandwidth of the proposed Viking '75 system. For Configuration C to map a full 180 degrees true anomaly, special radar antenna techniques are required (such as those described in Volume III, Section IV) including a combined variable side look angle and multiple beamwidth antenna. Data relayed are at 100-meter resolution in range and azimuth with the maximum presumming option. RF powers shown were derived at maximum Earth-Venus slant range and with maximum Earth occultation impact. This is reasonable since, for the 250 day mission, maximum Earth occultation occurs at nearly maximum Earth-Venus slant range.

Table V-2 shows Configuration C in the 0.5 eccentricity orbit with comparison to eccentricity of 0.3 and 0. This case employs the simple radar antenna concept.

Table V-3 shows Configuration C relaying 100-meter resolution data but including the benefit of a larger 4-meter diameter communication antenna and the simple N radar antenna. The major impact of this antenna is an advanced attitude control concept. The coverage is 180 degrees true anomaly only in circular orbit. With this example the RF power with uncoded data is through completely feasible today. Again the derivation of RF power at maximum Earth-Venus range with peak occultation is imposed because these conditions occur simultaneously near mission (250 day reference) end.

Table V-4 shows Configuration C relaying potentially higher

---

[1] Optimal further reduction is possible at e = 0.5 by designing with an optimistic performance margin and neglecting the peak Earth occultation characteristic duration at some increase in risk.

resolution data in azimuth (33-meter res.) and the nominal 100-meter resolution in range. The antenna shown is 4 meters which requires an advanced ACS concept over the Viking '75 orbiter to meet the pointing requirement of 8.9 mrad at X-band. The RF power in circular orbit is unfeasible, but at eccentricities of 0.3 and 0.5 appears feasible. Using an encoded data channel (such as convolutional, rate 1/2, Viterbi decoding), the circular orbit power requirement becomes feasible.

Tables V-5 and V-6 show characteristics of Configuration A (single articulated antenna) over the example eccentricities. This configuration has a shared radar and communications antenna. It is noted that antennas of these dimensions cannot be pointed with sufficient accuracy for X-band operation with the current Viking Orbiter ACS concept. Additional precision would have to be incorporated to meet the communications requirement of these designs for the required X-band communications. This configuration is not favored because of the complicated antenna design necessary to meet both the radar and communications requirement, the need for advanced Viking Orbiter attitude control and the loss in communications time for antenna reorientation each mapping cycle. This configuration is assessed to have a higher risk than the preferred configuration. If the large antennas could be pointed, the RF power is reasonable except for circular orbit where channel encoding would be necessary.

Table V-8 shows that the RF power for Configuration A is unfeasible for relaying higher resolution (ρ_a = 33m, ρ_r = 100 m) data even with the benefit of channel encoding. This emphasizes the lack of performance flexibility and growth potential of this spacecraft

relative to the preferred configuration C.

Tables V-7 and V-8, for completeness, show the study results of investigations of an intermediate Configuration B spacecraft which has a fixed radar antenna and solar panels, and an articulated communications antenna of 3 meters. This configuration requires excessive rf power in all cases, is the most complicated in light of orbital maneuvers required to accomplish the mission, and is unnecessarily complex for the relative performance it offers.

In summary, Configuration C is shown to be the most flexible and possesses the greatest growth potential since it can accomplish the mission with reasonable data rate and power and with good growth margin. Configuration A can accomplish some missions, but has a complicated interrelated radar and communications antenna design requirement, and in most cases, the most complex communication data channel. The intermediate Configuration B just does not compete since the flexibility of dual antennas is not sufficiently exploited to justify this feature.

Comparative Evaluations and Technology Assessments

These paragraphs will summarize the relative performance potential of the basic spacecraft configurations which have evolved from this study relative to data management and communications characteristics. These comments are directed to the major elements of the subsystem identified in the introduction to this section and Figure V-9.

The discussion will identify salient spacecraft interactions and their effect on data management/communications subsystem speci-

fications. These primary interactions are power, thermal, dynamic, radiation, reliability, for the Venus mapper mission time requirement.

Subsystem Implementations Compared by Spacecraft Configuration - The study has considered a number of spacecraft candidate configurations for the radar mapping mission (Volume III, Section VI). Two basic configurations, denoted "C" (dual antennas, articulated solar panels) and "A" (single shared articulated antenna, fixed solar panels), survived the system evaluation sieve to remain as viable mission candidates. A third configuration ("B" configuration spacecraft) employing dual antennas and fixed solar panel also survived initial evaluations but does not provide sufficient benefit of dual antennas to be carried to the level of definition of the Configuration C spacecraft. System descriptions of these basic spacecraft types are found in Sections IV, V, VI in Volume II and Section VI in Volume III. Paragraphs of this section following below will discuss communications antenna vs configuration; communications power versus configuration; radar processing versus configuration; data mass storage versus configuration.

The specification of a communications antenna is straight forward with the dual antenna Configuration C spacecraft; communication design is not constrained by the radar mapping antenna constraints. Configuration C offers the greatest flexibility and the highest potential science data return of any configuration considered. Configuration A can do the nominal job of relaying the $\rho_a=\rho_r=100$ m data over the entire mission only when the mapping strategy allows an antenna with an area on the order of ≈ 9 m^2 or greater. This corresponds to the equivalent of 3.5 m diameter or greater parabolic antenna.

The Configuration B spacecraft offers the flexibility of employing a larger communication antenna to offset the penalties made by its requiring larger attitude maneuvering times, but requires excessive performance enhancement features to compete with either Configuration C or A.

Employing X-band communication ($F_o' \approx 8448$ MHz), the upper limit on parabolic antenna diameter is about 4 meters if an advanced attitude control and platform pointing concept is used without active radio frequency antenna pointing techniques. The desirability of employing larger communications antennas is offset by the requirement for attitude pointing precision in excess of that of the proposed Viking Orbiter class ($\sim$13 mrad). Attitude control parametric studies (Section VI, Volume III) have shown that by employing advance pointing concepts antennas up to 10 meters (parabolic) could probably be pointed with the aid of active radio frequency interferometric (vis advanced Pioneer Conscan) antenna orientation systems.

With up to 100 watts (CW) at X-band available for the communications amplifier unit, the 4 meter diameter parabola can provide significant increased design flexibility with Configuration C over other configurations.

The communication power required is potentially the highest with Configuration A (single antenna) although it is possible to identify an approach (viz e = 0.5, mapping every orbit) using a large radar antenna which allows nominal communication power at the expense of surface coverage. Even with a coding gain of approximately a factor of two or better due to relaxed signal-to-noise requirements, the communication power is potentially excessive

with the single antenna spacecraft because the radar and communications implementations are locked together through the antenna. Many tractable solutions yielding good quality data remain possible, however, with this spacecraft only, when the radar requires a large antenna. Further, mapping is constrained to less than 180 degrees argument of periapsis with Configuration A while a dual antenna spacecraft potentially maps 180 degrees argument of periapse.

The communications power is potentially the least with Configuration C for full coverage. The power requirement is lowered (over the Configuration A) by an increased time for communications (no attitude maneuvering penalty) and the flexibility to provide the largest antenna which can be oriented for communications. Since the communication antenna is continuously Earth oriented with Configuration C, data from mapping a full 180 degrees argument of periapse can be relayed at nominal radio frequency power employing only a 3 meter (reference) diameter communication antenna. When the long mission duration is considered, the RF amplifier power should be kept as low as possible, preferably on the order of 50-80 watts maximum at X-band based on current technology assessments.

The preferred policy for radar processing is to average (presum) the data on the spacecraft to the desired azimuth resolution, but relay higher resolution (less presumming) azimuth data whenever possible such as for the first 80 days of the mission, or during times when no occultation exists near the beginning of the mission. This policy is the same with all configurations shown. However, since Configuration C can relay more data at less power, the radar processor is potentially the simplest with this configuration since less data averaging is possible with this configuration.

Due to the restrained mapping (less than 180 degrees argument of periapse) with Configuration A, the temporary storage associated with a presum processor is the least at the expense of reduced science return potential compared to the preferred spacecraft.

The incorporation of mixed-integration processing (Section V - Volume III) would provide the greatest benefit to the single antenna Configuration A since this spacecraft is most performance limited. However with mixed integration processing aboard Configuration C the communications antenna and power would be correspondingly reduced while recovering high quality surface images.

A digital mass storage system to meet the radar data requirement can be met equally well with all configurations, and does not represent a system impact across configurations. The study recommends that the radar data be stored entirely digitally. Storage capacities for alternative processing options are presented in Volume III, Section V, and can be met with currently identifiable digital storage machines. The major concern with the digital tape machine is its long life reliability performance. Further study in this area would determine the need for additional redundancy to meet the needed reliability.

Summarized as Table V-10 are salient data management/communications characteristics as they vary according to the configurations which remain feasible. Most significant is that Configuration C allows the greatest flexibility in overall design (antennas are optimized separately for radar and communications), the greatest surface coverage, and best quality data at reasonable implementations. Configuration A can accomplish a respectable job with less overall coverage when the radar requires an antenna of area $\geq 9\ m^2$. A selectable telescope mode is possible with all configurations, but only Configuration C has the potential of not sacrificing overall coverage for the telescope feature.

Table V-10 Data Handling/Communication Subsystem Implementation Comparison

Data Management/ Communications Item	Configurations		
	Configuration C	Configuration A	Configuration B
Antenna	Independent from radar design Size limited only by pointing ability and weight Simplest lightest weight D $\leq$ 4m Advanced Viking class articulation. D $\leq$ 10 m new ACS + active pointing.	Locked to radar design. Range dimension limited by radar Complex antenna design; requires reflector type radar antenna for bandwidth Size limited by radar & ACS to $\leq$ 3.0 m	Independent from radar Larger than "preferred" to offset attitude maneuvering penalties. D $\leq$ 4 m uprated Viking. D $\leq$ 10 m - new ACS + active pointing.
RF Power @ X-Band	Potentially minimal $\leq$ 50 watts/3 m antenna, $\rho_a = \rho_r =$ 100 m Lower due to no ACS maneuver & possible comm during map.	Feasible only when radar requires larger ($\sim$3.5 m) Mutually exclusive mapping & comm. $\leq$ 100 watt	Full benefit of two antennas not possible due to ACS & solar arr'mt. $\leq$ 100 watt
Data Storage	Digital (tape)--largest volume potential, largest coverage	Digital (tape)--lowest volume lowest coverage.	Digital (tape)--medium volume, full planet coverage.
Radar Processor Potentially Best Res.	Minimum presumming: full coverage, 4 bit, complex $\rho_a' = 33$ m, $\rho_r = 100$ m	Maximum presumming, less coverage, 4 bit, complex.	Minimum presumming: less coverage, 4 bit, complex.
Auxiliary Science Recorded	Radar altimeter. Radar AGC. Eng. T/M.	Radar altimeter. Radar AGC. Eng. T/M.	Radar altimeter. Radar AGC. Eng. T/M.
Telescope Mode	Selectable: greatest time $\rho_a = \rho_r = 33$ m (nominal)	Selectable: least time $\rho_a = \rho_r = 33$ m (nominal)	Selectable: greater time $\rho_a = \rho_r = 33$ m (nominal)

TECHNOLOGY ASSESSMENTS/CONCERNS

In light of the set of derived requirements (Volume III) and feasibility testing through example implementations (Volume II), technology concerns are identified and discussed in this paragraph. These assessments relate to the major components and elements of the data management/communications system :

1. on-board radar data processor
2. mass storage
3. communications power amplifier (TWTA)
4. communications antenna
5. communication data channel
6. deep space network reception equipment

On-Board Data Processor

The recommended approach based in current technology is to perform presumming (data averaging) with no focusing on the spacecraft. (Final image formation would be done on earth). This could be implemented in solid state and can function reliably with relatively low power consumption. It is estimated that a presummer could negotiate 36 km swaths and consume less than 20 watts of power. The implementation could be based on MOSFET MSI and LSI technology.

Further study is recommended to determine the feasibility of implementing a mixed integration processor (image formation) on the spacecraft. It is currently assessed that the power could exceed 100 watts at a weight in excess of 50 kg for an image processor incorporated in the spacecraft. Image quality is potentially best with the non-coherent integration characteristic of the mixed-integration processor for a fixed data relay rate to Earth. However, a single channel image can be relayed with less presum averaging to achieve similar image improvement (which is the current recommended approach).

Investigations of this study recommend that all final image conversion and corrections be performed on Earth since once a computation is done on the spacecraft it is irreversible. This approach would allow additional frequency domain enhancement processing to enhance special classes of signal returns which could be found such as separating surface return from low altitude atmospheric turbulence or suspended particle interference.

On-Board Data Storage

Currently, a digital magnetic tape unit of the capacity comparable to the Viking Orbiter's 1300 Mbits would be sufficient with small modification to the Venus Mapper Mission. The major question would be the long life (250 day) reliability of the tape unit. The Viking mission will establish the shorter term 90-120 day mission reliability. The power and weight of such a unit should be less than 50 watts and less than 25 kg which is not excessive for this mapping mission.

In the time frame of the mission the present developmental magnetic bubble technology would be a likely replacement. This technology would allow greater reliability, a lower weight and power based on advance technology reports available.

Temporary storage can be met with a semiconductor solid state technology at a reasonable power and weight impact with good reliability.

Radio Frequency Power Amplifier

Derived requirements of data rate and spacecraft limitations on antenna size, (approx. 3 meter for Viking Orbiter baseline ACS) and high rate relay time of approx. 2000 hours firmly establish an X-band link. The traveling wave tube amplifier (TWTA) currently is the only technology which can potentially meet the typical 50-100 watt CW radio frequency power requirements. Recent technical breakthroughs such as multiple stage depressed collectors, and beam control techniques have greatly improved tube reliability and operating efficiencies. Current vendor contact results in the assessment that 50-80 watts at X-band is currently space qualifiable with the necessary reliability, and that a space qualification program would be required for power requirement in the 50-150 watt range. Due to this assessment, communications designs are recommended which require power at the end of the mission of 80 - 100 watts CW or less. Based on future funded qualification programs the projected potential of the X-band space type TWTA could be approximately 200 watts CW based on the literature and vendors' projection.

The long life reliability at required power levels should be further investigated to determine its impact on design projection. Power levels of 20 watts have been demonstrated for more than 10,000 hours continuous use. Potential typical high power communication time for the mission is on the order of 1500 to 2000 hours out of the 6000 hour total mission.

Communications Antenna

Relatively lightweight, furlable parabolic antennas operating a X-band are currently available or qualifiable up to 3 meters. Diameters up to 10 meters are planned for space demonstration. The primary concern is the articulation control. The primary performance limiting factor is the ability to orient the antenna on the spacecraft platform to within the half power beam width and maintain it there for up to 2 hours maximum between inertial attitude reference updates and the ability to articulate such antennas on a spacecraft in 2 degrees of freedom. A three meter fixed antenna was demonstrated in space by the Pioneer Jupiter spacecraft. Advance antenna work planned by JPL and others are examining furlable antennas up to 10 meters. Workers at the JPL antenna development laboratory have demonstrated very acceptable operating efficiencies at X-band (and Ku band) on up to 6 meter diameter antennas, with laboratory models of furlable antennas. The reference antenna size for this study is taken as 3 meter (at X-band) due to the attitude control and pointing system constraints. Incorporation of active radio frequency

interferometry based on an extension of the Pioneer conscan technology meet the typical 7-9 mrad typical overall pointing accuracy requirement of the large X-band communications antenna with an advanced attitude control concept using control moment gyros.

Communications Data Channel

The required relay rates for the mission were determined by the data volume that must be relayed and the time available for relay. Most mission possibilities required at least 80 KBPS if, for example, a rate 1/2 convolutional code were employed (disregarding any tail bits) for the telemetering of nominal 100 meter resolution data. At those data rates the least impact on the DSN would be to relay uncoded data. However, since the use of antennas larger than approximately 3 meters for communications may result in excessive cost for the attitude control concept needed to maintain the error performance to within the HPBW, the recommended approach is to relax power requirements by incorporating data channel encoding, preferably convolutional. Decoding would be Viterbi to maintain decoding computational feasibility at these data rates based on current assessments.

Deep Space Network Reception Equipment

This study indicates that three ground stations with 64 meter antennas will be required for the full 250 days of the typical mission of this study. An X-band carrier frequency

is necesary. Further study should examine possible programming competition with program envisioned for the 1980s era. Baseband equipment must possess sufficient bandwidth of from 80 to 250 KHz for the reception of nominal 100 meter resolution data and up to 2500 KHz for finer resolution data. For the reception of data of finer azimuth resolution (viz 33 meter) the data rates would be greater by a factor of three for this example. If 100 meter range resolution were maintained such data rates would be from 240 KHz to 750 KHz, or within the projected DSN capabilities for the 1980 decade. On-site recording must handle from 1000 to 3000 Mbit per day for nonredundant recording at the ground station. If the planned optical recording equipment is implemented this will pose no major problem.

Intra-station relay at a typical 6 MBPS (commercial television link would require about 9000 Mbit/(6 Mbit/sec x 3600 sec/hr) = 0.42 hr for relay to a central data processing facility.

Technology Balance Sheet

Summarized in Table V-11 are technology recommendations or conclusions compared on a "1974" and "1984" basis of assessment. Along with the recommendations is a collection of recommended continued technology development or continued study areas. This technology study has derived the requirements of the Venus Radar Mapping Mission and determined that data management and communications seems feasible for the relay of nominal 100 meter resolution data with reasonable modification of Viking Orbiter or

Table V-11 Technology Balance Sheet--Data Management & Communications Technology Conclusions/Recommendations

Item	Technology Recommendation 1974	1984	Recommended Action
On-Board Radar Data Processing	Presum averaging: 100 m res. nominal.	Mixed integration 4-10 azimuth channels 100 m nom. res.	Feasibility study of mixed integration. Tradeoff quantization vs degree of presumming.
Data Storage	Digital: mag tape 1300 MBit. MOS/LSI (temp'ary)	Digital: mag bubble or tape.	Initiate long life qual program for magnetic tape. Determine magnetic bubble availability or other new technologies. Determine auxiliary data support requirements.
Communica'ns Antenna	3 meters (furlable)	$3 \leq D \leq 6$ meters (furlable)	Qualify articulated, furlable antenna at X-band. Further ACS studies to permit precision pointing. Develop active RF interferometer pointing sensor.
Power Amplifier at X-Band	80 watt	to 200 watt	Initiate qualification program for high power X-band TWTA for 250 day mission (2000-3000 comm. hours)
Data Channel	Uncoded, or coded (block or convo.)	Coded - convolutional	Provide high rate convolutional decoder for DSN stations.
Deep Space Network			
Ground Sta.	3-64 m (at X-band)	Same	Conduct program competition study for mission era.
Intra-sta. Relay	Wide band-retro satellite	Same	Incorporate X-band, wide band reception. Determine/recommend data intrastation relay sufficiency.
Record. on-site	Digital predict. Analog & Digital Post-detection.	Same	Incorporate advance high capacity recording on DSN
Central Processing	Digital: main reduction Optical "quick look" Digital Enhance't	Digital	Define requirements/preliminary design of SLAR Central Data Reduction Facility

Summarized in Table V-12 is a normalized quantitative evaluation of the impact of performance enhancement items. The reference configuration is based on the following parameters.

Mapping:	Mapping every orbit (1:1), e = 0.5
Antenna:	3-meter parabolic
Comm. Frequency:	X-band (8448 MHz)
Data Channel:	Uncoded, coherent, p(e) 0.5×10^{-3}
On-Board Processor:	Presummer, multimode $\rho_a = \rho_r = 100$ meter,
Mass Memory:	Digital tape (1080 MBit)
True Anomaly Mapped:	180 degrees per cycle

Summarized in Table V-13 are the technology, risk and cost impact due to a number of identified performance enhancement items. These enhancement items include coded data channel (rate 1/2, convolutional, short constraint length typically), larger antenna radar on-board processor type, orbital strategy (multiple orbit cycles).

From the standpoint of image quality, the most desirable enhancement option footed in today's technology is the 4 meter antenna, coded data channel, and minimum presumming with an on-board processor. Pending further feasibility study of an on-board mixed integration processor (image formation), the most desirable enhancement based in future technology is that processor with the larger antenna and coded data channel. The significant penalty of the 4 meter antenna at X-band is the requirement of an advanced (over Viking Orbiter) attitude control concept (yielding a total pointing error on the order of 9 mrad total).

Table V-12 Performance Enhancement Alternatives Over Reference Configuration

	Antenna Communications(m)	RF Power (watt)	Data Channel[1]	On-Board Processor for Radar	Mass Memory
Reference Configuration[2]	3	88	Uncoded	Max. presumming $\rho_a=\rho_r=100$ m	1080 MBit
(1) Coded Data Channel	3	44	Coded [3]	ρ_a = m = 100 m	1080 MBit
(2) Larger Antenna	4	49	Uncoded	$\rho_a=\rho_r$= 100 m	1080 MBit
(3) Minimum Presummed Data	3	264	Uncoded	ρ_a'=33m, ρ_r=100m	3200 MBit
(4) Coded Data Larger Antenna	4	25	Coded	$\rho_a = \rho_r$ = 100 m	1080 MBit
(5) Minimum Presumming & Coded Data	3	132	Coded	ρ_a' = 33 m, ρ_r = 100 m	3200 MBit
(6) Minimum Pre summing Larger Ant. Coded Data	4	73.5	Coded	ρ_a' = 33 m ρ_r = 100 m	3200 MBit
(7) Smaller Ant. Coded Data	2	54.5	Coded	$\rho_a = \rho_r$ = 100 m	1080 MBit

(1) Coherent, p(e) 5×10^{-3}

(2) Mapping 1:1, ecc = .5

(3) Convolutional, rate 1/2, K=8

Table V-13 Performance Enhancement Item Impact Assessment

Enhancement Item	Advantage	Impact	Cost	Development Risk	Performance Risk
Data Channel Coding	T/M power on S/C	Increased symbol rate	DSN update A	L	L
		Develop hi rate decoder	L	L	L
Larger Antenna	T/M power on S/C	Develop new ACS on	M	L	M
		lower T/M power	L	L	L
Less Presum Processing	Better image quality	Higher relay rate	H	M	M
		High S/C T/M power	M	L	M
Mixed Integration Image	Best image quality overall.	Same data rate	L	L	L
		Complex processor on S/C	M	M	H
		Heavy, powerful			
Lower Eccentricity (multiple orbits)	Lower S/C power T/M	Propulsion or weight limited S/C	M	L	L

Reference configuration:

(1) Maximum presum processing

(2) Map 1:1, e = .5

(3) 3 meter antenna

(4) Uncoded data, coherent

(5) X-band carrier for comm.

Assessment Code:

L = Low

M = Medium

H = High

Mariner Jupiter/Saturn data handling and communications subsystem technology. Perhaps the most critical communication item in present technology is the X-band communications power amplifier (TWTA) if a power of 80 - 100 watts is required. However, if data channel encoding (preferably convolutional) is employed, the required power for the eccentric (e = 0.5) mission is within current qualified power levels of 20-40 watts at X-band. The reference radar processor is new in space, but a presum averaging processor is straightforward and not considered a significant technical risk. The mixed integration (image formation) processor using non-coherent integration of several (4-10) azimuth channels is considered feasible at a high technical risk currently and should be studied further.

Performance Enhancement Alternatives

This study has probed the characteristics of a radar mapping mission to Venus with an objective of determining technology requirements to accomplish 100 meter x 100 meter nominal resolution over nearly the entire planet. This section discusses alternative means of performance enhancement in the data management and communications area and assess their relative cost, development risk, and performance risk. An enhancement item can either reduce the spacecraft system impact (such as lower power, etc.) or provide even higher quality data than the already available good quality data provided by the reference mission.

VI. SPACECRAFT SYSTEMS

INTRODUCTION

The overall approach in conducting the study effort followed very closely the methodology that was used in performing the trade studies conducted during the first phase of the study.

The choice of the appropriate mission and systems design of an orbital radar mapper for Venus is much more interactive than most other unmanned planetary missions. The trade studies that constituted the first phase then, were aimed at meeting this challenge with lightweight, minimum cost, low risk technology systems. The large array of mission modes and systems options that were available for consideration produced a very large number of potential mission/system approaches that were worthy of investigation. This requirement necessitated that the study approach be designed to provide an early definition of the many potential mission/system approaches and a means for consistent screening and evaluation of alternates to arrive at the most promising concepts for further detailed analysis in this study phase. Maximum utilization of our parametric analyses conducted during the first phase of the study was made which allowed us to concentrate our efforts on three basic spacecraft designs. These three basic concepts then, utilized the results of the trade studies to determine the best options, or in lieu of any clear cut choices, the relevant factors were considered and a

conscious decision was made to use that particular concept. A comparative evaluation of these candidates, based on point design results, was then used to select a recommended Venus Radar Mapper Concept and leading alternative. These systems are described in detail in the following sections.

STUDY GROUND RULES AND GUIDELINES

Ground rules and guidelines were jointly established by SSD and the MMC Venus Radar Mapper study team just prior to the initiation of the second phase of the study. These ground rules are summarized in Table VI-1. Also, as preliminary results of the trade studies conducted during the first phase of the study were developed, a series of study generated ground rules evolved. These ground rules are tabulated in Table VI-2.

A general description of the spacecraft that were considered during this phase of the study as well as specific details of the baseline mission operations are delineated in subsequent portions of this section.

SYSTEM DESCRIPTIONS

System Overview

This section presents a summary of the Venus Radar Mapper spacecraft configurations that were studied. Specific details of the subsystems are presented in the subsequent portions of this section.

Table VI-1 SSD Study Directed Ground Rules

- Previous SSD and JPL study data to be used as basic reference data.
- Mission in mid to late 1980's.
- Mission science requirements have first priority.
- Viking/Mariner class spacecraft is basic design consideration with advanced spacecraft concepts where appropriate.
- Low cost missions to be prime consideration.
- Consider existing and new technologies as appropriate.
- Coverage and resolution (minimum)
  - 80% of surface at 1 km resolution.
  - 20% of surface at 100 m resolution.

Three spacecraft configurations were evaluated in depth. These three configurations fell into two major categories of design; these being, a shared antenna concpet, and a dedicated antenna configuration. Configuration A is representative of the shared antenna concept in which the same antenna is utilized for both mapping and transmission of data to Earth. Configuration B is the result of efforts to design a representative dedicated antenna configuration in which separate antennas are used for mapping and communication. Configuration C is also a dedicated antenna design, but unlike Configuration B it is inertially oriented which served to overcome some of the problems associated with Configuration B (e.g., excessive ACS propellant requirements, and the requirement to gimbal the Canopus tracker). Detail

Table VI-2 Study Derived Guidelines and Conclusions

- Orbit eccentricity of 0.50 preferred.
- Periapsis attitude of 400 km selected with polar orientation.
- VO '75 cold gas attitude control system selected.
- Articulated reflector antennas preferred.
- Shared antenna concept minimizes spacecraft integration problems.
- Solar array/battery system is recommended.
- Radiator/heat pipe thermal control concpet provides highly flexible thermal design.
- Space storable insertion propulsion system necessary for orbital eccentricities between 0.30 and 0.00.
- Off-loaded or stretched VO'75 propulsion system assumed for orbital eccentricities of 0.30 to 0.50.

descriptions of each of these spacecraft configurations will be found in the Structural Design portion of this section.

Table VI-3 summarizes the principal design features of the three configurations that were studied from the various alternatives on the basis of system analysis, mission design, design tradeoffs, and engineering judgment.

Table VI-3 Venus Radar Mapper Spacecraft Design Matrix

	CONFIGURATION A			CONFIGURATION B			CONFIGURATION C		
	0.00	0.30	0.50	0.00	0.30	0.50	0.00	0.30	0.50
Propulsion	Space Storable (2) 2670 N Engines	Stretched VO Type S/S (3) 1330N Eng.	Off-Loaded VO Type S/S (3) 1330N Eng.	Space Storable (2) 2670 N Engines	Stretched VO Type S/S (3) 1330N Eng.	Off-Loaded VO Type S/S (3) 1330N Eng.	Space Storable (2) 2670 N Engines	Stretched VO Type S/S (3) 1330N Eng.	Off-Loaded VO Type S/S (3) 1330N Eng.
Power	Fixed VO Type Panels + NiCd Batteries	Fixed VO Type Panels + NiCd Batteries	Fixed VO Type Panels + NiCd Batteries	Fixed VO Type Panels + NiCd Batteries	Fixed VO Type Panels + NiCd Batteries	Fixed VO Type Panels + NiCd Batteries	Tilted VO Type Panels + NiCd Batteries	Titled VO Type Panels + NiCd Batteries	Titled VO Type Panels + NiCd Batteries
Radar									
Antenna	Art. Reflector	←	Art. Reflector	Fixed Roll-out	←	Fixed Roll-out	Art. Reflector	←	Art. Reflector
Side Look Angle	Fixed 30°	←				Fixed 30°	Var. 10-50°	Var 10-50°	Var 10-50°
Swath Width	65 KM	44 KM	36 KM	65 KM	44 KM	36 KM	65 KM	44 KM	36 KM
Overlap	20%	←						→	20%
Wavelength	10 CM(S-Band)	←						→	10 CM (S-Band)
Coverage	90°	65°	55°	90°	65°	55°	55°	90°	90°
Strategy	N=5	N=2	N = 1	N=5	N=2	N=1	N=5	N=2	N=1
Comm & Data Handlg									
Antenna	Art. Reflector	←						→	Art. Reflector
Processing	Max Presumm.	Min. Presumm.	Min. Presumm.	Min. Presumm.	←			→	Min. Presumm.
Storage	Mag. Tape	←						→	Mag. tape
Frequency	X-Band	←						→	X-Band
RF Pwr (W)	100 Watts	←						→	100 Watts
Attitude Control	VO Type GN_2 Relocate Yaw Thrusters & Star Tracker	←	VO Type GN_2 Relocate Yaw Thrusters & Star Tracker	VO Type GN_2 + CMB's. Relocate Yaw Thrusters & Star Tracker	←	VO Type GN_2 + CMG's.Relocate Yaw Thrusters & Star Tracker	VO Type GN_2 Relocate Yaw Thrusters	←	VO Type GN_2 Relocate Yaw Thrusters
Thermal Control	Integral Radiators + Multilayer Insulation	←				Integral Radiators + Multilayer Insulation	Detached Radiator + Multilayer Insulation	←	Detached Radiator + Multilayer Insulation
Structure	Modified VO Bus Prop. Mod. Modified for Space Storables	Modified VO Bus, Prop. Tanks Stretched	Modified VO Bus,	Modified VO Bus Prop.Mod. Modified for Space Storables	Modified VO Bus. Prop. Tanks Stretched	Modified VO Bus	Modified VO Bus Prop. Mod. Modified for Space Storables	Modified VO Bus Prop. Tanks Stretched	Modified VO Bus

Mission Operations

A typical mapping strategy that will work throughout the mapping mission has to be determined to guarantee antenna travel and spacecraft design. For this reason antenna and spacecraft pointing was determined for six positions throughout the mapping mission as shown in Figure VI-1 for the shared antenna configuration. Configuration C will be discussed later.

This figure shows the position of the planets, Venus and Earth, at six positions along the typical Venus mapping mission. The corresponding positions of these planets are indicated by numbers, where positions 1 and 7 indicate the planet positions at the start and end of the mapping mission. Vectors are shown to indicate the Sun and Earth pointing direction. The spacecraft orbit was assumed to have an inertial orientation with no spacecraft perturbations. The side of the orbit that is mapped is indicated by shaded side of the planet. The spacecraft orientations are shown for the mapping and communication phases.

The spacecraft sketch with the shaded antenna shows the antenna orientation at the mapping extremities. During the mapping phase, the azimuth gimbal is commanded to be perpendicular to the orbital plane by a stored command. This stored command is calculated by Earth based computers and stored in the control computer to be used on their designated orbits. The elevation gimbal is controlled by the clutterlock system to point the antenna boresight along the zero doppler direction. The radar antenna rotates 180 degrees during the mapping phase.

At the end of the mapping phase, the antenna is rotated 90 degrees about the elevation gimbal to point in the ecliptic and the azimuth gimbal is commanded to point toward the Earth. Both

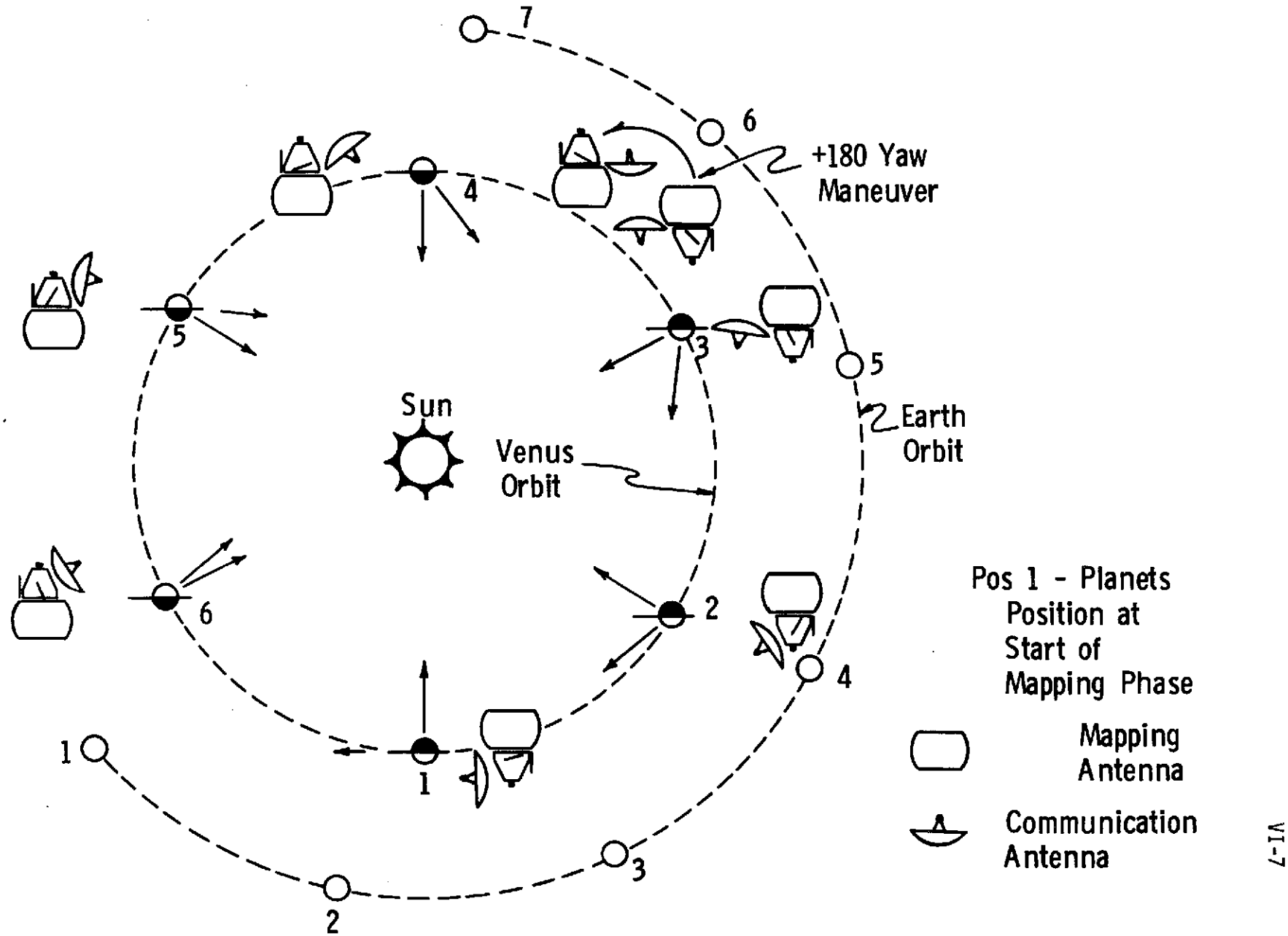

Figure VI-1 Typical Mapping Strategy
(Shared Antenna)

these commands are stored in the control computer (CC). These commands are calculated by Earth based computers and stored per orbit in the CC. As estimated time of 18 minutes is allowed for the Earth acquisition. The antenna has to be pointed toward the Earth within the beamwidth of the antenna by commands relative to an inertial coordinate system. The inertial reference has to be accurate enough to point the antenna within its beamwidth with a spacecraft 1/4 degree limit cycle. If very large antennas are used, then an automatic beam position pointing system may be needed to point the antenna more accurately than is possible with the attitude control system.

An equivalent period will be needed at the end of the communication phase to re-acquire the zero doppler line for the start of the mapping phase. Eighteen minutes were allotted for this phase also. The clutterlock system should be able to acquire and point the antenna along the zero doppler line (ZDL) in a fraction of a minute, if the antenna can be pointed within a degree of the ZDL. The clutterlock system will determine the initial pointing error within a few milliseconds; the initial acquisition time is determined principally by the time it takes to slew the antenna to the zero doppler direction.

The other spacecraft sketch on the figure shows the orientation during the communication phase. The vehicle can map and communicate until the spacecraft can no longer map the surface somewhere between planet positions 3 and 4. At this point the mapping side is changed to complete the mapping mission. Changing the mapping side has interesting mission augmenting

advantages because a certain portion of the surface is remapped on the second pass. Since the planet is mapped from different directions on the second pass, good stereo pictures can be obtained in the overlap areas. Additionally the data from the first pass can be processed to show where interesting topographic features are located. The spacecraft can then use its fine resolution mode to get high resolution pictures of these areas of interest. This overlap time can also be used for extra data transmission or battery charging time for additional flexibility to the mission. This configuration can be used to complete the mapping mission as shown in the last figure.

When the vehicle is occulted from the Sun, the vehicle is controlled by body mounted rate gyros in the pitch and yaw axis. The roll rate gyro is used to control the vehicle during Canopus acquisition.

Figure VI-2 shows the typical mapping strategy using Configuration C when separate antennas (dedicated antennas) are used to map and communicate. This figure shows the same elements that the previous figure showed. The spacecraft is always inertially oriented, so the vehicle roll axis is controlled to be perpendicular to the vehicle orbital plane. Since the vehicle is always inertially oriented, no modifications are required to be made to the Canopus sensor, except that the sensor has to be remounted to look down the edge of the south pointing solar panel similar to the other configurations. These modifications are discussed in the attitude control portion of this section. The orientations of the articulated solar panels are also shown in this figure. The mapping mission is conducted similar to the shared antenna

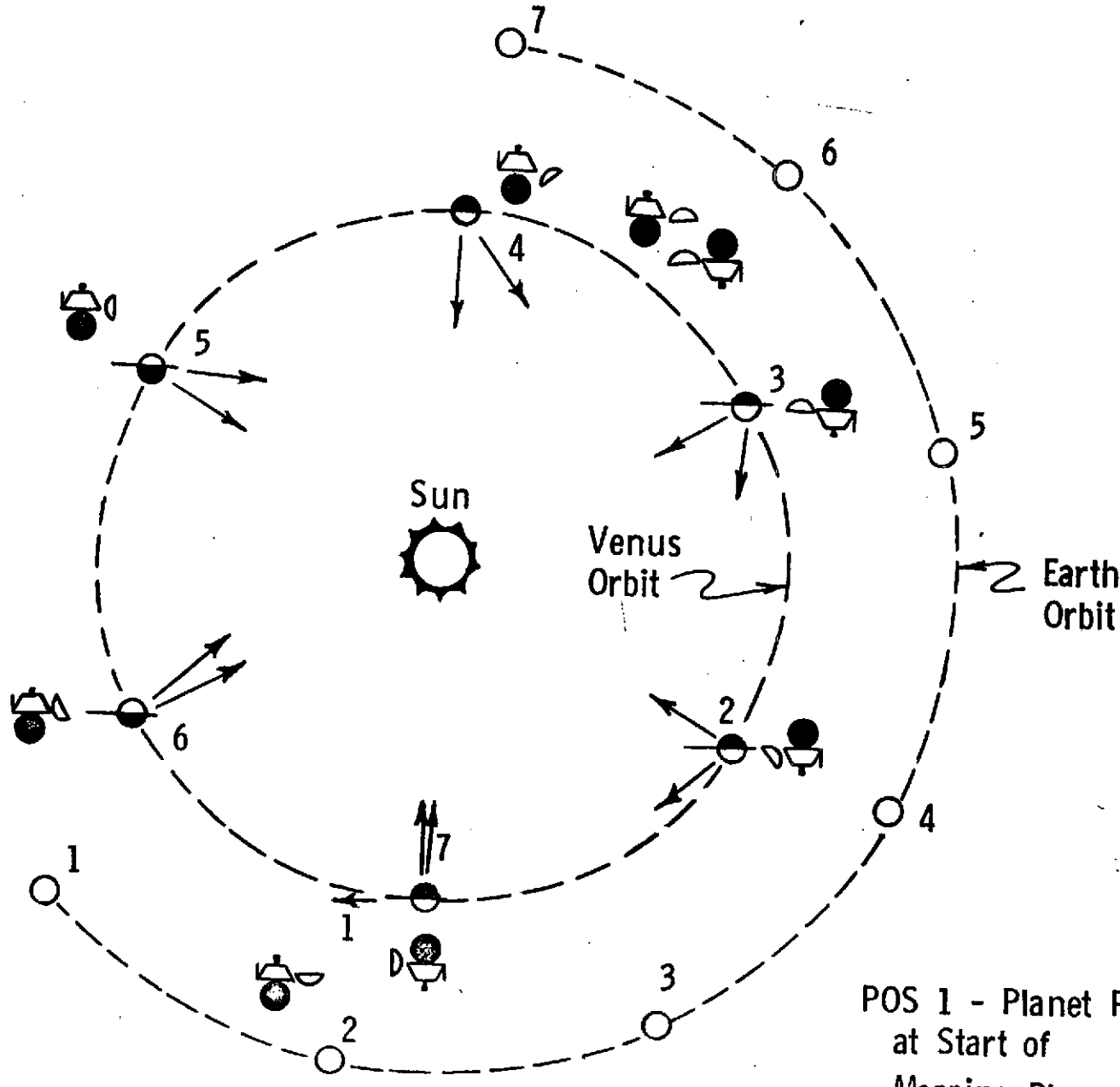

POS 1 - Planet Position at Start of Mapping Phase

configuration, except a maneuver is needed to change the mapping side. This maneuver is needed so the vehicle can communicate to Earth after a certain point in the mission. A 180-degree maneuver is needed to re-orient the vehicle so it can communicate with Earth. Changing the mapping side gives the same advantages as described for the shared antenna configuration.

Attitude Control

A detailed sizing analysis using a nitrogen cold gas ACS is presented for configurations A and C. The effects of orbital eccentricities of 0.00 and 0.50 on each of the configurations are evaluated. The list of mission requirements and ground rules that were used in the ACS sizing analysis that appear in Volume III, Section VI are also applicable to the analysis shown here. However, there are two important departures in the work shown herewith from the analysis procedures given in Volume III. In Volume III, the effect of external torques on ACS propellant usage was included. In this analysis, zero external torques were assumed. In Volume III, a total system weight is given for each candidate ACS. In this section, only the total GN_2 gas weight is presented. Determination of the weight contributions of tanks, support structure, nozzles, valves, regulators, plumbing, sensors, main engine actuators, flight control computer, antenna articulation control actuators, and ullage allowance is presented in the mass properties description. The reason for this is to obtain consistency in spacecraft design and also because of the fact that the work presented in Volume III is more parametric in nature.

The reason that zero external torques are assumed in this writeup is explained as follows:

The effect of external torques on a spacecraft can increase or decrease impulse consumption depending on the size of the external torque. As the external torque increases from zero, the impulse consumption initially drops under the no-external torque condition until a minimum is reached. Thereafter the impulse consumption increases monotonically with increases in external torque. External torque sources are solar pressure, gravity gradient, and aerodynamic torques due to lift and drag. In Volume III, external torques were computed by using the spacecraft configuration and orbit eccentricity that resulted in the largest values from each torque source. The contributions from each torque source were added directly to obtain a worst case peak external torque. Preliminary analyses of the orbiter limit cycle showed that impulse consumption under the influence of this peak external torque is approximately equal, on the average, to the impulse consumption with no external torques. Therefore, all impulse usage estimates in this section assume zero external torques. This is apparently a conservative assumption.

Configuration Descriptions - Figures VI-3 and VI-4 define the coordinate system and the spacecraft configurations that are used in the ACS sizing analysis. As shown in these figures, the Venus Mapper spacecraft has four more ACS jets in pitch and in yaw than the VO'75 spacecraft. The Venus Mapper spacecraft has four + pitch jets, four - pitch jets, four + yaw jets, four - yaw jets, two + roll jets, and two - roll jets. As is the case for VO'75, each jet produces 0.133 newtons (0.030 lb) of thrust. Roll torque using a 4.8 m moment arm is $\pm$ 1.29 N-m

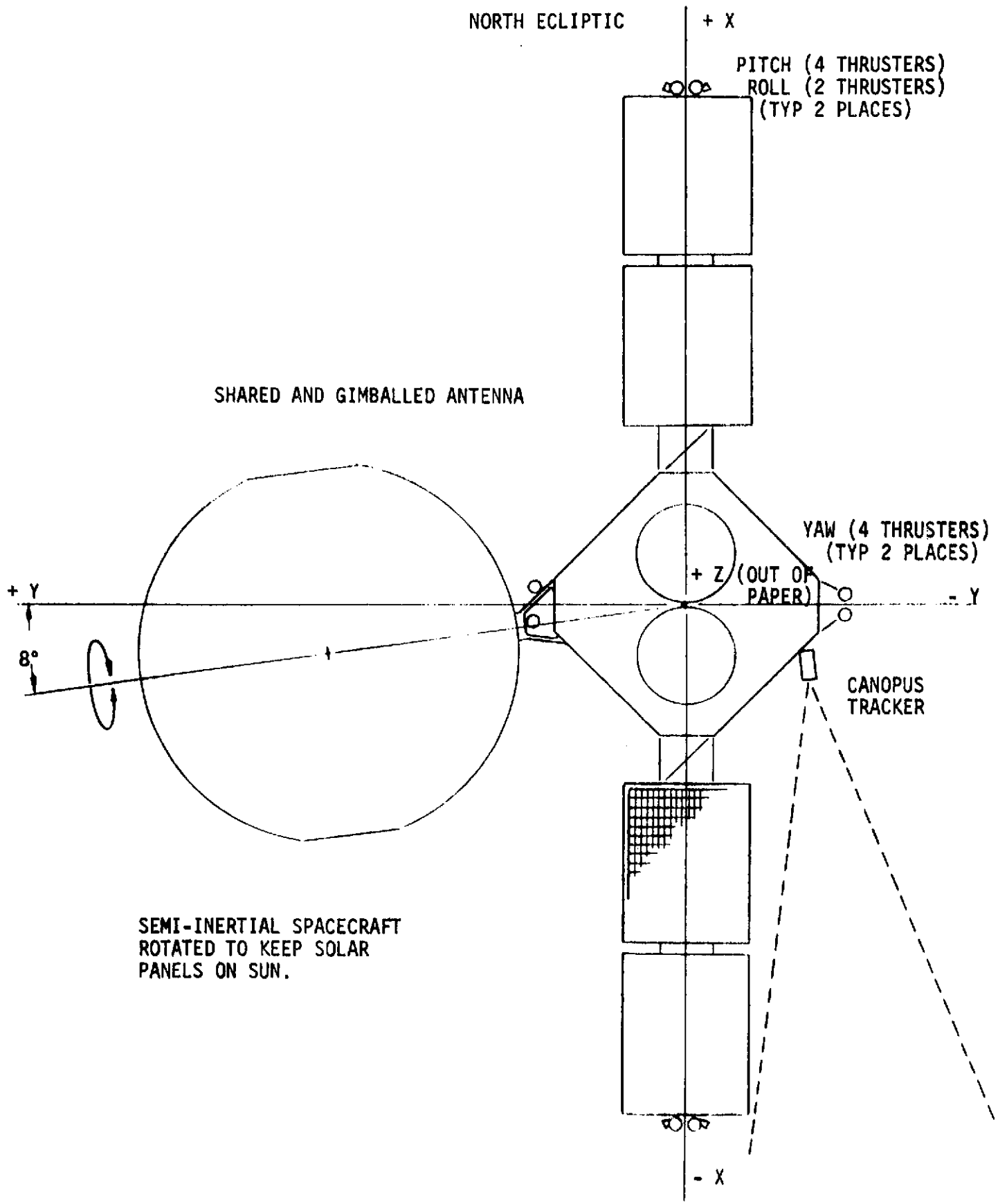

Figure VI-3 Configuration A

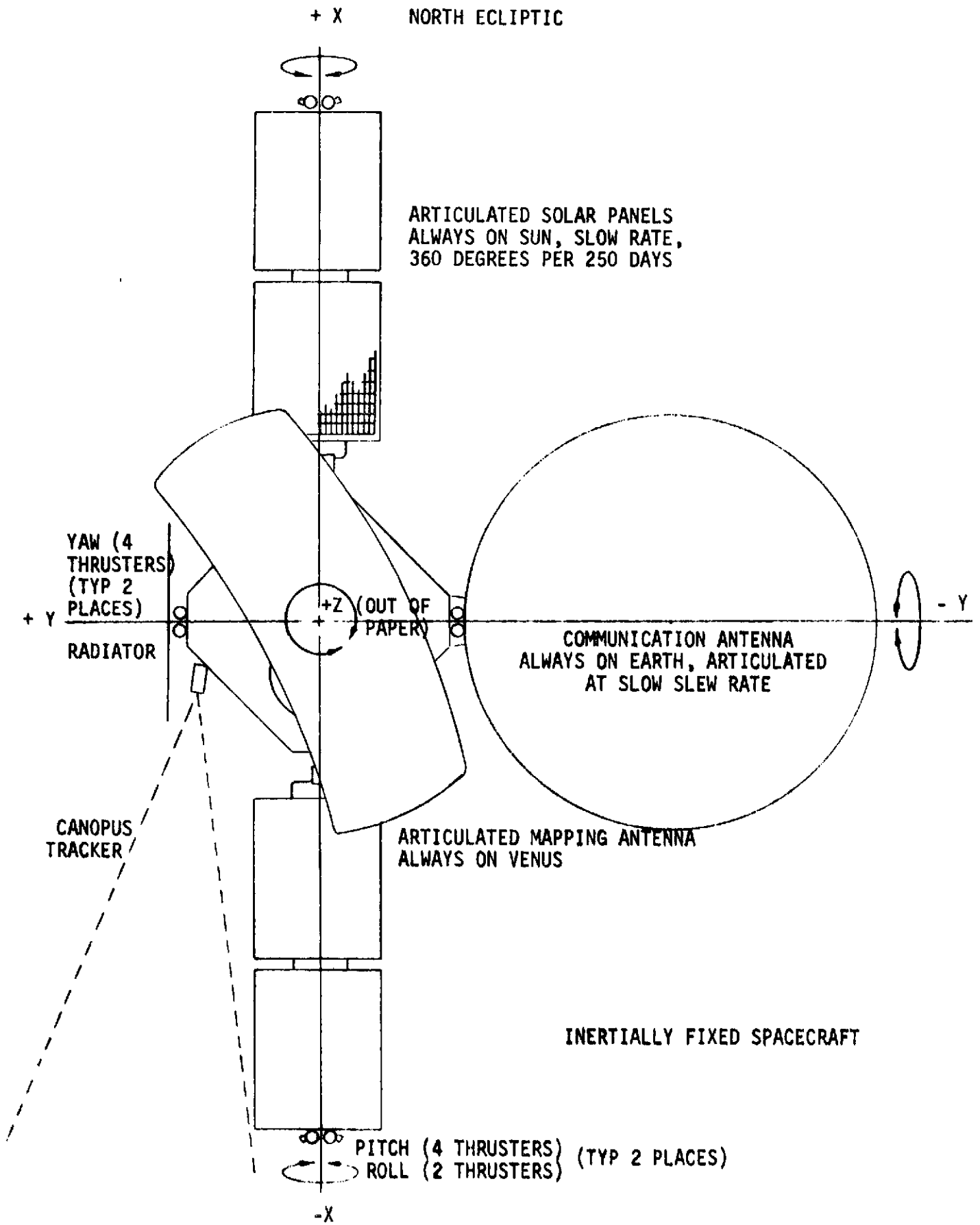

Figure VI-4 Configuration C

and pitch torque also using a 4.8 m moment arm is $\pm$ 2.56 N-m. Yaw torque depends on where the yaw ACS jets are mounted. If they are mounted on the spacecraft body on brackets the moment arm is 1.6 m and the torque is $\pm$ 0.85 N-m.

The principal reason for doubling the number of pitch and yaw jets is to obtain a conservative analysis. Also, the communication antenna boom is presently located along the spacecraft pitch axis which coincides with the desirable location for the yaw jets. This problem is avoided if two yaw jets are mounted on a yoke-type bracket which places one jet on each side of the boom. Another consideration is that the Venus Mapper may need more ACS thrust to control thrust vector misalignments on a multiple engine spacecraft. However, more detailed analysis may also show that fewer ACS jets are needed for the mapper application.

Mass properties used for Configurations A and C, e = 0 and 0.5, are given in Table VI-4.

Results - Table VI-5 gives the results of the GN_2 ACS sizing analysis for Configurations A and C, e = 0 and 0.5. The events correspond to the timeline defined in Volume III, Section VI. The total gas weight does not include the factor of three for the half-gas system. This factor is included when the total ACS system weight is calculated.

Configuration A, without a CMG system, requires the highest ACS gas weight mainly because of antenna maneuvering. Approximately 45% of the total ACS gas requirement is due to antenna maneuvering. These numbers represent worst case conditions. The principal worst case condition is that the major effect of antenna motion occurs about the spacecraft yaw axis. This unfavorably coincides with the spacecraft axis with a small thruster moment

Table VI-4 Mass Properties Used for Configurations A and C GN_2 Sizing Analysis

	e = 0				e = 0.5			
	Weight (kg)	Inertia N-m-sec^2			Weight (kg)	Inertia N-m-sec^2		
		I_x Yaw	I_y Pitch	I_z Roll		I_x Yaw	I_y Pitch	I_z Roll
Configuration A								
Booster separation to prior to orbit insertion, antenna stowed.	2910	3110	3790	1770	2020	1196	2110	1845
Orbit insertion to end of mission, antenna extended	1090	1670	2095	1765	1012	1190	1555	1855
Configuration C								
Booster separation to prior to orbit insertion, antenna stowed.	3005	3310	4025	1825	2100	1510	2320	1990
Orbit insertion to end of mission, antenna extended	1120	1760	2210	1810	1050	1233	1675	1810

Table VI-5 ACS Sizing Results for Configurations A and C, e = 0, and .5

Event	Configuration A									Configuration C					
	e = 0 Impulse n-sec			e = 0.5 Impulse n-sec			e=0.5 (RTGs) Impulse n-sec			e = 0 Impulse n-sec			e = 0.5 Impulse n-sec		
	Yaw	Pitch	Roll	Yaw	Pitch	Roll	Yaw	Pitch	Roll	Yaw	Pitch	Roll	Yaw	Pitch	Roll
I	39.30	16.00	7.50	15.12	8.90	7.80	15.12	26.70	23.40	40.60	17.00	7.80	19.10	9.80	8.40
II A&S	48.80	19.88	9.70	18.80	11.04	9.68	18.80	33.12	29.04	50.40	21.10	10.00	23.70	12.15	10.45
IIIA	0.0	39.70	19.38	0.0	22.08	19.36	0.0	66.24	58.08	0.0	42.10	19.95	0.0	24.30	20.90
IIIB1	0.0	0.0	21.28	0.0	0.0	21.28	0.0	0.0	21.28	0.0	0.0	21.28	0.0	0.0	21.28
IIIB2	78.60	32.00	0.0	30.24	17.80	0.0	30.24	35.10	0.0	81.40	34.00	0.0	38.30	19.60	0.0
IIIB3	478.00	478.00	239.40	323.00	323.00	161.60	323.00	323.00	161.60	478.00	478.00	239.40	323.00	323.00	161.60
IV	50.00	123.00	65.80	130.00	221.00	63.25	130.00	73.70	21.10	47.00	116.00	63.80	103.00	201.00	58.60
VA	0.0	19.85	9.69	0.0	11.04	9.68	0.0	33.12	29.04	0.0	21.10	9.98	0.0	12.15	10.45
VB1	0.0	0.0	212.80	0.0	0.0	212.80	0.0	0.0	212.80	0.0	0.0	212.80	0.0	0.0	212.80
VB2	21.20	8.86	0.0	15.06	6.56	0.0	15.06	19.68	0.0	22.30	9.40	0.0	15.60	7.10	0.0
VI	150.10	358.00	200.00	198.10	464.20	160.00	198.10	154.70	53.00	142.40	339.40	188.70	190.70	433.10	164.10
VIIA	NA	NA	NA	0.0	16.30	19.30	0.0	48.70	58.29	NA	NA	NA	0.0	17.55	19.00
VIIB1	NA	NA	NA	0.0	0.0	21.28	0.0	0.0	21.28	NA	NA	NA	0.0	0.0	21.28
VIIB2	NA	NA	NA	30.12	13.12	0.0	30.12	29.36	0.0	NA	NA	NA	31.20	14.12	0.0
VIIB3	NA	NA	NA	161.90	161.90	80.80	161.90	161.90	80.80	NA	NA	NA	161.90	161.90	80.80
VIII	890.00	1715.00	0.0	2460.00	216.00	0.0	2460.00	648.00	0.0	NA	NA	NA	NA	NA	NA
TOTAL	1756.00	2810.30	1569.90	3382.30	1492.90	786.90	3382.30	1653.30	769.70	862.10	1078.10	773.70	906.50	1235.80	789.70
TOTAL	6136.20 n-sec			5662.20 n-sec			5805.36 n-sec			2713.90 n-sec			2931.90 n-sec		
Gas Wt. I_{sp} GN_2 = 65S n-sec / kg	9.368 kg (42.5% due to antenna maneuvering.)			8.645 kg (47.2% due to antenna maneuvering.)			8.875 kg			4.14 kg			4.14 kg		

arm 1.6 m in yaw as compared with 4.8 m in pitch and roll. Also a radar altimeter is assumed to be mounted on the antenna dish which increases antenna inertia.

Antenna motion does not present a serious ACS problem because ACS gas requirements are not excessive even under these worst case conditions and several steps can be taken to optimize spacecraft and antenna design. These steps might include mounting the radar altimeter or some of its electronics elsewhere, reduction of antenna rotational inertia, and moving the antenna attach point slightly so that more of the antenna motion could be absorbed in a spacecraft control axis other than yaw.

Canopus Tracker Mounting Considerations - VO'75 presently has the Canopus tracker mounted in bay 12, pointing 45 degrees away from the -Y axis toward the -X axis. Ideally, the Venus Mapper spacecraft should have this sensor pointing along the - X axis. Therefore, there is a definite requirement to remount the Canopus sensor to point more or less along the Venus Mapper -X axis. However, if the Canopus sensor "looks" along the -X axis, there is a field of view (FOV) interference problem from the -X axis solar panel. Reference VI-1 states that the Orbiter configuration will provide an unobstructed rectangular FOV of $\pm$ 15 degrees in clock and $\pm$ 33 degrees in cone, centered at a cone angle of 90 degrees and a clock angle of 0 degrees.

The FOV problem for the Venus Mapper is the $\pm$ 15 degree clock angle requirement. Two solutions are suggested. The spacecraft could be flown with an approximate 15 degree roll bias. This would rotate the solar panels out of the Canopus tracker's FOV, but it would also point the solar panels away from the Sun 15 degrees, resulting in a slight solar power degradation. Also the mapping antenna yaw gimbal would need to be mounted at a compensating 15 degree angle.

A second solution to this problem would be to reduce the ± 15 degree clock angle requirement enough to effectively shield the solar panel from the sensor's FOV. Whether or not this can be done for the Venus Mapper application is a subject of future tradeoff studies and it would depend on a detailed study of the Canopus tracker sensor.

The Canopus tracker could possibly be mounted on a boom to clear the FOV requirement. A boom length of 1 meter for the ± 15 degree clock angle is needed. A boom of this length is required to be hinged to clear the payload shroud during boost, and mechanical alignment problems between the sensor and the spacecraft reference planes would be greater than if no boom were used.

Another potential problem for Configurations A and B is that the Canopus tracker may need to be gimballed in clock. This is because the mapping antenna arm must remain perpendicular to the orbital plane. As the spacecraft follows the planet around the Sun, the spacecraft yaws 180 degrees causing the Canopus angle to change through a range of approximately 30 degrees. VO'75 does not have this problem because the spacecraft can be rolled to compensate for change in the direction of Canopus. An alternative to gimballing the Canopus sensor is to add another gimbal to the mapping antenna.

Propulsion

The size and type of propulsion system selected is dependent upon the desired Venus orbit and the non-propulsive mass to be inserted into that orbit. Insertion delta V magnitude is partially determined by finite burn losses. These losses are inversely related to the vehicle thrust-to-mass ratio. Further, a large portion of the total spacecraft mass is its propulsion system, thus propulsion system selection is tempered by launch

vehicle capability and the potential economies of a multiple spacecraft launch. For these reasons a variety of propulsion systems were examined during the early phases of this study (Volume III). From these studies three basic propulsion systems were selected, one for each of the three orbit eccentricities that were studied in detail.

For an orbit eccentricity of 0.5 a V0'75 propulsion system modified to accommodate 3 engines is selected.

Investigation of finite burn losses indicated that one engine required a long time marginal burn to achieve orbit. Therefore, the jump was made to three engines to allow for S/C growth and reduce orbit insertion time. Three-engine design is accomplished by mounting two fixed engines on either side of the present gimballed engine along the "X" axis. These fixed engines will be used only during orbit insertion, therefore, a pair of pyrotechnic valve isolation assemblies will control propellant to both engines. V0'75 isolation valve assemblies will be used for the center engine. Figure VI-5 is a schematic of the resulting system, and the schematic of the pyrotechnic valve isolation assembly is shown in Figure VI-6.

Configurations designed for an orbit eccentricity of 0.5 will utilize existing V0'75 tankage off-loaded, taking advantage of economies offered by an existing design.

To achieve an orbit of $e = 0.3$ the same three engine arrangement will provide adequate thrust. However, the V0'75 tankage will be stretched by approximately 30 percent to provide sufficient propellant. JPL has indicated that a stretch of this magnitude will require some analysis and new testing, but is a reasonable modification to the system.

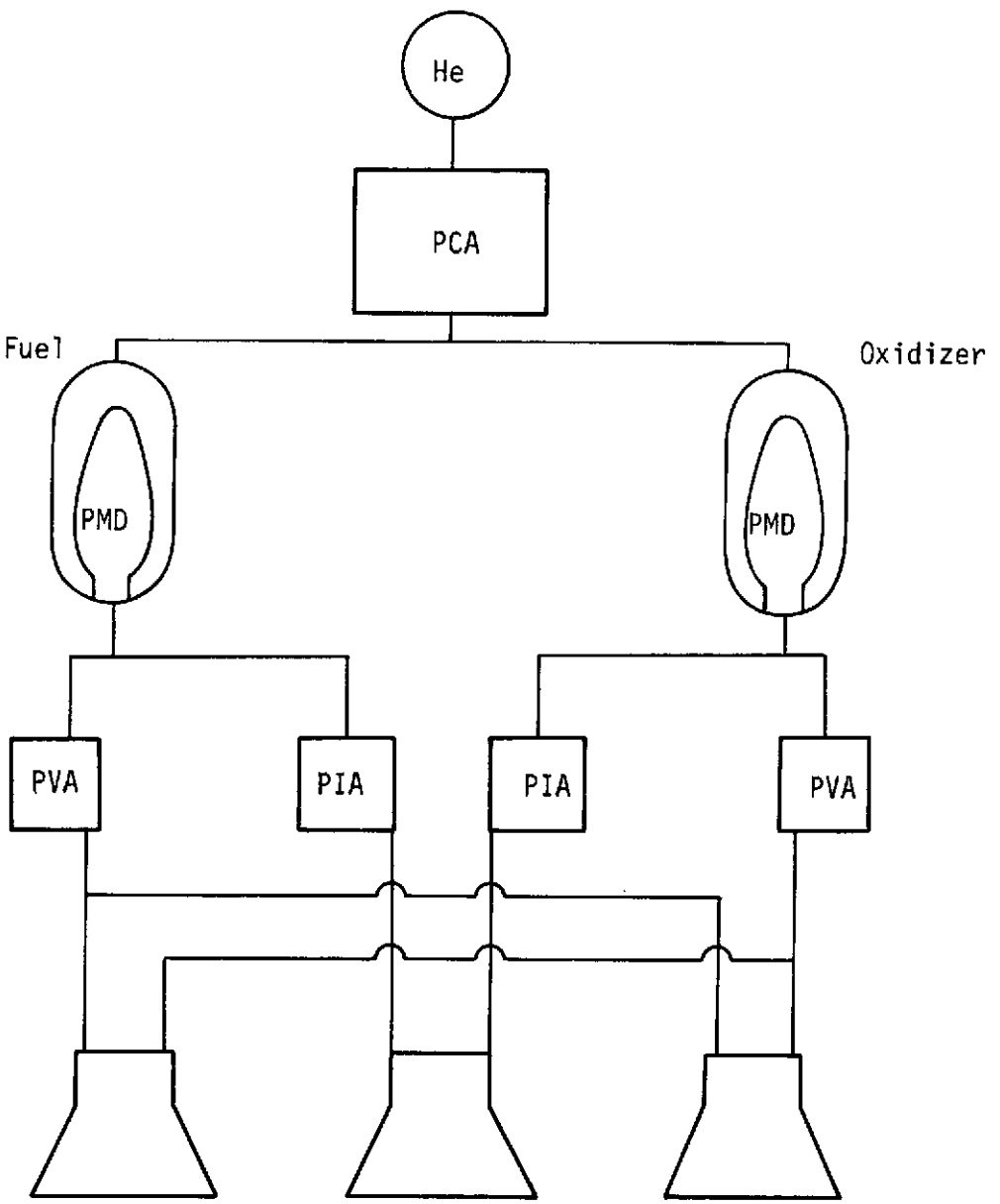

Figure VI-5 VO'75 Propulsion System 3 Engine Modification Schematic

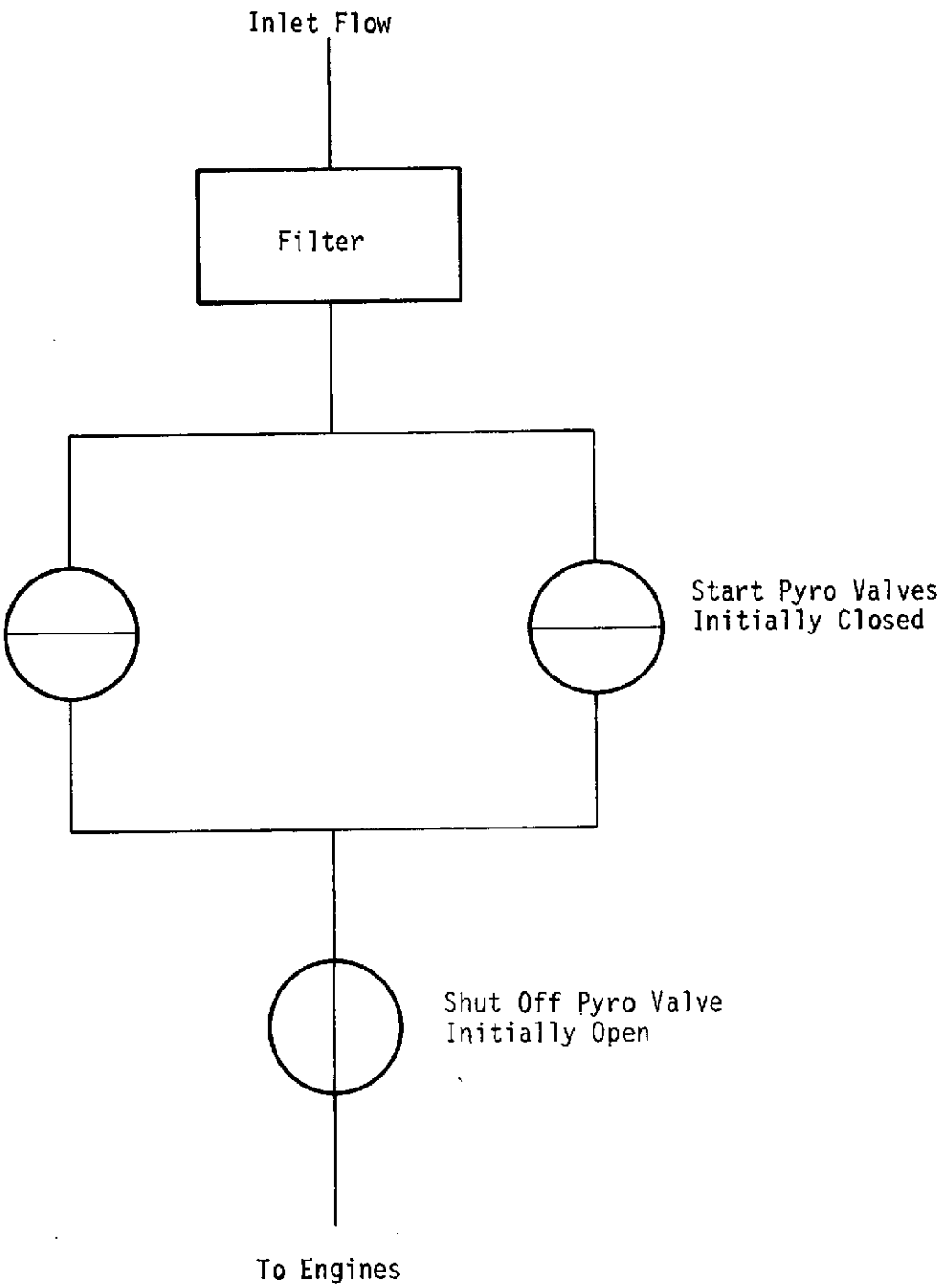

Figure VI-6 Pyrotechnic Valve Isolation Assembly Schematic

The higher insertion delta V required to achieve orbits of e = 0 led to the selection of space storable systems for these configurations. Further stretch of the VO'75 system was rejected because of the large tank size and propellant mass.

A space storable propulsion system using fluorine (F_2) and hydrazine (N_2H_4) appears most advantageous for these spacecraft. The system design is based to a large extent upon results of work conducted by JPL. The following is assumed as appropriate engine and propellant parameters.

Engines, 2-2669 Newton Thrust

Bipropellant Isp (Vacuum)	3677.5 N sec/kg
Monopropellant Isp (Vacuum)	2255.5 N sec/kg
Mixture Ratio	1.5
Fluorine (F_2) 155°R (Density)	1505.6 kg/m^3
Hydrazine (N_2H_4) (Density)	1001.0 kg/m^3
Pressurant	Helium
Reserve propellant	2%

The configurations assume two spherical propellant tanks. The oxidizer tank is fabricated of aluminum and the fuel tank of titanium. The tank arrangement is shown in Figure VI-7. The use of spherical tanks minimizes tank mass and simplifies the oxidizer tank shield.

A system schematic is shown in Figure VI-8. To completely separate the two propellants two distinct pressurization systems are used. Isolation assemblies are similar to those used on VO'75 but are increased in size to handle increased flow. Because both engines operate at all times, both are gimballed; however, for midcourse maneuvers the engines operate in the monopropellant mode utilizing hydrazine only. The hydrazine is thermally decomposed in this operational mode.

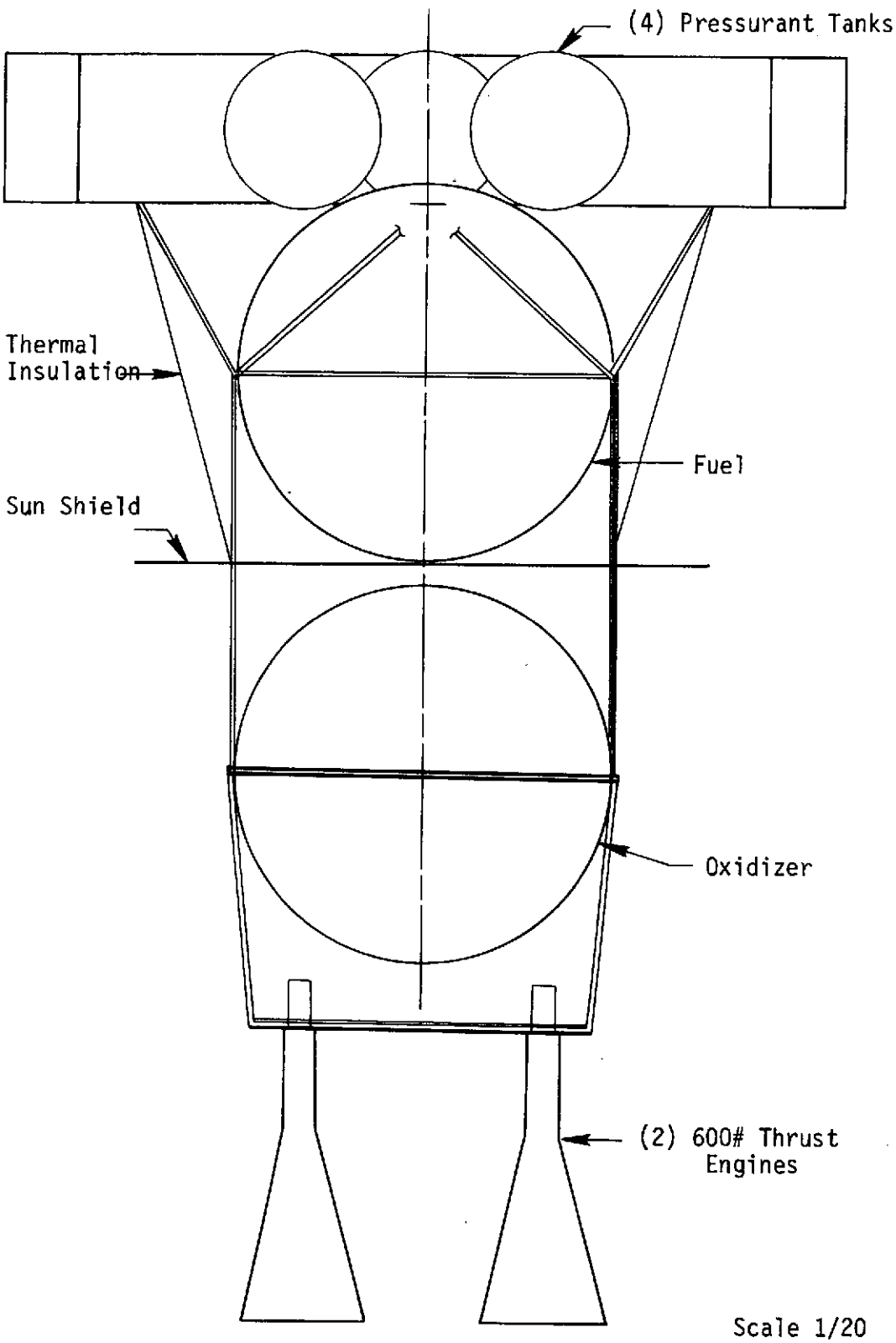

Figure VI-7 Space Storable Propulsion System Arrangement

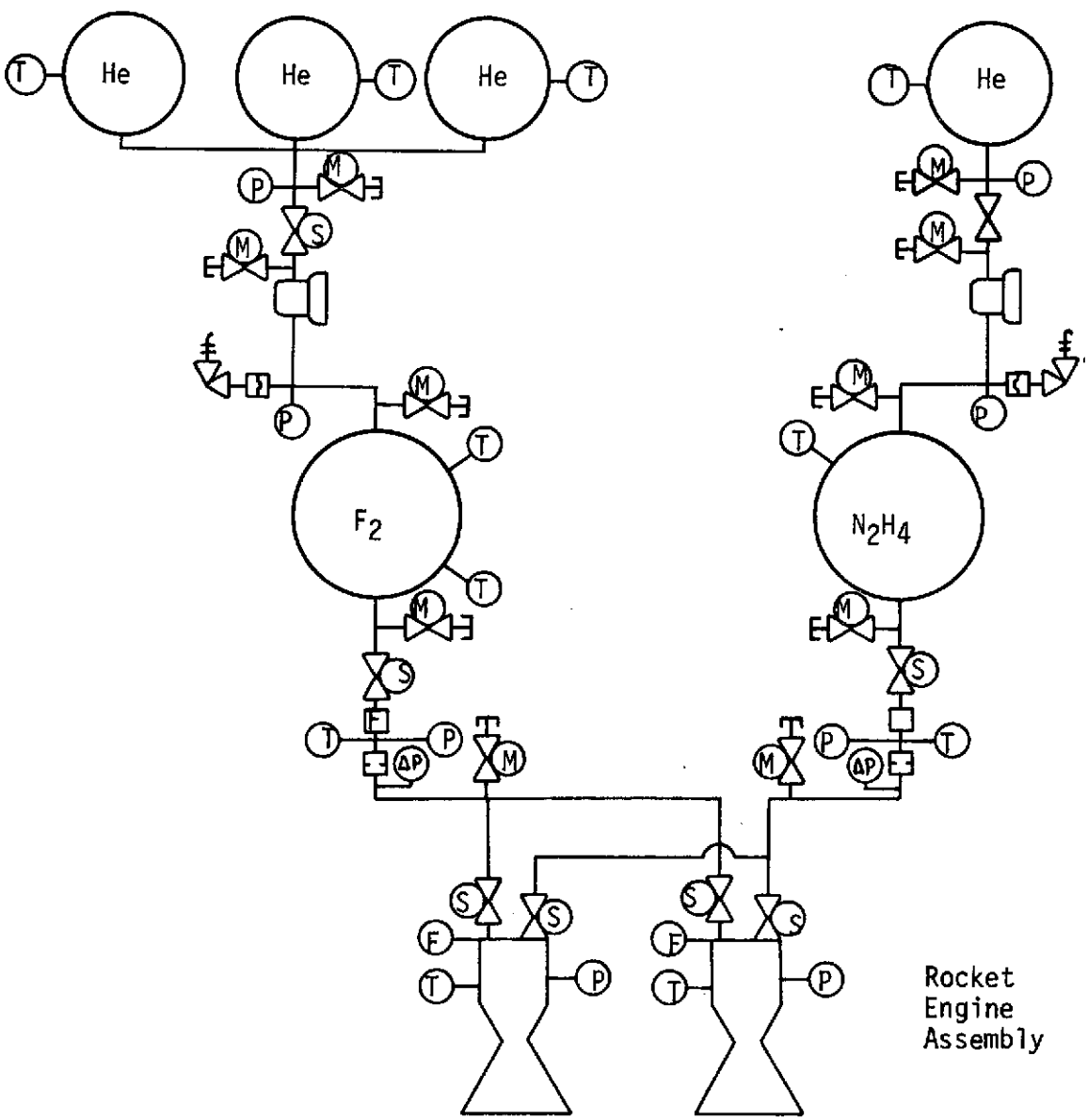

Figure VI-8 Space Storable Propulsion System Schematic

Power

This section describes the power subsystem utilized for the Venus Radar Mission Spacecraft. Also describes is the impact of the mission mode selection on the power subsystem. Power requirement tables are devised for each of the three configurations (Configuration A and C) studied. Energy balance calculations as a function of orbital period and spacecraft power requirements are generated for each configuration for orbital eccentricities of 0.0, 0.3, and 0.5.

The VO'75 power subsystem, modified for the Venus Radar Mapping mission, is used in this study. The major subassemblies of the unmodified subsystem are shown in Figure VI-9. The subsystem is further described in reference VI-2 but consists of three major groups as listed below:

a. Power Source Group
    1. Solar Array
    2. Array Zener Diodes
    3. Array Blocking Diodes
b. Energy Storage Group
    1. Orbiter Batteries
    2. Battery Chargers
    3. Boost Converter
    4. Share Mode Detector
    5. Battery Blocking Diodes
c. Power Conditioning and Distribution Group
    1. Boost Regulator
    2. 2.4 KHz Inverter
    3. 400 Hz, 3-Phase Inverter
    4. 30 VDC Converter
    5. Power Control
    6. Power Distribution

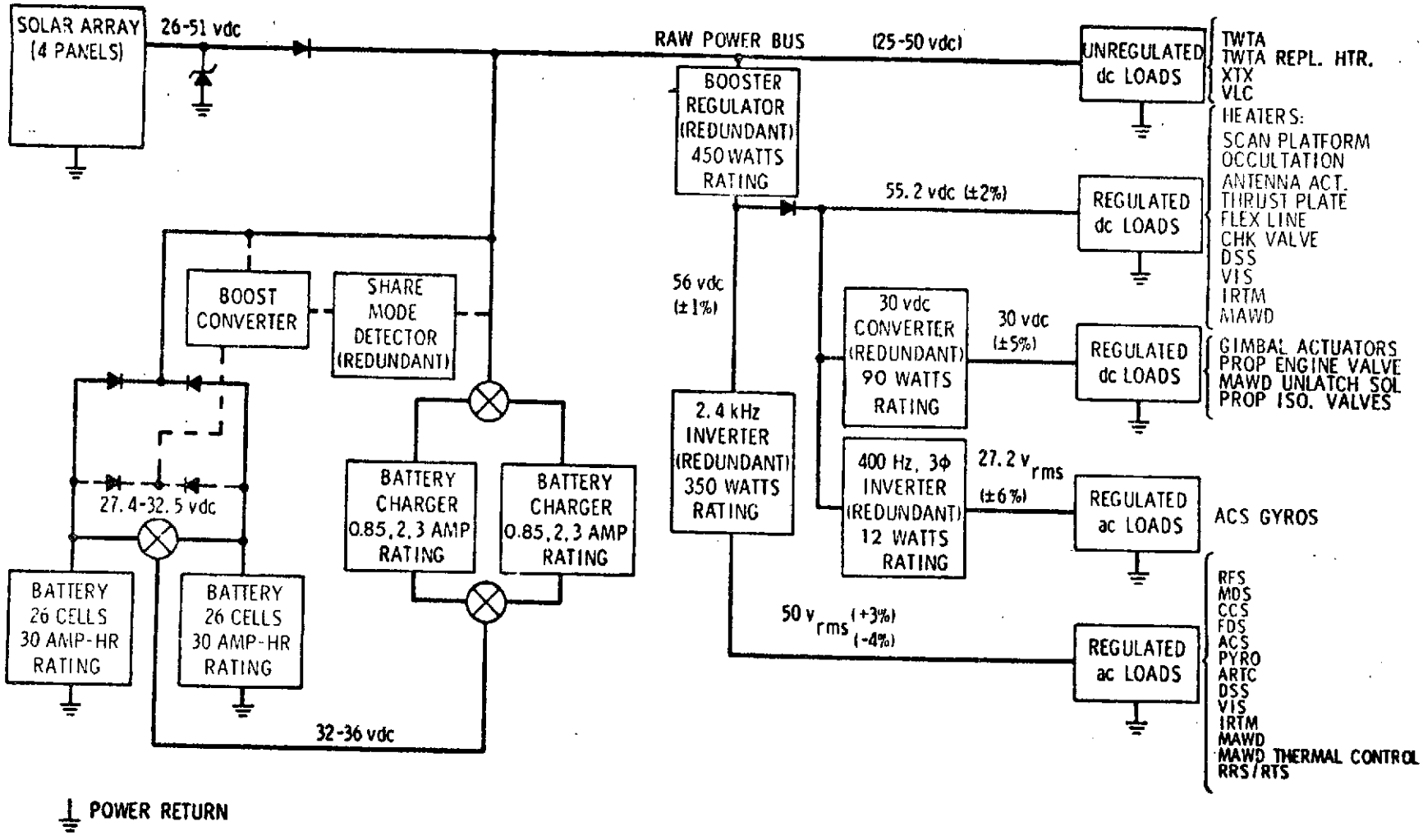

Figure VI-9 Unmodified VO'75 Power Subsystem Characteristics

The solar array for VO'75 consists of eight photovoltaic solar panels grouped in array segments of two panels each. For the Venus Radar Mapping Mission only four panels are used with two panels mounted on each of two array segments.

The higher temperatures encountered in the Venus orbit, compared to those in Mars orbit, make it necessary to use more solar cells in a series string to obtain the required system voltage. Hence 145 cells are used in series rather than the 87 used on VO'75. The existing panel area can be effectively used by a layout consisting of four series - parallel strings; three having seven cells in parallel and one having eight cells in parallel. The layout is shown in Figure VI-10 with the string identified as A, B, C and D. This arrangement is used in the computer simulation studies.

Other modifications permit a maximum battery charge current of 20 amperes and allow a dead zone of two volts in the battery charger.

The ability of the solar array power subsystem to meet the power requirements imposed by the family of compatible groupings is examined for three different orbits. Comparisons are made for the limiting cases, that is, for maximum occultations of the Sun. As demonstrated in Section III of this volume, maximum occultation occurs during only a fraction of the 250 day mission. During the rest of the time the power subsystem capability will be greater.

Power requirements are analyzed for Configurations A and C when operated in orbits with eccentricities of 0.5, 0.3 and 0.0. Tables VI-6, 7 and 8 show the power requirements for individual phases of the mapping and relay orbits for Configuration A, while Tables VI-9, 10 and 11 show the requirements for Configuration C. Power requirements for engineering items are based upon

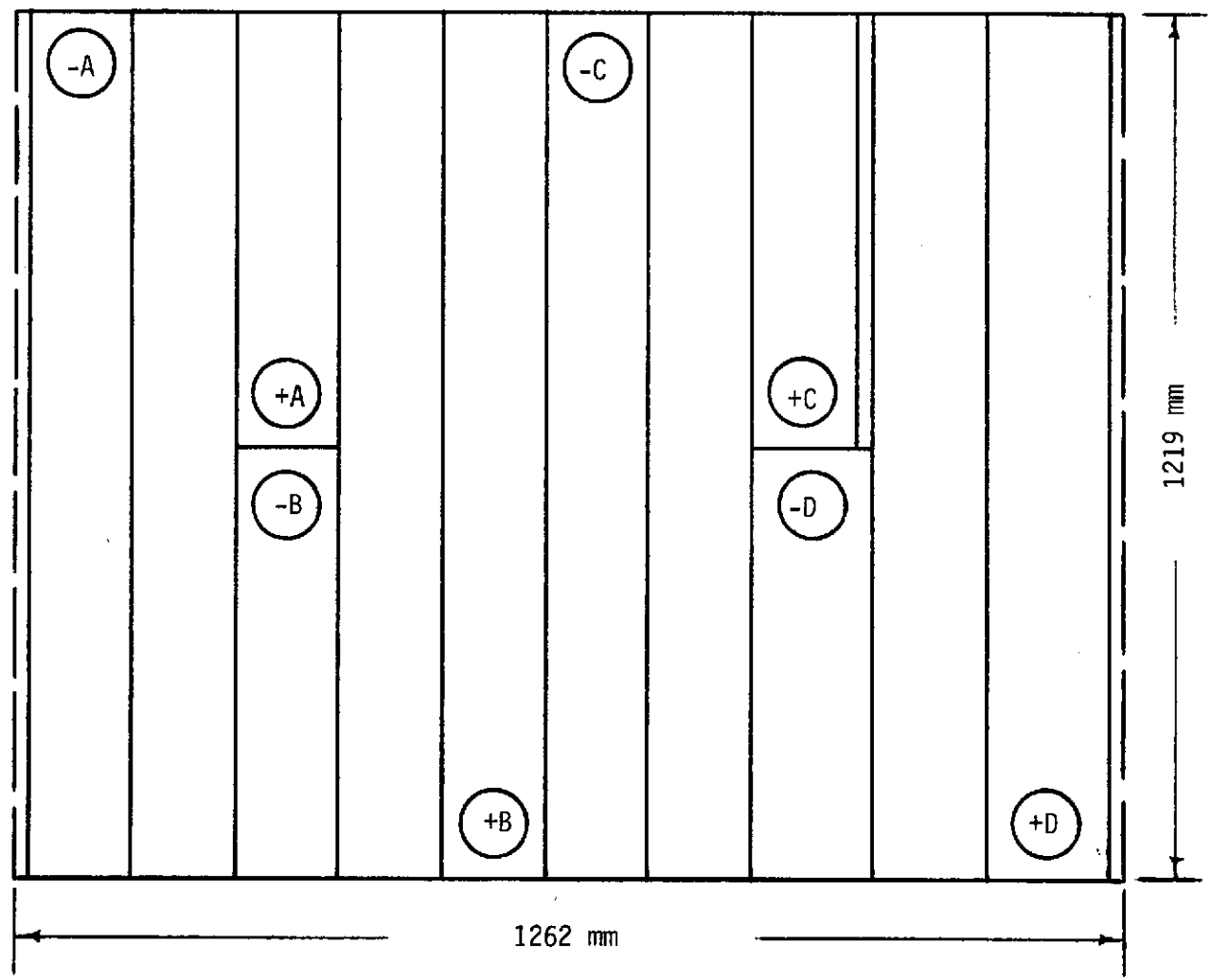

Figure VI-10 Panel Solar Cell Layout

Table VI-6 Power Allocation for Configuration A, e = 0.5 (Watts)

Equipment Name	Occultation Anticipation	Earth Occultation	Standby	Attitude Maneuver 1	Map	Attitude Maneuver 2	Signal Acquisition	High Rate Relay
	1	2	3	4	5	6	7	8
Engineering								
Modulation Demodulation S/S	8.70	8.70	8.70	8.70	8.70	8.70	8.70	8.70
Flight Data S/S	44.30	44.30	44.30	44.30	44.30	44.30	44.30	44.30
Computer Command S/S	15.00	15.00	15.00	15.00	15.00	15.00	15.00	15.00
Pyrotechnics	1.00	1.00	1.00	1.00	1.00	1.00	1.00	1.00
Power Distribution	13.00	13.00	13.00	13.00	13.00	13.00	13.00	13.00
Attitude Control S/S Electronics	15.50	15.50	15.50	15.50	15.50	15.50	15.50	15.50
Radio Frequency S/S	29.30	29.30	29.30	29.30	29.30	29.30	29.30	29.30
ACS Inertial Reference Unit	0.0	13.70	0.0	0.0	0.0	0.0	0.0	0.0
Articulation Control S/S	0.0	0.0	0.0	35.30	35.30	35.30	18.00	35.30
Data Storage S/S	0.0	0.0	0.0	0.0	45.00	0.0	0.0	45.00
Total Engineering (2.4 kHz)	126.80	140.50	126.80	162.10	207.10	162.10	131.30	207.10
Science								
Radar Receiver					100.00			
Altimeter				10.00	10.00	10.00		
Total Science (2.4 kHz)				10.00	110.00	10.00		
Total 2.4 kHz Output	126.80	140.50	126.30	172.10	317.10	172.10	131.30	207.10
2.4 kHz Inverter Efficiency	0.89	0.89	0.89	0.90	0.915	0.90	0.89	0.91
Total 2.4 kHz Inverter Input	142.47	157.86	142.47	191.22	346.56	191.22	147.53	227.58

Table VI-6 Power Allocation for Configuration A, e = 0.5 (Watts) concluded

Equipment Name	Occultation Anticipation	Earth Occultation	Standby	Attitude Maneuver 1	Map	Attitude Maneuver 2	Signal Acquisition	High Rate Relay
	1	2	3	4	5	6	7	8
ACS Gyro Motors	9.00	9.00	9.00	9.00	9.00	9.00	9.00	9.00
400 Hz 3 Ph Inverter Efficiency	0.84	0.84	0.84	0.84	0.84	0.84	0.84	0.84
Total 400 Hz 3 Ph Inverter Input	10.71	10.71	10.71	10.71	10.71	10.71	10.71	10.71
Booster Regulator								
Total 2.4 kHz Inverter Input	142.47	157.86	142.47	191.22	346.56	191.22	147.53	227.58
Total 400 Hz Inverter Input	10.71	10.71	10.71	10.71	10.71	10.71	10.71	10.71
Scan Platform Heaters	0.0	0.0	0.0	0.0	0.0	0.0	0.0	0.0
Data Storage S/S 1 Bay Heater	10.00	10.00	10.00	10.00	10.00	10.00	10.00	10.00
Data Storage S/S 2 Bay Heater	0.0	0.0	0.0	0.0	0.0	0.0	0.0	0.0
Occultation Heaters	0.0	0.0	0.0	0.0	0.0	0.0	0.0	0.0
High Gain Antenna Actuator Heater	0.0	0.0	0.0	0.0	0.0	0.0	0.0	0.0
B/R Power Distribution	5.0	5.0	5.0	5.0	5.0	5.0	5.0	5.0
Propellant Lockup Heaters	0.0	0.0	0.0	0.0	0.0	0.0	0.0	0.0
Total Booster Regulator Load	168.18	183.57	168.18	216.93	372.27	216.93	173.24	253.29
Booster Regulator Efficiency	0.89	0.90	0.89	0.90	0.90	0.90	0.90	0.90
Total Booster Regulator Input	188.97	203.97	188.97	241.03	413.63	241.03	192.49	281.43
Unregulated Power								
Total Booster Regulator Input	188.97	203.97	188.97	241.03	413.63	241.03	192.49	281.43
Power Failure Sensor	1.50	1.50	1.50	1.50	1.50	1.50	1.50	1.50
TWT System	0.0	0.0	0.0	0.0	0.0	303.00	303.00	303.00
Radar Mapper Transmitter	0.0	0.0	0.0	0.0	500.00	0.0	0.0	0.0
Total Unregulated Power	190.47	205.47	190.47	242.53	915.13	545.53	496.99	585.93
PSL Efficiency	0.982	0.982	0.982	0.982	0.982	0.982	0.982	0.982
Total Raw Power	193.96	209.24	193.96	246.98	931.90	555.53	506.10	596.67

Table VI-7 Power Allocation for Configuration A, e = 0.3 (Watts)

Equipment Name	Occultation Anticipation	Earth Occultation	Standby	Attitude Maneuver 1	Map	Attitude Maneuver 2	Advance Signal Acquisition	Occultation Anticipation	Earth Occultation	Signal Acquisition	High Rate Relay
	1	2	3	4	5	6	7	8	9	10	11
Engineering											
Modulation Demodulation S/S	8.70	8.70	8.70	8.70	8.70	8.70	8.70	8.70	8.70	8.70	8.70
Flight Data S/S	44.30	44.30	44.30	44.30	44.30	44.30	44.30	44.30	44.30	44.30	44.30
Computer Command S/S	15.00	15.00	15.00	15.00	15.00	15.00	15.00	15.00	15.00	15.00	15.00
Pyrotechnics	1.00	1.00	1.00	1.00	1.00	1.00	1.00	1.00	1.00	1.00	1.00
Power Distribution	13.00	13.00	13.00	13.00	13.00	13.00	13.00	13.00	13.00	13.00	13.00
Attitude Control S/S Electronics	15.50	15.50	15.50	15.50	15.50	15.50	15.50	15.50	15.50	15.50	15.50
Radio Frequency S/S	29.30	29.30	29.30	29.30	29.30	29.30	29.30	29.30	29.30	29.30	29.30
ACS Inertial Reference Unit	0.0	13.70	0.0	0.0	0.0	0.0	0.0	0.0	13.70	0.0	0.0
Articulation Control S/S	0.0	0.0	0.0	35.30	35.30	35.30	18.00	0.0	0.0	18.00	35.30
Data Storage S/S	0.0	0.0	0.0	0.0	45.00	0.0	45.00	0.0	0.0	0.0	45.00
Total Engineering (2.4 kHz)	126.80	140.50	126.80	162.10	207.10	162.10	176.30	126.80	140.50	131.30	207.10
Science											
Radar Receiver					100.00						
Altimeter				10.00	10.00	10.00					
Total Science (2.4 kHz)				10.00	110.00	10.00					
Total 2.4 kHz Output	126.80	140.50	126.80	172.10	317.10	172.10	176.30	126.80	140.50	131.30	207.10
2.4 kHz Inverter Efficiency	0.89	0.89	0.89	0.90	0.915	0.90	0.91	0.89	0.89	0.91	0.91
Total 2.4 kHz Inverter Input	142.47	157.86	142.47	191.22	346.56	191.22	193.74	142.47	157.86	147.53	227.58

Table VI-7 Power Allocation for Configuration A, e = 0.3 (Watts) concluded

Equipment Name	Occultation Anticipation	Earth Occultation	Standby	Attitude Maneuver 1	Map	Attitude Maneuver 2	Advance Signal Acquisition	Occultation Anticipation	Earth Occultation	Signal Acquisition	High Rate Relay
	1	2	3	4	5	6	7	8	9	10	11
ACS Gyro Motors	9.00	9.00	9.00	9.00	9.00	9.00	9.00	9.00	9.00	9.00	9.00
400 Hz 3 Ph Inverter Efficiency	0.84	0.84	0.84	0.84	0.84	0.84	0.84	0.84	0.84	0.84	0.84
Total 400 Hz 3 Ph Inverter Input	10.71	10.71	10.71	10.71	10.71	10.71	10.71	10.71	10.71	10.71	10.71
Booster Regulator											
Total 2.4 kHz Inverter Input	142.47	157.86	142.47	191.22	346.56	191.22	193.74	142.47	157.86	147.53	227.58
Total 400 Hz Inverter Input	10.71	10.71	10.71	10.71	10.71	10.71	10.71	10.71	10.71	10.71	10.71
Scan Platform Heaters	0.0	0.0	0.0	0.0	0.0	0.0	0.0	0.0	0.0	0.0	0.0
Data Storage S/S 1 Bay Heater	10.00	10.00	10.00	10.00	10.00	10.00	10.00	10.00	10.00	10.00	10.00
Data Storage S/S 2 Bay Heater	0.0	0.0	0.0	0.0	0.0	0.0	0.0	0.0	0.0	0.0	0.0
Occultation Heaters	0.0	0.0	0.0	0.0	0.0	0.0	0.0	0.0	0.0	0.0	0.0
High Gain Antenna Actuator Heater	0.0	0.0	0.0	0.0	0.0	0.0	0.0	0.0	0.0	0.0	0.0
B/R Power Distribution	5.0	5.0	5.0	5.0	5.0	5.0	5.0	5.0	5.0	5.0	5.0
Propellant Lockup Heaters	0.0	0.0	0.0	0.0	0.0	0.0	0.0	0.0	0.0	0.0	0.0
Total Booster Regulator Load	168.18	183.57	168.18	216.93	372.27	216.93	219.45	168.18	183.57	173.24	253.29
Booster Regulator Efficiency	0.89	0.90	0.89	0.90	0.90	0.90	0.90	0.89	0.90	0.90	0.90
Total Booster Regulator Input	188.97	203.97	188.97	241.03	413.63	241.03	243.83	188.97	203.97	192.49	281.43
Unregulated Power											
Total Booster Regulator Input	188.97	203.97	188.97	241.03	413.63	241.03	243.83	188.97	203.97	192.49	281.43
Power Failure Sensor	1.50	1.50	1.50	1.50	1.50	1.50	1.50	1.50	1.50	1.50	1.50
TWT System	0.0	0.0	0.0	0.0	0.0	428.00	428.00	0.0	0.0	428.00	428.00
Radar Mapper Transmitter	0.0	0.0	0.0	0.0	375.00	0.0	0.0	0.0	0.0	0.0	0.0
Total Unregulated Power	190.47	205.47	190.47	242.53	790.13	670.53	673.33	190.47	205.47	621.99	710.93
PSL Efficiency	0.982	0.982	0.982	0.982	0.982	0.982	0.982	0.982	0.982	0.982	0.982
Total Raw Power	193.96	209.24	193.96	246.98	804.61	682.82	685.67	193.96	209.24	633.39	723.96

Table VI-8 Power Allocation for Configuration A, e = 0 (Watts)

Equipment Name	Occultation	Attitude Maneuver 1	Map	Attitude Maneuver 2	Occultation	Signal Acquisition	High Rate Relay	Occultation Anticipation
	1	2	3	4	5	6	7	8
	←	Mapping Orbit	→		←	Relay Orbits (4)	→	
Engineering								
Modulation Demodulation S/S	8.70	8.70	8.70	8.70	8.70	8.70	8.70	8.70
Flight Data S/S	44.30	44.30	44.30	44.30	44.30	44.30	44.30	44.30
Computer Command S/S	15.00	15.00	15.00	15.00	15.00	15.00	15.00	15.00
Pyrotechnics	1.00	1.00	1.00	1.00	1.00	1.00	1.00	1.00
Power Distribution	13.00	13.00	13.00	13.00	13.00	13.00	13.00	13.00
Attitude Control S/S Electronics	15.50	15.50	15.50	15.50	15.50	15.50	15.50	15.50
Radio Frequency S/S	29.30	29.30	29.30	29.30	29.30	29.30	29.30	29.30
ACS Inertial Reference Unit	13.70	0.0	0.0	0.0	13.70	0.0	0.0	0.0
Articulation Control S/S	0.0	35.30	35.30	35.30	0.0	18.00	35.30	0.0
Data Storage S/S	0.0	0.0	45.00	0.0	0.0	0.0	45.00	0.0
Total Engineering (2.4 kHz)	140.50	162.10	207.10	162.10	140.50	131.30	207.10	126.80
Science								
Radar Receiver			100.00					
Altimeter		10.00	10.00	10.00				
Total Science (2.4 kHz)		10.00	110.00	10.00				
Total 2.4 kHz Output	140.50	172.10	317.10	172.10	140.50	131.30	207.10	126.80
2.4 kHz Inverter Efficiency	0.89	0.90	0.915	0.90	0.89	0.89	0.91	0.89
Total 2.4 kHz Inverter Input	157.86	191.22	346.56	191.22	157.86	147.53	227.58	142.47

Table VI-8 Power Allocation for Configuration A, e = 0 (Watts) concluded

Equipment Name	Occultation	Attitude Maneuver 1	Map	Attitude Maneuver 2	Occultation	Signal Acquisition	High Rate Relay	Occultation Anticipation
	1	2	3	4	5	6	7	8
	← Mapping Orbit →				← Relay Orbit (4) →			
ACS Gyro Motors	9.00	9.00	9.00	9.00	9.00	9.00	9.00	9.00
400 Hz 3 Ph Inverter Efficiency	0.84	0.84	0.84	0.84	0.84	0.84	0.84	0.84
Total 400 Hz 3 Ph Inverter Input	10.71	10.71	10.71	10.71	10.71	10.71	10.71	10.71
Booster Regulator								
Total 2.4 kHz Inverter Input	157.86	191.22	346.56	191.22	157.86	147.53	227.58	142.47
Total 400 Hz Inverter Input	10.71	10.71	10.71	10.71	10.71	10.71	10.71	10.71
Scan Platform Heaters	0.0	0.0	0.0	0.0	0.0	0.0	0.0	0.0
Data Storage S/S 1 Bay Heater	10.00	10.00	10.00	10.00	10.00	10.00	10.00	10.00
Data Storage S/S 2 Bay Heater	0.0	0.0	0.0	0.0	0.0	0.0	0.0	0.0
Occultation Heaters	0.0	0.0	0.0	0.0	0.0	0.0	0.0	0.0
High Gain Antenna Actuator Heater	0.0	0.0	0.0	0.0	0.0	0.0	0.0	0.0
B/R Power Distribution	5.0	5.0	5.0	5.0	5.0	5.0	5.0	5.0
Propellant Lockup Heaters	0.0	0.0	0.0	0.0	0.0	0.0	0.0	0.0
Total Booster Regulator Load	183.57	216.93	372.27	216.93	183.57	173.24	253.29	168.18
Booster Regulator Efficiency	0.90	0.90	0.90	0.90	0.90	0.90	0.90	0.89
Total Booster Regulator Input	203.97	241.03	413.63	241.03	203.97	192.49	281.43	188.97
Unregulated Power								
Total Booster Regulator Input	203.97	241.03	413.63	241.03	203.97	192.49	281.43	188.97
Power Failure Sensor	1.50	1.50	1.50	1.50	1.50	1.50	1.50	1.50
TWT System	0.0	0.0	0.0	568.00	0.0	568.00	568.00	0.0
Radar Mapper Transmitter	0.0	0.0	83.00	0.0	0.0	0.0	0.0	0.0
Total Unregulated Power	205.47	242.53	498.13	810.53	205.47	761.99	850.93	190.47
PSL Efficiency	0.982	0.982	0.982	0.982	0.982	0.982	0.982	0.982
Total Raw Power	209.24	246.98	507.26	825.39	209.24	775.96	866.53	193.96

Table VI-9 Power Allocation for Configuration C, e = 0.5 (Watts)

Equipment Name	Occultation Anticipation	Earth Occultation	Signal Acquisition	High Rate Relay	Map/Low Rate Relay	High Rate Relay
	1	2	3	4	5	6
Engineering						
Modulation Demodulation S/S	8.70	8.70	8.70	8.70	8.70	8.70
Flight Data S/S	44.30	44.30	44.30	44.30	44.30	44.30
Computer Command S/S	15.00	15.00	15.00	15.00	15.00	15.00
Pyrotechnics	1.00	1.00	1.00	1.00	1.00	1.00
Power Distribution	13.00	13.00	13.00	13.00	13.00	13.00
Attitude Control S/S Electronics	15.50	15.50	15.50	15.50	15.50	15.50
Radio Frequency S/S	29.30	29.30	29.30	29.30	29.30	29.30
ACS Inertial Reference Unit	0.0	13.70	0.0	0.0	0.0	0.0
Articulation Control S/S	0.0	0.0	18.00	35.30	35.30	35.30
Data Storage S/S	0.0	0.0	0.0	45.00	45.00	45.00
Total Engineering (2.4 kHz)	126.80	140.50	131.30	207.10	207.10	207.10
Science						
Radar Receiver					100.00	
Altimeter				10.00	10.00	
Total Science (2.4 kHz)				10.00	110.00	
Total 2.4 kHz Output	126.80	140.50	131.30	217.10	317.10	207.10
2.4 kHz Inverter Efficiency	0.89	0.89	0.89	0.91	0.915	0.91
Total 2.4 kHz Inverter Input	142.47	157.87	147.53	238.57	346.56	227.58

Table VI-9 Power Allocation for Configuration C, e = 0.5 (Watts) concluded

Equipment Name	Occultation Anticipation	Earth Occultation	Signal Acquisition	High Rate Relay	Map/Low Rate Relay	High Rate Relay
	1	2	3	4	5	6
ACS Gyro Motors	9.00	9.00	9.00	9.00	9.00	9.00
400 Hz 3 Ph Inverter Efficiency	0.84	0.84	0.84	0.84	0.84	0.84
Total 400 Hz 3 Ph Inverter Input	10.71	10.71	10.71	10.71	10.71	10.71
Booster Regulator						
Total 2.4 kHz Inverter Input	142.47	157.87	147.53	238.58	346.56	227.58
Total 400 Hz Inverter Input	10.71	10.71	10.71	10.71	10.71	10.71
Scan Platform Heaters	0.0	0.0	0.0	0.0	0.0	0.0
Data Storage S/S 1 Bay Heater	10.00	10.00	10.00	10.00	10.00	10.00
Data Storage S/S 2 Bay Heater	0.0	0.0	0.0	0.0	0.0	0.0
Occultation Heaters	0.0	0.0	0.0	0.0	0.0	0.0
High Gain Antenna Actuator Heater	0.0	0.0	0.0	0.0	0.0	0.0
B/R Power Distribution	5.0	5.0	5.0	5.0	5.0	5.0
Propellant Lockup Heaters	0.0	0.0	0.0	0.0	0.0	0.0
Total Booster Regulator Load	168.18	183.58	173.24	264.29	372.27	253.29
Booster Regulator Efficiency	0.89	0.90	0.90	0.90	0.90	0.90
Total Booster Regulator Input	188.97	203.98	192.49	293.66	413.63	281.43
Unregulated Power						
Total Booster Regulator Input	188.97	203.98	192.49	293.66	413.63	281.43
Power Failure Sensor	1.50	1.50	1.50	1.50	1.50	1.50
TWT System	0.0	0.0	352.00	352.00	40.00	352.00
Radar Mapper Transmitter	0.0	0.0	0.0	0.0	233.00	0.0
Total Unregulated Power	190.47	205.48	545.99	647.16	688.13	634.93
PSL Efficiency	0.982	0.982	0.982	0.982	0.982	0.982
Total Raw Power	193.96	209.25	556.00	659.02	700.74	646.57

Table VI-10 Power Allocation for Configuration C, e = 0.3 (Watts)

Engineering Name	Occultation Anticipation	Earth Occultation	Signal Acquisition	Joint Signal Acqui'n/Map	Map/Low Rate Relay	High Rate Relay	Occultation Anticipation	Earth Occultation	Signal Acquisition	High Rate Relay
	1	2	3	4	5	6	7	8	9	10
	← Mapping Orbit →						← Relay Orbit →			
Engineering										
Modulation Demodulation S/S	8.70	8.70	8.70	8.70	8.70	8.70	8.70	8.70	8.70	8.70
Flight Data S/S	44.30	44.30	44.30	44.30	44.30	44.30	44.30	44.30	44.30	44.30
Computer Command S/S	15.00	15.00	15.00	15.00	15.00	15.00	15.00	15.00	15.00	15.00
Pyrotechnics	1.00	1.00	1.00	1.00	1.00	1.00	1.00	1.00	1.00	1.00
Power Distribution	13.00	13.00	13.00	13.00	13.00	13.00	13.00	13.00	13.00	13.00
Attitude Control S/S Electronics	15.50	15.50	15.50	15.50	15.50	15.50	15.50	15.50	15.50	15.50
Radio Frequency S/S	29.30	29.30	29.30	29.30	29.30	29.30	29.30	29.30	29.30	29.30
ACS Inertial Reference Unit	0.0	13.70	0.0	0.0	0.0	0.0	0.0	13.70	0.0	0.0
Articulation Control S/S	0.0	0.0	18.00	18.00	35.30	35.30	0.0	0.0	18.00	35.30
Data Storage S/S	0.0	0.0	0.0	45.00	45.00	45.00	0.0	0.0	0.0	45.00
Total Engineering (2.4 kHz)	126.80	140.50	131.30	189.80	207.10	207.10	126.80	140.50	131.30	207.10
Science										
Radar Receiver					100.00					
Altimeter				10.00	10.00					
Total Science (2.4 kHz)				10.00	110.00					
Total 2.4 kHz Output	126.80	140.50	131.30	199.80	317.10	207.10	126.80	140.50	131.30	207.10
2.4 kHz Inverter Efficiency	0.89	0.89	0.89	0.90	0.915	0.91	0.89	0.89	0.89	0.91
Total 2.4 kHz Inverter Input	142.47	157.87	147.53	222.00	346.56	227.58	142.47	157.87	147.53	227.58

Table VI-10 Power Allocation for Configuration C, e = 0.3 (Watts) concluded

Equipment Name	Occultation Anticipation	Earth Occultation	Signal Acquisition	Joint Signal Acqui'n/Map	Map/Low Rate Relay	High Rate Relay	Occultation Anticipation	Earth Occultation	Signal Acquisition	High Rate Relay
	1	2	3	4	5	6	7	8	9	10
	← Mapping Orbit →						← Relay Orbit →			
ACS Gyro Motors	9.00	9.00	9.00	9.00	9.00	9.00	9.00	9.00	9.00	9.00
400 Hz 3 Ph Inverter Efficiency	0.84	0.84	0.84	0.84	0.84	0.84	0.84	0.84	0.84	0.84
Total 400 Hz 3 Ph Inverter Input	10.71	10.71	10.71	10.71	10.71	10.71	10.71	10.71	10.71	10.71
Booster Regulator										
Total 2.4 kHz Inverter Input	142.47	157.87	147.53	222.00	346.56	227.58	142.47	157.87	147.53	227.58
Total 400 Hz Inverter Input	10.71	10.71	10.71	10.71	10.71	10.71	10.71	10.71	10.71	10.71
Scan Platform Heaters	0.0	0.0	0.0	0.0	0.0	0.0	0.0	0.0	0.0	0.0
Data Storage S/S 1 Bay Heater	10.00	10.00	10.00	10.00	10.00	10.00	10.00	10.00	10.00	10.00
Data Storage S/S 2 Bay Heater	0.0	0.0	0.0	0.0	0.0	0.0	0.0	0.0	0.0	0.0
Occultation Heaters	0.0	0.0	0.0	0.0	0.0	0.0	0.0	0.0	0.0	0.0
High Gain Antenna Actuator Heater	0.0	0.0	0.0	0.0	0.0	0.0	0.0	0.0	0.0	0.0
B/R Power Distribution	5.0	5.0	5.0	5.0	5.0	5.0	5.0	5.0	5.0	5.0
Propellant Lockup Heaters	0.0	0.0	0.0	0.0	0.0	0.0	0.0	0.0	0.0	0.0
Total Booster Regulator Load	168.18	183.58	173.24	247.71	372.27	253.29	168.18	183.58	173.24	253.29
Booster Regulator Efficiency	0.89	0.90	0.90	0.90	0.90	0.90	0.89	0.90	0.90	0.90
Total Booster Regulator Input	188.97	203.98	192.49	275.23	413.63	281.43	188.97	203.98	192.49	281.43
Unregulated Power										
Total Booster Regulator Input	188.97	203.98	192.49	275.23	413.63	281.43	188.97	203.98	192.49	281.43
Power Failure Sensor	1.50	1.50	1.50	1.50	1.50	1.50	1.50	1.50	1.50	1.50
TWT System	0.0	0.0	286.00	286.00	40.00	286.00	0.0	0.0	286.00	286.00
Radar Mapper Transmitter	0.0	0.0	0.0	106.00	106.00	0.0	0.0	0.0	0.0	0.0
Total Unregulated Power	190.47	205.48	479.99	668.73	561.13	568.93	190.47	205.48	479.99	568.93
PSL Efficiency	0.982	0.982	0.982	0.982	0.982	0.982	0.982	0.982	0.982	0.982
Total Raw Power	193.96	209.25	488.79	680.99	571.42	579.36	193.96	209.25	488.79	579.36

Table VI-11 Power Allocation for Configuration C, e = 0 (Watts)

Equipment Name	Occultation	Attitude Maneuver 1	Map	Attitude Maneuver 2	Occultation	Signal Acquisition	High Rate Relay	Occultation Anticipation
	1	2	3	4	5	6	7	8
	← Mapping Orbit →				← Relay Orbits (4) →			
Engineering								
Modulation Demodulation S/S	8.70	8.70	8.70	8.70	8.70	8.70	8.70	8.70
Flight Data S/S	44.30	44.30	44.30	44.30	44.30	44.30	44.30	44.30
Computer Command S/S	15.00	15.00	15.00	15.00	15.00	15.00	15.00	15.00
Pyrotechnics	1.00	1.00	1.00	1.00	1.00	1.00	1.00	1.00
Power Distribution	13.00	13.00	13.00	13.00	13.00	13.00	13.00	13.00
Attitude Control S/S Electronics	15.50	15.50	15.50	15.50	15.50	15.50	15.50	15.50
Radio Frequency S/S	29.30	29.30	29.30	29.30	29.30	29.30	29.30	29.30
ACS Inertial Reference Unit	13.70	0.0	0.0	0.0	13.70	0.0	0.0	0.0
Articulation Control S/S	0.0	35.30	35.30	35.30	0.0	18.00	35.30	0.0
Data Storage S/S	0.0	0.0	45.00	0.0	0.0	0.0	45.00	0.0
Total Engineering (2.4 kHz)	140.50	162.10	207.10	162.10	140.50	131.30	207.10	126.80
Science								
Radar Receiver			100.00					
Altimeter		10.00	10.00	10.00				
Total Science (2.4 kHz)		10.00	110.00	10.00				
Total 2.4 kHz Output	140.50	172.10	317.10	172.10	140.50	131.30	207.10	126.80
2.4 kHz Inverter Efficiency	0.89	0.90	0.915	0.90	0.89	0.89	0.91	0.89
Total 2.4 kHz Inverter Input	157.86	191.22	346.56	191.22	157.86	147.53	227.58	142.47

Table VI-11 Power Allocation for Configuration C, e = 0 (Watts) concluded

Equipment Name	Occultation	Attitude Maneuver 1	Map	Attitude Maneuver 2	Occultation	Signal Acquisition	High Rate Relay	Occultation Anticipation
	1	2	3	4	5	6	7	8
	← Mapping Orbit →				← Relay Orbits (4) →			
ACS Gyro Motors	9.00	9.00	9.00	9.00	9.00	9.00	9.00	9.00
400 Hz 3 Ph Inverter Efficiency	0.84	0.84	0.84	0.84	0.84	0.84	0.84	0.84
Total 400 Hz 3 Ph Inverter Input	10.71	10.71	10.71	10.71	10.71	10.71	10.71	10.71
Booster Regulator								
Total 2.4 kHz Inverter Input	157.86	191.22	346.56	191.22	157.86	147.53	227.58	142.47
Total 400 Hz Inverter Input	10.71	10.71	10.71	10.71	10.71	10.71	10.71	10.71
Scan Platform Heaters	0.0	0.0	0.0	0.0	0.0	0.0	0.0	0.0
Data Storage S/S 1 Bay Heater	10.00	10.00	10.00	10.00	10.00	10.00	10.00	10.00
Data Storage S/S 2 Bay Heater	0.0	0.0	0.0	0.0	0.0	0.0	0.0	0.0
Occultation Heaters	0.0	0.0	0.0	0.0	0.0	0.0	0.0	0.0
High Gain Antenna Actuator Heater	0.0	0.0	0.0	0.0	0.0	0.0	0.0	0.0
B/R Power Distribution	5.0	5.0	5.0	5.0	5.0	5.0	5.0	5.0
Propellant Lockup Heaters	0.0	0.0	0.0	0.0	0.0	0.0	0.0	0.0
Total Booster Regulator Load	183.57	216.93	372.27	216.93	183.57	173.24	253.29	168.18
Booster Regulator Efficiency	0.90	0.90	0.90	0.90	0.90	0.90	0.90	0.89
Total Booster Regulator Input	203.97	241.03	413.63	241.03	203.97	192.49	281.43	188.97
Unregulated Power								
Total Booster Regulator Input	203.97	241.03	413.63	241.03	203.97	192.49	281.43	188.97
Power Failure Sensor	1.50	1.50	1.50	1.50	1.50	1.50	1.50	1.50
TWT System	0.0	0.0	0.0	209.00	0.0	209.00	209.00	0.0
Radar Mapper Transmitter	0.0	0.0	83.00	0.0	0.0	0.0	0.0	0.0
Total Unregulated Power	205.47	242.53	498.13	451.53	205.47	402.99	491.93	190.47
PSL Efficiency	0.982	0.982	0.982	0.982	0.982	0.982	0.982	0.982
Total Raw Power	209.24	246.98	507.26	495.81	209.24	410.38	500.95	193.96

Viking Orbiter power status reports and follow the same format with loads classified by type of power furnished. The majority of loads are provided with single-phase squarewave power from 2.4 kHz inverters. The TWT system and the radar mapper transmitter have their own power supplies fed from the unregulated main bus. Differences in load requirements between the two configurations and the three orbits result from varying radar transmitter and TWT system requirements. Power requirements were not analyzed for Configuration B since it was not a strong contender for selection. Radar receiver power is held at 100 watts for all orbits but transmitter power vary as shown in Tables VI-12 and 13.

Table VI-12 Radar Transmitter Power Input

	Orbit		
	e = 0.5	e = 0.3	e = 0
Configuration A	500 W	375 W	83 W
Configuration C	233 W	106 W	83 W

TWT system power requirements during high rate relay are:

Table VI-13 TWT System Power Input

	Orbit		
	e = 0.5	e = 0.3	e = 0
Configuration A	303 W	428 W	568 W
Configuration C	352 W	286 W	209 W

Ability of the solar array power subsystem to support the spacecraft loads was determined by simulating its operation as the spacecraft passed through the different orbital cycles. This was carried out by using a power systems computer program (Ref-VI-3) for energy balance calculations. A subroutine option was used employing a shunt dissipator to limit the maximum voltage on the solar array bus to 51 volts. This simulates the VO'75 spacecraft which uses zener diodes across the solar array to limit voltages to the power conditioning equipment. High array voltages can occur as the spacecraft comes out of occultation since the array at this time is cold.

Time lines used in the power subsystem orbital simulation are shown in Tables VI-14 and 15 for the two configurations. As previously described both mapping and data relay phases are provided for in the 0.5 eccentricity orbit. For the 0.3 eccentricity orbit, one orbit is used for mapping and one for data transmission; while for the circular orbit, four orbits are required for data transmission. The numbered phases in the first column correspond with the phase names identified in Tables VI-6 through VI-11.

Solar array temperatures encountered with maximum Sun occultation are shown in Figure VI-11 for the three eccentricities.

Results of the simulation are plotted in Figures VI-12 through VI-21 where values of the array power utilized during the orbit and voltages and currents are shown. The simulation employed a 24-cell (NiCd) battery with a capacity of 60 ampere hours, the same as that used on VO'75. Shown in Table VI-16 is a summary of depth of discharge for each condition simulated.

Table VI-14 Time Lines for Configuration A (Shared Antenna Option)

	Phase	Time at Start of Phase		
		Orbital Hours	Power Hours	Power Minutes
	e = 0.5, Period = 4.487 hr			
	1	2.77	0.02	1.2
	2	2.80	0.05	3.0
	3	3.82	1.07	64.2
	4	4.12	1.37	82.2
	5	4.27	1.52	91.2
	6	0.22	1.96	117.6
	7	0.37	2.11	126.6
	8	0.95	2.69	161.4
	e = 0.3, Period = 2.708 hr			
Mapping Orbit	1	1.28	0.0	0.0
	2	1.31	0.03	1.8
	3	2.11	0.83	49.8
	4	2.28	1.00	60.0
	5	2.43	1.15	69.0
	6	0.28	1.71	102.6
	7	0.43	1.86	111.6
	8	1.28	2.71	162.6
Relay Orbit	9	1.31	0.03	1.8
	10	2.11	0.83	49.8
	11	2.45	1.17	70.2
	e = 0, Period = 1.586 hr			
Mapping Orbit	1	0.49	0.0	0.0
	2	1.04	0.54	32.6
	3	1.19	0.69	41.4
	4	0.40	1.50	90.0
Relay Orbits (4)	5	0.49	0.0	0.0
	6	1.10	0.61	36.6
	7	1.44	0.95	57.0
	8	0.46	1.56	93.6

Table VI-15 Time Lines for Configuration C (Specialized Spacecraft)

	Phase	Time at Start of Phase		
		Orbital Hours	Power Hours	Power Minutes
	e = 0.5, Period = 4.487 hr			
	1	1.668	0.026	1.56
	2	1.698	0.056	3.36
	3	2.902	0.260	15.60
	4	3.482	1.840	110.40
	5	4.048	2.406	144.36
	6	0.439	3.284	197.04
	e = 0.3, Period = 2.708 hr			
Mapping Orbit	1	0.936	0.0	0.0
	2	0.967	0.030	1.80
	3	1.792	0.855	51.30
	4	2.286	1.349	80.94
	5	2.372	1.435	86.10
	6	0.422	2.193	131.58
Relay Orbit	7	0.937	0.0	0.0
	8	0.967	0.030	1.80
	9	1.792	0.855	51.30
	10	1.896	0.959	57.54
	e = 0, Period = 1.586 hr			
Mapping Orbit	1	0.49	0.0	0.0
	2	1.04	0.54	32.6
	3	1.19	0.69	41.4
	4	0.40	1.50	90.0
Relay Orbits (4)	5	0.49	0.0	0.0
	6	1.10	0.61	36.6
	7	1.44	0.95	57.0
	8	0.46	1.56	93.6

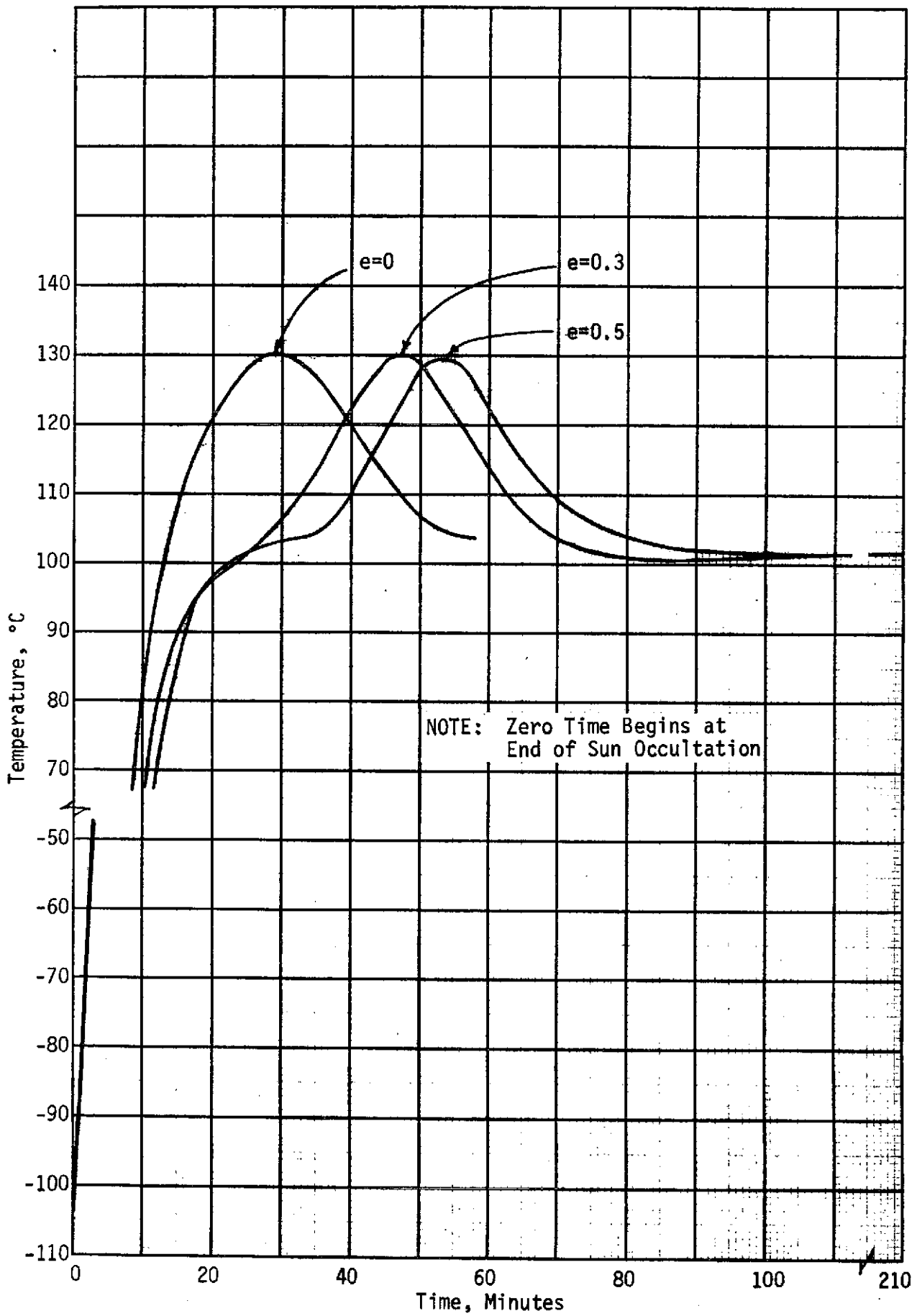

Figure VI-11 Solar Array Time-Temperature Relationships

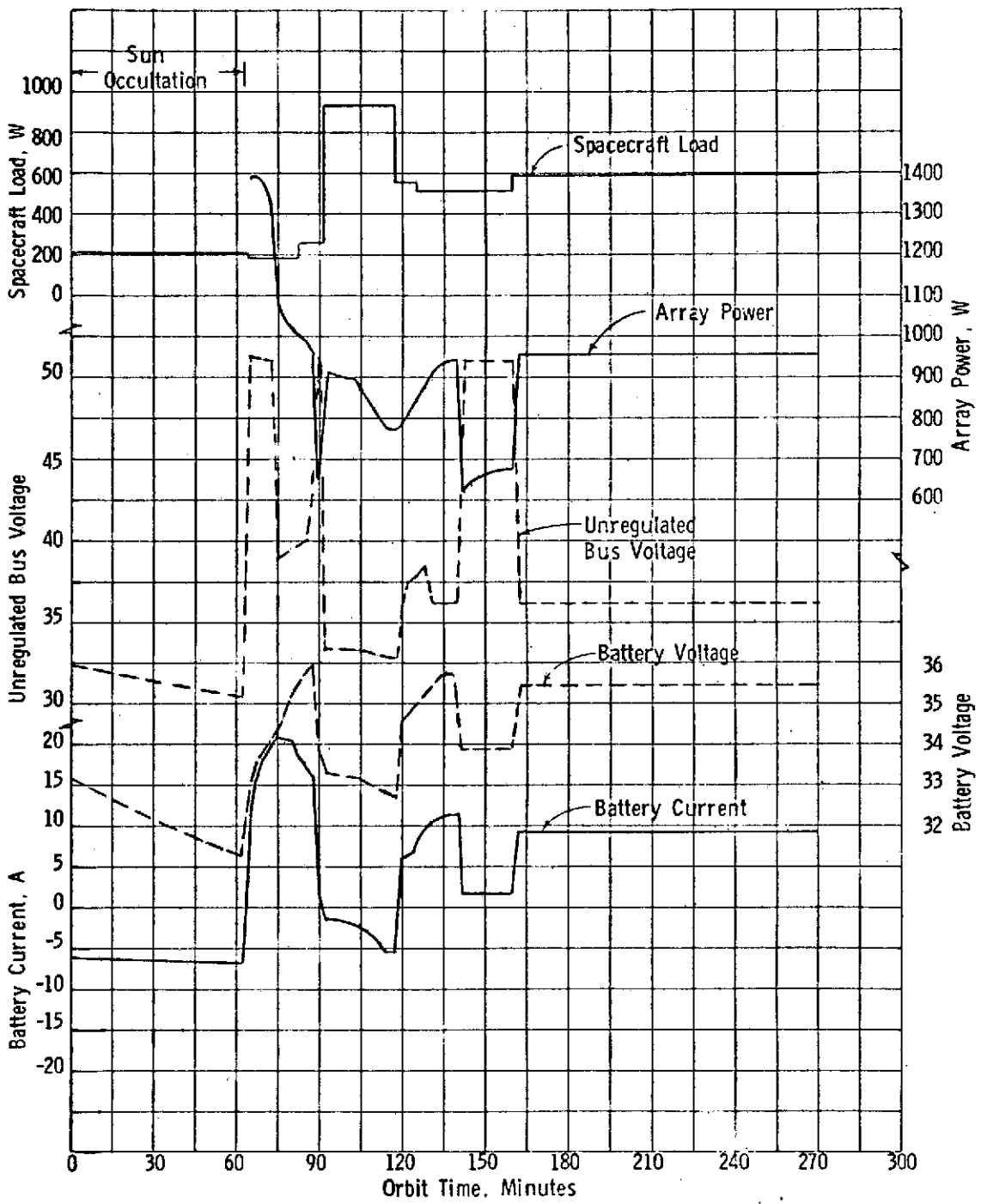

Figure VI-12 Power System Orbital Performance Configuration A, e = 0.5

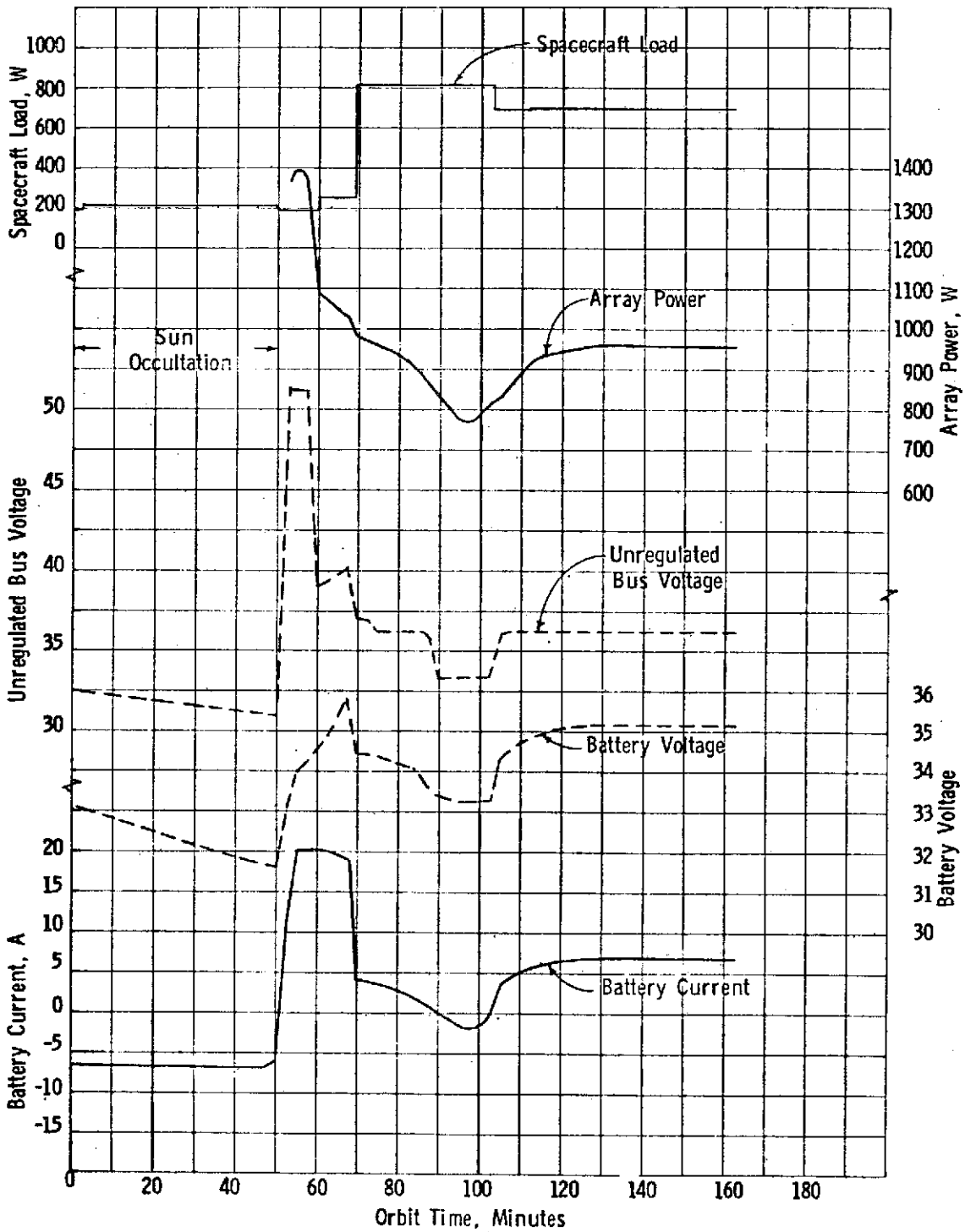

Figure VI-13 Power System Orbital Performance, Configuration A, e = 0.3 Mapping Orbit

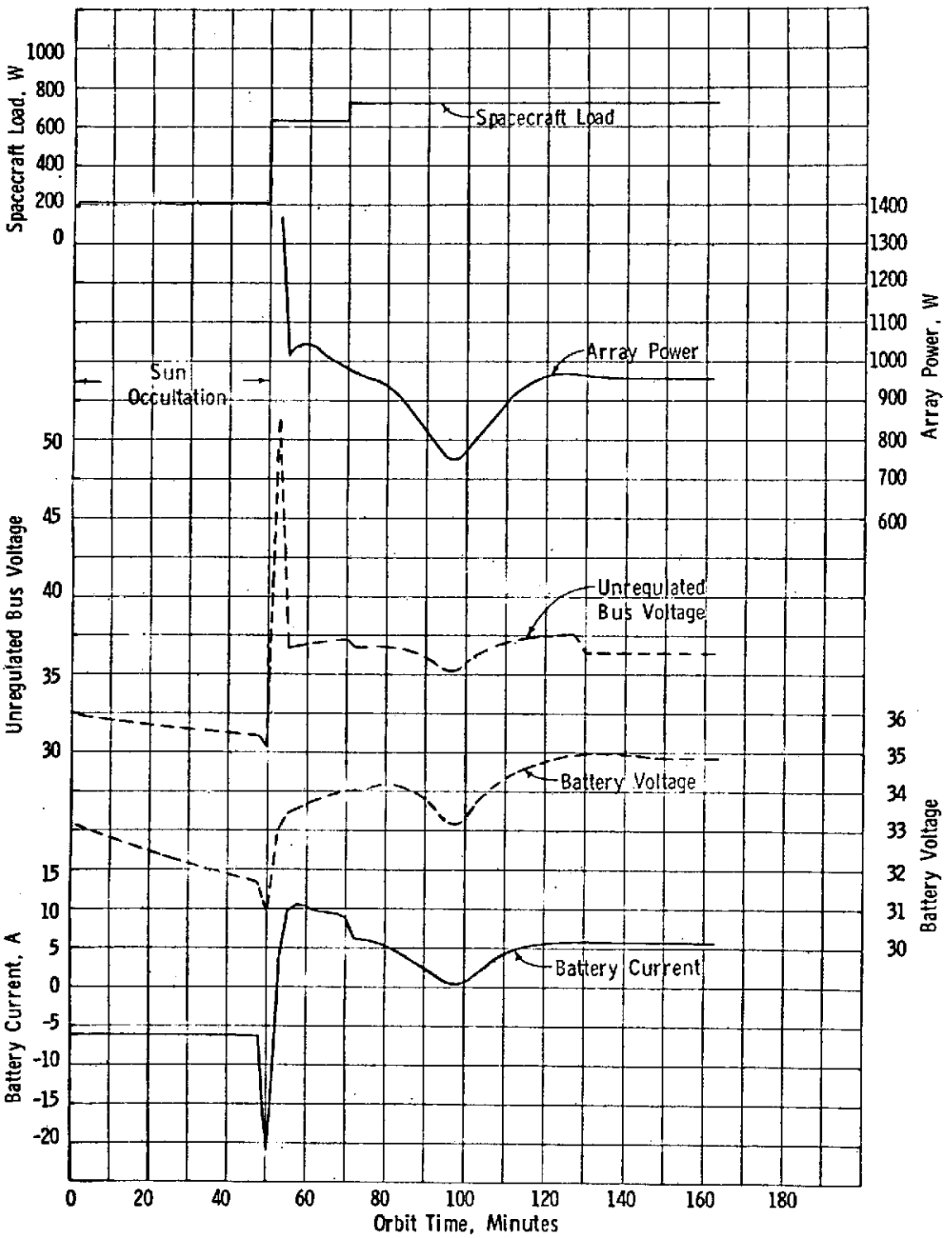

Figure VI-14 Power System Orbital Performance, Configuration A, e = 0.3 Relay Orbit

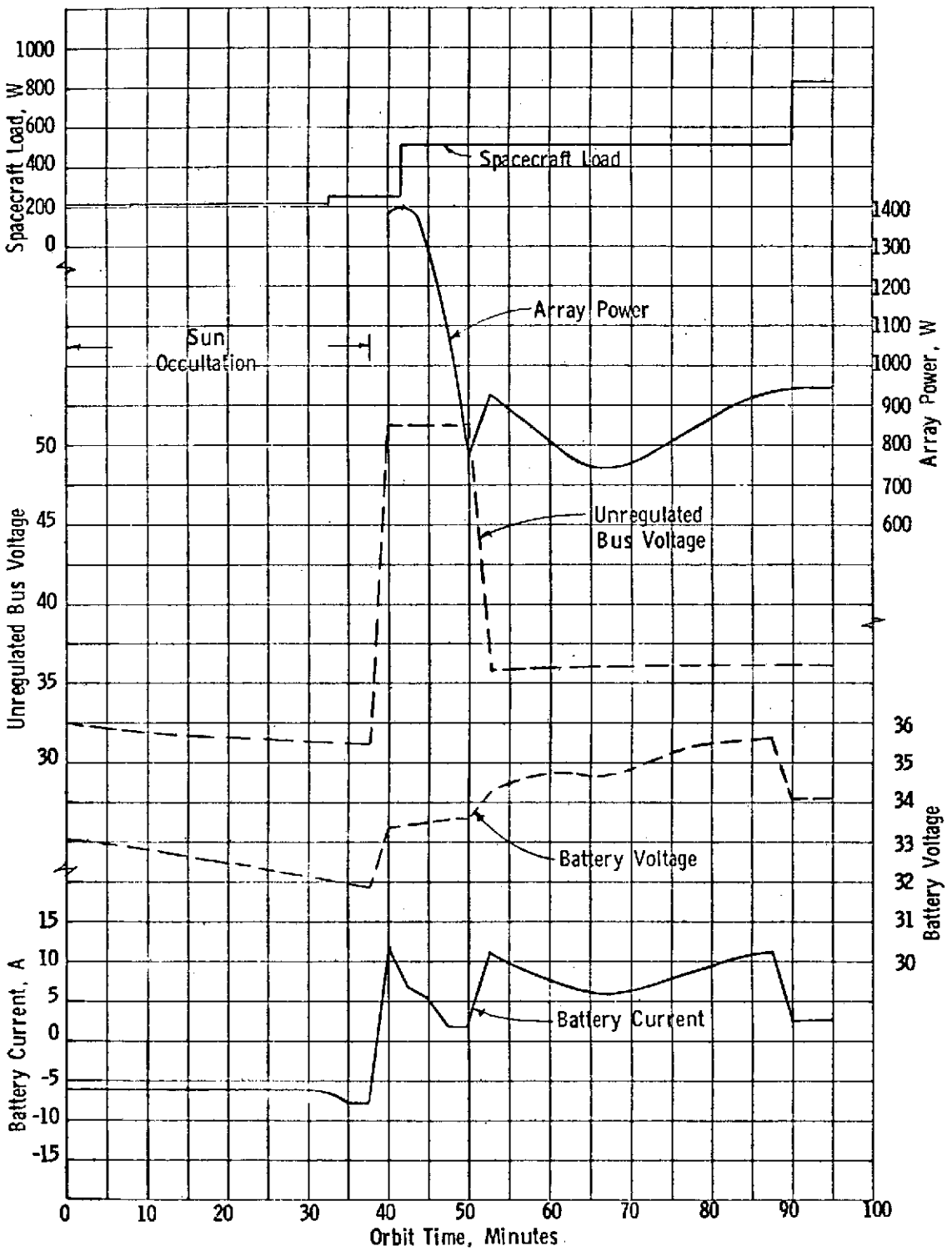

Figure VI-15 Power System Orbital Performance, Configuration A, e = 0 Mapping Orbit

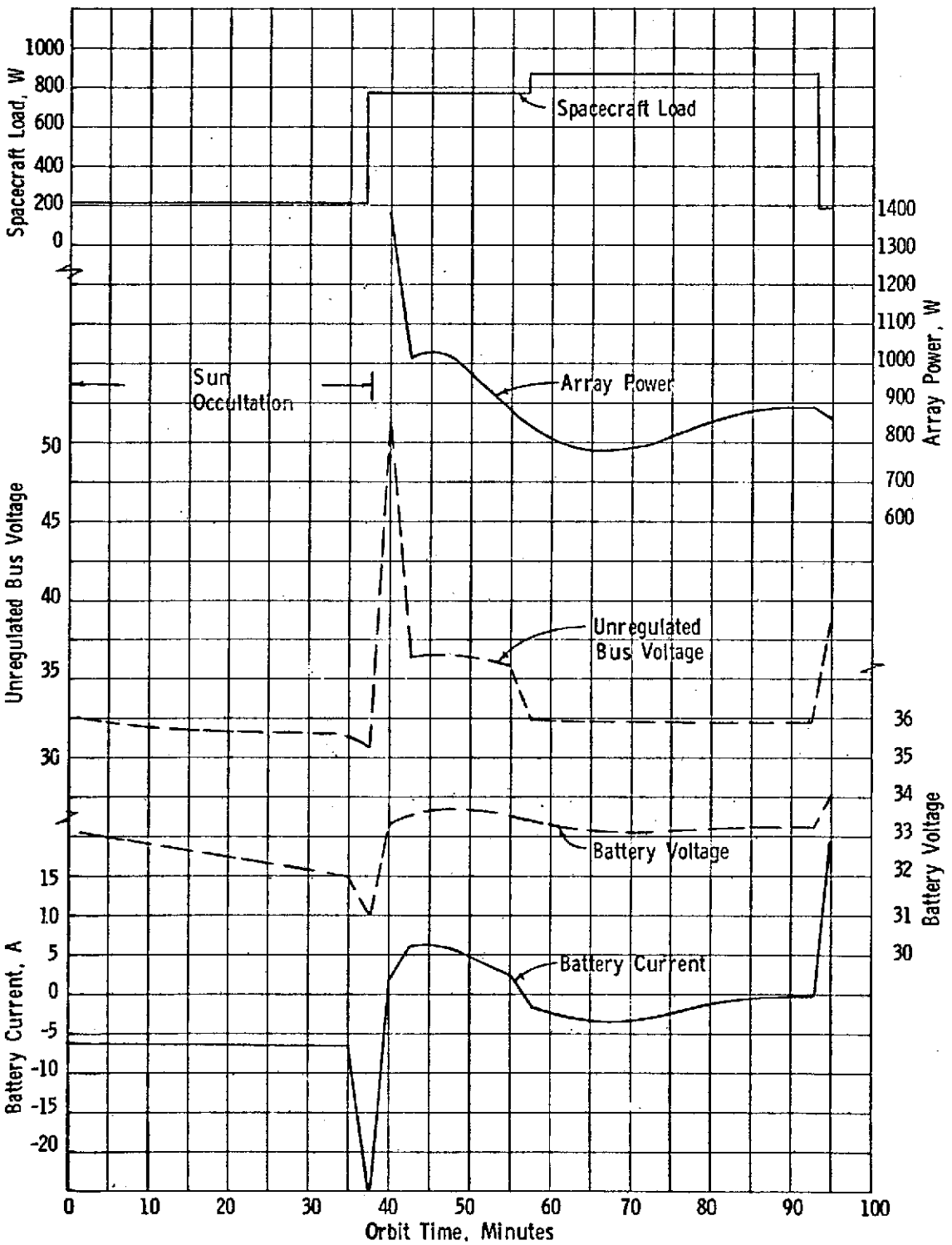

Figure VI-16 Power System Orbital Performance, Configuration A, e = 0, Relay Orbit

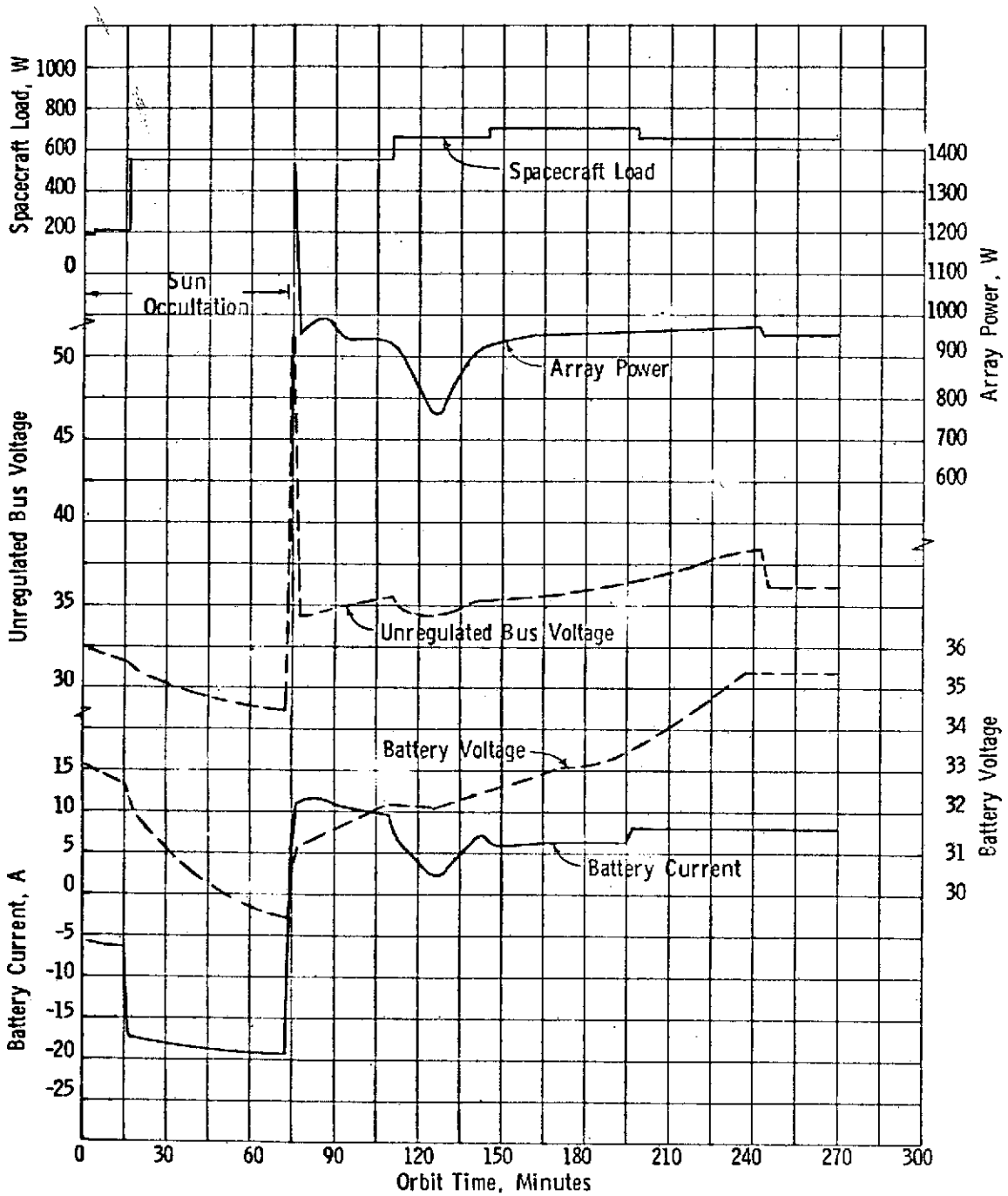

Figure VI-17 Power System Orbital Performance, Configuration C, e = 0.5

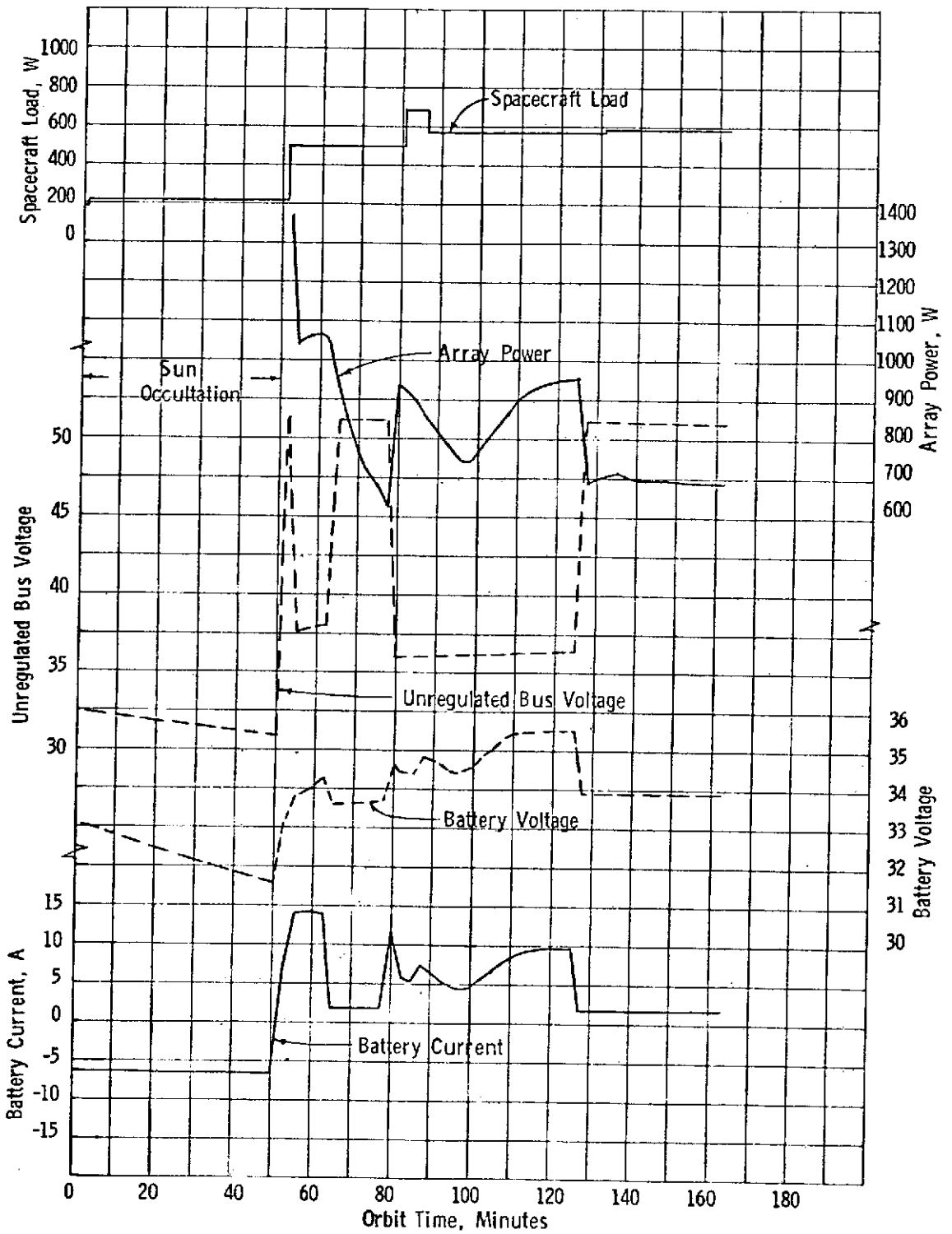

Figure VI-18 Power System Orbital Performance, Configuration C, e = 0.3 Mapping Orbit

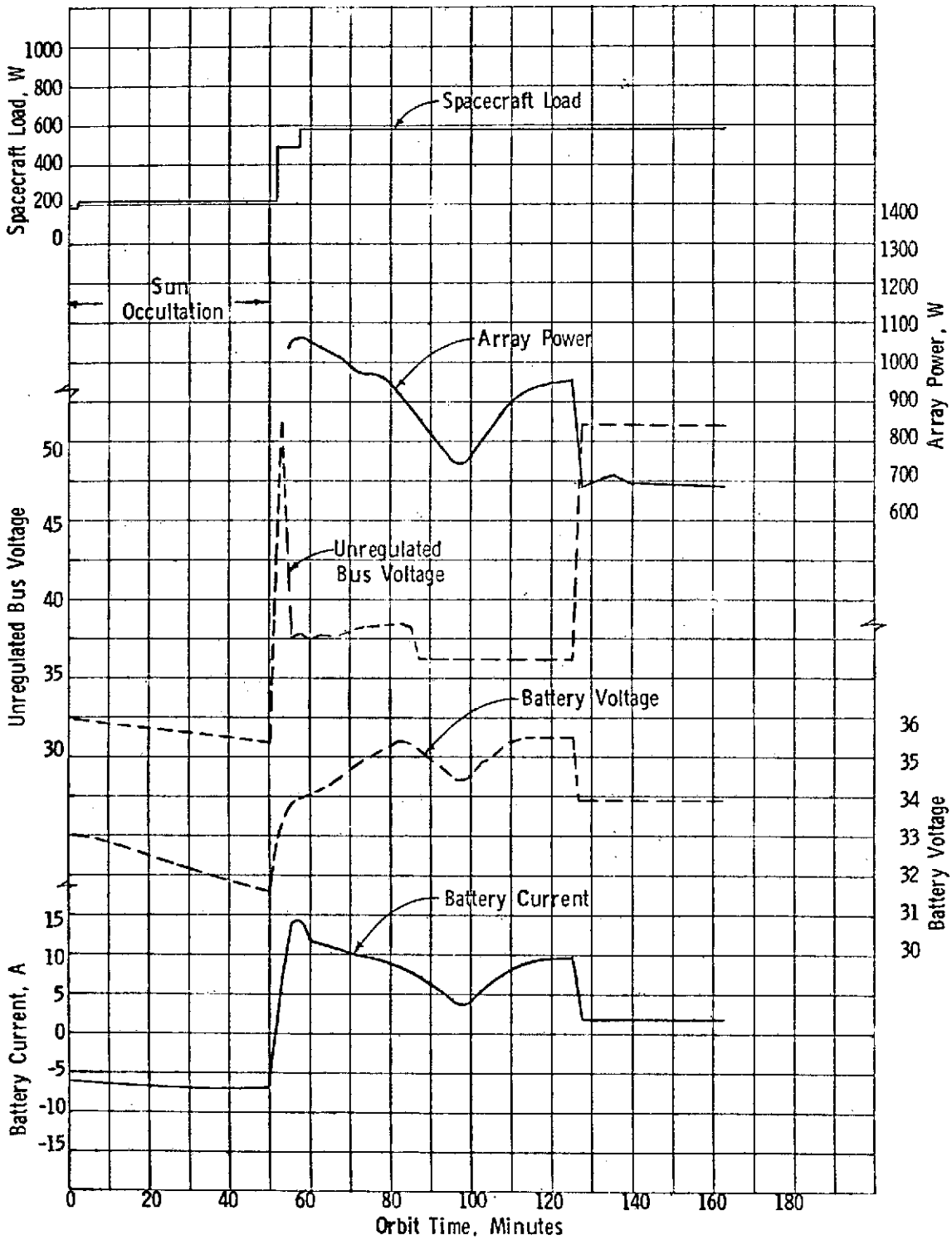

Figure VI-19 Power System Orbital Performance, Configuration C, e = 0.3 Relay Orbit

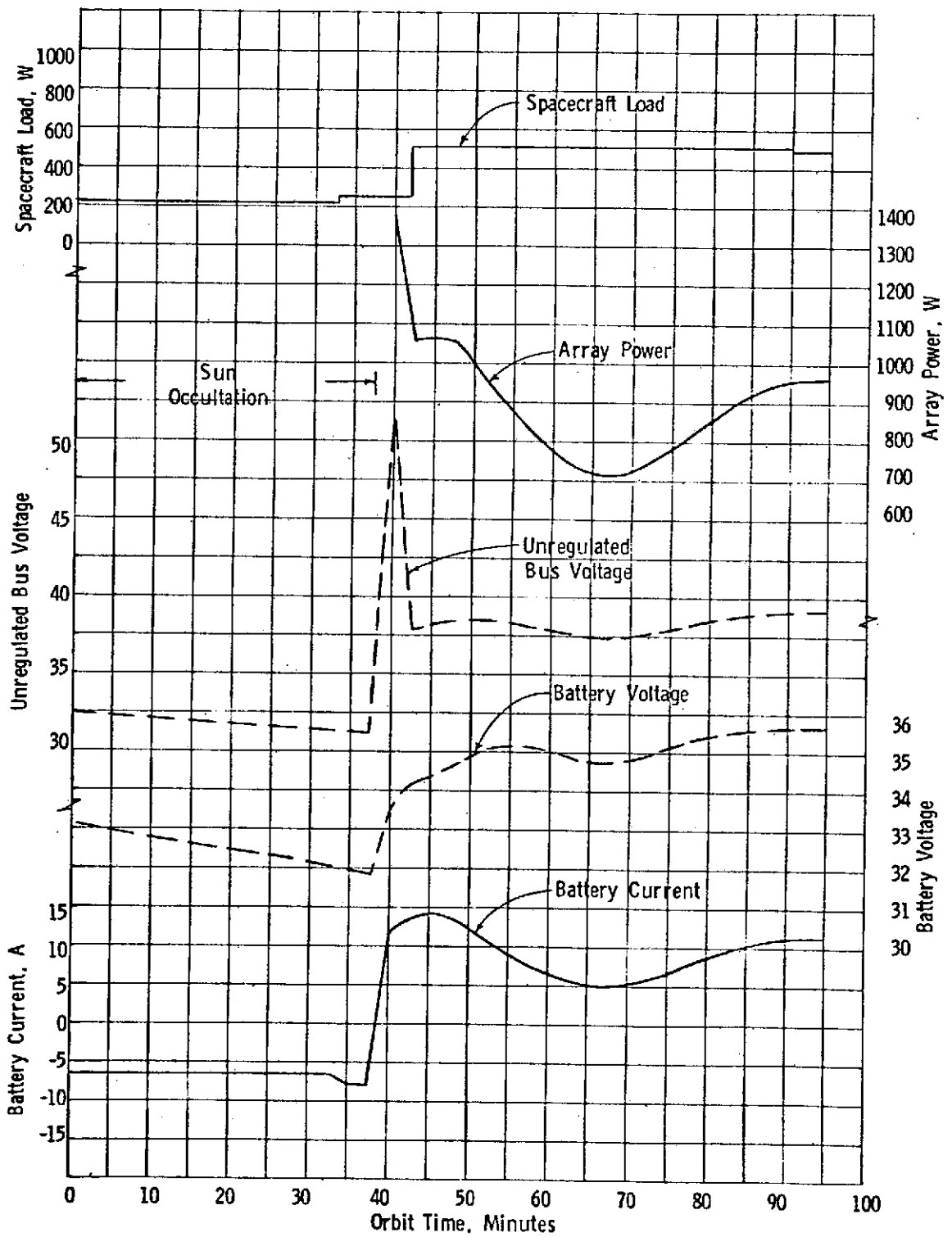

Figure VI-20 Power System Orbital Performance, Configuration C, e = 0 Mapping Orbit

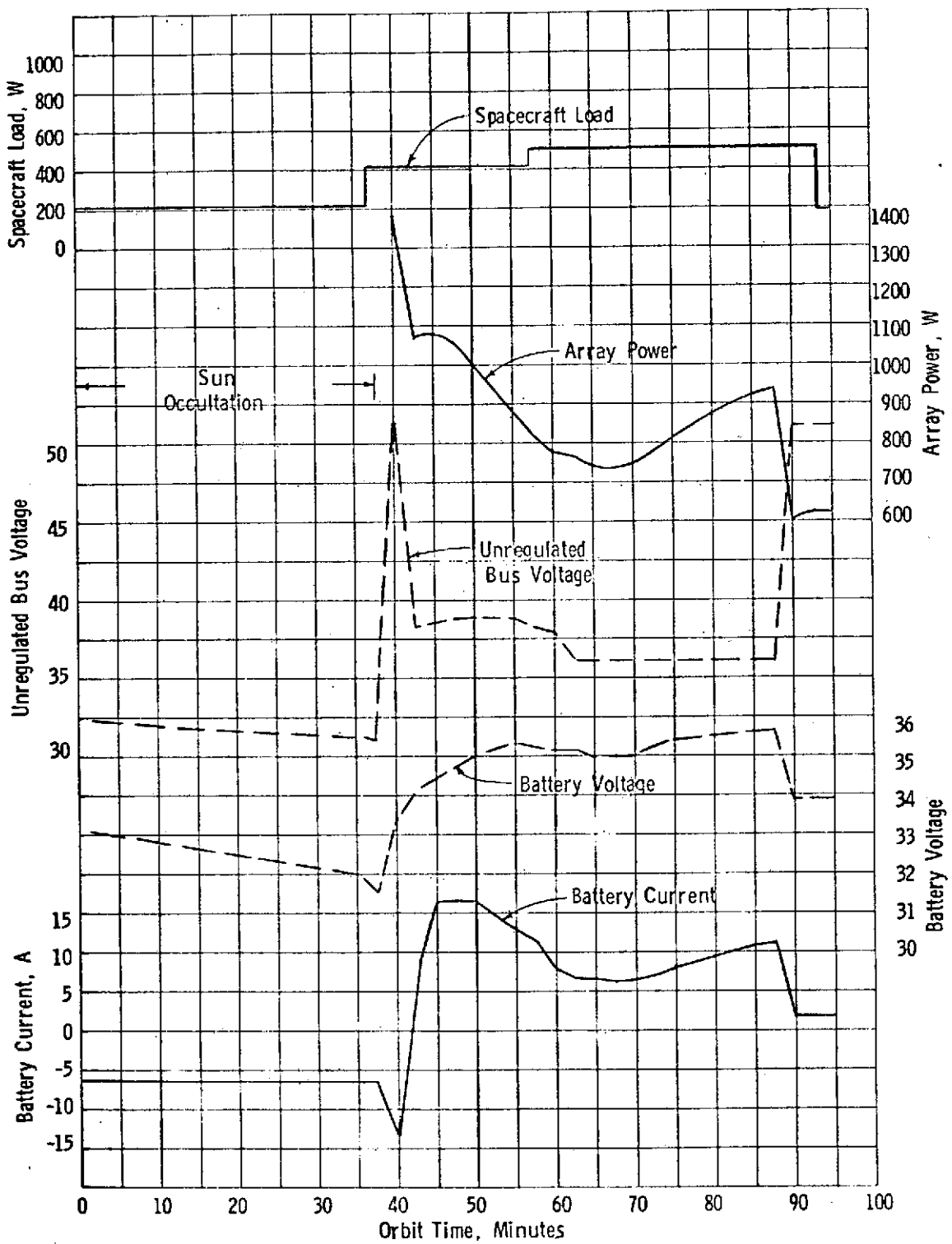

Figure VI-21 Power System Orbital Performance, Configuration C, e = 0
Relay Orbit

Table VI-16 Battery Depth of Discharge Summary

Configuration	Orbit Eccentricity	Depth of Discharge (%)	
		Mapping Orbit	Relay Orbit
A	0.5	11.5	11.5
	0.3	9.2	10.2
	0.0	7.0	8.2
C	0.5	32.5	32.5
	0.3	9.2	9.2
	0.0	7.0	7.3

It is estimated from data in Section III that 535 orbits will be encountered in the 0.5 orbit that required the maximum depth of discharge from the battery. As seen from the 25°C, 3-hour cycle line in Volume III, Figure VI-9 expected life under this condition is 9600 cycles which is well over the 535 cycles expected to be encountered during the mission. It is therefore concluded that the capacity of the battery is adequate.

The adequacy of the solar array is determined by its ability to supply spacecraft loads as well as to provide for replenishing energy taken from the battery during occultation. For this study the criterion used is that the battery be recharged to capacity. Table VI-17 summarizes the time required and the corresponding percentage of orbit needed to achieve the desired recharge.

Table VI-17 Times and Percentage of Orbit Required for Recharge

Configuration	Orbit Eccentricity	Mapping Orbit		Relay Orbit	
		Minutes	Percentage of Orbit	Minutes	Percentage of Orbit
A	0.5	162.5	60.2	162.5	60.2
	0.3	135.0	83.0	153.8	94.5
	0	------	-----	----	-----
C	0.5	257.5	95.3	257.5	95.3
	0.3	122.5	75.3	111.3	68.5
	0	86.2	90.8	81.7	86.0

The summary shows that the desired recharge was achieved for all orbits except the circular one with Configuration A. In this one 104.2% of recharge was achieved for the mapping orbit and 93.3% of recharge for the relay orbit. Again, it is emphasized that these data are for orbits in which maximum Sun occultation occurs. Power and energy margins are very sensitive also to the degree of loading which occurs during occultation, for instance in the case of the 0.5 eccentric orbit with Configuration C, signal acquisition occurs during a portion of Sun occultation resulting in a greater battery depth-of-discharge than for other orbits and a lower power margin. It is concluded that the power subsystem is adequate to supply all configurations and orbits except for Configuration A in a circular orbit.

A desirable option, discussed under the attitude control section, is to employ a control moment gyro (CMG) system for fine antenna pointing in Configuration A. This is particularly needed should a 4-meter rather than a 3-meter antenna be employed. The CMG system would require 10 watts average, 14 watts peak, of 400 Hz power. Power margins of Configuration A are such that these additional requirements would have an insignificant impact upon the power subsystem.

Thermal Control

The principal areas of concern in the thermal design of the VRM spacecraft, their effects on performance, and potential design solutions are summarized on Table VI-18. Also indicated are the proposed configurations on which the various design approaches play a significant or predominant role. It is noted that alternate approaches to those proposed for Configurations A, B and C are possible within each of the concern-areas, and an optimum combination of these should be the result of detailed design. The level of detail in the present study is that required to prove feasibility, and evaluate technology requirements.

Equipment Compartment Thermal Design - Thermal control schematics of the three configurations are shown in Figure VI-22. The proposed thermal design employs the "enclosure concept" whereby the equipment compartment is partially isolated from the thermal environment by the use of high-performance (multilayer) insulation, and partially coupled to it by heat rejection surfaces referred to as radiators. In the case of Configurations A and B the radiators are integral with the basic structure, whereas they are detached in the case of Configuration C.

The radiator surfaces are highly reflective in the solar wavelength (0.25 to 0.75 microns) in order to minimize the effects of the external environment during the orbital phases of the mission, which is "hot" in the solar wavelength only. As a result, the principal thermal transients in orbit are due to the

Table VI-18 Thermal Concerns and Potential Solutions

THERMAL CONCERNS	EFFECT ON THERMAL PERFORMANCE	POTENTIAL SOLUTIONS	APPLICABLE CONFIGURATION
Near-Venus Environment: Solar Intensity Twice Near-Earth Value Albedo 76 %	Reduced S/C Internal Heat-Rejection Capability	Use Solar-Reflector Type Heat Rejection Surfaces, such as:	
		-Second-Surface Mirror Flat Radiators	A, B, C
		-Specular Louver Blade Assemblies	A, B,
		Minimize Incident Environmental Fluxes by Judicious Location and Orientation of Radiators	C
		Absorb Penalty via Increased Radiator Area	A, B
	Increased Solar Panel Temperature & Reduced Solar Cell Efficiency	Absorb Penalty via Increased Panel Area	A, B, C
		Reduce Panel Temperature via -Active Thermal Control -Special Panel Design (e.g. "Helios")	
Near-Earth & Cruise: External Heat Loads Potentially Zero	Widens Range of Thermal Design Requirements	Use Active Thermal Control to Accommodate Range	A, B, C
		Narrow Range by Minimizing Near-Venus Effects per above	C
Configuration Design: Thermal Blockage by Antennas	Reduced S/C Internal Heat-Rejection Capability	Locate & Orient Radiator(s) to Minimize View-Factor to Antennas	C
		Absorb Penalty via Increased Radiator	A, B
Mission Design: S/C -Venus - Sun Radiation Geometry Unfavorable	Unavoidable External Heat Loads	Locate & Orient Radiator(s) to Minimize View Factors to Sun/Venus	C
		Impact Mission Design	
Internal Power Profile: Radar- and Communications Electronics are Concentrated Heat Sources	Potential "Hot Spots" and Excessive Equipment Temperatures	"Isothermalize" Equipment Compartment by the Use of Heatpipes	A, B, C
		Reduce Local Temperature Peaks by the Use of Phase Change Material (PCM)	
		Use "Distributed" Packaging of High-Heat Dissipating Electronics	
		Impact Equipment Design and Qualification to Increase Permissible Temp. Levels	

relatively high peak-to-average ratios of internal power dissipation during mapping and high-rate relay. The proposed solution employs an internal heat pipe system whose purpose is to "isothermalize" the equipment compartment, making its entire thermal mass (product of weight and specific heat) effective in smoothing out the internal temperature fluctuations.

Since the orbital-average internal heat dissipation rate is relatively constant throughout the orbital phases of the mission, the use of the heat-pipe concept minimizes the need for variable heat-rejection capability. However, some control of heat rejection is provided on all three configurations (in the form of specular louvers or temperature-controlled heat pipe) in order to accommodate differences in power dissipation levels during the various phases of the mission, and to compensate for design uncertainties. The louvers control the effective emissivity of the radiator surface by the position of the blades, and they are expected to be in a fully-open position during the orbital phases of the mission. The operation of the temperature-controlled heat pipe is based on the expansion and contraction of an inert gas "bubble" which causes the effective condenser area of the radiator/heat pipe to vary on demand. The effective area is expected to remain essentially constant during the orbital phases of the mission.

The required radiator areas - including margins - are indicated on Figure VI- 22. The largest uncertainty in arriving at these figures is due to the lack of reliable data pertaining to the shadowing effect (thermal blockage) of the antennas. A

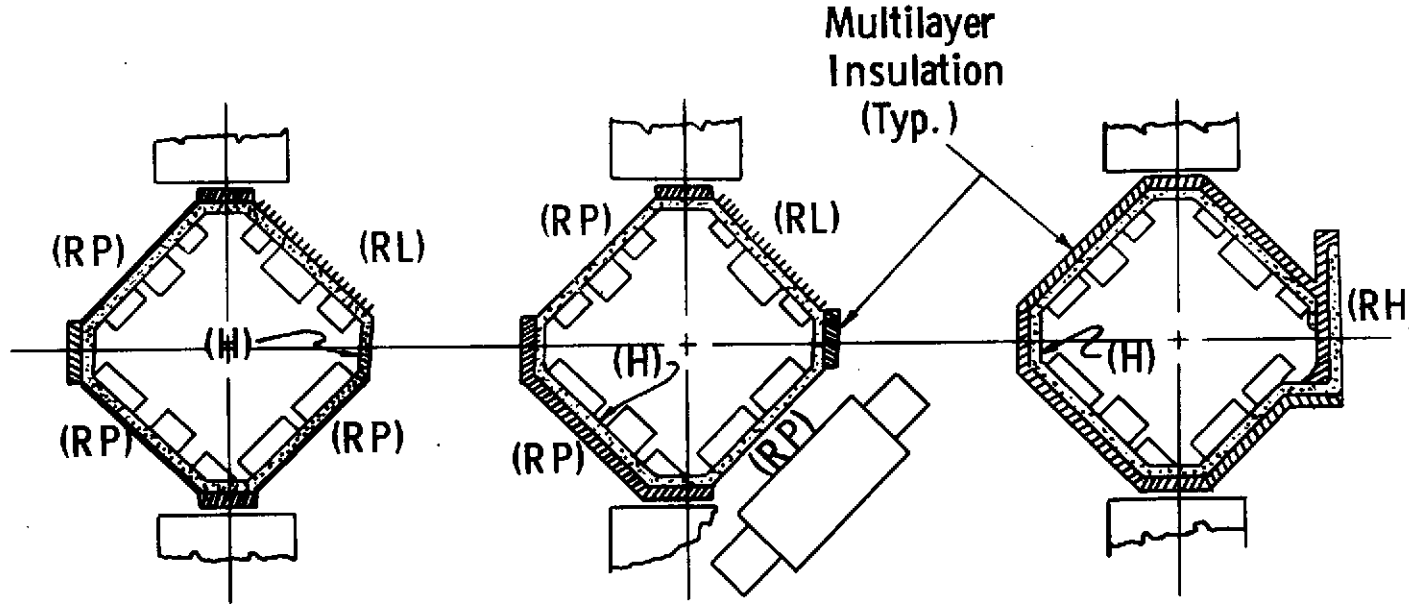

Configuration A

A_R = 2.6 m^2 @ e=0
= 2.0 m^2 @ e=0.3
= 1.9 m^2 @ e=0.5

Configuration B

A_R = 2.9 m^2 @ e=0
= 2.2 m^2 @ e=0.3
= 2.0 m^2 @ e=0.5

Configuration C

A_R = 2.3 m^2 @ e=0
= 1.6 m^2 @ e=0.3
= 1.6 m^2 @ e=0.5

LEGEND: (RP) = Passive Radiator (Second-Surface Mirror)
(RL) = Radiator-Louver Assembly (Base=Second Surface Mirror; Blades=Specular)
(RH) = Radiator-Heat Pipe Assembly (Radiator=Second Surface Mirror; Heat Pipe = Inert Gas Controlled)
(H) = Internal Heat Pipe for Temperature Equalization

Figure VI-22 Thermal Control Schematic

15% blockage is assumed to be a minimum (based on unit area of the antenna), however this figure may increase considerably at sub-normal view angles. Consequently, the estimated effect was arbitrarily doubled when determining the required radiator sizes for Configurations A and B.

The radiator sizes are based on the assumption of no significant direct solar impingement. Since Configuration C is inertially oriented, a 180 degree yaw maneuver of this spacecraft will be required midway during the orbital phase, in order to comply with the "no sun" requirement.

Thermal Performance - The thermal performance of the proposed thermal control concepts is illustrated by the heat balance diagrams on Figures VI-23 and VI-24. The graphical representation is based on a Kepler analogy, and serves the purpose to illustrate the relative magnitudes - and variation in orbit - of the four principal components of radiator heat balance, viz.: (1) heat absorbed from the environment; (2) internal equipment heat dissipation; (3) heat stored and/or liberated by the thermal mass of the compartment; and (4) the heat emitted by the radiator. It is a fundamental requirement that the sum of the first three, balance the fourth.

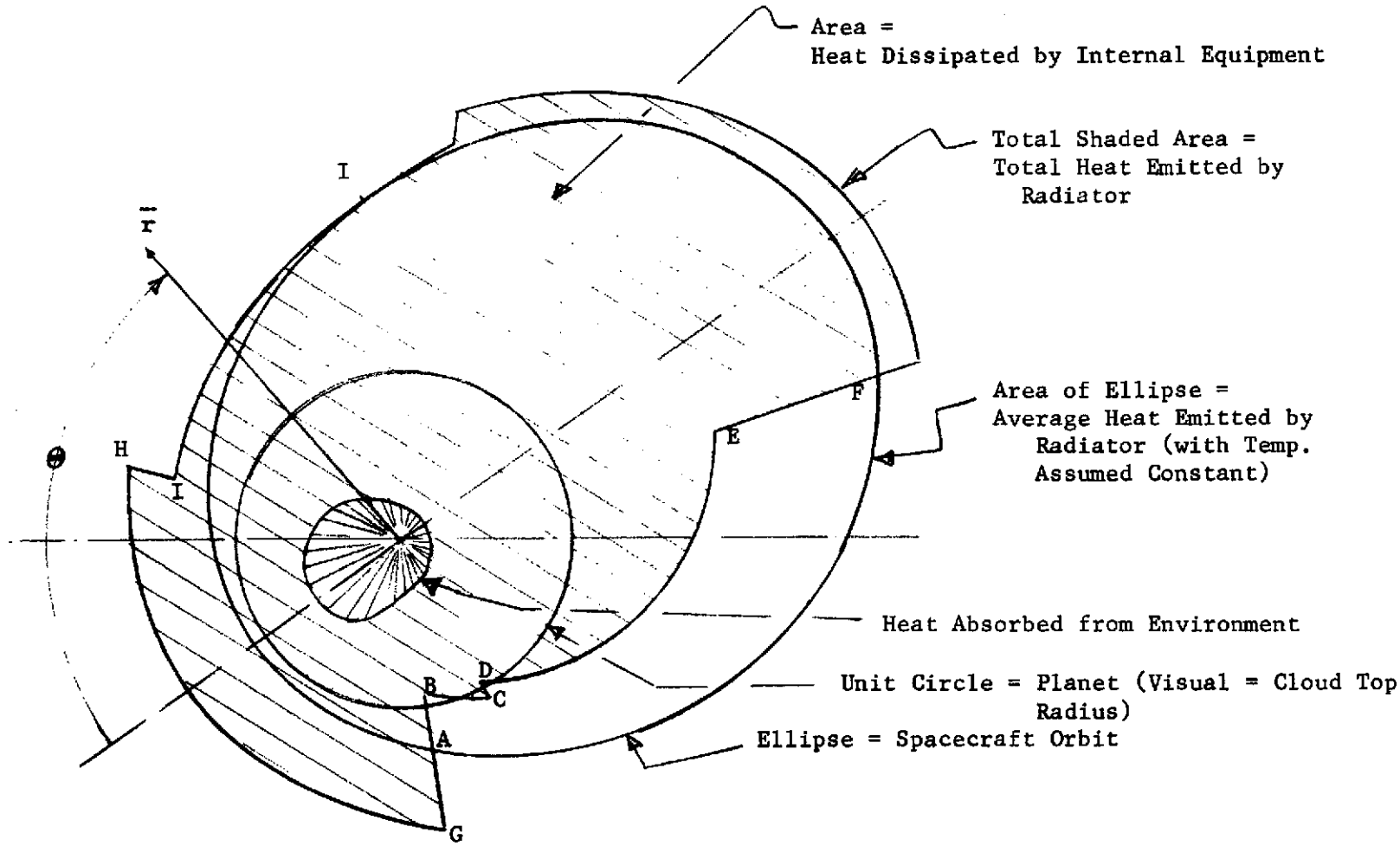

Figure VI-23 Typical Heat Balance Diagram

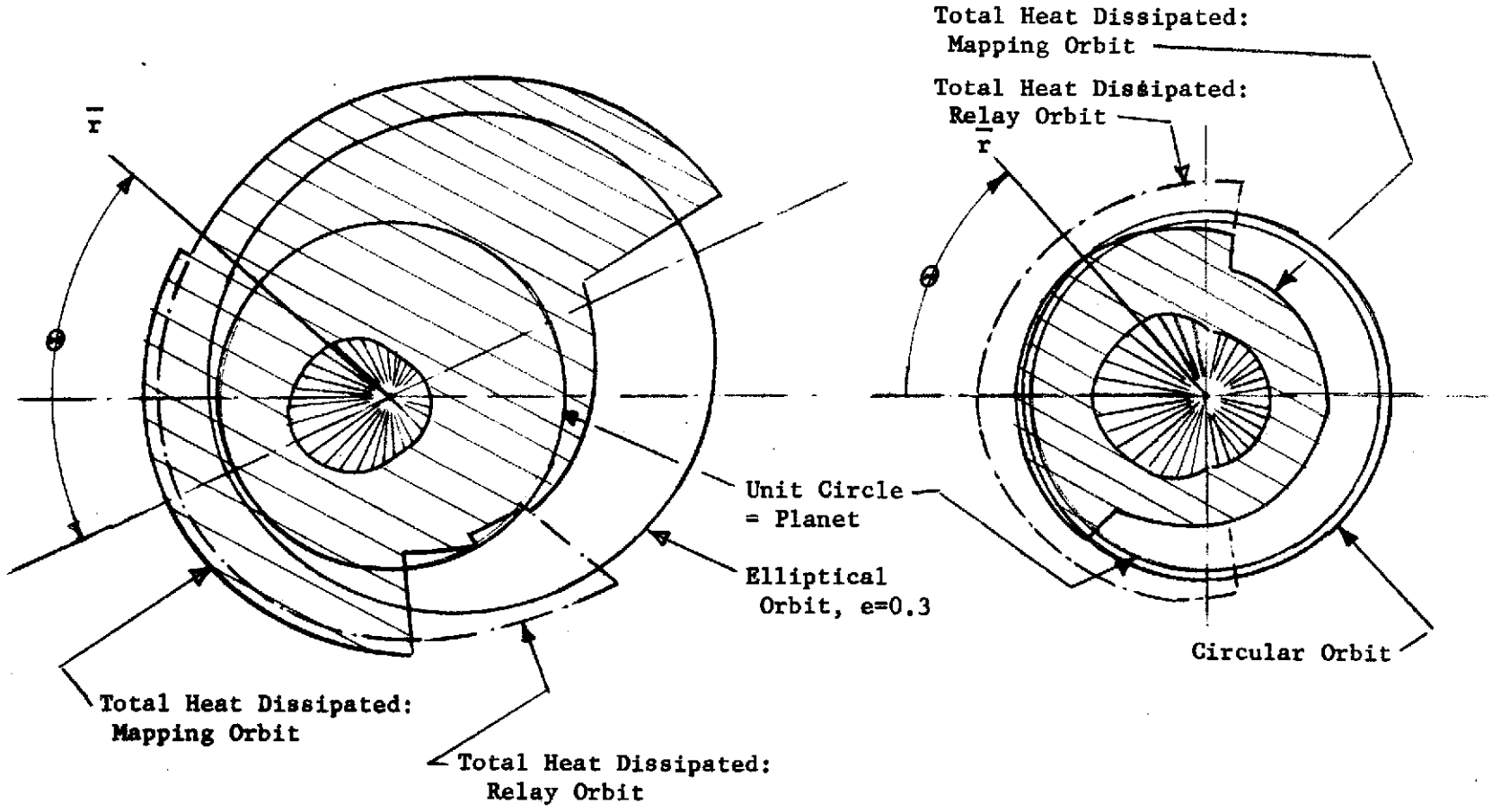

Figure VI-24 Heat Balance Diagram

The polar presentation shows the various heat quantities of interest (represented by areas on the diagram) as a function of spacecraft position in orbit, i.e, of true anomaly θ . The following notations apply:

The unit circle represents the "cloud top" of Venus with a radius of 6120.km.

The ellipse in the case of $e \neq 0$ or circle in the case $e = 0$ represent the orbit of the spacecraft drawn on scale with respect to the unit circle.

The position vector $\bar{r}$ indicates the (arbitrary) position of the spacecraft as a function of true anomaly.

The radially shaded small area around the focus represents the heat absorbed by the radiator from the environment. That portion of the area swept by the position vector $\bar{r}$ while rotating from $\theta = 0$ to θ , is proportional to the total heat absorbed (in $Kcal/m^2$) per unit area of the radiator as a function of θ .

The larger diagonally shaded area represents the internal heat dissipated by the equipment divided by the area of the radiator. That portion of the area swept by the position vector $\bar{r}$ is proportional to the internal heat load per unit radiator area for the period the position vector describes the angle θ.

The area of the ellipse (or circle) representing the orbit is proportional to the heat emitted by the radiator per unit area per orbit, and must equal the sum of the shaded areas. That portion swept by $\bar{r}$ represents the average heat emission as a function of θ .

For any given sector swept by $\bar{r}$ the difference between the sum of the shaded areas and the ellipse (or circle) is proportional to the heat stored or liberated by the thermal mass of the equipment compartment. For example, the ratio of the areas ABCDEFA and OEFABO represents that fraction of the heat rejected by the radiator which is liberated by the thermal mass of the equipment.

From an examination of the heat balance diagrams it is evident that the relative effect of the environment of the heat dissipation capability of the ;highly-reflective radiators is small, although increases somewhat with decreasing eccentricity. On the whole, the heat balance is dominated by internal heat dissipation. The VRM power profiles represent significant thermal transients, requiring heat storage capabilities from 15 to 25 percent of average heat dissipated. The transients due to transitions from mapping to relay orbits are comparable in magnitude with the transients within each orbit, and do not present special thermal control problems. (They can be accommodated by the thermal mass of the compartment).

Solar Panel Temperatures - Solar panel temperature profiles for worst case occultations of the e = 0.5, 0.3 and 0.0 orbits are shown on Figures VI-25, 25 and 27 respectively. The temperatures were based on a cell-side α/ε of 0.78/0.82, and a back-side α/ε of 0.33/0.95. The latter represents a Silicon Oxide white paint in a degraded condition after 8×10^3 ESH (Equivalent Sun Hours) of UV exposure. The initial α/ε of this paint is 0.17/0.92, consequently somewhat lower solar panel temperatures (and higher conversion efficiencies) will be realized at the beginning of the mission.

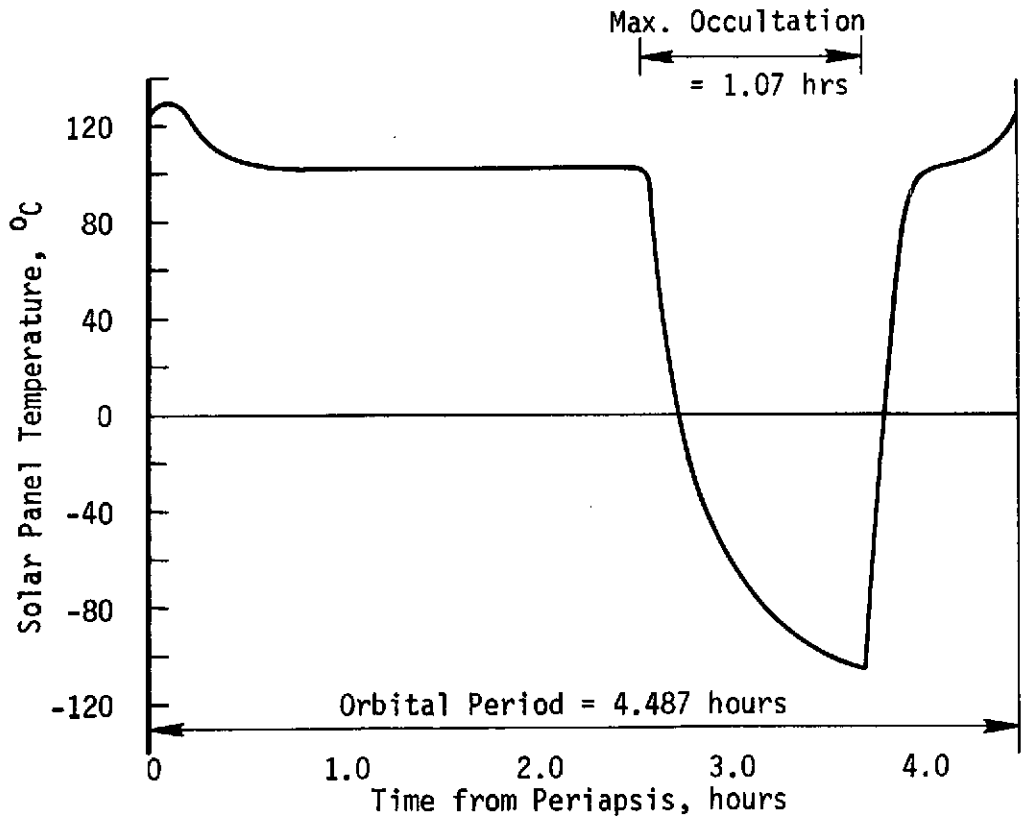

Figure VI-25 Solar Panel Temperature Profile
e = 0.5, Shared Antenna Concept

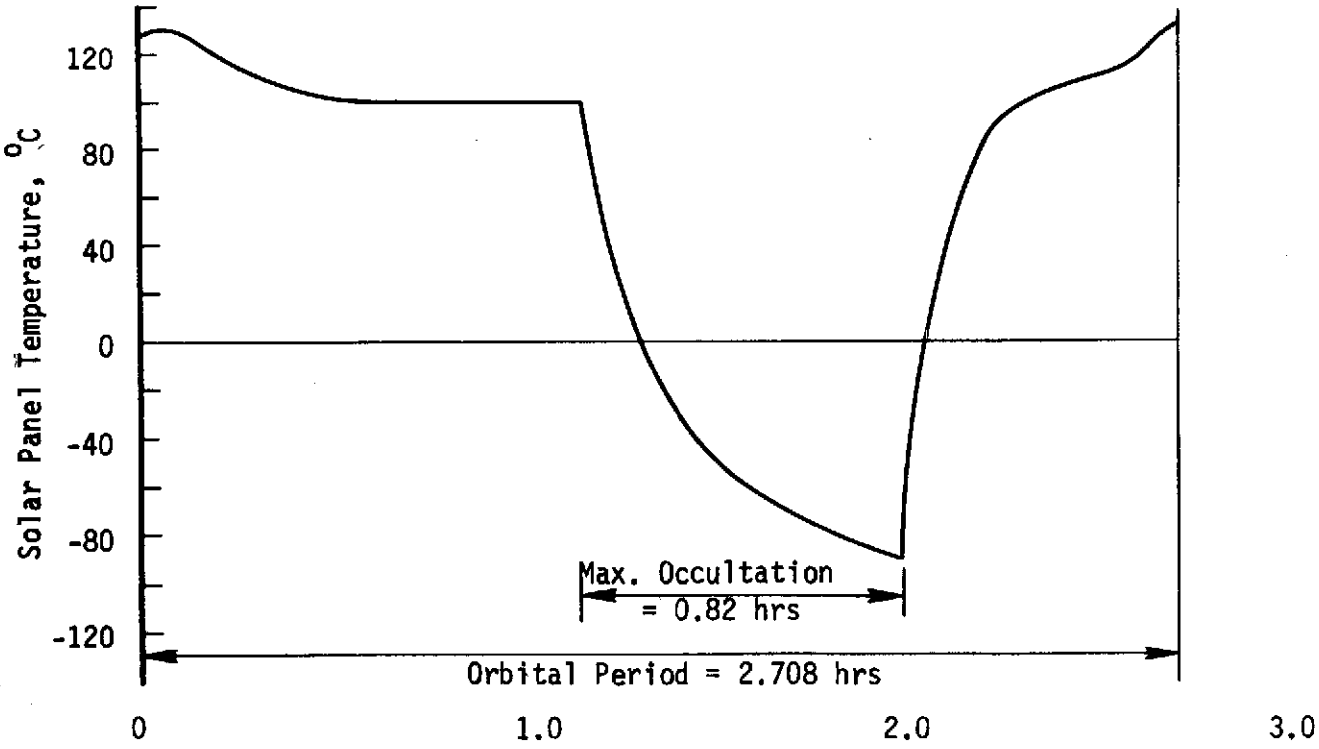

Figure VI-26 Solar Panel Temperature Profile
e = 0.3, Shared Antenna Concept

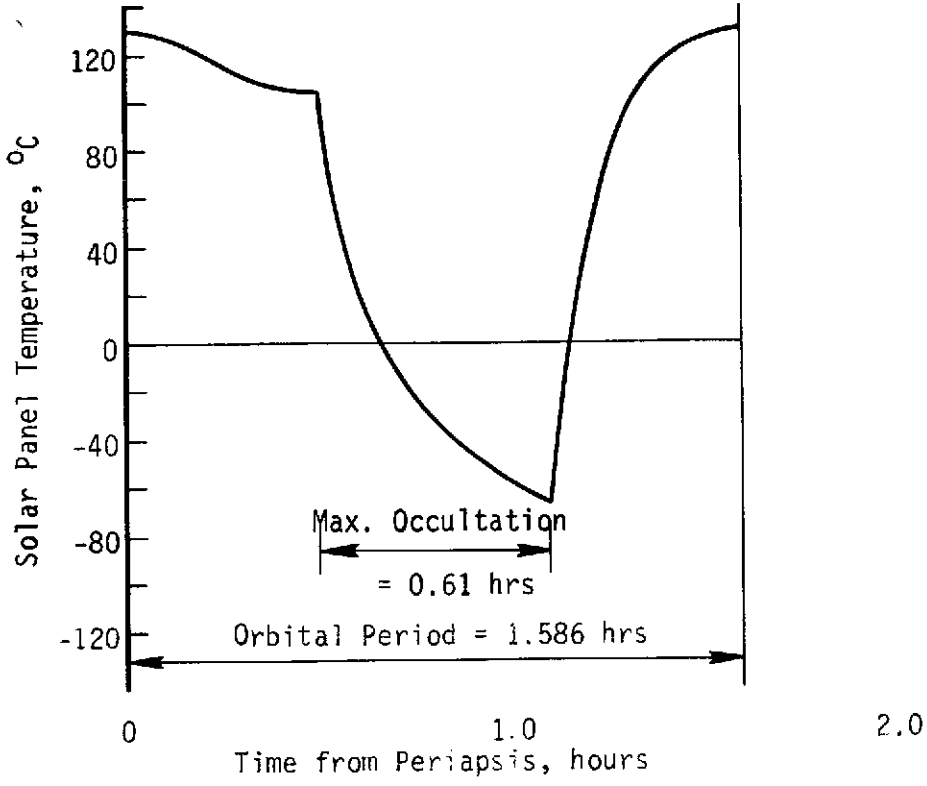

Figure VI-27 Solar Panel Temperature Profile
e = 0, Shared Antenna Concept

Mass Properties

Primary objectives of the mass properties activity during this study were to prepare mass estimates of the various configurations and to develop center of gravity and inertia data needed for design of the attitude control system. Mass estimates relied heavily on Viking Orbiter '75 mass data, however, some estimating such as that for the large antennas and the space storable propulsion systems required data from other sources with parametric techniques tailored to the particular application. Parametric estimating data and estimating methods are covered in Volume III.

The MMC computerized preliminary design mass properties computer program (CBK) was used to develop c.g. and inertia data required for ACS design. While CBK has the ability to handle the complete accounting of any configuration it was only used for a few configurations of particular interest and a simplified weight only summary sheet was used to prepare overall estimates of the remaining configurations. The final C-3 configuration CBK print out is given as Table VI-19.

The following discussion of this print out will show how the mass properties activity was conducted and aid in understanding of the print out. Weights in the run are added downward for various levels of indenture thus each indenture to the left is the total of all items above it up to the previous same level of indenture. The run lists first the stripped bus by contents in each bay, bus equipment and structure. This

TABLE VI-19 VENUS RADAR MAPPER CONFIGURATION C-3 e = 0.5 MASS PROPERTIES DETAILS
VEHICLE DRY WEIGHT

DESCRIPTION	MASS	CENTER OF GRAVITY			RADIUS OF GYRATION		
		X	Y	Z	KX	KY	KZ
	(KG)		(CM)			(CM)	
CONTENTS BAY 1	23.49	118.6	-1.2	23.6	17.2	14.4	13.7
CONTENTS BAY 2	23.63	101.8	38.8	22.6	15.2	15.2	12.6
CONTENTS BAY 4	16.41	39.8	102.3	23.3	15.2	15.2	12.6
CONTENTS BAY 5	24.72	0.	118.6	25.1	13.9	16.2	12.6
CONTENTS BAY 6	21.00	-37.5	100.5	23.3	16.0	16.0	13.7
CONTENTS BAY 9	34.33	-123.6	0.	23.3	17.0	12.6	11.9
CONTENTS BAY 10	20.13	-103.8	-39.3	23.3	15.4	15.4	13.9
CONTENTS BAY 12	25.53	-33.7	-109.7	21.8	14.2	13.9	10.1
CONTENTS BAY 13	34.01	0.	-123.6	23.3	12.6	16.5	11.4
CONTENTS BAY 14	18.41	39.8	-102.3	23.3	15.2	15.2	12.6
CONTENTS BAY 15	6.44	70.6	-71.8	22.8	14.2	14.2	11.6
CONTENTS BAY 16	18.14	102.3	-41.1	22.8	15.2	15.2	13.9
THERMAL CONTROL BLANKET	3.03	10.1	10.1	47.2	63.2	63.2	86.9
BUS EQUIP	31.25	.7	23.3	19.8	93.4	86.1	110.7
BUS STRUCT	57.06	2.5	2.7	25.3	81.0	90.9	104.3
VIKING ORBITER BUS STRIPPED	359.58	3.3	-6.0	23.5	85.5	82.2	113.5
LOW GAIN ANTENNA	3.53	-127.0	0.	-96.5	55.8	55.8	5.0
SOLAR PANEL +X DEPLOYED	25.80	332.7	0.	2.5	35.3	94.4	100.6
SOLAR PANEL -X DEPLOYED	25.71	-332.7	0.	2.5	35.3	94.4	100.8
S/P OUTRIGGER +X	1.72	142.2	0.	30.4	14.7	19.8	22.0
S/P OUTRIGGER -X	1.72	-142.2	0.	30.4	14.7	19.8	22.0
CABLE TROUGH ASSEMBLY	22.86	0.	0.	40.6	72.3	51.0	51.0
STRIPPED (INCL 14.6 kg CONT)	440.92	1.7	-4.9	21.0	81.2	141.8	158.3
PROPULSION MODULE STRUCT	11.88	0.	-.2	-157.4	51.0	62.4	70.6
PROP BLANKET ATTACH HARDWARE	.54	0.	0.	0.	107.9	76.4	76.4
FUEL TANK SHELL -X	56.78	-46.7	0.	-69.8	44.7	44.7	41.9
OXID TANK SHELL +X	56.78	46.7	0.	-69.8	44.7	44.7	41.9
TEMP CONTROL BLANKET PROP	8.75	0.	0.	-75.9	72.3	72.3	78.4
TANKAGE INSTALLATION	134.73	0.	-.0	-77.6	54.2	69.8	64.7

TABLE VI-19 VENUS RADAR MAPPER CONFIGURATION C-3 e = 0.5 MASS PROPERTIES DETAILS
VEHICLE DRY WEIGHT

DESCRIPTION	MASS (KG)	CENTER OF GRAVITY X (CM)	Y (CM)	Z (CM)	RADIUS OF GYRATION KX (CM)	KY (CM)	KZ (CM)
PRESSURANT CONTROL ASSEM	15.14	.7	-50.2	-23.6	9.3	21.3	20.0
PROPULSION PRESSURANT SHELL	37.19	0.	-1.2	24.3	27.6	26.6	26.9
PROPULSION PRESSURANT GAS	4.44	0.	0.	19.8	20.8	20.3	20.8
PRESSURANT SHELL SUPPORT	2.81	0.	-1.2	24.3	27.6	26.5	26.9
PRESSURIZATION INSTALLATION	59.58	.2	-13.6	11.8	38.1	32.4	32.8
THRUST PLATE + HARDWARE	9.52	0.	0.	-154.9	19.3	34.5	40.1
BLANKET THERMAL SWITCH	3.62	0.	0.	-154.9	5.0	7.6	8.8
ISOLATION ASSEM	5.76	0.	25.3	-147.3	9.9	14.7	12.6
ISOLATION ASSEM	5.76	0.	-25.3	-147.3	9.9	14.7	12.6
PYRO ISOLATION UNIT	4.71	40.6	25.3	-147.3	9.9	14.7	12.6
PYRO ISOLATION UNIT	4.71	40.6	-25.3	-147.3	9.9	14.7	12.6
PIPING AND MISC	1.36	0.	0.	0.	30.4	15.2	30.4
ENGINE 1	8.48	35.5	0.	-177.2	11.4	11.4	7.1
ENGINE 2	8.48	0.	0.	-177.2	11.4	11.4	7.1
ENGINE 3	8.48	-35.5	0.	-177.2	11.4	11.4	7.1
ENGINE ACTUATORS	2.49	0.	0.	-157.4	5.0	5.0	6.3
ENGINE PACKAGE (3 ENGINES)	63.37	6.0	0.	-156.1	33.1	39.8	33.1
PROPULSION INSTALLATION	237.68	1.5	-3.1	-76.8	74.9	81.4	52.4
HEAT PIPES + HE RESERVOIR	3.17	0.	0.	22.8	70.1	70.1	99.0
RADIATOR PANEL	14.37	0.	-152.3	63.5	43.1	43.1	43.1
INSULATION	2.44	0.	0.	22.8	84.5	84.5	119.3
THERMAL CONTROL	19.98	0.	-109.5	52.1	89.5	57.6	96.5
COMMUNICATIONS TWTA BAY7+8	19.50	-91.4	55.8	22.8	17.7	17.7	13.9

TABLE VI-19 VENUS RADAR MAPPER CONFIGURATION C-3 e = 0.5 MASS PROPERTIES DETAILS
VEHICLE DRY WEIGHT

DESCRIPTION	MASS	CENTER OF GRAVITY			RADIUS OF GYRATION		
		X	Y	Z	KX	KY	KZ
	(KG)		(CM)			(CM)	
ADDITION TO RADIO FREQ SYS	19.50	-91.4	55.8	22.8	17.7	17.7	13.9
A TO D CONVERTER BAY 6	5.66	-37.5	100.5	23.3	16.0	16.0	13.7
VIDIO PROCESSOR BAY 6	7.03	-37.5	100.5	23.3	16.0	16.0	13.7
ADDITION TO FLIGHT DATA SYS	12.69	-37.5	100.5	23.3	16.0	16.0	13.7
RADAR ANT DISH	3.40	0.	-73.6	200.6	99.0	142.2	99.0
RADAR ANT FEED	1.36	0.	-101.5	200.6	36.8	2.5	36.8
RADAR ANT HUB	8.16	0.	-35.5	200.6	11.4	16.0	11.4
UPPER GIMBAL	2.49	0.	0.	200.6	5.0	5.0	5.0
UPPER SUPPORT	6.21	0.	0.	139.6	33.0	33.0	5.0
LOWER GIMBAL	3.40	0.	0.	78.7	5.0	5.0	5.0
LOWER SUPPORT	3.17	0.	0.	50.7	25.3	25.3	30.4
ANTENNA FEED + MISC	2.72	30.7	-91.4	40.6	25.3	25.3	35.5
RADAR ANTENNA	30.91	4.5	-30.0	145.5	81.5	82.1	53.0
COMM ANT DISH (STOWED)	2.76	0.	50.7	190.5	40.6	38.0	25.3
COMM ANT FEED (STOWED)	1.36	0.	45.7	184.1	35.5	30.4	22.8
COMM ANT HUB (STOWED)	8.16	0.	12.6	129.5	11.4	7.6	15.2
COMM ANT UPPR GIMB (STOWED)	3.22	0.	10.1	127.0	5.0	5.0	5.0
COMM ANT BOOM (STOWED)	5.12	0.	76.1	86.3	45.7	24.1	41.9
COMM ANT MOVABLE (STOWED)	20.62	0.	33.3	130.1	32.8	39.3	37.5
LOWER GIMBAL + SUPPORT	4.98	0.	134.6	35.5	6.3	6.3	6.3
LATCH MECH	3.22	0.	5.0	113.0	12.6	12.6	12.6
COMMUNICATION ANTENNA	28.82	0.	43.0	111.9	69.9	49.0	51.3
RADAR UNIT BAY 15	28.75	70.6	71.8	22.8	16.5	16.5	12.6
RADAR INSTALLATION	28.75	70.6	71.8	22.8	16.5	16.5	12.6

TABLE VI-19 VENUS RADAR MAPPER CONFIGURATION C-3 e = 0.5 MASS PROPERTIES DETAILS
VEHICLE DRY WEIGHT

DESCRIPTION	MASS (KG)	CENTER OF GRAVITY X (CM)	Y (CM)	Z (CM)	RADIUS OF GYRATION KX (CM)	KY (CM)	KZ (CM)
RADAR ALT ELECTRONICS	4.58	0.	-25.3	213.3	6.3	6.3	3.8
RADAR ALT ANTENNA	.58	0.	-93.9	373.3	2.5	3.8	2.5
RADAR ALT COAX	.72	0.	-58.4	287.0	50.7	50.7	2.5
RADAR ALTIMETER	5.88	0.	-36.1	238.1	58.3	54.1	22.2
SOLAR PANEL DRIVE +X	4.53	152.3	0.	2.5	4.3	4.3	4.5
SOLAR PANEL DRIVE -X	4.53	-152.3	0.	2.5	4.3	4.3	4.5
SOLAR PANEL DRIVE	9.06	0.	0.	2.5	4.3	152.4	152.4
GAS TANK + SUPPORT BAY 3	5.35	57.1	57.1	20.5	16.7	16.7	16.7
GAS BAY 3	4.35	57.1	57.1	20.5	12.9	12.9	12.9
H1 PRESSURE MODULE BAY 3	2.67	81.2	81.2	16.5	12.6	12.6	9.1
GAS TANK + SUPPORT BAY 11	5.35	-57.1	-57.1	20.5	16.7	16.7	16.7
GAS BAY 11	4.35	-57.1	-57.1	20.5	12.9	12.9	12.9
H1 PRESSURE MODULE BAY 11	2.67	-81.2	-81.2	16.5	12.6	12.6	9.1
TANKAGE INSTALLATION	24.74	-.0	-.0	19.6	64.8	64.8	90.3
NOZZLES +X ADDED	.40	508.0	0.	2.5	1.2	1.2	1.2
NOZZLES -X ADDED	.40	-508.0	0.	2.5	1.2	1.2	1.2
NOZZLES +Y	.74	0.	162.5	2.5	1.2	1.2	1.2
NOZZLES -Y	.74	0.	-162.5	2.5	1.2	1.2	1.2
TUBING ADDED	.99	12.6	0.	0.	66.0	45.7	45.7
NOZZLE ADDITION	3.27	3.8	0.	1.7	115.2	252.6	275.2
ADDITION TO ACS SYSTEM	28.01	.4	-.0	17.5	72.7	105.3	126.7
ADDITIONAL HARNESS	8.16	0.	0.	25.3	91.4	86.3	106.6

TABLE VI-19 VENUS RADAR MAPPER CONFIGURATION C-3 e = 0.5 MASS PROPERTIES DETAILS
/EHICLE DRY WEIGHT

DESCRIPTION	MASS (KG)	CENTER OF GRAVITY X (CM)	Y (CM)	Z (CM)	RADIUS OF GYRATION KX (CM)	KY (CM)	KZ (CM)
TOTAL ADDITIONS	449.44	.7	3.8	-16.7	112.9	114.0	79.3
CONTINGENCY (10PC -14.6)	72.98	1.2	-.5	1.9	100.3	130.0	124.9

TABLE VI-19 VENUS RADAR MAPPER CONFIGURATION C-3 e = 0.5 MASS PROPERTIES DETAILS
VEHICLE DRY WEIGHT

GRAND TOTAL

MASS 963.34 KGS

CENTER OF GRAVITY

X =	1.21	CM
Y =	-.51	CM
Z =	1.97	CM

RADIUS OF GYRATION

KX =	100.34	CM
KY =	129.90	CM
KZ =	124.90	CM

MOMENT OF INERTIA

IX=	970	KG-M2
IY=	1626	KG-M2
IZ=	1503	KG-M2

PRODUCT OF INERTIA

PXY=	16	KG-M2
PXZ=	1	KG-M2
PYZ=	-15	KG-M2

MOMENT OF INERTIA

IX=	9698541	KG-CM2
IY=	16255703	KG-CM2
IZ=	15027566	KG-CM2

PRODUCT OF INERTIA

PXY=	163971	KG-CM2
PXZ=	12536	KG-CM2
PYZ=	-150155	KG-CM2

TABLE VI-19 VENUS RADAR MAPPER CONFIGURATION C-3 e = 0.5 MASS PROPERTIES DETAILS
VEHICLE WEIGHT AT END OF MISSION BURNOUT

GRAND TOTAL

MASS 1001.74 KGS

CENTER OF GRAVITY

X =	1.62	CM
Y =	-.49	CM
Z =	-.78	CM

RADIUS OF GYRATION

KX =	99.60	CM
KY =	128.64	CM
KZ =	122.97	CM

MOMENT OF INERTIA

IX=	994	KG-M2
IY=	1658	KG-M2
IZ=	1515	KG-M2

PRODUCT OF INERTIA

PXY=	16	KG-M2
PXZ=	-2	KG-M2
PYZ=	-15	KG-M2

MOMENT OF INERTIA

IX=	9937168	KG-CM2
IY=	16576841	KG-CM2
IZ=	15146761	KG-CM2

PRODUCT OF INERTIA

PXY=	164174	KG-CM2
PXZ=	-15973	KG-CM2
PYZ=	-151510	KG-CM2

TABLE VI-19 VENUS RADAR MAPPER CONFIGURATION C-3 e = 0.5 MASS PROPERTIES DETAILS
VEHICLE IN VENUS ORBIT ANTENNA STOWED

GRAND TOTAL

MASS 1005.27 KGS

CENTER OF GRAVITY

X =	1.65	CM
Y =	-.49	CM
Z =	-1.02	CM

RADIUS OF GYRATION

KX =	99.53	CM
KY =	128.52	CM
KZ =	122.79	CM

MOMENT OF INERTIA

IX=	996	KG-M2
IY=	1661	KG-M2
IZ=	1516	KG-M2

PRODUCT OF INERTIA

PXY=	16	KG-M2
PXZ=	-2	KG-M2
PYZ=	-15	KG-M2

MOMENT OF INERTIA

IX=	9958375	KG-CM2
IY=	16605659	KG-CM2
IZ=	15157744	KG-CM2

PRODUCT OF INERTIA

PXY=	164186	KG-CM2
PXZ=	-17602	KG-CM2
PYZ=	-151630	KG-CM2

TABLE VI-19 VENUS RADAR MAPPER CONFIGURATION C-3 e = 0.5 MASS PROPERTIES DETAILS
VEHICLE IN VENUS ORBIT NO ANTENNA

GRAND TOTAL

MASS 984.65 KGS

CENTER OF GRAVITY

X =	1.68	CM
Y =	-1.21	CM
Z =	-3.77	CM

RADIUS OF GYRATION

KX =	96.30	CM
KY =	123.31	CM
KZ =	123.85	CM

MOMENT OF INERTIA

IX=	951	KG-M2
IY=	1621	KG-M2
IZ=	1510	KG-M2

PRODUCT OF INERTIA

PXY=	17	KG-M2
PXZ=	-1	KG-M2
PYZ=	-24	KG-M2

MOMENT OF INERTIA

IX=	9513733	KG-CM2
IY=	16210731	KG-CM2
IZ=	15104524	KG-CM2

PRODUCT OF INERTIA

PXY=	165378	KG-CM2
PXZ=	-13056	KG-CM2
PYZ=	-239681	KG-CM2

TABLE VI-19 VENUS RADAR MAPPER CONFIGURATION C-3 e = 0.5 MASS PROPERTIES DETAILS
VEHICLE IN VENUS ORBIT ANTENNA EXTENDED

GRAND TOTAL

MASS 1005.27 KGS

CENTER OF GRAVITY

X =	1.65	CM
Y =	4.32	CM
Z =	-2.51	CM

RADIUS OF GYRATION

KX =	105.16	CM
KY =	127.38	CM
KZ =	120.65	CM

MOMENT OF INERTIA

IX=	1112	KG-M2
IY=	1631	KG-M2
IZ=	1664	KG-M2

PRODUCT OF INERTIA

PXY=	16	KG-M2
PXZ=	-2	KG-M2
PYZ=	10	KG-M2

MOMENT OF INERTIA

IX=	11116109	KG-CM2
IY=	16312249	KG-CM2
IZ=	16638778	KG-CM2

PRODUCT OF INERTIA

PXY=	156233	KG-CM2
PXZ=	-15137	KG-CM2
PYZ=	98304	KG-CM2

TABLE VI-19 VENUS RADAR MAPPER CONFIGURATION C-3 e = 0.5 MASS PROPERTIES DETAILS
VEHICLE PRIOR TO ORBIT INSERTION ANTENNA STOWED

GRAND TOTAL

MASS 1987.24 KGS

CENTER OF GRAVITY

X =	5.07	CM
Y =	-.23	CM
Z =	-35.01	CM

RADIUS OF GYRATION

KX =	82.57	CM
KY =	105.90	CM
KZ =	95.68	CM

MOMENT OF INERTIA

IX=	1355	KG-M2
IY=	2229	KG-M2
IZ=	1819	KG-M2

PRODUCT OF INERTIA

PXY=	17	KG-M2
PXZ=	-25	KG-M2
PYZ=	-16	KG-M2

MOMENT OF INERTIA

IX=	13547623	KG-CM2
IY=	22266176	KG-CM2
IZ=	18191320	KG-CM2

PRODUCT OF INERTIA

PXY=	165733	KG-CM2
PXZ=	-254454	KG-CM2
PYZ=	-162300	KG-CM2

TABLE VI-19 VENUS RADAR MAPPER CONFIGURATION C-3 e = 0.5 MASS PROPERTIES DETAILS
VEHICLE AT LIFT OFF

GRAND TOTAL

MASS 2008.09 KGS

CENTER OF GRAVITY

X =	5.11	CM
Y =	-.23	CM
Z =	-35.37	CM

RADIUS OF GYRATION

KX =	82.29	CM
KY =	103.57	CM
KZ =	95.35	CM

MOMENT OF INERTIA

IX=	1360	KG-M2
IY=	2238	KG-M2
IZ=	1826	KG-M2

PRODUCT OF INERTIA

PXY=	17	KG-M2
PXZ=	-26	KG-M2
PYZ=	-16	KG-M2

MOMENT OF INERTIA

IX=	13599078	KG-CM2
IY=	22361630	KG-CM2
IZ=	18255429	KG-CM2

PRODUCT OF INERTIA

PXY=	165750	KG-CM2
PXZ=	-256939	KG-CM2
PYZ=	-162468	KG-CM2

method of presentation was used because of the type of mass properties data available on this portion of the Viking Orbiter '75. All items of equipment to be replaced or changed by this study were deleted. A list of VO'75 equipment which was retained is given in Table VI-20.

The low gain antenna, two of the four VO'75 solar panels and the cable through assembly are added to obtain the "stripped orbiter" which carries 14.6 kg of contingency. Additions to the stripped orbiter is the second portion of the dry weight derivation.

Ten percent of the total dry weight is provided for contingency. The value shown in the run is less the 14.6 kg already in the stripped orbiter.

Total mass properties are shown on the grand total sheet. The dry weight grand total sheet is followed by additional grand totals without showing intermediate details. These sheets run the mission backwards from burnout to liftoff with special intermediate conditions developed for attitude control studies such as no antenna and extended antenna.

Total estimates were made for nine configurations using the parametric data from Volume III. In the following section each subsystem is examined for variations caused by these configurations.

Propulsion - For orbits with e = 0.5 the VO'75 tankage (offloaded) proved adequate. For e = 0.3 VO'75 stretched tankage is utilized. Further stretch might possibly accommodate circular orbits. However, space storable propulsion systems appeared more attractive and therefore are used for this study.

Table VI-20 Viking Orbiter '75 Bus Equipment Assumed Retained for Venus Mapper

Item	Mass (kg)	Location
Radio Frequency Subsystem		
Receivers 2 @ 3.70	7.40	Bay 1
Control Unit	0.68	Bay 1
Coaxial Cables	0.45	Bay 1
Output Filter	0.54	Bay 16
HGA Switch	1.50	
LGA Switch	1.95	
Filter Hybrid	0.95	
Exciters	4.44	
Preselect Mixers 2 @ 2.36	4.72	
Receiver RF Switch	0.73	
Coaxial Cables	0.59	
RFS End Circuits Isolation	0.54	
Provide Receiving for HGA	0.54	
Provide RFS Status Word	0.54	Bay 16
Modulation Demodulation System		
Command Detector Subassembly	1.13	Bay 1
Command Detector/Power Supply	2.99	Bay 1
Mode Control/Block Coder Subassembly	1.27	Bay 1
Modulator Power Supply	2.99	Bay 1
Power Subsystem		
Batteries (incl. wire, potting, etc.) 2 @ 30.53	61.06	Bays 9 & 13
Solar Array Electronics Subassembly	4.54	Bay 10
Battery Electronics Subassembly	4.54	Bay 10
Battery Chargers 2 @ 1.50	3.00	Bay 10
30 VDC Converter	2.13	Bay 10
Booster Regulators 2 @ 3.53	7.06	Bay 12
Power Control	3.36	Bay 12
Power Distribution	2.77	Bay 12
2.4 KHz Inverters 2 @ 2.12	4.24	Bay 12
3 Phase 400 Hz Inverter 2 @ 1.81	3.62	Bay 12
Computer Command Subsystem		
Memory 2 @ 3.41	6.82	Bay 2
Output Unit 2 @ 2.05	4.10	Bay 2
Processor 2 @ 1.54	3.08	Bay 2
Power Supply 2 @ 2.07	4.14	Bay 2
Flight Data Subsystem		
Power Converter	2.58	Bay 6
Analog Com/Disc CKT	2.14	Bay 6
Eng/Logic	2.19	Bay 6
Memory/ID	2.32	Bay 6
CC/Inst. Cont./Logic	2.05	Bay 6
M.O./Timing/Logic	1.73	Bay 6

(continued)

Table VI-20 Viking Orbiter '75 Bus Equipment Assumed Retained for Venus Mapper (concluded)

Item	Mass (kg)	Location
Attitude Control Subsystem		
Inertial Sensors 2 @ 2.27	4.54	Bay 5
Inertial Electronics 2 @ 2.72	5.44	Bay 5
Cruise Sun Sensor	0.18	Bay 5
Sun Gate Assembly	0.09	Bay 5
Attitude Control Electronics 2 @ 3.69	7.38	Bay 5
Canopus Tracker	4.22	Bay 12
Acquisition Sun Sensors 4 @ 0.034	0.14	Solar Panels
Thrusters 4 @ 0.374	1.50	Solar Panels
Tubing	1.36	Solar Panels
Cabling Subsystem		
ACS Harness	1.87	Bay 5
ARTC Harness	1.36	Bay 5
RFS Harness 2 @ 0.5	1.00	Bays 1 and 16
MDS Harness	2.10	Bay 1
DSS-1 Harness	1.91	Bay 14
RTS Harness	0.91	Bay 15
FDS Harness	3.27	Bay 6
DSS-2 Harness	1.66	Bay 4
Power Reg. Harness	1.81	Bay 10
Power Conv. Harness	1.52	Bay 12
Pyro Harness	1.59	Bay 15
CCS Harness	3.63	Bay 2
Upper Ring Signal Harness	5.67	Bus Intercomm.
Upper Ring Power Harness	5.67	Bus Intercomm.
Lower Ring Harness	2.58	Bus Intercomm.
Pyro Interconnect Harness	1.95	Bus Intercomm.
Data Storage Subsystem		
DSS-DTR Assemblies 2 @ 14.36 (includes: power supply, motor driver timing control, command decoder, record logic, buffer, data detection, tech channel, DST S/A).	18.72	Bays 4 and 14
Antenna Subsystem		
Low Gain Cable Assembly	0.73	Bays 9 and 16
Low Gain Feed and Probe	0.18	Bay 9
Articulation Subsystem		
ARTC Electronics Subassembly	3.99	Bay 5
SEC Actuators 4 @ 0.34	1.36	Bays 4,6,12,14

As mentioned above for the e = 0.5 configurations, the tankage and pressurization system are identical to VO'75. However, three engines are required; therefore, two nongimballed engines and associated pyrotechnic valve isolation assemblies are added for use during orbit insertion. The present VO'75 isolation assemblies will be retained for propellant control to the center or gimballed engine. Weight estimates for the pyro isolation assembly was derived from the VO'75 unit using its pyro valves, service valves, transducer, an increased size filter, and factors for structures and tubing. Configurations designed to achieve e = 0.3 use the same three engine arrangements and stretch the tankage and pressurization systems as required. Space storable systems are new designs and mass estimates are developed using data from Volume III. Table VI-21 shows summary design and mass data for the nine configurations.

Thermal Control - Completely new thermal control system is developed for the configurations, consisting of heat pipes which are routed inside of the bus, external insulation, and on some configurations, a separate radiator. A summary of thermal control system mass estimates is given in Table VI-22.

Communications - Communications average output power varies depending upon the communications concept and radar coverage. Some of these concepts and coverages considered during the study and mass estimates from Figure VI-19 (Vol. III) are given in Table VI-23. The conditions used for the nine configuration mass estimates are noted.

Table VI-21 Propulsion Dependent Mass Summary

Configuration	A-3	B-3	C-3
% Offload (mass)	26.5	21.6	26.9
Tank Length (meters)	1.37	1.37	1.37
Mass Data - kg			
Tankage Installation	134.8	134.8	134.8
Pressurization Installation	59.6	59.6	59.6
Engine Installation	63.4	63.4	63.4
Propulsion (dry)	257.8	257.8	257.8
Trapped Propellant	18.3	18.3	18.3
Usable & Reserve Propellant	1032.3	1101.4	1026.4
Total	1308.4	1377.5	1302.5

Configuration	A-2	B-2	C-2
% Tank Stretch (mass)	15.4	26.4	14.0
Tank Length (meters)	1.53	1.63	1.51
Mass Data - kg			
Tankage Installation	153.0	164.6	151.18
Pressurization Installation	67.2	71.7	66.60
Engine Installation	63.4	63.4	63.4
Propulsion (dry)	283.6	299.7	281.2
Trapped Propellant	18.3	18.3	18.3
Usable & Reserve Propellant	1621.8	1776.2	1601.2
Total	1923.7	2094.2	1900.7

Configuration	A-1	B-1	C-1
Tank Diameter (meters)	1.17	1.21	1.18
Mass Data - kg			
Tankage Installation	117.1	127.2	120.7
Pressurization Installation	130.0	138.6	131.3
Engine Installation	68.5	68.5	68.5
Propulsion (dry)	315.6	334.3	320.5
Trapped Propellant	20.4	20.4	20.4
Usable & Reserve Propellant	1900.1	2035.6	1908.8
Total	2236.1	2390.3	2249.7

Table VI-22 Thermal Control Mass Estimate Summary (kg)

	A-1	A-2	A-3	B-1	B-2	B-3	C-1	C-2	C-3
Radiator or OSR Area m^2	2.6	2.0	1.9	2.9	2.2	2.0	2.3	1.6	1.6
Louvers	2.45	2.45	2.45	2.45	2.45	2.45			
Heat Pipes	2.27	2.27	2.27	2.27	2.27	2.27	3.18	3.18	3.18
Radiator							17.96	12.50	12.50
Radiator Support							2.27	1.81	1.81
Insulation	1.22	1.22	1.22	1.22	1.22	1.22	2.45	2.45	2.45
Second Surface Mirrors (ORS)	2.16	1.66	1.58	2.41	1.83	1.66			
Total	8.10	7.60	7.52	8.35	7.77	7.60	25.86	19.94	19.94

Table VI-23 Communications Transmitter Mass & Power Comparison

		e = 0.	e = 0.3	e = 0.5
Configuration A				
Max Presumming	P	142*	38.5	25.6
Reduced Radar Coverage	M	54.4	21.0	15.5
Min Presumming	P	422	107*	75.8*
Reduced Radar Coverage	M	123.0	43.1	34.0
Configuration B				
Max Presumming	P	84.5	38.5	69.5
Reduced Radar Coverage	M	37.5	21.0	32.4
Min Presumming	P	250*	203*	206*
Reduced Radar Coverage	M	86.2	74.8	74.8
Configuration C				
3 Meter Antenna				
Max Presumming	P	52.2	71.5	88.0
180° Radar Coverage	M	26.5	33.2	38.8
Max Presumming	P	68.3*	39.6*	34.4*
Reduced Radar Coverage	M	32.2	21.3	19.5
4 Meter Antenna				
Max Presumming	P	37.9	22.0	19.2
Reduced Radar Coverage	M	20.8	13.8	12.5
Min Presumming	P	112.0	61.8	57.0
Reduced Radar Coverage	M	43.0	30.0	28.0

* - Used for mass estimate.

P - Average transmitted power, watts.

M - Mass, kg.

Flight Data - Flight data system additions are the same for all configurations and are estimated based on existing equipment of the required capacity.

Antenna System - In addition to the antenna and drive system covered in Volume III, all radar systems require a 2.72 kg waveguide installation in the orbiter bus to interconnect with the antenna. Table VI-24 is a summary of the antenna systems used for the configurations studied.

Radar Electronics - Radar electronics mass estimates are developed from the JPL equations given in Volume III. Estimates from these equations and pertinent estimating parameters for nine configurations are shown in Table VI-25

Table VI-25 Radar Electronics Mass Estimates

Configuration	A-1	A-2	A-3	B-1	B-2	B-3	C-1	C-2	C-3
P Watts	28	105	166	28	105	166	28	35	78
PRF	4000	3750	5000	4000	3750	5000	4000	4500	4500
Wt. Kilograms	21.32	32.52	36.29	21.32	32.52	36.29	21.32	22.41	28.76

Radar Altimeter - The radar altimeter is mounted to the radar antenna so that it may be bore sighted to the radar. Mass estimates for the altimeter are based on Viking Lander.

Power - The VO'75 power system is unchanged except that only two solar arrays are required and for the Configuration C 9.1 kg of solar panel rotation mechanism is added.

Table VI-24 Radar Antenna and Mechanism Summary

Configuration	A-1	A-2	A-3	B-1	B-2	B-3	All B	C-1	C-2	C-3	All C
Antenna	← Shared →			← Radar →			← Comm →	← Radar →			← Comm →
Size (meters)	1.0x4.0	2.9x4.57	3.5x3.66	1.0x4.0	2.9x4.57	3.5x3.66	3 Dia	1.0x4.0	3.24x4.1		
Area (square meters)	3.96	12.20	10.40	3.96	12.20	10.40	7.00	3.96	11.60	8.69	7.00
Type Antenna	← Furled →		← Rigid →	← Furled →							
Type Support	← Boom →			← Fixed →			← Boom →	← Center →			← Boom →
Mass-Kilograms											
Dish	1.54	4.76	15.25	1.54	4.76	4.06	2.73	1.54	4.52	3.39	2.73
Hub	8.16	8.16	.45	8.16	8.16	8.16	8.16	8.16	8.16	8.16	8.16
Feed	1.81	1.81	1.81	1.81	1.81	1.81	.91	1.36	1.36	1.36	1.36
Sup't & Deploy't	18.58	18.58	18.58	1.81	1.81	1.81	16.54	11.79	14.18	15.27	16.54
Waveguide in Bus	2.72	2.72	2.72	2.72	2.72	2.72		2.72	2.72	2.72	
TOTAL	32.81	36.03	38.81	16.04	19.26	18.56	28.34	25.57	30.94	30.90	28.79

Cabling - Cabling is added as part of the engine installation and to account for added electronics, etc. 6.8 kg is added for Configurations A and B and 8.2 kg to Configuration C to accommodate the solar panel drive system and the addtional antenna drives.

Attitude Control System - The sensing and computation components of the ACS are assumed identifical to the VO'75 components. New mass estimates are required for the maneuver system. For the nine configurations studied mass explusion systems proved optimum for Configurations A and C and five CMG momentum exchange systems are optimum for Configuration B. Cold gas nozzles are VO'75 units relocated as required for the particular configuration and where additional thrust is required parallel nozzles are used. Cold gas is used to desaturate the CMG momentum exchange systems.

The method used for mass estimates of attitude control maneuver systems is covered in Volume III and summarized for configurations studied in detail in Table VI-26.

For this study two types of weight breakdowns have been used. One is a functional breakdown which is convenient for estimating purposes, the preceding estimating section is on this basis, and for c.g., and inertia work. The other breakdown is the one used by JPL for VO'75 which is used here to facilitate comparison with VO'75. Table VI-27 consists of 9 weight summary sheets for the 9 configurations presented in the JPL format.

Center of Gravity and Inertia Data - Center of gravity and inertia data was developed to size the attitude control system. Detail runs were made on four of the nine configurations at

Table VI-26 Attitude Control Maneuver System Mass Summary

Type System	Mass Expulsion	Mass Expulsion	Mass Expulsion	Momentum Exchange	Mass Expulsion
Configuration	A-1	A-2	A-3	A11 B	A11 C
Gas Required - kg (no margin)	(9.368)	(8.950)	(8.875)	(6.7)	(4.14)
Control Moment Gyros				12.75	
CMG Electronics				10.00	
Total Gas Provided	19.67	18.79	18.64	14.00	8.69
Sphere	24.20	23.12	22.92	17.22	10.69
Pressure Mod	5.31	5.31	5.31	5.31	5.31
Nozzles & Piping	6.23	6.23	6.23	3.78	6.23
Total (kg)	55.41	43.45	53.10	63.06	30.92

Table VI-27 Nine Configuration Mass Estimate

Configuration A-1, e = 0, Mass Estimate (kg)

	Stripped Orbiter	Basic	ACS	Radar & Comm.	Propulsion Dependent	Total
Structure & Thermal	131.6	① 8.1		13.5	51.7	204.9
Radio Frequency	25.3			54.4		79.7
Mod/Demod	8.4					8.4
Power	115.6					115.6
Command Comp	18.1					18.1
Flight Data	13.0	12.7				25.7
Attitude Control	24.7		52.5		5.4	82.6
Pyrotechnics	4.7				0.5	5.2
Cabling	39.3	6.8			6.5	52.6
Mechanical Devices	10.7					10.7
Articulation Control	5.4		1.4	2.3		9.1
Data Storage	28.7					28.7
Radar Altimeter	0.0			5.9		5.9
Antenna - Low Gain	0.9					0.9
- Shared				17.0		17.0
Radar	0.0			21.3		21.3
Reserve	14.6	54.0				68.6
Total	441.0	81.6	53.9	114.4	64.1	755.0

Propulsion (Dry)	260.0
Reserve 10%	26.0
Trapped	20.4
Burnout	1061.4
Propellant	1900.1
Liftoff	2961.5

S/C Less Propulsion Dependent Mass 684.5

① Thermal

Table VI-27 Nine Configuration Mass Estimate

Configuration A-2, e = 0.3 Mass Estimate (kg)

	Stripped Orbiter	Basic	ACS	Radar & Comm.	Propulsion Dependent	Total
Structure & Thermal	131.6	① 7.6		13.5	39.6	192.3
Radio Frequency	25.3			43.1		68.4
Mod/Demod	8.4					8.4
Power	115.6					115.6
Command Comp	18.1					18.1
Flight Data	13.0	12.7				25.7
Attitude Control	24.7		50.6		2.5	77.8
Pyrotechnics	4.7				0.8	5.5
Cabling	39.3	6.8			10.1	56.2
Mechanical Devices	10.7					10.7
Articulation Control	5.4		1.4	2.3		9.1
Data Storage	28.7					28.7
Radar Altimeter	0.0			5.9		5.9
Antenna - Low Gain	0.9					0.9
- Shared				20.3		20.3
Radar	0.0			32.5		32.5
Reserve	14.6	53.0				67.6
Total	441.0	80.1	52.0	117.6	53.0	743.7

		Propulsion (Dry)	230.6
		Reserve 10%	23.1
S/C Less Propulsion		Trapped	18.3
Dependent Mass	685.4	Burnout	1015.7
① Thermal		Propellant	1621.8
Tank Stretch 0.157 m		Liftoff	2637.5

Table VI-27 Nine Configuration Mass Estimate

Configuration A-3, e = 0.5 Mass Estimate (kg)

	Stripped Orbiter	Basic	ACS	Radar & Comm.	Propulsion Dependent	Total
Structure & Thermal	131.6	① 7.5		13.5	37.1	189.7
Radio Frequency	25.3			34.0		59.3
Mod/Demod	8.4					8.4
Power	115.6					115.6
Command Comp	18.1					18.1
Flight Data	13.0	12.7				25.7
Attitude Control	24.7		50.2		2.5	77.4
Pyrotechnics	4.7				0.8	5.5
Cabling	39.3	6.8			9.1	55.2
Mechanical Devices	10.7					10.7
Articulation Control	5.4		1.4	2.3		9.1
Data Storage	28.7					28.7
Radar Altimeter	0.0			5.9		5.9
Antenna - Low Gain	0.9					0.9
- Shared				23.0		23.0
Radar	0.0			36.3		36.3
Reserve	14.6	52.3				66.9
Total	441.0	79.3	51.6	115.0	49.5	736.4

Propulsion (Dry)	208.1
Reserve 10%	20.8
Trapped	18.3
Burnout	983.6
Propellant	1032.3
Liftoff	2015.9

S/C Less Propulsion Dependent Mass 982.0

① Thermal

Table VI-27 Nine Configuration Mass Estimate

Configuration B-1, e = 0 Mass Estimate (kg)

	Stripped Orbiter	Basic	ACS	Radar & Comm.	Propulsion Dependent	Total
Structure & Thermal	131.6	① 8.3		② 13.3	53.0	206.2
Radio Frequency	25.3			86.1		111.4
Mod/Demod	8.4					8.4
Power	115.6					115.6
Command Comp	18.1					18.1
Flight Data	13.0	12.7				25.7
Attitude Control	24.7		61.6		5.4	91.7
Pyrotechnics	4.7				0.5	5.2
Cabling	39.3	6.8			6.6	52.7
Mechanical Devices	10.7					10.7
Articulation Control	5.4		1.4	2.3		9.1
Data Storage	28.7					28.7
Radar Altimeter	0.0			5.9		5.9
Antenna - Comm	0.9			14.6		15.5
- Radar				14.2		14.2
Radar	0.0			21.3		21.3
Reserve	14.6	59.4				74.0
Total	441.0	87.2	63.0	157.7	65.5	814.4

Propulsion (Dry)	275.0
Reserve 10%	27.5
Trapped	20.4
Burnout	1137.3
Propellant	2035.6
Liftoff	3172.9

S/C Less Propulsion Dependent Mass 742.4

① Thermal

② Comm 11.47 Radar 1.81

Table VI-27 Nine Configuration Mass Estimate

Configuration B-2, e = 0.3 Mass Estimate (kg)

	Stripped Orbiter	Basic	ACS	Radar & Comm.	Propulsion Dependent	Total
Structure & Thermal	131.6	① 7.8		② 13.3	40.9	193.6
Radio Frequency	25.3			74.8		100.1
Mod/Demod	8.4					8.4
Power	115.6					115.6
Command Comp	18.1					18.1
Flight Data	13.0	12.7				25.7
Attitude Control	24.7		61.6		2.5	88.8
Pyrotechnics	4.7				0.8	5.5
Cabling	39.3	6.8			10.8	56.9
Mechanical Devices	10.7					10.7
Articulation Control	5.4		1.4	2.3		9.1
Data Storage	28.7					28.7
Radar Altimeter	0.0			5.9		5.9
Antenna - Comm	0.9			14.6		15.5
- Radar				17.4		17.4
Radar	0.0			32.5		32.5
Reserve	14.6		58.6			73.2
Total	441.0	85.9	63.0	160.8	55.0	805.7

Propulsion (Dry)	244.8
Reserve 10%	24.5
Trapped	18.3
Burnout	1093.3
Propellant	1776.2
Liftoff	2869.5

S/C Less Propulsion Dependent Mass 745.2

① Thermal

② Comm 11.47 Radar 1.81

Stretch 0.258 m

Table VI-27 Nine Configuration Mass Estimate

Configuration B-3, e = 0.5 Mass Estimate (kg)

	Stripped Orbiter	Basic	ACS	Radar & Comm.	Propulsion Dependent	Total
Structure & Thermal	131.6	① 7.6		② 13.3	37.1	189.6
Radio Frequency	25.3			74.8		100.1
Mod/Demod	8.4					8.4
Power	115.6					115.6
Command Comp	18.1					18.1
Flight Data	13.0	12.7				25.7
Attitude Control	24.7		61.6		2.5	88.8
Pyrotechnics	4.7				0.8	5.5
Cabling	39.3	6.8			9.1	55.2
Mechanical Devices	10.7					10.7
Articulation Control	5.4		1.4	2.3		9.1
Data Storage	28.7					28.7
Radar Altimeter	0.0			5.9		5.9
Antenna - Comm	0.9			14.6		15.5
- Radar				16.7		16.7
Radar	0.0			36.3		36.3
Reserve	14.6	57.7				72.3
Total	441.0	84.8	63.0	163.9	49.5	802.2

S/C Less Propulsion Dependent Mass 748.4

① Thermal

② Comm 11.47 Radar 1.81

Propulsion (Dry)	208.1
Reserve 10%	20.8
Trapped	18.3
Burnout	1049.4
Propellant	1101.4
Liftoff	2150.8

Table VI-27 Nine Configuration Mass Estimate

Configuration C-1, e = 0 Mass Estimate (kg)

	Stripped Orbiter	Basic	ACS	Radar & Comm.	Propulsion Dependent	Total
Structure & Thermal	131.6	① 25.9		② 17.2	51.8	226.5
Radio Frequency	25.3			32.2		57.5
Mod/Demod	8.4					8.4
Power	115.6					115.6
Command Comp	18.1					18.1
Flight Data	13.0	12.7				25.7
Attitude Control	24.7		28.1		5.4	58.2
Pyrotechnics	4.7				0.5	5.2
Cabling	39.3	8.2			6.6	54.1
Mechanical Devices	10.7	9.1				19.8
Articulation Control	5.4			③ 4.5		9.9
Data Storage	28.7					28.7
Radar Altimeter	0.0			5.9		5.9
Antenna - Comm	0.9			15.0		15.9
- Radar				17.5		17.5
Radar	0.0			21.3		21.3
Reserve	14.6	54.2				68.8
Total	441.0	110.1	28.1	113.6	64.3	757.1

Propulsion (Dry)	262.4
Reserve 10%	26.2
Trapped	20.4
Burnout	1066.1
Propellant	1908.8
Liftoff	2974.9

S/C Less Propulsion Dependent Mass 686.4

① Thermal

② Comm 11.47 Radar 5.75

③ Comm 2.27 Radar 2.27

Table VI-27 Nine Configuration Mass Estimate

Configuration C-2, e = 0.3 Mass Estimate (kg)

	Stripped Orbiter	Basic	ACS	Radar & Comm.	Propulsion Dependent	Total
Structure & Thermal	131.6	① 19.9		② 18.8	39.5	209.8
Radio Frequency	25.3			21.3		46.6
Mod/Demod	8.4					8.4
Power	115.6					115.6
Command Comp	18.1					18.1
Flight Data	13.0	12.7				25.7
Attitude Control	24.7		28.1		2.5	55.3
Pyrotechnics	4.7				0.8	5.5
Cabling	39.3	8.2			10.0	57.5
Mechanical Devices	10.7	9.1				19.8
Articulation Control	5.4			③ 4.5		9.9
Data Storage	28.7					28.7
Radar Altimeter	0.0			5.9		5.9
Antenna - Comm	0.9			15.0		15.9
- Radar				21.3		21.3
Radar	0.0			22.4		22.4
Reserve	14.6	52.1				66.7
Total	441.0	102.1	28.1	112.2	52.8	733.1

Propulsion (Dry)	228.5
Reserve 10%	22.8
Trapped	18.3
Burnout	1002.7
Propellant	1601.2
Liftoff	2603.9

S/C Less Propulsion Dependent Mass 675.0

① Thermal

② Comm 11.47 Radar 7.33

③ Comm 2.27 Radar 2.27

Tank Stretch 0.142 m

Table VI-27 Nine Configuration Mass Estimate

Configuration C-3, e = 0.5 Mass Estimate (kg)

	Stripped Orbiter	Basic	ACS	Radar & Comm.	Propulsion Dependent	Total
Structure & Thermal	131.6	① 19.9		② 19.5	37.1	208.1
Radio Frequency	25.3			19.5		44.8
Mod/Demod	8.4					8.4
Power	115.6					115.6
Command Comp	18.1					18.1
Flight Data	13.0	12.7				25.7
Attitude Control	24.7		28.1		2.5	55.3
Pyrotechnics	4.7				0.8	5.5
Cabling	39.3	8.2			9.1	56.6
Mechanical Devices	10.7	9.1				19.8
Articulation Control	5.4			③ 4.5		9.9
Data Storage	28.7					28.7
Radar Altimeter	0.0			5.9		5.9
Antenna - Comm	0.9			15.0		15.9
- Radar				20.6		20.6
Radar	0.0			28.8		28.8
Reserve	14.6	52.2				66.8
Total	441.0	102.1	28.1	113.8	49.5	734.5

Propulsion (Dry)	208.1
Reserve 10%	20.8
Trapped	18.3
Burnout	981.7
Propellant	1026.4
Liftoff	2008.1

S/C Less Propulsion Dependent Mass 680.0

① Thermal

② Comm 11.47 Radar 8.06

③ Comm 2.27 Radar 2.27

various phases of development. Only Configuration C-1 is updated to the final configuration status. Using available data, updated c.g.s and inertias are estimated for all configurations as summarized in Table VI-28.

Structural Design

Configuration A is representative of the shared antenna design concept and is shown in Figure VI-29. The configuration as shown is sized for an orbital eccentricity of 0.50. The basic vehicle for this configuration is the Viking Orbiter octagonally shaped bus. The Viking Orbiter propulsion module, offloaded by approximately 25%, and the adapter truss which attaches the Orbiter to the Titan III/Centaur launch vehicle is also used. Power requirements for the mapping mission are such that they can be adequately handled by two of the four solar panels presently being used on Viking '75. The solar arrays have a total cell mounting area of 7.6 m^2 and generate somewhat less than 900 watts of gross power in Venus orbit. A symmetrically cut parabolic antenna, 3.66 meter by 3.50 meter is mounted to the upper surface of the basic orbiter bus. This antenna is used for both mapping and communications and is articulated with two degrees of freedom.

An order to reduce insertion burn time and losses, three 1330 N thrust engines are used instead of the single engine used on Viking '75. The three engines would be mounted in line along the yaw axis with the two additional outboard engines and the center engine gimballed. Studies of the impact of orbital eccentricities on the propulsion requirements indicated that for an eccentricity of 0.50 the present Viking '75 propulsion tanks

Table VI-28 Venus Orbiter Mapper Mass Properties
Summary of Nine Configurations

	Mass kg	c.g. (cm)			Moment of inertia ($kg-m^2$)		
		X	Y	Z	I_X	I_Y	I_Z
Configuration A-1 ①							
Lift Off	2961.5	-1.1	0.8	-88.1	3221.5	3915.6	1791.0
Pre-Insertion	2922.6	-1.1	0.8	-88.6	3211.8	3907.0	1786.0
In Orbit (Ant. Ext.)	1098.6	-3.0	-4.8	-21.8	1715.6	2153.1	1776.8
In Orbit (Ant.Stowed)	1098.6	-3.0	2.2	-21.8	1462.9	2153.1	1529.3
Configuration A-2 ②							
Lift Off	2637.5	4.6	0.9	-48.3	1659.2	2925.2	2401.0
Pre-Insertion	2610.1	4.6	0.9	-48.0	1653.6	2911.6	2391.3
In Orbit (Ant. Ext.)	1047.5	0.7	-8.4	- 6.3	1318.5	1724.6	1947.9
In Orbit (Ant.Stowed)	1047.5	0.7	0.7	- 6.3	955.6	1724.6	1593.5
Configuration A-3 ①							
Lift Off	2015.9	4.6	0.9	-38.2	1191.6	2099.7	1835.0
Pre-Insertion	1995.0	4.6	0.9	-37.8	1186.9	2090.5	1828.6
In Orbit (Ant. Ext.)	1007.4	0.7	-8.5	- 6.1	1190.9	1558.0	1856.2
In Orbit (Ant.Stowed)	1007.4	0.7	1.8	- 6.1	863.2	1558.0	1528.4
Burn Out	1003.8	0.6	1.9	- 5.9	861.3	1555.3	1527.3
Configuration B-1 ②							
Lift Off	3172.9	3.0	2.8	-92.2	3446.3	3959.5	1918.8
Pre-Insertion	3131.3	3.0	2.8	-92.7	3434.3	3961.0	1913.4
In Orbit (Ant. Ext.)	1177.2	-3.6	3.6	-22.3	1712.0	2287.0	1821.9
In Orbit (Ant. Stowed)	1177.2	-3.6	8.4	-22.3	1654.9	2287.0	1638.6
Configuration B-2 ②							
Lift Off	2869.5	2.9	3.9	-48.8	1846.9	3027.8	2523.8
Pre-Insertion	2839.7	2.9	3.9	-48.8	1830.0	2997.8	2497.7
In Orbit (Ant.Ext.)	1128.1	-3.6	3.5	- 7.6	1323.7	1881.7	1843.4
In Orbit (Ant.Stowed)	1128.1	-3.6	8.5	7.4	1121.9	1881.7	1724.6

Table VI-28 Venus Orbiter Mapper Mass Properties (concluded)
Summary of Nine Configurations

	Mass kg	c.g. (cm)			Moment of inertia (kg-m^2)		
		X	Y	Z	I_X	I_Y	I_Z
Configuration B-3①							
Lift Off	2150.7	2.9	3.9	-41.0	1251.7	2051.2	1890.2
Pre-Insertion	2128.4	2.9	3.9	-41.0	1239.5	2031.1	1871.8
In Orbit (Ant. Ext.)	1074.7	-3.6	3.5	- 6.2	1139.5	1560.1	1756.1
In Orbit (Ant.Stowed)	1074.7	-3.6	8.5	- 7.7	965.1	1560.1	1642.6
Burn Out	1071.0	-3.6	8.5	- 7.5	963.1	1557.4	1641.4
Configuration C-1②							
Lift Off	2974.9	5.1	-0.1	-83.8	3173.3	3938.5	1842.8
Pre-Insertion	2935.9	5.1	-0.1	-83.8	3231.0	3929.8	1818.6
In Orbit (Ant. Ext.)	1103.5	1.6	3.8	-17.0	1725.3	2165.8	1638.9
In Orbit (Ant. Stowed)	1103.5	1.6	-0.5	-17.0	1471.3	2198.9	1538.0
Configuration C-2②							
Lift Off	2603.9	5.1	-0.2	-45.7	1867.9	3088.9	2369.1
Pre-Insertion	2576.8	5.1	-0.2	-45.2	1860.7	3061.1	2360.7
In Orbit (Ant. Ext.)	1034.1	1.6	4.3	- 3.0	1210.8	1776.1	1712.0
In Orbit (Ant.Stowed)	1034.1	1.6	-0.5	- 1.3	1085.8	1796.8	1564.0
Configuration C-3③							
Lift Off	2008.5	5.1	-0.2	-35.4	1361.7	2240.2	1827.2
Pre-Insertion	1987.7	5.1	-0.2	-35.0	1356.6	2230.7	1820.8
In Orbit (Ant. Ext.)	1005.7	1.6	4.3	- 2.5	1112.7	1632.4	1665.0
In Orbit (Ant.Stowed)	1005.7	1.6	0.5	- 1.0	996.9	1661.8	1516.8
Burn Out	1002.2	1.6	0.5	- .7	994.7	1658.9	1515.7

c.g. Locations Ref. Figure VI-28

① Ratioed from Old Run

② Estimate

③ From Up-Dated Run

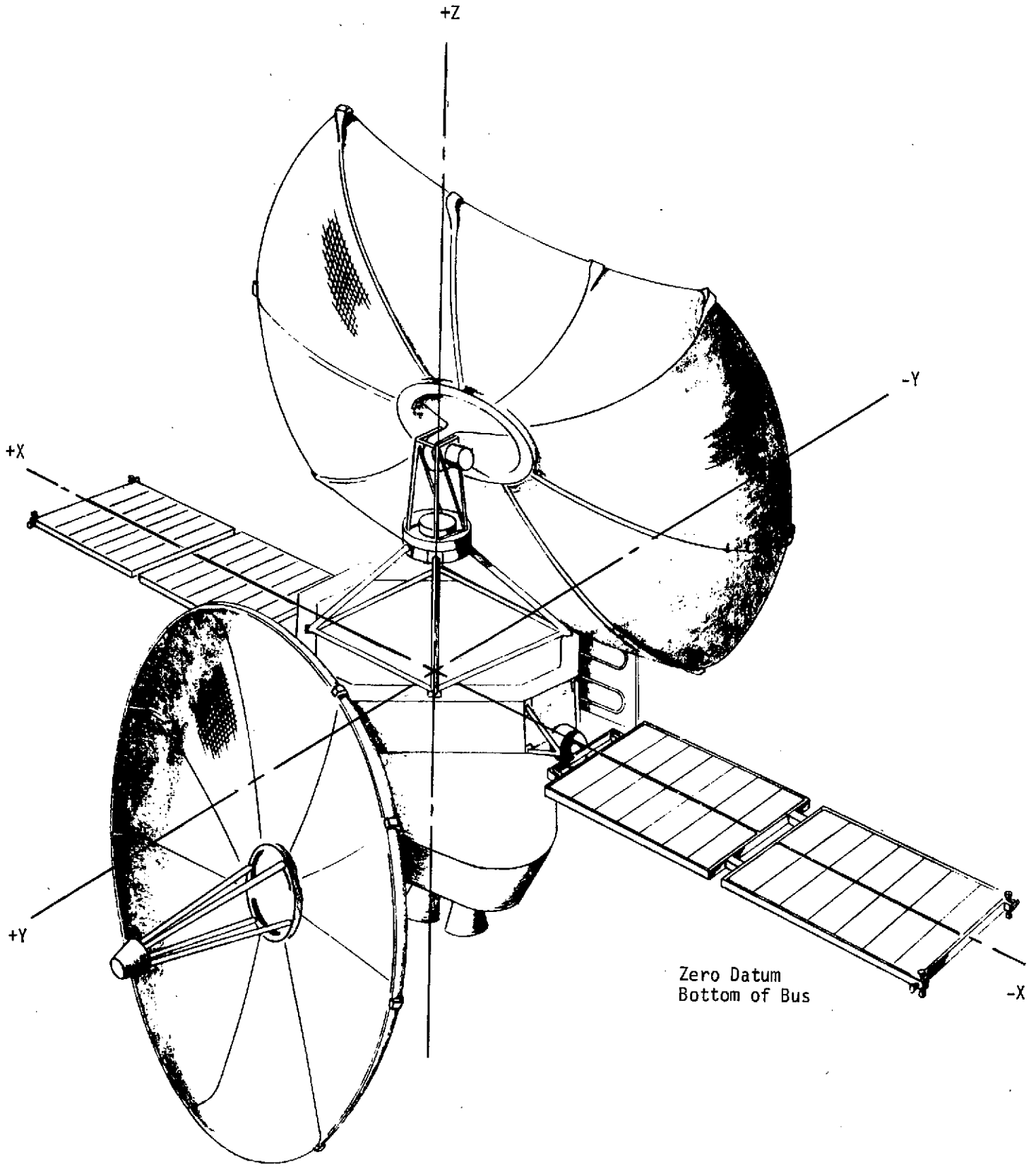

Figure VI-28 Venus Radar Mapper (Configuration C-3) Reference Axis System

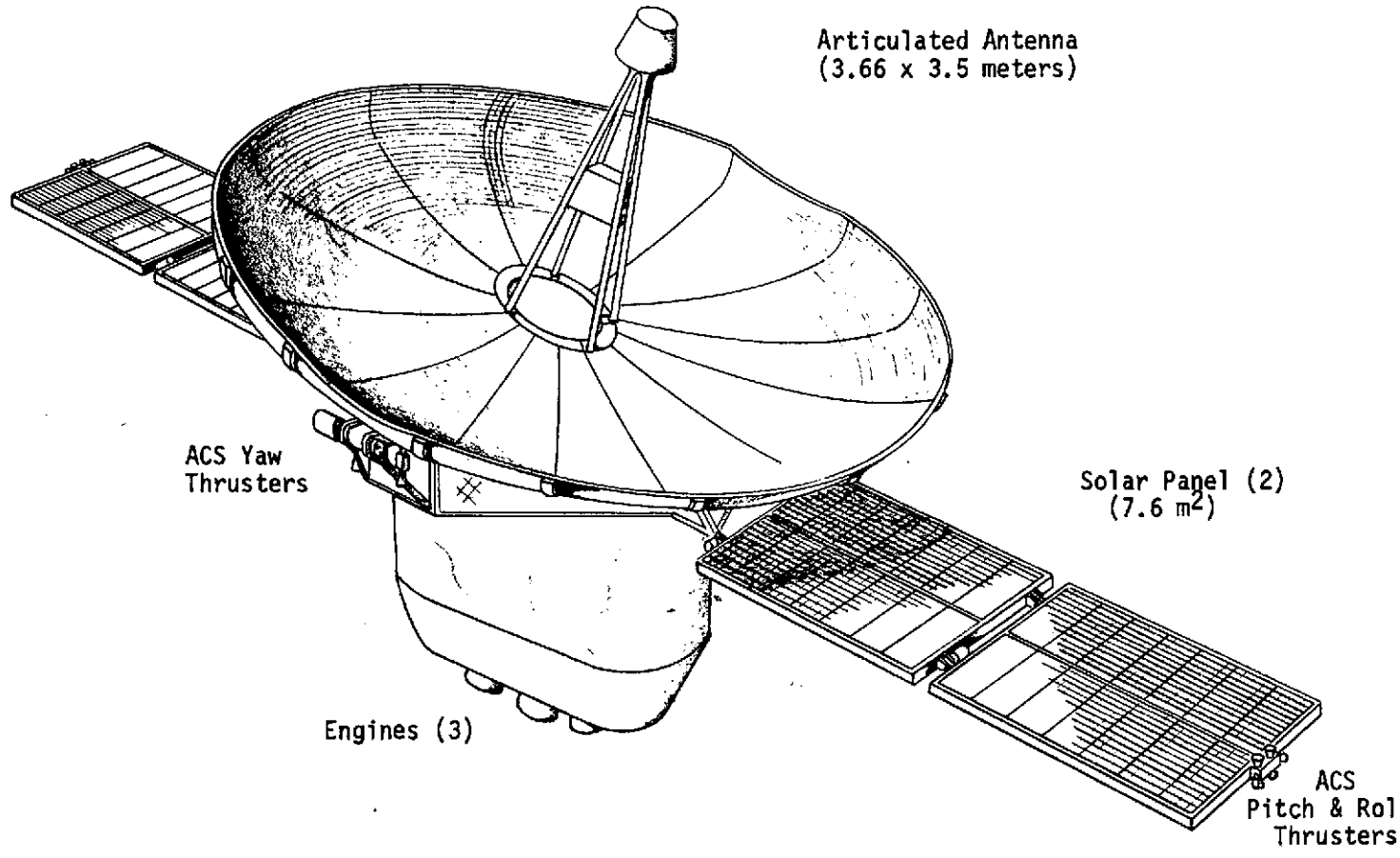

Figure VI-29 Spacecraft Configuration A

were adequate, utilizing an offloaded (26.5%) configuration. An orbital eccentricity of 0.30 reqùires a stretched (15.4%) Viking orbiter tankage while an orbital eccentricity of 0.00 dictates that space storable propellants with tankage the same diameter as the 1975 Viking Orbiter be used. Two 2670 N thrust engines would also be employed.

The radar subsystem and communication equipment are housed inside the basic octagon bus together with the other spacecraft housekeeping subsystems. The internal arrangement of these subsystems is shown in Figure VI-30 and Table VI-29.

Thermal control is accomplished by means of radiator surfaces and specular louvers forming the outside panels of the orbiter body in place of the louvered structure on the Viking 1975 vehicle. An internal heat pipe routed around the orbiter is used to maintain temperature equalization for the equipment compartment. The electronic components required to support the radar and communications subsystems are installed in the equipment compartment in space now occupied by Viking '75 components not required for this mission.

The 3.66 meter by 3.50 meter antenna uses S-band frequency for radar mapping purposes and x-band for data return. A fixed side look angle is also used for mapping purposes. During launch, the antenna is stowed across the upper surface of the orbiter. The radar altimeter system is mounted on the antenna and therefore is automatically aligned when the spacecraft is in the mapping cycle.

Three-axis attitude control of the vehicle is provided by the Viking Orbiter cold gas nitrogen system with some increase in the amount of GN_2 onboard. Pitch and roll thrusters consisting

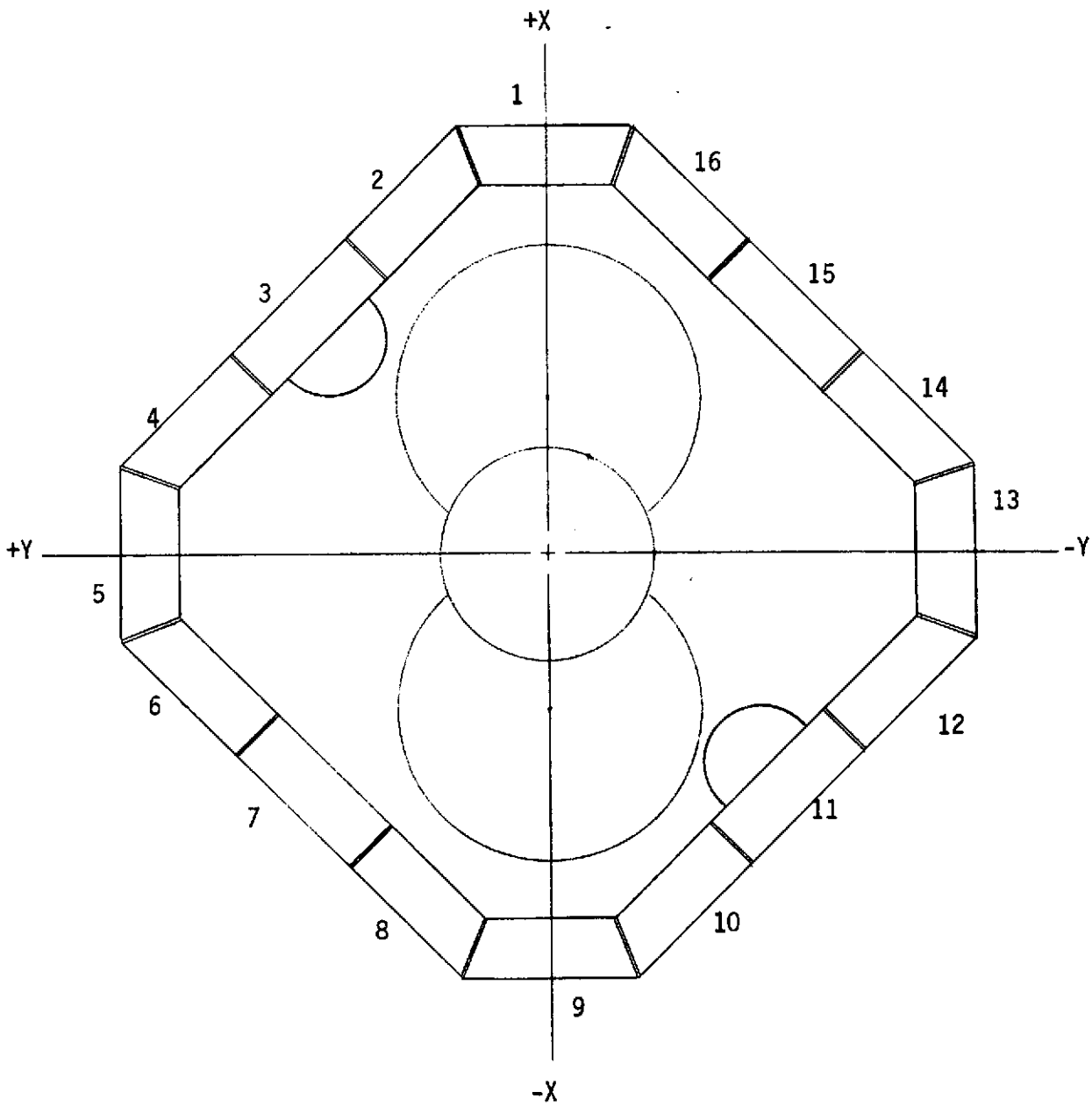

Figure VI-30 Orbiter Equipment Bay Identification

Table VI-29 Orbiter Subsystem Arrangement

Bay 1	Radio Frequency Subsystem
Bay 2	Computer Command Subsystem
Bay 3	ACS Pressure Module
Bay 4	Data Storage Subsystem
Bay 5	Attitude Control Subsystem
Bay 6	Flight Data Subsystem A to D Converter (New) Video Processor (New)
Bay 7	Communication TWTA (New)
Bay 8	Communication TWTA (New)
Bay 9	Power Subsystem (Battery)
Bay 10	Power Subsystem
Bay 11	ACS Pressure Module
Bay 12	Power Subsystem
Bay 13	Power Subsystem (Battery)
Bay 14	Data Storage Subsystem
Bay 15	Radar Unit (New)
Bay 16	Radio Frequency Subsystem

of four clusters of three thrusters each are mounted on the tip of each solar panel. Yaw thrusters are located on the orbiter bus.

Celestial sensors, composed of a Canopus sensor, cruise and acquisition sun sensors, sun gate, and a stray light sensor, are mounted on the appropriate sides of the bus and solar panels to meet the required field of view of the instruments.

The mass of the shared antenna concept is summarized in Table VI-27 at the subsystem level. Useful weight in orbit, which is defined as the total spacecraft weight less propulsion dependent mass, and propellants, is approximately 682 kg. Total injected mass is 2016 kg.

Configuration B is representative of the dedicated antenna concept and is presented in Figure VI-33. This configuration also uses a modified Viking orbiter. Two antennas are used, a 2 meter communications antenna which is articulated with two degrees of freedom and a fixed roll out planar array radar antenna. The communication antenna stows across the top of the orbiter, while the 3.66 meter by 3.50 meter radar antenna is mounted along the side of the orbiter. After separation of the payload fairing the radar antenna is deployed and locked into its proper attitude with a 30 degree side look angle. S-band is used for mapping while x-band is employed for data transmission to Earth.

Electrical power is provided by solar array panels with a cell array of 7.6 meters^2. Nickel cadmium batteries supply power during periods of sun occultation.

As in the shared antenna concept the primary propulsion system is the basic Viking Orbiter system with the 1330 N thrust engines mounted in a similar manner as the shared antenna case. Because

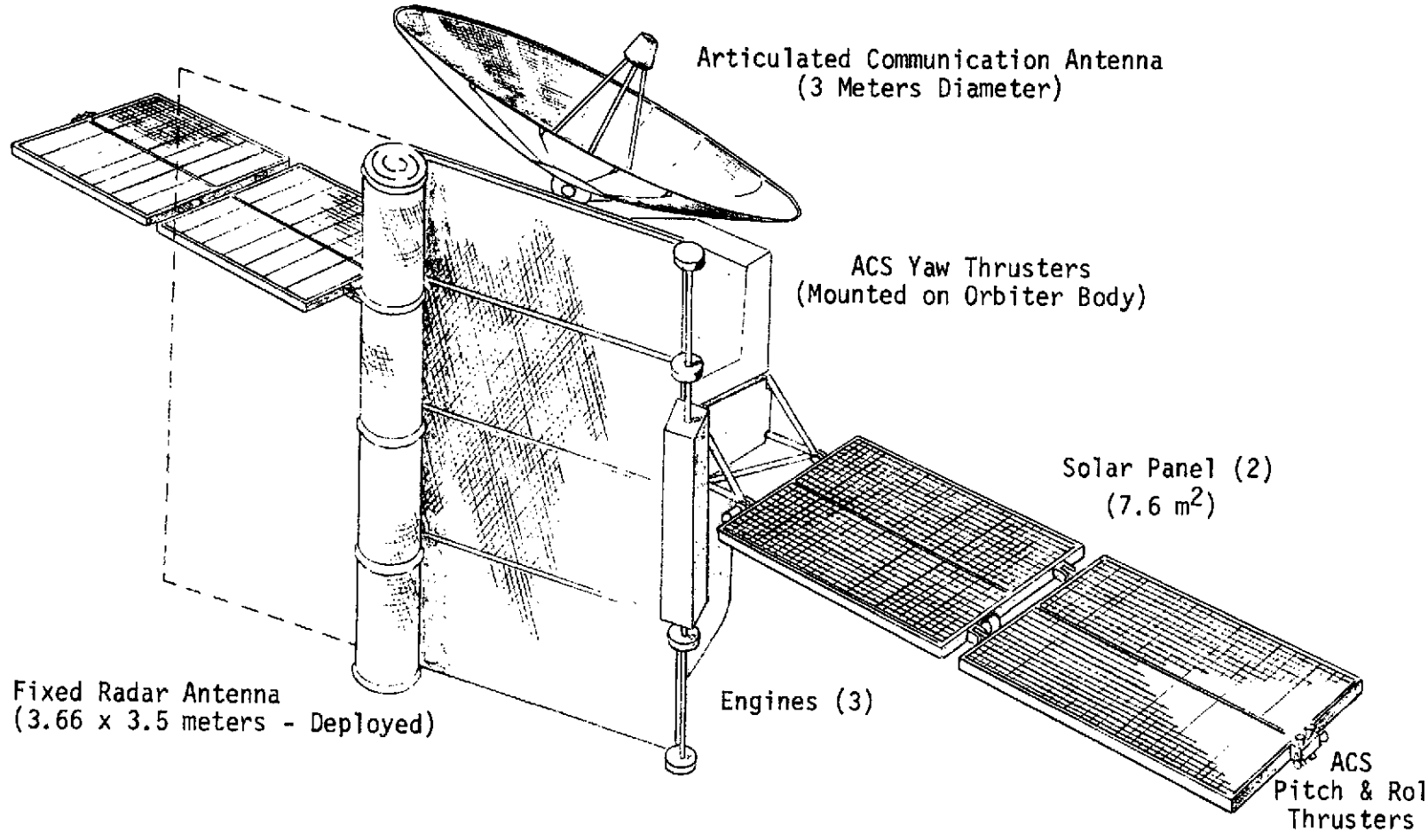

Figure VI-31 Spacecraft Configuration B

of the slightly increased spacecraft inert mass less propulsion dependent mass compared to the shared antenna case (viz., 746 kg vs 682 kg) the 0.50 orbital eccentricity requires the propellant to be offloaded less than for the shared antenna concept (21.6% compared to 26.5% for configuration A). Similarly, for the 0.30 eccentricity case the tanks are stretched 26.4% compared to 15.4% for Configuration A. Again space storables are required for insertion into a circular orbit.

Unlike the shared antenna concept, three-axis attitude control is provided by a combination of control moment gyros (CMGs) and GN_2. Pitch and roll control is provided by four clusters of three thrusters each mounted on the top of each solar panel. Yaw thrusters are located on the orbiter bus.

Celestial sensors, comprised of a Canopus sensor, cruise and acquisition Sun sensors, Sun gate and a stray light sensor, are mounted on the appropriate sides of the bus and solar panels to meet the required fields of view of the instruments and to eliminate interference from the solar panels. Propellant for the ACS system is housed in spherical bottles located within the bus structure. The inertial reference units consisting of gyros, inertial sensors, and electronic controls are also mounted within the orbiter bus structure.

Thermal control is similar to Configuration A in that radiator surfaces and specular louvers make up most of the outside panels on the orbiter body. More multilayer insulation is required compared to Configuration A to compensate for the spacecraft pointing the radar antenna toward Venus.

A mass summary, by subsystems, is given in Table VI-27.

Since a dedicated antenna configuration is desirable from a data return aspect, an effort was made to overcome some of the problems that became evident with Configuration B.

The excessive ACS propellant requirements of Configuration B were overcome by adding gimbals to the solar panels and making the spacecraft inertially oriented. Each of the antennas is mounted so as to have gimbals with two degrees of freedom.

Configuration C is illustrated in Figure VI-32. Again, the spacecraft is configured around a modified Viking Orbiter. These modifications include; deletion of two of the solar panels, moving the yaw thrusters to the orbiter body and adding two 1330 N thrust main engines. Keeping the spacecraft inertially oriented eliminates the requirements for adding a gimbal system to the Canopus tracker, and the amount of GN_2 on board would be decreased by approximately 10 kg to 8.7 kg for ACS maneuvers. The main propellant tanks and their support structure would remain unchanged for orbits with an eccentricity of 0.5, the tanks would be stretched for 0.3 orbits, and space storables would be required for circular orbits.

Unlike Configurations A and B, Configuration C has a radiator which is separate from the orbiter body with the entire external surface of the octagonal structure covered with a multilayer insulation. Temperature equalization within the spacecraft is again accomplished by means of a heat pipe.

The communications antenna, 3 meter parabolic is mounted at the support points for one of the deleted solar panels as shown in Figure VI-32. The radar antenna, 4.1 x 3.24 meters, symmetrically cut parabolic, is supported at the VLC truss attach points on Viking 75. The radar antenna gimbals in such a way as to allow a varying side look angle.

A mass summary, at the subsystem level, is given in Table VI-27.

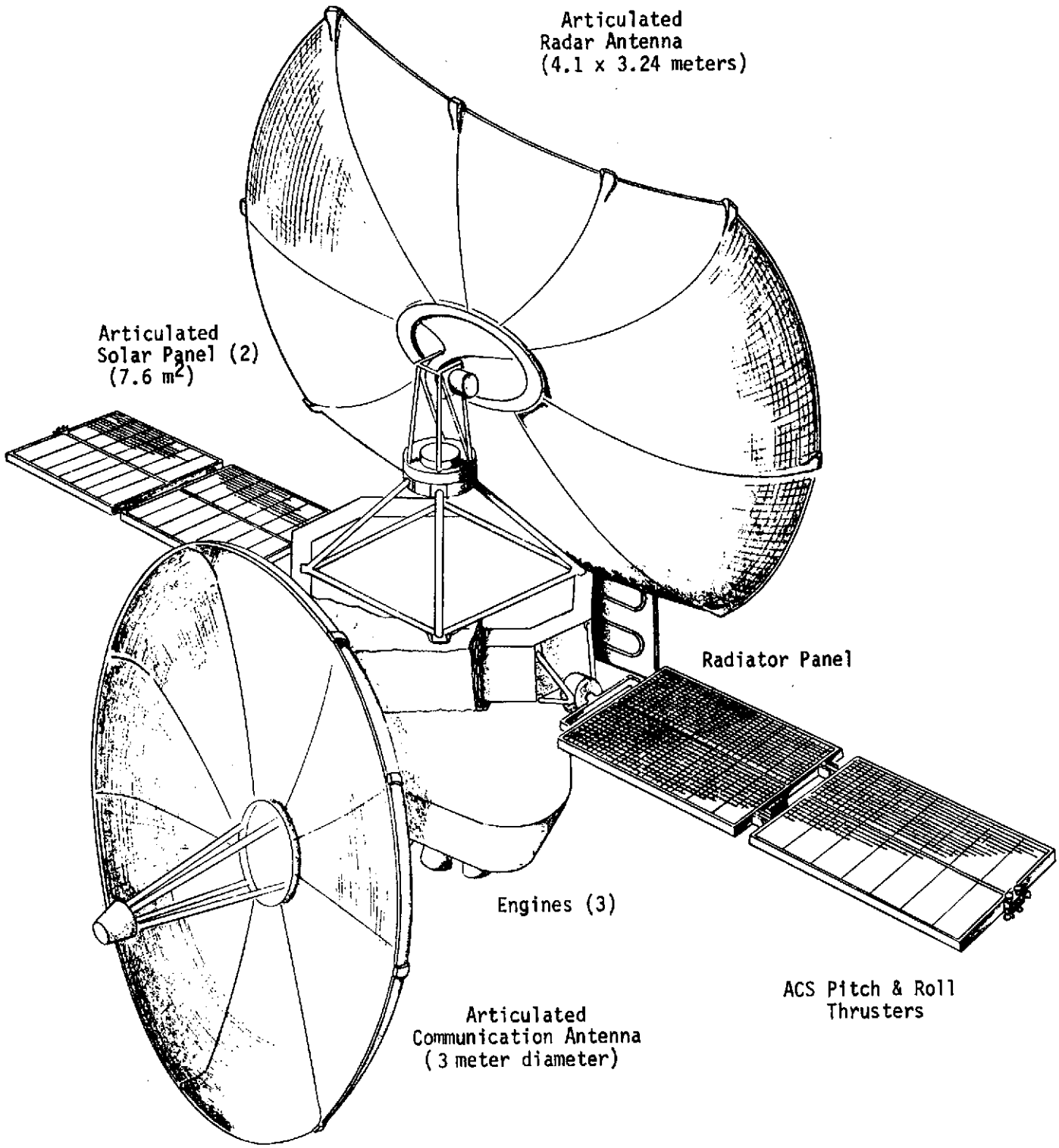

Figure VI-32 Spacecraft Configuration C

LONG LIFE RELIABILITY

Introduction

The success of a Venus Radar Mapper mission is obviously dependent on the reliability of the spacecraft and its subsystems. Other factors affecting mission success are the requirements for complex maneuvers, the long term operation of the spacecraft, the number of launch opportunities, and the technological developments required. Mission success is thus probablistic in nature and becomes an important study parameter in formulating various spacecraft design and operational concepts. Probably the most important parameter affecting mission success is the required mission lifetime. The duration of typical Venus Radar Mapper missions that have been evaluated in this study are in the order of 400 days. Mission lifetimes of this duration are not expected to pose any significant problems in significant spacecraft systems since a number of spacecraft are still operable after 5 to more than 8 years in space, including Syncoms, Intelsato, OGO's, Pioneers, Velas and Explorers, see Table VI-30. As a point of reference, the Viking '75 Orbiter which is proposed as the basic delivery vehicle for a Venus Radar Mapper mission has a design lifetime of approximately 510 days.

Table VI-30 Long-Life Spacecraft Experience

SPACECRAFT	LIFE
OGO	Since 1964
Pioneer	Since 1965
Vela	Since 1963
Syncom II	Since 1963
Intelsat I	Since 1965
Alouette I	Since 1962
Explorer 31	Since 1965
Tiros 6	Since 1962

Basic Design Considerations

Some spacecraft components need not perform throughout the mission. Those parts that operate only during deployment early in the mission require the ultimate in reliability, but long life is not a particular problem. Motors, gear trains, deployment defices and associated electrical control elements are examples.

Other devices are dormant until as long as near the end of the mission. Pyrotechnics and some propellant valves are examples. Here there should be no wear or stress fatigue cycling. The main concerns would deal with potential chemical changes or cold welding possibilities that could freeze up mechanical actions, or impair pyrotechnics, etc.

Another category is the devices that function on a daily or hourly intervals. The radar, communication and data handling fall into this category. Devices with "wear-out" characteristics, such as TWT's, tape recorders, and thrusters could benefit from this "on-off" time, although the cycling stresses could become more of a factor. Means of controlling or ruggedizing for on-off stressing should be kept in mind.

Conclusions

Since the majority of the subsystems proposed for use in the Venus Radar Mapper missions are being developed for programs presently in being (Viking) it is essential that continuing monitoring and sufficient program insight be maintained in order to comprehensively catalog failure modes and their effects in order of importance, together with an evaluation of possible design solutions.

For these subsystems, such as the radar, communications, and data handling systems which use off-the-shelf components with an inherent 5 to 12-year mission capability a stringent reliability program plan must be kept up. Typically, the reliability program plan would involve the following steps:

1. Establishment of reliability goals.
2. Allocation of reliability with respect to mission phases.
3. Establishment of subsystem/part reliability allocations, and
4. Determination of failure modes effects.

TECHNOLOGY ASSESSMENT

This section presents the results of the system analysis and design studies that were made to identify the technology requirements necessary for the implementation of a Venus Radar Mapper. The required spacecraft systems are evaluated with their related technology assessment and recommended design approaches. The principal conclusion drawn from the study indicated that no technology areas could be identified which required research studies to substantiate the feasibility of implementing the spacecraft design.

This section addresses the technology requirements for all subsystems, with the exception of the radar, communication and data handling subsystems. The technology requirements associated with these subsystems are treated independently in Sections IV and V of this volume, respectively.

Thermal Control System

The thermal control system design is one of the most vital elements in the spacecraft upon which most all other vehicle subsystems are to some degree dependent. The proposed thermal design employs the "enclosure concept" whereby the equipment compartment is partially insulated from the surrounding thermal environment by the use of high performance multilayer insulation,

and partially coupled to it by heat rejection surfaces (radiators). The radiator surfaces are highly reflective in the solar wavelength in order to minimize the effects of the external environment during the orbital phases of the mission. An internal heat pipe system is used to smooth out the internal temperature fluctuations and to minimize the requirement for a variable heat rejection capability. However, control of heat rejection is provided in the form of specular louvers which control the effective emissivity of the radiator surface by the position of the blades.

The thermal design may be accomplished by the use of state-of-the art concepts, and thermal control elements that are either flight proven, or in the advanced developmental stage . No technological breakthroughs are necessary to assure the thermal feasibility of the mission, but the following events, while not critical, should be given detailed consideration:

1. Flight-qualification of temperature-controlled heat pipe concepts meeting the specific detailed requirements of the mission, including life testing.
2. Flight-qualification of Phase Change Heat Sink Materials applicable to the Venus Radar Mapper thermal control.
3. Design and optimization of specular louver assemblies for diffuse short-wave length environments.
4. Flight-qualification of isothermal heat pipe concepts for "isothermalization" of the equipment compartment.
5. Detailed definition of thermal characteristics of radar and communications electronics applicable to the mission.

6. Detailed definition of "blockage" characteristics of radar and communications antennas.
7. Development and optimization of solar panel temperature control techniques.
8. Development of stable inexpensive solar-reflective coatings or finishes to replace second-surface mirrors.

Electrical Power System

Increased power system capability would permit greater flexibility in design tradeoffs for the Venus radar mapping spacecraft. Present stuides show that the reference power system is inadequate for only one of the operational cases examined. However, if science enhancement or greater terrain resolution is desired, power requirements will increase considerably. For example, with the specialized spacecraft operating in a 0.5 eccentricity orbit, an improvement in resolution by a factor of three will increase the TWT system needs from 352 watts to 1056 watts.

If the spacecraft becomes mass limited, desired power capability can then only be obtained through use of improved technology.

One of the prime candidates for improvement is the battery. The nickel-cadmium battery is the only one which has been proven in cycling service. Although the silver batteries have high energy density a number of problems have limited their application to long life spacecraft. Due to the low specific

output of the nickel cadmium battery (5 W hr/kg) its mass represents one of the major portions of the power system. In the reference system in this study, the battery amounts to 43 percent of the total mass. Weight, however, has not been a constraining factor in this study.

A promising replacement for the nickel-cadmium battery is the nickel hydrogren battery. The cells making up the battery have advantages over the nickel cadmium cells from the standpoint of improved energy density and inherent overcharge and reversal protection. These accrue to the Ni-H_2 system because it combines the best electrode (Ni) from the Ni-Cd system and the best electrode (H_2) from the H_2- O_2 (fuel cell) system. Initial development work on this system is described in Ref. VI-4.

The cell modules consist of a nickel hydrocide electrode sandwiched between two electrolyte matrices and two platinized hydrogen electrodes. The modules, separated by diffusion screens, are electrically connected in parallel and enclosed in a cylindrical pressure vessel. The authors calculate that a cell can be built with an energy density of 88 Whr/kg over a pressure range of 34 atm with 70 percent utilization of the active nickel. Voltage characteristics under load closely follow those of the nickel cadmium cell. Its one disadvantage is that it suffers somewhat greater self-discharge than the Ni-Cd cell. Actual construction and testing of multi-cell batteries is necessary to investigate cell life and thermal effects.

The second area for technology advancement is in the solar array area. In the reference design the solar cell and supporting substrate amount to 29 percent of the total mass. Roll out arrays using thin solar cells and coverglasses mounted upon flexible substrates provide specific outputs on a mass basis of two or three times that of cells mounted on rigid substrates. One array of this type was launched 17 October 1971 and performs satisfactorily in space (Ref. VI-5).

In addition to structural advances, silicon processing has produced cells with an efficiency of 13.5 percent under standard conditions (ref. VI-6), as contrasted to a theoretical limit of 18 percent (ref. VI-7). The combination of these two activities promise to provide arrays with specific output much higher than those which have seen service on past spacecraft. The use of these cells with their lower efficiency tends to increase the specific areas needed for arrays, but this will be counterbalanced by the higher efficiency resulting from silicon semiconductor improvements.

Propulsion System

Proven spacecraft bipropellant, MM'71 and Viking Orbiter '75 liquid propulsion systems support a non-critical technology evaluation for these systems.

A medium criticality, defined as similar requirements having been met through design studies and implementation of system level or conceptual design, must be assigned to the space storable propulsion system. It is felt that the technologies associated with space storable propellant propulsion systems that have been accumulated by such companies as Rocketdyne, Pratt & Whitney, and Aerojet are sufficient for the successful development of a pressure-fed or pump-fed propulsion module. There are certain propulsion subsystem development requirements that must be resolved before an integrated flight qualified multistart long burn duration space storable propulsion module can be successfully developed. A compilation of these requirements include:

1) Demonstrate propellant tank and component materials compatibility;
2) Demonstrate leak-free fluorine oxidizer storage and pressurization systems;
3) Develop safe fluorine oxidizer management techniques;
4) Develop efficient propellant thermal control systems.

Attitude Control System

Cold gas systems proposed for use are identical to the cold gas system presently being used for Viking Orbiter 1975 and therefore are assigned a non-critical evaluation. The concept employing CMGs require a rating of medium to high criticality.

Structure System

The basic Viking Orbiter 1975 structural arrangement is proposed for use with only minor packaging arrangements to be made, therefore this subsystem has been assigned a non-critical technology evaluation.

REFERENCES

VI-1 *VO'75 Project Lander System Specification, SS-3703004.* Prepared for NASA-Langley Research Center by Martin Marietta Aerospace, February 26, 1971.

VI-2 *Functional Requirement Viking Orbiter 1975 Flight Equipment Power Subsystem.* Jet Propulsion Laboratory No. VO75-4-2004A, 4 December 1972.

VI-3 *Power System Computer Program.* Prepared by RCA Corporation for Goddard Space Flight Center, March 1, 1970.

VI-4 J. F. Stockel, G. Van Ommering, L. Swelte, L. Gaines: "A Nickel-Hydrogen Secondary Cell for Synchronous Orbit Application." *IECEC Conference Proceedings,* 1972.

VI-5 G. Wolff and A. Wittmann: "The Flight of the FRUSA." *Conference Record of the Ninth Photovoltaic Specialists Conference,* May 1972.

VI-6 J. Lindmayer and J. Allison: "An Improved Silicon Solar Cell--The Violet Cell." *Conference Record of the Ninth Photovoltaic Specialists Conference,* May 1972.

VI-7 H. W. Brandhorst, Jr.: "Silicon Solar Cell Efficiency - Practice and Promise." *Conference Record of the Ninth Photovoltaic Specialists Conference,* May 1972.

VII. TECHNOLOGY, COST AND SCHEDULE IMPLICATIONS

INTRODUCTION

In the original concept of this study it was expected that new technology areas would be identified as being required to achieve the Venus mapping mission. However, as the study progressed it became apparent that many current technology solutions existed to meet the mission objectives. For this reason, no specific new technologies are identified, costed and scheduled as required items. All technology areas identified are enhancement items whose value lies in expanding the capability and flexibility of the mission. Hence, the basic mission costs are presented and the possible enhancement areas are presented as "add-ons". The focus of the study is directed at the 1980-1989 time period with 1984 chosen as a representative performance case. NASA Headquarters interest in the earliest possible launch opportunity has led to the presentation of a schedule based on a 1981 launch.

COST

General Costing Approach

Two approaches have been taken in developing a Venus mapper program cost estimate range for the recommended configuration. The first approach assumes that the mission could be performed by a spacecraft derived from the Viking '75 Orbiter. Since the VO'75 was developed from the Mariner '71, a subsystem by subsystem comparison of the transition from MM'71 to VO'75 with the changes required to develop a Venus mapper from a VO'75, could form a realistic costing reference. Where the transition from VO'75 to the Venus mapper was

more complex than the growth from MM '71 to VO '75, as in the case of the spacecraft structures for example, suitable cost deltas were added to the VO '75 costs.

The second approach was use of the Planning Research Corporation (PRC) cost model which establishes more general Cost Estimating Relationships (CER's) with other unmanned space exploration missions. Both of the cost estimating activities were based on the following ground rules:

- Program execution span of approximately 40 months from full go-ahead to launch preceded by two years of long-lead development.
- Two spacecraft mission with 240-day orbital lifetime each
- Spacecraft Configuration C assumed
- Test and flight hardware as follows:
  - Design development models at component level
  - Qualification models at component level
  - Proof test model at systems level
  - Two flight spacecraft
  - One set of selected spares
- Radar mapper system and altimeter for mission science - no other science experiments
- Assumes DSN availability for mission data
- Launch Vehicle, facilities, DSN and other NASA support costs are not scoped in these reflected costs
- Costing is FY '73 dollars

Approach 1 - Comparison to VO'75 Costs

Task	Estimate Assumption	Venus Mapper FY'73 ($ M)
Project Management and Management Technical Support	Similar to VO '75	$ 20
Systems Engineering, Analysis, Integration, Reliability, Quality Assurance and Mission Design	Similar to VO '75	65
Systems Test and Operation at ETR	Similar to VO '75	6
Telecommunications	Estimated from comparative data for various telecommunications systems	23
Data Storage	Similar to VO '75	6
Command Control and Sequencer	Similar to VO '75	7
Power	Similar to VO '75	11
Attitude Control System	Similar to VO '75 with modification to size and strength of GN_2 spheres, modification of antenna gimbal servos, and lower drift rate gyros in IRU. Increase in complexity by approximately 10% over VO '75 costs	18
Structure	Significant structural and mechanical changes from VO '75. Approximately 140% of VO '75.	15
Cabling	Similar to VO '75	2
Pyrotechnic	Similar to VO '75.	3

Task	Estimate Assumption	Venus Mapper FY'73 ($ M)
Propulsion	Venus Mapper three (3) engine configuration vs. one engine system on VO '75 - Increase over VO '75 estimated in detail and adds approximately 20% for Venus Mapper	$ 18
Modulation Demodulation Subsystem	Similar to VO '75	4
Flight Data System	Similar to VO '75 plus new radar processor. Cost includes $3M above VO '75 cost for radar processor development.	13
Radar Mapper (New)	Estimated based upon similar complexity development program	10
Radar Altimeter (New)	Estimated based upon similar complexity development program	7
Communications and Radar Antennas (New)	Parametric estimate of antenna size to cost	2
Mission Operations	Similar to VO '75	25
	TOTAL VENUS MAPPER COST	$ 255M

Approach 2 - PRC Cost Model

Redesign and redevelopment cost with inheritance from other programs and recurring hardware costs.	$ 104
Radar Mapper Systems cost	16
Program Management, Systems Test and Operations cost	66
Financial Risk	14
TOTAL COST	$ 200M

Venus Mapper Options

Certain options have been technically considered for the Venus Mapper Program. The majority of these options will require additional analysis, development and qualification before they can become viable for hardware optimization on the Venus Mapper Program and therefore, specific costs cannot be defined with confidence. However, an attempt has been made to range costs of these options based on similar types of development programs. Table VII-1 reflects these options and the costs reflected are delta costs to the $200 - $255 million Configuration C defined as the baseline configuration.

Table VII-1 Venus Mapper Option Deltas

	$ Million Range	
Option	Low	High
Dual Frequency	$ 2 (1)	$ 5 (2)
Dual Polarization	1 (1)	3 (2)
Larger Communications Antenna	1	2
Space Storable System (3)	2	6
Control Moment Gyros	.5	1
120 Days vs. 240 Day Mission (4)	2	4

NOTES: (1) Low dollar range assumes redundant system is on part time basis and has negligible impact on data handling system.

(2) High dollar range assumes redundant system is on full time basis and has significant impact to data handling system.

(3) $18 million is already in the baseline for propulsion. Cost reflected is for delta over existing three engine configuration and is for space storable system design, qualification and integration into existing baseline assuming development costs have already been charged to other programs. New space storable system adaptation to Venus mapper including design, integration, qualification and hardware is approximately $20 - $24 million.

(4) Savings or credit to baseline system in flight operations area.

Conclusions

In view of the foregoing, it is felt a Venus Mapper Mission unmanned spacecraft, technically defined as Configuration C in this report, can be provided for a range of $200 million to $255 million. Additional options, if selected, could add as much as $6 million to the lower range and $17 million to the upper range of Configuration C.

SCHEDULE

A program development outline for a 1981 Venus Radar Mapping Mission is presented in Figure VII-1. This is representative of the earliest launch date anticipated and imposes the tightest schedule.

The plan offers several features that can be highlighted as follows:

(1) Identification of technical problems and demonstration of practical solutions with pyrototype hardware prior to the commitment of major program funds.

(2) Restricted program go-ahead in FY'77 to establish line item recognition and allow the initiation of long lead development without heavy impact on the Planetary Programs budget.

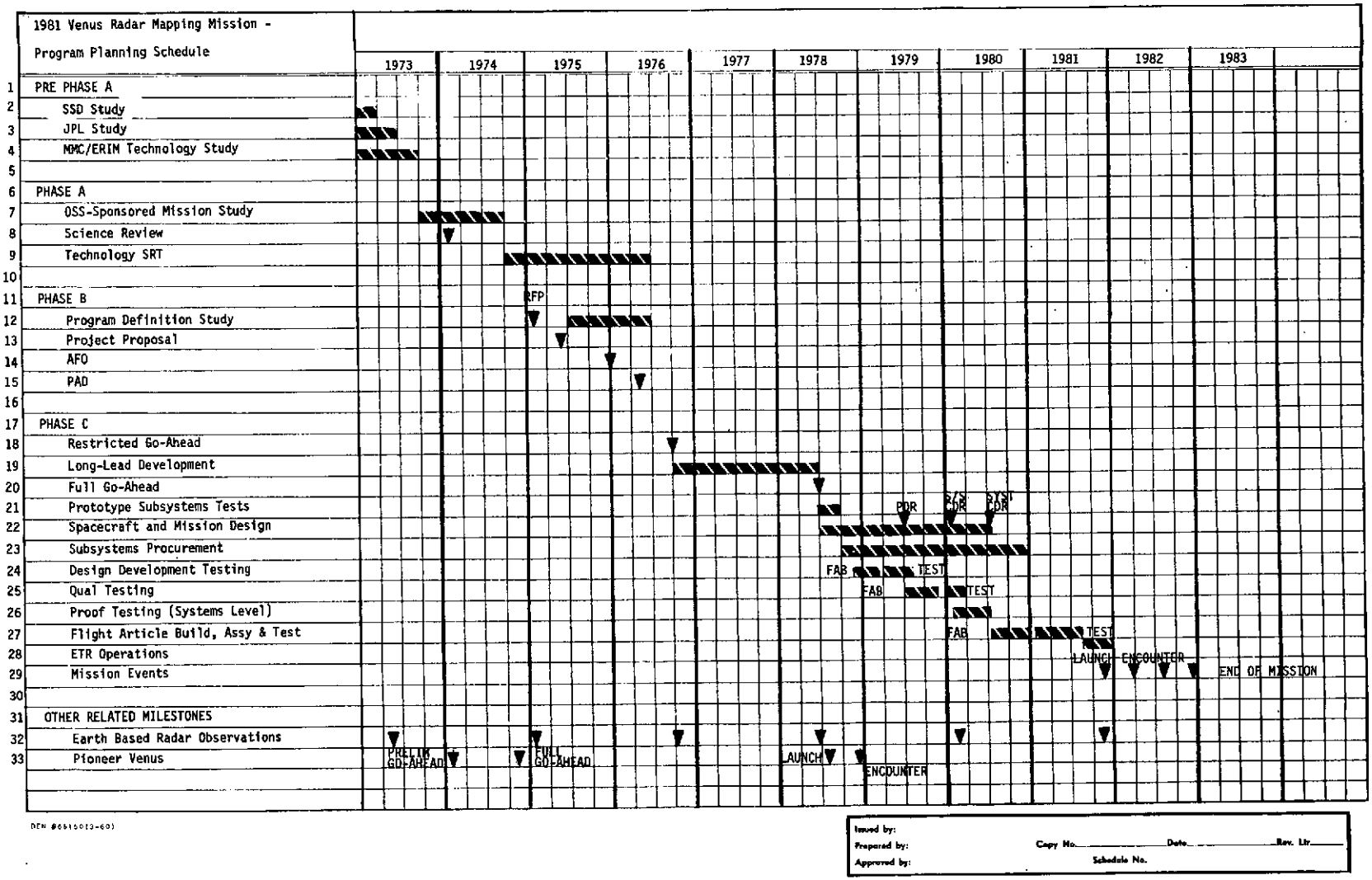

Figure VII-1 1981 Venus Radar Mapping Mission - Program Planning Schedule

(3) Full go-ahead in FY '79 (about 40 months prior to launch) to compress major funding into an efficient time-span to hold down total program costs.

The program phases shown in the outline follow the pattern currently being used on the Pioneer Venus program. Phase A is preliminary design, Phase B is program definition, and Phase C is design and implementation. These phases combine the old Phase A, B, C, and D activities.

The work done to date by SSD, JPL and the Martin Marietta team has established that the Venus Mapper Mission can be done as early as 1981 with technology that is in hand today. There is, however, a good deal of "sorting out" to do among the mission and spacecraft concepts recommended in these studies to provide a good planning base for the program.

The rationale and explanation of items in the plan is discussed line-by-line in the following paragraphs.

Line 7. Mission Study - This study would provide the planning base for the Venus Mapper program development plan. It would establish a recommended mission/spacecraft approach and the initial detailed program cost estimate. The outputs of the study would also support the preparation of the NASA-prepared Project Proposal.

Line 8. Science Reviews - A forum or symposium sponsored by NASA Headquarters to focus the attention of the science community on the Venus Mapper mission and to identify science objectives and requirements. The results of this review will support the mission study, provide quidance for the preparation of the AFO and serve as the first step in the development of the mission definition document.

Line 9. Technology SRT - A program of supporting research and technology aimed at solving specific Venus Mapper technology problems. Tasks would address problems in the areas of: radar and antenna, data handling and communications, supporting spacecraft subsystems,

and mission analysis. The results of these SRT tasks will identify where long-lead prototype hardware development will be required.

Line 12. Program Definition Study - A competitive Phase B activity to develop preliminary mission and spacecraft designs and to produce the technical and management plans required to conduct the full program. The output of the study will also include proposals for Phase C.

Line 13. Project Proposal - A NASA generated document that supports the request for line item recognition in the NASA budget. It is essentially a scaled down version of the Project Plan that demonstrates that sufficient ground work has been done to establish a clear understanding of the program and its problems and requirements. The Project Proposal would be produced in the second quarter of calendar year 1975 at the time the FY '77 NASA budget exchanges begin between Headquarters and OMB.

Line 14. Announcement of Flight Opportunity (AFO) - Notification to the planned 1981 Venus Radar Mapping mission to solicit offers from potential science team members and principal investigators.

Line 15. Project Approval Document - The official NASA approval of the program prior to initial go-ahead.

Line 18. Restricted Go-Ahead - The restricted go-ahead establishes program identity at low funding levels to permit long-lead development and planning to start. Funding liabilities are held to less than 10% of total program run-out costs during the period prior to full go-ahead (FY '79).

Line 19. Long-Lead Development - Design and build of prototype hardware for those critical subsystems or components identified in the technology SRT tasks and the Program Definition Studies. Prototypes should be built at minimum cost with minimum paper-work to establish proof of function and operation.

Line 20. Full Go-Ahead - The point at which major program funding is turned on. This is about 40 months prior to launch.

Line 21. Prototype Subsystems Test - Evaluation of the prototype hardware developed in the long-lead program. This evaluation will feed directly into the spacecraft and mission design effort.

Line 22. Spacecraft and Mission Design - Design effort covers 24 months and produces procurement specifications, design drawings, and test plans and specs for the development test, qual test, proof test and flight hardware phases of the program.

Line 23. Subsystems Procurement - Placement of subcontracts and delivery of hardware for the total program requirements.

Line 24. Design Development Testing - Selected subsystems will be produced to as near flight configuration as possible to allow testing and "smoking-out" of potentially serious problems ahead of qual test.

Line 25. Qual Testing - Proof of flight qualification at the component and subsystem level by testing to specs that contain appropriate margins in excess of anticipated flight conditions.

Line 26. Proof Testing - Systems level testing under simulated mission environments of an all-up flight version of the spacecraft (Proof Test Mapper).

Line 27. Flight Article Build Assembly and Test - Production and test of flight spacecraft (one or two) and flight spares. Flight article delivery to Cape Kennedy will be about three to four months prior to launch.

Line 28. ETR Operations - Prelaunch and launch operations

Line 29. Mission Events - The launch period will be approximately 11/11/81 to 11/30/81. Encounter will be 3/6/82 to 3/17/82. End of mission will be approximately 250 days after encounter for an elliptical mapping orbit or could be as low as 120 days after encounter for a circular orbit.

Line 32. Earth Based Radar Observations - Earth-Venus inferior conjunctions that will provide good radar coverage from Arecibo, Goldstone and Haystack. Information will help establish mapping strategy and priorities for high resolution coverage for the orbital mapping mission.

Line 33. Pioneer Venus - Significant milestones in the PV flyby/orbiter/probe program. Information will assist in verifying mapping radar frequency selection, orbit perturbation predictions and ancillary science instrument selection.

VIII. SCIENCE ACHIEVEMENT

INTRODUCTION

An orbital mapping mission (providing topographic resolution at approximately 100 meters) can be expected to increase our knowledge of Venus by several orders of magnitude. This has been demonstrated in the case of Mars exploration. The thin Martian atmosphere allowed telescopic and video fly-by observation of the surface before the Mariner IX orbiter mission. Based on these early observations,scientists developed many theories regarding Martian geology, planetology and atmospheric physics. The medium and high resolution imagery produced by Mariner IX provided dramatic data which completely changed or disproved many of these theories. Current theories on the nature of Venus are based on vague and ambiguous data at best, and the science impact of quality surface imagery will indeed be tremendous.

This section will consider the Configuration C mission which will employ a dedicated antenna system and a variable side-look angle. Configuration C appears to offer the maximum science return benefit within the current cost limitations. Each mission variable which impacts the science return (discussed in detail in Volume III) will be evaluated in terms of Configuration C parameters.

RESOLUTION

A baseline resolution of 100 meters has been determined as desirable for a global geologic analysis. A fine resolution mode, allowing limited coverage at resolutions on the order of 10 meters, is desired for detailed geologic and terrain analysis for lander site selection. By using a variable look-angle Configuration C is able to obtain 100 percent coverage but resolution is variable. At periapsis, resolution is 50 meters, which is a factor 2 better than the baseline resolution. This resolution will allow considerable detail in studying stratigraphy and discriminating rock types. At $\pm 60^{\circ}$ true anomaly resolution equals 100 meters and falls off to 200 meters at 90° true anomaly. Resolution in the polar region is somewhat less than desired. However, this deficiency is compensated for by the repeat coverage available in this area. The repeat coverage will allow selected small areas in the polar regions to be inspected with a higher resolution mode of operation. This telescopic mode of operation can be used at any time if a smaller swath width (less coverage) is acceptable. The best resolution obtainable in this mode of operation is about 33 meters and can be obtained over most areas of the planet. Although this is less than desired for precision landing site selection, these data will aid in selecting the proper type of terrain for a safe, scientifically rewarding landing site.

FREQUENCY

Radar system frequency is 3.0 GHz providing a wavelength of 10 cm. This frequency insures atmospheric penetration and high topographic data content of the resultant imagery. Antenna dimensions needed for a 3.0 GHz system are favorable for an orbital mission.

STEREO COVERAGE

A minimum of 20% stereo overlap is considered necessary to provide control for the construction of a topographic map and identification of representative geomorphic features. Configuration C exceeds this minimum requirement providing 30% "same side" stereo coverage at periapsis and 100% at 90^{o} true anomaly (See Figure III-20). The increasing percentage of stereo coverage at higher latitudes tends to compensate for the decreasing resolution and will result in a topographic map of more uniform overall quality. As explained in Volume III, same-side viewing of the target terrain provides the most easily interpreted stereo image. If a squint mode of operation is incorporated into Configuration C, a 900 km wide belt, centered on the equator, will receive opposite-side stereo imaging. Although this type of coverage is unsuitable for stereo viewing by the human interpreter, the exaggerated stereo parallax is ideal for computer analysis and display.

COVERAGE, PERIAPSIS LATITUDE AND ECCENTRICITY

Configuration C achieves the desired 100% global coverage despite an eccentricity of 0.5 because of the variable side-look angle. This fact has strongly influenced the selection of Configuration C as providing the highest science return. In the case of mission configurations that provide less than 100% coverage it is recommended that periapsis be shifted to a higher latitude to include coverage of at least one pole and to provide more uniform data quality in the equational, temperarate and polar regions in one hemisphere. Configuration C images both poles and provides adequate uniformity of data with periapsis located on the equator.

RADAR LOOK ANGLE

Configuration C is unique in the handling of radar look angle. Since "grazing angle" is more relevant to the resultant imagery than "look angle", only the term grazing angle will be used. The two terms denote equal quantities in a flat target model but vary significantly when dealing with a curved (planet curvature) surface. At periapsis (0^{o} latitude) the grazing angle is 50^{o} and decreases to 12^{o} at the poles (See Figure IV-9, Volume III). This variation allows the maximum grazing angle to be used with the power and range constraints encountered as a function of latitude. As discussed in Volume III, it is probable that problems with radar layover distortion will occur at grazing angles less than 20^{o} which would exist at

latitudes greater than about 60^{o}. At worst, this will reduce interpretability of the imagery to determination of general terrain type but would probably produce superior surface roughness data. Hopefully, most of the topographic data can be resolved with processing techniques. This is a probable thing since repetitive coverage at higher latitude may reduce ambiguities resulting from layover distortion. It should be noted that the 20^{o} grazing angle limit on radar layover is based on SLAR imagery of mountainous Earth terrain (See Figure II-8, Volume III). Layover effects are less significant, and occur at smaller grazing angles, over terrain of low surface slopes as may be encountered on Venus.

AUXILIARY INSTRUMENTATION

Auxiliary instrumentation and experiments are recommended as optional to the basic mission configuration. In general, these experiments provide useful secondary information at minimum cost. As mentioned in the Introduction, it is assumed that experimentation regarding the atmosphere, dynamic figure of reference, planetary dimensions and shape, mass distribution, spherical harmonics and magnetic field will be largely completed prior to the mapper mission as part of Pioneer Venus. However, the orbital mapper mission offers an opportunity to enhance and verify previously obtained data. Precise tracking of the spacecraft in the 0.5 eccentricity orbit will provide spherical harmonics and planetary shape data. The S-band imaging system and x-band communication link could be used for a dual frequency occulation experiment to provide valuable information about the Venusian atmosphere and planet shape. The following paragraphs suggest specific additional instrumentation that can add significantly to the science return.

Radar Altimeter - Radar altimetry is the most beneficial auxiliary instrumentation and is included in configuration C. The topographic profiles produced by this instrument can be used to check and calibrate the relative height data provided by the imaging system. Special computer processing of stereo imagery to facilitate stereo viewing will require the altimeter data input. The science value return of the altimetry equipment can be increased by using a dual frequency mode of operation. The proper selection of the two frequencies may allow the determination of relative atmospheric surface pressure. Comparison of the topographic profile data with the pressure data may reveal the presence of mass concentrations such as those detected on Mars.

Radiometer - Microwave radiometry can provide valuable secondary geologic information. Although the sensitivity of a radiometer measuring surface emittance through the Venusian atmosphere probably would not detect temperature variations due to surface thermal properties, geothermal activity would provide sufficient temperature constant to be measured. Additionally, the lower atmosphere lapse rate, estimated to be 8^{o} C/KM, would result in a thermal map of the topography and provide a double check of the imaging system.

Aerial Magnetometer - If the existence of a magnetic field is established by early fly-by missions the inclusion of an aerial magnetometer on board the mapping spacecraft would provide useful scientific information. Mapping the direction, inclination and magnitude of the field can indicate the nature of the planet core. The distribution and amounts of ferromagnetically rich rocks will be indicated by deviations from the regional field trends.

Dual Polarization and Dual Frequency - The use of dual polarization and dual frequency radar imagery has received limited experimental use in geoscience applications. Investigators have variously claimed that information on surface roughness, vegetation, soil moisture content and cultural features are increased by the use of these techniques. Of these, only surface roughness is both useful and existent on Venus. Since the basic imaging system will provide some surface roughness information, without the aid of dual frequency and polarization, it seems that additional complexity, data handling requirements, and cost of adding these features is not worth the increase, if any, in the science return.